Mind the gap:
modelling event-based and millennial-scale landscape dynamics

Jantiene E.M. Baartman

Mind the gap:
modelling event-based and millennial-scale landscape dynamics

Jantiene E.M. Baartman

Mind the gap:
modelling event-based and millennial-scale landscape dynamics

Jantiene Elise Marianne Baartman

Thesis
submitted in fulfilment of the requirements for the degree of doctor
at Wageningen University
by the authority of the Rector Magnificus
Prof. dr. M.J. Kropff,
in the presence of the
Thesis Committee appointed by the Academic Board
to be defended in public
on Wednesday 9 May 2012
at 4 p.m. in the Aula.

Dankwoord

Een proefschrift schrijven is iets dat je zelfstandig doet. Het tot stand komen van de inhoud van een proefschrift is echter (gelukkig!) een kwestie van samenwerking, overleg, inspiratie en terugkoppeling. Hierbij zijn gedurende de vijf jaar dat ik aan dit proefschrift heb gewerkt veel mensen van groot belang geweest. Bij dezen wil ik hen allen hartelijk bedanken!

Ten eerste wil ik mijn promotors Tom Veldkamp en Coen Ritsema bedanken. Tom bedankt voor de inspirerende en motiverende gesprekken, je wist altijd de vinger op de zere plek te leggen. Met jou en Jeroen rondlopen in het veld was een feest: je kijkt, analyseert, interpreteert en produceert een niet-aflatende stroom hypothesen die je vervolgens probeert te ontkrachten met verdere waarnemingen. Ik heb veel van je mogen leren. Coen, bedankt dat je mijn promotieonderzoek wilde inbedden in het DESIRE project en voor de vrijheid die je me gaf. Je deur stond altijd voor me open, dat waardeer ik zeer. In dit rijtje hoort natuurlijk ook co-promotor en LAPSUS-vraagbaak Jeroen Schoorl. Jeroen, bedankt voor de motivatie, de kritische blik op mijn schrijfsels, je enthousiasme en humor. Helaas niet officieel in dit rijtje, maar daarom zeker niet minder belangrijk voor het tot stand komen van dit proefschrift is Arnaud Temme. Arnaud, zonder jouw hulp op vele vlakken (LAPSUS, OSL-sampling, artikel-revisies etc etc) zou dit proefschrift hier nu niet liggen. Ik wil je hiervoor heel hartelijk bedanken, maar met name ook voor je enthousiasme, inspiratie en motivatie! Ik hoop dat we in de toekomst kunnen blijven samenwerken.

Werken bij twee vakgroepen heeft zijn voor- en nadelen: je blijft heen-en-weer lopen, maar je profiteert van dubbele vakgroepuitjes, -borrels en taart! Ik wil mijn collega's van beide groepen van harte bedanken voor de gezelligheid: Peter, Jetse, Marthijn, Jeroen, Martha, Gerard, Violette, Gert, Bas P., Kasper, Arnaud, Lieven (LAD) en Leo, Saskia, Manuel, Aad, Jan, Michel, Erik, Piet, Alma (LDD). Marnella, Henny en Mieke wil ik hartelijk bedanken voor alle onmisbare administratieve hulp. Met name wil ik ook de aio-collega's van beide groepen bedanken. Een aantal personen in het bijzonder. Bas: Gaia-kamergenoot, arcGIS helpdesk, R-vraagbaak, koffiemeisje en concurrent (!). We hebben heel wat goede momenten en frustraties gedeeld tijdens onze koffie-hang-pauzes in Atlas. Bedankt voor je adviezen, luisterend oor en gezelschap de afgelopen vijf jaar. Wouter wil ik hartelijk bedanken voor de inspirerende geomorfologische en LAPSUS sessies. Ik kom graag nog eens in Turkije kijken! Monique, hartelijk bedankt voor je enthousiasme, je nuchtere manier van aanpakken en leuk dat je mee ging skiën ;)! Wouter, Monique, Derek, Claudius en Lieven: hartelijk bedankt voor het (mede)organiseren van de Kenya cursus!

Catherine: bedankt voor het delen van ons Gaia-kantoor op maandag, het verzorgen van Bas' plantjes ;) en het samen organiseren van Spatial Methods.

Mijn kamergenootjes op onze mooie hoekkamer op Atlas wil ik ook graag hartelijk danken: Cathelijne, Demie, Louis, Jan en Klaas. Bedankt voor de goede sfeer, jullie luisterend oor en het halen van koffie! Jan, hartelijk dank voor je programmeerkunsten, het gebruik van je rekencomputer en het delen van calibratie- en modelleer perikelen!
Bij dezen wil ik ook graag de collega's van DESIRE hartelijk bedanken. Mike Kirkby ben ik zeer erkentelijk voor het verschaffen van essentiële afvoer- en regenval data. Joris, Carolina en Albert Sole Benet in Spanje ben ik zeer dankbaar voor de introductie en het rondleiden in het veldgebied en het zeer snel beantwoorden van mijn vele vragen via e-mail. Carolina wil ik extra bedanken voor het redigeren van de Spaanse samenvatting! Victor Jetten wil ik hartelijk danken voor het beantwoorden van al mijn LISEM vragen en het updaten van en knutselen aan OpenLISEM. Verder wil ik graag Erik Cammeraat hartelijk danken voor zijn introductie in het veld. Jakob Wallinga en NCL-collega's wil ik bedanken voor de hulp bij het dateren van mijn Spaanse sedimenten.

Minstens zo belangrijk tijdens mijn promotie was voor mij het ontspannen na het werk. Hiervoor wil ik vooral de ibex (oude lullen...) -vriendjes en –vriendinnetjes bedanken. Behalve het (bijna) wekelijkse halklimmen, hebben we vele leuke activiteiten ondernomen zoals (in willekeurige volgorde en frequentie): mtb-en, koffie drinken, alpineren, biertjes drinken, sauna, dansen, toerskiën/freeriden met of zonder camper, schaatsen en (berg)wandelen. Bedankt: Arnaud, Michiel, Danny, Peter, Pim, Paula, Lieke, Kirsten, Mark, Monique, Baukje, Marije, Joris, Suus, Roemer, Joost, Monique, Miranda, Tijs, Folmer en Jorien. Kirsten wil ik als (oud) huisgenootje nog speciaal bedanken: voor je gezelligheid en luisterend oor. Ook mijn jaarclubvriendinnetjes Nora, Willemijn, Marlinde, Marleen, Margriet, Marjolein en Marije wil ik hartelijk bedanken. Vooral het weekend bij Marleen afgelopen november vond ik super.

Een aantal mensen zijn niet alleen deze vijf jaar maar al veel langer belangrijk voor me. Ten eerste mijn paranimfen Marije en Liesbeth. Marije, we zijn al vriendinnen vanaf de kleuterschool. Bedankt voor deze levenslange vriendschap: door dik en dun en waar ook ter wereld! Liesbeth, mijn grote zus en grote voorbeeld! Ondanks (sporadische) zussen-onenigheden kan ik me geen betere zus wensen. Een hoogtepunt vormde toch wel ons Bolivia-avontuur, waar Eric natuurlijk ook een belangrijk deel van uitmaakte. Ik ben enorm trots tante te zijn van het liefste nichtje en neefje van de wereld: Lotte en Daniel!
Natuurlijk gaat ook mijn liefste dank naar mijn ouders Jan en Nella. Ik ben jullie heel dankbaar voor jullie onaflatende en onvoorwaardelijke steun en liefde.

Lieve David: mijn steun en toeverlaat en mijn grote liefde. Dank je dat je er voor me bent. Nu mag je weer met me op vakantie!

Table of Contents

Chapter 1

General introduction

1.1. Introduction

Soil erosion is defined as 'the wearing away of the land surface by water, wind, ice, gravity or other natural or anthropogenic agents that abrade, detach and remove soil particles or rock material from one point on the earth's surface, for deposition elsewhere, including gravitational creep and so-called tillage erosion' (European Commission, 2011) and erosion is listed as the first of eight main soil threats (European Commission, 2006). According to Parsons *et al.* (2004) it is important to know rates of soil erosion by water for two principal reasons: first, it is essential to our understanding of landform development. Second, on agricultural land, these rates determine the long-term sustainability of agricultural practices and have profound economic consequences. The first of these two reasons, landform development, involves erosion over long (millennial) time-scales. However, erosion by water occurs as a consequence of (a sequence of multiple) rainfall events. There is a gap in time-scales between an erosive rainfall event (hours to days) and landscape evolution (centuries to millennia). The contribution of, for example, an extreme event to total erosion can only be evaluated if long-term average erosion rates are known. Furthermore, different sequences of events can lead to different erosional response. The effect of two consecutive large events will have a different effect than if these two events occur several years apart. In a recent review, Hoffmann *et al.* (2010) propose that future research should focus on quantifying the relative roles of allogenic and autogenic forcing on fluvial regimes, extreme events and sediment fluxes. This behaviour can be evaluated with landscape evolution models (LEMs; e.g. Tucker and Hancock, 2010) using information on long-term erosion rates derived from for instance, dated sediment archives. In addition, the consequences of climate change, for instance if more extreme events are being predicted to occur, can be simulated with these kinds of models.

The second reason mentioned by Parsons *et al.* (2004) involves human activity. As stated by Hooke (2000), humans have arguably become the most important geomorphic agents in sculpting the landscape. However, appreciating the actual importance of humans as agents of global soil erosion necessitates knowledge of prehistoric erosion rates imposed only by natural processes (Wilkinson, 2005). By comparing long-term and contemporary erosion rates, some studies have found similar rates (e.g. Matmon *et al.*, 2003), others found elevated contemporary rates, attributed to human impact (e.g. Gellis *et al.*, 2004, Vanacker *et al.*, 2007), but also lower contemporary rates were found, explained by the absence of high-magnitude, low-frequency (extreme) events in the contemporary record (e.g. Kirchner *et al.*, 2001, Tomkins *et al.*, 2007, Meyer *et al.*, 2010). To prevent or mitigate the effects of land degradation and erosion, soil and water conservation measures should be sustainable and targeted at the accelerated erosion due to human impact on the landscape. This is not possible without understanding the natural landscape dynamics (erosion and deposition processes).

If erosion due to human impact can be separated from natural erosion, sustainable measures to combat erosion can be developed (Vanacker *et al.*, 2007, Boix-Fayos *et al.*, 2008).

While the definition of erosion separates natural from anthropogenic causes of erosion, in many erosion studies, the assumption is made that all observed erosion features are the direct and indirect results of human actions (e.g. Bork *et al.*, 2001, Vanacker *et al.*, 2003). In geosciences, however, erosion is viewed upon as a natural denudational process. Consequently, in erosion research, spatial and temporal scales as well as research methods differ: plot-slope-small catchment scale, event based change, 'human' time-scales (Kroonenberg, 2006) and field experiments on the one hand, landscape regional scale, decadal change, time-scales of landscape evolution (Quaternary) and landscape evolution models as tools on the other hand. The aim of this thesis is to bridge the gap between these two contrasting approaches with focus on the time-scale gap between rainfall events and landscape evolution and the relative contribution of human activity to natural erosion. Tools of both approaches (i.e. field measurements and modelling on different time-scales) are combined.

The remainder of this introductory chapter introduces the role of natural versus human induced erosion in section 1.2. In section 1.3 the gap in time-scale between rainfall - runoff events and landscape evolution is introduced. Section 1.4 introduces modelling of landscape dynamics (erosion and sedimentation). In sections 1.5 and 1.6 the research questions and thesis outline are given. The study area in SE Spain is described in section 1.7. Finally, in section 1.8 details of two models used in this study are described.

1.2. Natural and human-induced erosion

Generally, it is believed that human pressure upon the soil increased erosion rates (e.g. Hooke, 2000, Syvitski *et al.*, 2005, Knox, 2006), due to for instance urbanization, deforestation, agricultural practices, mining and reservoir development. Moreover, humans also indirectly influence erosion, for example when land use changes increase the sensitivity of river dynamics to climate fluctuations (Verstraeten *et al.*, 2009a). To quantify the importance of humans as agents of erosion, knowledge of erosion rates due to solely natural processes is required (Wilkinson, 2005, Vanacker *et al.*, 2007). Two interconnected problems that arise are that the onset of anthropogenic influence frequently predates historical records (Wilkinson, 2005) and that undisturbed areas where natural rates can be assessed are difficult to find (Gellis *et al.*, 2004).
Comparing estimates of world-wide modern rates of erosion to estimates of ancient and geologic erosion rates, Hooke (2000) and Wilkinson (2005) conclude that humans have become the most important geomorphic agents, moving more than an order of

13

magnitude more sediment than the sum of all other natural processes operating on the Earth's surface. Syvitski *et al.* (2005) use a modelling approach to estimate the global sediment flux on a river-by-river basis under modern and pre-human conditions, concluding that humans have increased the sediment transport by global rivers trough soil erosion but reduced the sediment flux reaching the coast due to retention within reservoirs. Apart from these global estimates, many case studies exist that qualitatively or quantitatively relate erosion to natural and/or human causes. Several examples illustrate different methodologies to assess human versus natural sediment dynamics.

Many (case) studies use field observations and dating of sediment bodies, for example river terraces, and qualitatively correlate the episodes of erosion or deposition to periods of increased human impact or climate change (e.g. Little Ice Age). Examples include Schulte (2002), Faust *et al.* (2004), Avni *et al.* (2006), Knox (2006), Fuchs (2007), De Moor *et al.* (2008), Dearing *et al.* (2008) and Zielhofer *et al.* (2008). Carrión *et al.* (2007) use pollen data to correlate the vegetation history to human and/or natural perturbations. Dotterweich (2008) reviews past soil erosion and gullying in small catchments of central Europe, concluding that sediment fluxes in small catchments are highly sensitive to local land use changes, while river sediments show regional trends in land use and climate changes.

Lang (2003) use a semi-quantitative approach in which a frequency distribution of optical dates on colluvial sediments is constructed. Phases of increased colluviation are correlated to periods of stronger human impact. Using a similar approach, Panin *et al.* (2009) emphasizes the role of climate changes to trigger gullying in the last five millennia and only since the Middle Ages human impact has amplified gully erosion.

Cosmogenic nuclide analysis can be used to quantitatively calculate long-term erosion rates. These can be compared with present-day sediment yields, for example calculated from reservoir sedimentation in steep mountain catchments (Vanacker *et al.*, 2007), or calculated using sediment traps and straw dams (Gellis *et al.*, 2004). In both studies, present-day sediment yields showed large spatial variation and modern erosion rates are similar to the pre-anthropogenic benchmark rates if the area is well-covered by vegetation. Removal of the vegetation cover leads to an exponential acceleration of erosion rates. Gellis *et al.* (2004) relate the higher erosion rates to grazing activity.

Another approach to quantitatively evaluate sediment dynamics and their causes (e.g. human or natural) is the sediment budget concept (e.g. Houben *et al.*, 2009, Notebaert *et al.*, 2009, Verstraeten *et al.*, 2009b). Verstraeten *et al.* (2009b) visualize not only the human influence on erosion, but also the changing connectivity of hillslopes, colluvia and floodplain area throughout the Holocene.

A third quantitative method to study landscape responses to human-induced changes is to use simulation models. Govers *et al.* (2006) used an adapted version of the SPEROS model to study the interaction of water erosion, tillage erosion and rock fragment cover

under various land use scenarios over decadal time-scales. Van Oost *et al.* (2000) assess the effect of changes in landscape structure on both water and tillage erosion using the WATEM model. Although these applications simulate the effects of (human) land use changes, they do not compare to non-human situations. Verstraeten and Prosser (2008) apply the WATEM/SEDEM model to an Australian catchment by first modelling erosion and sedimentation under pre-European land use and second, they use recent land use patterns in the model. Long-term (i.e. millennial) modelling of the effects of human impact on erosion and landscape dynamics are rare. Using the landscape evolution model CAESAR Coulthard *et al.* (2000) modelled the effects of deforestation and climate change separately and in combination for a UK catchment over 100 years. Using the same model but over 9 millennia, Coulthard and Macklin (2001) conclude that Holocene river evolution in temperate regions is driven primarily by climate change, but that it is also influenced by land cover changes. Different from the previous is the use of agent-based models (AGMs) to evaluate human interactions with geomorphic processes (Wainwright and Millington, 2010).

1.3. The time-scale gap in landscape dynamics

There is an obvious gap in time-scales between runoff and erosion during a storm event and the long-term landscape evolution of a catchment (Tucker and Hancock, 2010), i.e. between hydrometeorologic time-scales (minutes to weeks) and geomorphic time-scales (centuries to millennia and even geologic era; Tucker and Bras, 2000). As Schumm and Lichty (1965) illustrate, dependent on the time-span involved, variables of a landscape system may change status from independent to dependent or not relevant. On a millennial time-scale, the independent variables are, for instance, lithology, climate and vegetation, while hillslope and channel morphology are dependent variables and observed discharge and flow characteristics are considered indeterminable on this (millennial) time-scale. On the short time-scale (defined as < 1 year), the latter become the dependent variables and hillslope and channel morphology become independent variables.

Extreme events of low frequency but high magnitude seem to contribute disproportionally to total erosion (e.g. Brunsden and Thornes, 1979, Hooke and Mant, 2000, Boardman, 2006, Gonzalez-Hidalgo *et al.*, 2010). Comparing long-term and contemporary erosion rates, some studies have found similar rates (e.g. Matmon *et al.*, 2003), others found elevated contemporary rates, attributed to human impact (see section 1.2; e.g. Gellis *et al.*, 2004, Vanacker *et al.*, 2007), but also lower contemporary rates were found, explained by the absence of high-magnitude, low-frequency (extreme) events in the contemporary record (e.g. Kirchner *et al.*, 2001, Tomkins *et al.*, 2007, Meyer *et al.*, 2010). Due to the episodic nature of sediment fluxes, they can easily be missed in

contemporary, short time, sediment measures, leading to underestimation of calculated average erosion rates (Kirchner *et al.*, 2001). Conversely, if an extreme event was included in the measurements, average rates can be overestimated compared to long-term average flux-rates. As Kirkby (2010) states, soil erosion measurements should not be reported without their interpretation in terms of long-term average rates and magnitude-frequency distributions.

Of importance for the interpretation of events in landscape evolution, e.g. from records of deposited sediments, is the mechanism of shredding of environmental signals (Jerolmack and Paola, 2010). Due to nonlinearity of sediment transport and autogenic (self-organized) behaviour in the landscape system, an external signal will not show in the sediment output if its frequency is smaller than the characteristic time-scale of the system, unless its magnitude is large enough (Jerolmack and Paola, 2010). In line with this, Van De Wiel and Coulthard (2010) showed that the application of identical rainfall events (i.e. events of equal magnitude and regular sequencing) in their landscape evolution model gave considerably different sediment outputs. This implies that sediment records, used to infer past climate or environmental conditions could simply reflect the internal system dynamics instead of external forcing such as climate variability (Van De Wiel and Coulthard, 2010).

Although often modelled as a continuous process, landscape evolution is in fact driven by discrete events (Tucker and Bras, 2000), which have a characteristic frequency distribution varying in space and time.

In their review on modelling the response of river systems to environmental change, Van De Wiel *et al.* (2011) state that the temporal resolution (i.e. the time step) of model simulations should be sufficiently small to capture landform altering events. Many landscape evolution models (LEMs) use a 'geomorphologically effective' runoff event to drive erosion in the model (Tucker and Hancock, 2010). However, it is not defined what a 'geomorphic effective' or 'landform altering event' is or should be. Tucker and Hancock (2010) also state that time variability in hydrologic forcing can have an impact on landscape dynamics and should normally be incorporated in models. In an analysis on the effect of rainfall variability as opposed to mean rainfall, Tucker and Bras (2000) found that long-term average sediment transport capacity (and sediment flux) in rivers and on eroding hillslopes should be higher under a more variable climate, all else being equal. The degree of sensitivity to climate variability depends on (1) the intrinsic nonlinearity in transport dynamics and (2) the magnitude of thresholds for runoff production (e.g. the infiltration threshold) and sediment particle detachment.

1.4. Approaches to modelling landscape dynamics

First of all it should be remembered that every model is by definition a simplified representation of (parts of) reality (e.g. Mulligan and Wainwright, 2004, Nicholas and Quine, 2007). Depending on the objective and scale of the modelling exercise, few or more elements of reality can be incorporated in a model. The so-called reductionist approach strives towards understanding and explaining a system by reducing it to its fundamental components and attempting to analyse the behaviour of these components and the interactions between them (Harrison, 2001). Thus, larger-scale system characteristics are predicted as the product of lower-level process interactions, rather than being defined explicitly (Nicholas and Quine, 2007). Often, reductionist models aim to include as many primary and secondary processes as feasible, assuming that the inclusion of more processes will result in enhanced realism in the simulations (Van De Wiel *et al.*, 2011). The disadvantages of this approach are, firstly, that there will always be a number of processes which are not explicitly included and, secondly, that inclusion of more processes increases the model's complexity and thus simulation uncertainty and parameter requirements (Van De Wiel *et al.*, 2011). According to Preston *et al.* (2011), the reductionist paradigm dominated geomorphic enquiry from 1960 – 1990, but the challenge should now be to synthesize and extend understanding beyond the mechanics of process and into the holistic function of complex landscape systems. The synthesist approach (e.g. Paola, 2011), is underpinned by the recognition that process-form interactions operate across a hierarchy of scales and by the belief that only certain aspects of the dynamics at any level are essential to understanding system behaviour at the level above (Nicholas and Quine, 2007). Complexity, in general, is ordered and hierarchical, meaning that it is not additive (Paola, 2011). Harrison (2001) notes that geomorphological landscapes may be 'more than the sum of their parts'. Synthesists advocate that understanding what is really essential requires simplification and that this is essential if the goal is insight (Paola, 2011). Simplified representations of the complex small-scale mechanics of flow or sediment movement capture the self-organization processes that create apparently complex patterns (Paola, 2011). However, this simplification introduces other problems, such as weakly-physical or empirical parameterization instead of previously well-constrained properties or variables (Brasington and Richards, 2007).

Most models are not strictly reductionist or synthesist. For example, models that are considered reductionist, rarely resolve sediment transport at the level of individual particle trajectories. Synthesist models may represent the same suite of processes at the same scale, be underpinned by the same principles (e.g. conservation of mass) and retain the same basic structure as traditional flow-sediment transport models (Nicholas and Quine, 2007). The term reduced-complexity is therefore often used, which implies only emphasis on simplicity (Nicholas and Quine, 2007).

Reduced-complexity models may form the necessary bridge between the short-term, small-scale, process-oriented and the long-term, large-scale elements of geomorphology (Brasington and Richards, 2007).

1.5. Objectives and research questions

To better understand landscape response in terms of erosion and deposition dynamics, there is a need to understand the role of human activity on the (naturally) eroding landscape and the role of (extreme) events in long-term landscape evolution. In a recent review on human impact on Holocene fluvial regimes and sediment fluxes, Hoffmann *et al.* (2010) propose that more sophisticated datasets should be developed that combine (i) contemporary and long-term hydrological and geomorphological information; (ii) DEMs of contemporary floodplain topography and land use; and (iii) reconstructed DEMs of palaeo-floodplain environments. For the future, Hoffmann *et al.* (2010) propose that research should focus on quantifications of the relative role of allogenic and autogenic forcing on fluvial regimes, extreme events and sediment fluxes and on improvement of long-term river basin modelling.

Indeed, it is the main focus of this thesis to combine long-term (millennial) landscape evolution and short-term (hours – days) rainfall runoff events using models that have been developed for both extremes (i.e. of time-scales). On the one hand physically based erosion models simulate the topographic effects during and after a single rainfall event while, on the other hand, landscape evolution models simulate the topographic development of a catchment as the effect of one (or more) landscape forming processes over thousands of years. In this thesis, two such models are applied to the study area in SE Spain (see section 1.7) and eventually combined in order to evaluate the effects of rainfall events on long-term landscape evolution. Moreover, using these models, the effects of human influence on erosion can be assessed, both in the long-term (millennia) and on the shorter term (decades). Separating human from natural erosion is important to appreciate the impact of human activities on the landscape and to be able to target erosion mitigation measures to human induced erosion instead of to natural erosion.

Therefore, the main objectives of this thesis are to get insight in (i) the time-scale gap between landscape dynamics (erosion and deposition) as a result of rainfall events on the one hand and over landscape evolution time-scales on the other hand; and (ii) the relative importance of natural processes versus human influence on landscape dynamics. The following research questions are divided according to the first objective; the second objective is addressed in chapters 2, 4 and 6 (see section 1.6. Thesis outline).

1. Long-term landscape evolution:
    a) What are the main processes and drivers of long-term landscape evolution in the research area?
    b) What is the relative importance of natural versus human influence on erosion and sedimentation dynamics over time?
    c) How large are erosion rates for different time periods?
    d) Can sequences of erosion and deposition be quantitatively modelled for the research area?
    e) Did tillage erosion contribute to long-term landscape development in the research area and can this be evaluated with a landscape evolution model?

2. Event-based erosion:
    a) Can typical Mediterranean storm events of different magnitudes of rainfall intensity and duration be modelled?
    b) How do these different magnitude storms contribute to total erosion?

3. Bridging the time-scale gap:
    a) Can results of an event-based and a landscape evolution model be compared?
    b) How can event information be incorporated into longer-term (e.g. centennial) landscape modelling?
    c) What are the effects of rainfall variability, extreme events and land use change on landscape evolution?

1.6. Thesis outline

This thesis comprises seven chapters, including this introduction. Chapters 2 to 6 form the core of this thesis (Fig. 1.1) and address the objectives and research questions presented in section 1.5. Because this thesis focusses more on differences in temporal scale (as opposed to spatial scale), the thesis chapters are related to temporal scales in Fig. 1.1. Usually, but not necessarily, smaller temporal scales go together with smaller spatial scales and vice versa.
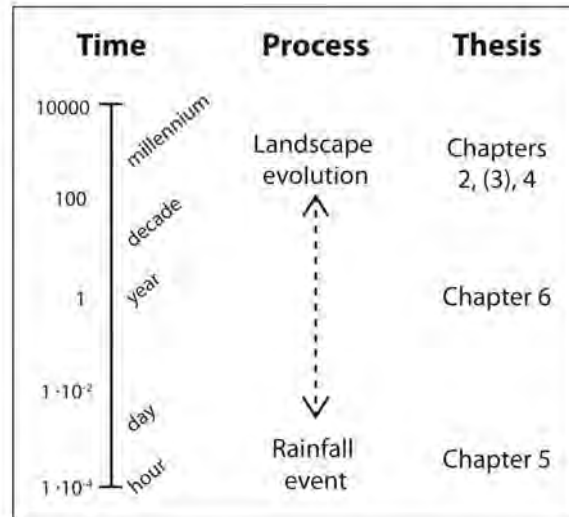
Fig. 1.1. Schematic outline of the core chapters of this thesis

In *Chapter 2*, the geomorphological background of the research area is investigated with the aim to get insight in the Late Pleistocene and Holocene landscape development. A schematic model of erosion and sedimentation dynamics is developed and the character (local or regional) of landscape forming factors are investigated (Question 1a). A tentative correlation between episodes of erosion and deposition and natural or human impact was made (Question 1b). From dated sediment archives, erosion rates were estimated for different time periods (Question 1c). In *Chapter 3* the originally hillslope-focused LAPSUS landscape evolution model is adapted to incorporate fluvial behaviour. The adapted model should be able to reproduce alternating aggradation and incision behaviour in a river floodplain area, which was tested by using an artificial DEM and experimental set-up. This addresses Question 1d in a theoretical way. Subsequently, in *Chapter 4* the adapted model is calibrated for the research area, thus quantitatively answering Question 1d. In this chapter the potential contribution of tillage erosion to observed erosion – sedimentation – erosion sequences is analysed on the millennial time-scale using the adapted LAPSUS model (Question 1e). The observed erosion and deposition sequences were derived from the geomorphological inventory described in chapter 2.

In *Chapter 5* the event-based soil erosion model OpenLISEM is used to simulate typical Mediterranean storms of different magnitudes of rainfall intensity and duration (Question 2a). Moreover, the relative contribution of these different magnitude storms to total erosion is explored (Question 2b). In *Chapter 6* the event-based OpenLISEM model and the landscape evolution model LAPSUS are compared (Question 3a). Based on this comparison, a way of incorporating event information into longer-term landscape evolution modelling is explored (Question 3b). Furthermore, the effects of rainfall

variability and extreme events are quantitatively evaluated and the effects of climate and land use changes are explored (Question 3c).

Finally, *Chapter 7* concludes with a synthesis of the findings of the previous chapters and general conclusions of the thesis. In addition, suggestions for further research are given in this chapter.

1.7. Study area

Research for this thesis was carried out in the semi-arid Guadalentín Basin (~3300 km^2), located in Murcia province, SE Spain. The research focused on the upper part of the Guadalentín river, upstream of the city of Lorca (Fig. 1.2; UTM 30N 614800; 4171000). In this section, the general characteristics of the study area are described; relevant specific information is given in each chapter. Starting with the Guadalentín, Velez and Torrealvilla rivers in chapter 2, chapter 4 focuses on the Rambla (Spanish for 'ephemeral river') Torrealvilla (~250 km^2), while chapters 5 and 6 zoom in to the Prado catchment (~50 km^2), which is a sub-catchment of the Torrealvilla (Fig. 1.2b).

Altitudes in the catchment range from ~300 to ~1500 meter above sea level. Current climate is semi-arid Mediterranean. Average annual precipitation is about 250 mm in the lower areas near Lorca to 530 mm in the northern mountains, with 75% of rainfall in spring (mainly April) and autumn (mainly October). Inter-annual variability of precipitation is high (Navarro Hervás, 1991). Average annual temperatures are ~17ºC, with lowest mean temperatures of 3 ºC and highest mean temperatures of 34ºC (Navarro Hervás, 1991). Evapotranspiration exceeds precipitation during most of the year, resulting in an annual moisture deficit (De Wit, 2001). Semi-natural vegetation in the research area consists mainly of natural shrubs (matorral, mainly *Stipa tenacissima*) and forest (*Pinus halepensis*). Land use is mainly dryland farming (cereals and almonds) and irrigated crops (olives, almonds, vines and horticultural crops). Dominant rock types in the area are limestone, calcarenite and conglomerates, with marls, sandstones and some conglomerates occurring mainly in the lower parts of the catchment (IGME, 1981). Dominant soil types are calcaric Cambisols, Regosols and Fluvisols, (petric) Calcisols, (petric) Gypsisols and Leptosols (LUCDEME, 1988, 1993).
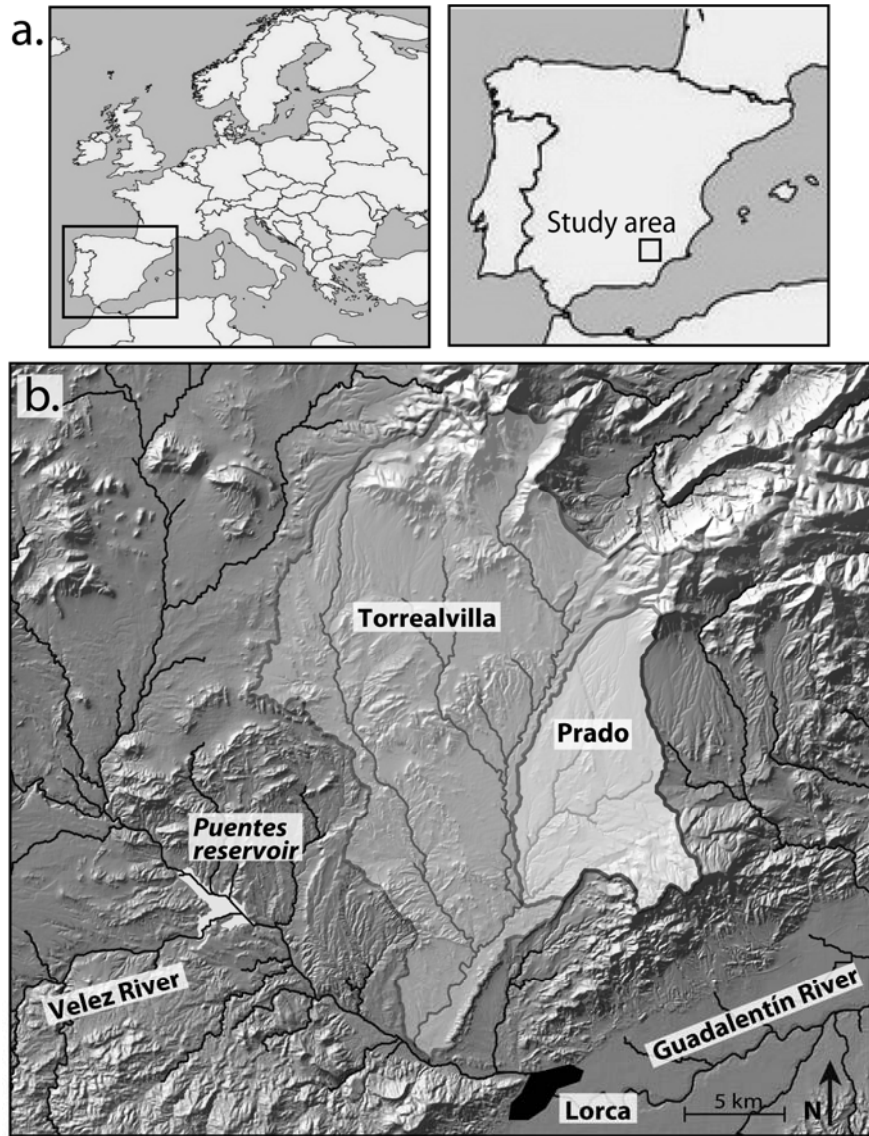
Fig. 1.2. a) Location of the research area in SE Spain; b) DEM of the research area with Guadalentín and Velez rivers indicated. The white area is the Puentes reservoir, the black area the town of Lorca. Black lines and grey shading delineate the Torrealvilla and Prado catchments.

1.8. Model descriptions

In this thesis, two different models are used: the event- and physically based OpenLISEM soil erosion model and the landscape evolution model LAPSUS. Of these two models, LAPSUS is the more synthesist, reduced complexity model, while OpenLISEM

incorporates more processes and is more inclined towards the reductionist type of models. In chapter 3 and 4, the LAPSUS model is adapted for and calibrated to the study catchment, respectively. In the chapter 5, the OpenLISEM model is applied to the study catchment. Finally, in chapter 6, the two models are compared. To avoid repeating model descriptions in these chapters, both models are introduced here.

1.8.1. The event-based OpenLISEM soil erosion model

The OpenLISEM model is a physically based runoff and soil erosion model, based on the original Limburg Soil Erosion Model (LISEM; De Roo et al., 1996b, Jetten and De Roo, 2001). It simulates runoff and erosion during and immediately after a rainfall event. Fig. 1.3 shows a modelling scheme for the OpenLISEM model.

Following a standard surface water balance, OpenLISEM first calculates the net precipitation by subtracting the actual interception storage, based on canopy storage functions as described in De Jong and Jetten (2007). Subsequently the infiltration rate is calculated by a one-layer Green and Ampt, based on a direct use of the Darcy equation for one-dimensional flow (Kutílek and Nielsen, 1994). There is no need for an iterative estimation of time to ponding as the model time step is very short (15 s). The infiltration rate q (in m s^{-1}) is calculated as:

$$q = -K_{sat}\left(\frac{dh}{dz} + 1\right) = -K_{sat}\left(\frac{d-h}{L} + 1\right) \qquad \text{Eq. 1.1}$$

with K_{sat} the saturated hydraulic conductivity (m s^{-1}); L the depth of the wetting front (m) calculated as the cumulative infiltration (m) divided by the available soil storage (m^3 m^{-3}); h the negative matrix suction at the wetting front (m); and d the overpressure depth of the water layer at the soil surface (m). The infiltration cannot exceed the soil depth in case of impermeable sub soils so that saturation overland flow is eventually generated when the soil storage is exceeded. The model considers different sub-pixel surfaces such as fraction of crusted, compacted or impenetrable surfaces, or grass strips, for which separate infiltration calculations can be done. In case of runoff, OpenLISEM assumes that the micro roughness causes not only surface storage (Kamphorst *et al.*, 2000), but also determines the flow width through a fraction of the grid cell that is ponded and hydraulic radius if there is ponding.

The flow width is calculated form the surface roughness using the empirical equation (Jetten and De Roo, 2001):

$$w = dx \cdot f_{pa} = dx \cdot \left(1 - e^{-1.875d/RR}\right) \qquad \text{Eq. 1.2}$$

23
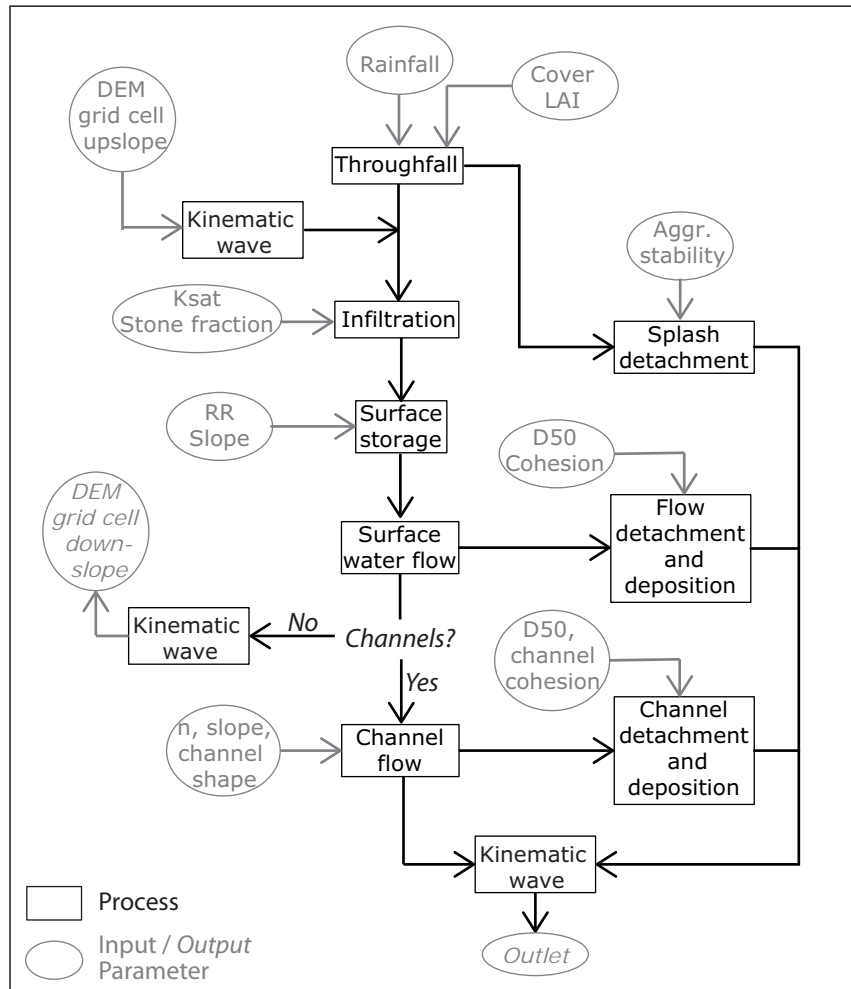
Fig. 1.3. OpenLISEM modelling scheme.

with *w* flow width (m); f_{pa} fraction of ponded area (-); *d* the depth of the runoff water (m); and *RR* the standard deviation of micro roughness surface heights (m). Runoff water is routed with an implicit solution of the kinematic wave (Chow *et al.*, 1988). In case of natural or artificial channels the stream flow is routed with its own kinematic wave, determined by the channel dimensions, roughness and bed slope. Infiltration in channel beds is possible, but once water has entered a channel it cannot leave it, in other words there is no flooding possibility in OpenLISEM.

Sediment is generated by rainfall splash detachment and detachment by overland and channel flow. Splash detachment D_s (kg s^{-1}) is based on rainfall kinetic energy (Van Dijk, 2002) multiplied by an empirical aggregate stability factor based on splash tests:

$$D_s = \left(\frac{2.82}{As} \cdot KE \cdot e^{-1.48d} + 2.96\right) \cdot P_{net} \cdot \frac{dx^2}{dt} \qquad \text{Eq. 1.3}$$

With *As* the soil aggregate stability from the Lowe drop test (kg J^{-1}); *KE* the rainfall kinetic energy (J m^{-2} mm^{-1}); *d* the depth of the surface water layer (mm); P_{net} net precipitation (mm); dx^2 grid cell surface; and *dt* the time step (s). The model accounts for fractions of the grid cell covered by vegetation or that are ponded.

Flow detachment, sediment transport and deposition are calculated with a streampower based transport capacity equation (Govers, 1990; see also Morgan *et al.*, 1998):

$$TC = \rho \cdot Cl \cdot (\omega - \omega_c)^{Dl} = \rho \cdot Cl \cdot (S \cdot V - 0.004)^{Dl} \qquad \text{Eq. 1.4}$$

With *TC* the transport capacity (kg m^{-3}); ω and ω_c the unit streampower and critical unit streampower (m s^{-1}); *S* slope gradient (m m^{-1}); ρ the particle density (2650 kg m^{-3}); *V* mean flow velocity (m s^{-1}); and *Cl* and *Dl* empirically derived coefficients, depending on the texture median (*D50*) of the upper soil layers. Sediment from splash detachment is added to the amount of sediment in transport. It is assumed that the flow will cause detachment (*Df* in kg s^{-1}) as long as the transport capacity *TC* is larger than the concentration of the suspended sediment *C* (kg m^3), while a soil strength factor has to be overcome (based on cohesion):

$$Df = Y \cdot (TC - C) \cdot Q \qquad \text{Eq. 1.5}$$

with *Y* the detachment efficiency based on the reverse of the soil cohesion (Morgan *et al.* 1998, see below) and *Q* the discharge (m^3 s^{-1}). Deposition (*Dp* in kg s^{-1}) occurs whenever the transport capacity is less than the total suspended sediment in flow:

$$Dp = w \cdot dx \cdot v_s \cdot (TC - C) \qquad \text{Eq. 1.6}$$

with *w* width of flow (m) and v_s settling velocity of the particles (m s^{-1}).

It is important to note that the same equations are used for overland flow and for channel flow, where a separate stream power is calculated based on channel velocity and bed slope.

1.8.2. The LAPSUS landscape evolution model

Landscape evolution model LAPSUS (Landscape Process Modelling at Multi-Dimensions and Scales) is a reduced complexity model, based on early works of Kirkby (1971, 1986) and Foster and Meyer (1972) and is described in detail in Schoorl *et al.* (2000, 2002). To ensure wide applicability of the model, mathematical descriptions of the processes have been formulated to use a limited amount of input data and to represent annual averages. The original model simulates erosion and deposition by overland flow. Model development started with programming, validation and calibration in Spain (Schoorl *et al.*, 2000, 2002, 2004, Schoorl and Veldkamp, 2001). In later versions of the model more processes were added: biological and frost weathering, tectonics, soil creep, vegetation effects and solifluction (Temme and Veldkamp, 2009), tillage erosion (Schoorl *et al.*, 2004, Heuvelink *et al.*, 2006), landsliding (Claessens *et al.*, 2005, 2006a,b, 2007a,b, 2009, 2010, Keijsers *et al.*, 2011) and saturated overland flow (Buis and Veldkamp, 2008). In addition, issues of DEM resolution and the treatment of pits and sinks in the landscape have been investigated (Temme *et al.*, 2006). The model has been used in regional nutrient balance studies in Africa (Haileslassie *et al.*, 2005, 2006, 2007), to investigate phosphor pathways in the Netherlands (Sonneveld *et al.*, 2006) and to assess the role of connectivity, agricultural terraces and land abandonment on erosion dynamics (Lesschen *et al.*, 2007, 2009). Fig. 1.4 shows a methodological scheme of the LAPSUS model.

Water, sediment flux and transport capacity is routed using the multiple flow algorithm (Freeman, 1991, Quinn *et al.*, 1991, Holmgren, 1994):

$$F_i = \frac{(\Lambda)_i^p}{\sum_{j=1}^{\max 8}(\Lambda)_i^p}$$
Eq. 1.7

where fraction F_i of flow out of a cell in direction i, is equal to the slope gradient Λ (tangent) in direction i, to the power of convergence factor p, divided by the summation of Λ for all (maximum eight) downslope neighbouring cells j, to the power of convergence factor p.

For sediment transport, continuity of transport and conservation of mass principles apply. For each cell sediment transport capacity C (m³ a⁻¹) is calculated (Eq. 1.8) as a function of discharge Q (m³ a⁻¹) and tangent of slope Λ (Kirkby, 1971):

$$C = \alpha \cdot Q^m \cdot \Lambda^n$$
Eq. 1.8

with discharge exponent m, slope exponent n and variable α the constant for unit conversion. Transport capacity C is compared to the incoming amount of sediment in transport S_0 (m³ a⁻¹) to calculate the amount of sediment S (m³ a⁻¹) that is actually transported:
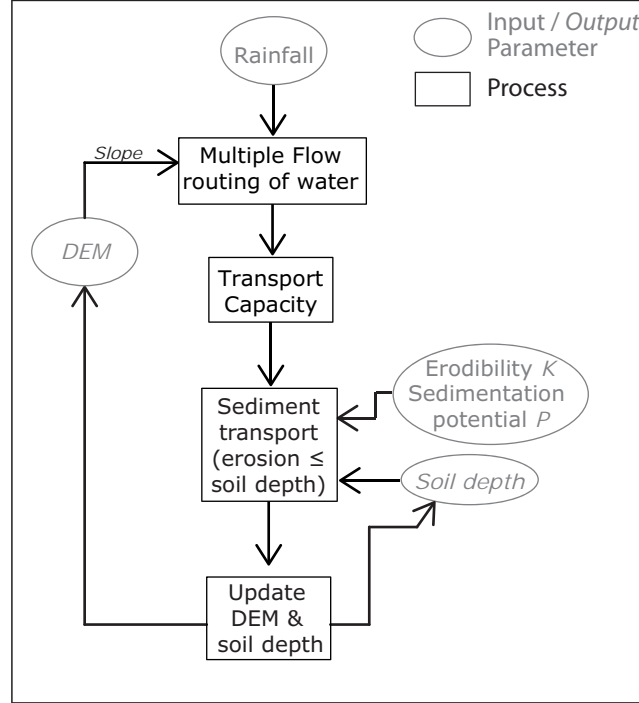
Fig. 1.4. LAPSUS modelling scheme.

$$S = C + (S_0 - C) \cdot e^{-dx/h} \hspace{4cm} \text{Eq. 1.9}$$

with dx the cell size (m). Term h (m) refers to the transport capacity divided by the detachment capacity (D; m^2 a^{-1}) in case of erosion, and transport capacity divided by settlement capacity (T; m^2 a^{-1}) in case of sedimentation:

$$D = K \cdot Q \cdot \Lambda \hspace{5cm} \text{Eq. 1.10}$$

$$T = P \cdot Q \cdot \Lambda \hspace{5cm} \text{Eq. 1.11}$$

where K (m^{-1}) is an aggregated surface factor representing the erodibility (the ease to erode) of the surface. P (m^{-1}) is a similar factor for sedimentation potential. These lumped factors include the effects of vegetation. A high K-factor indicates that sediments are easily eroded (e.g. little vegetation) and a low K-factor means low erodibility. A high P-factor means that sediments are easily deposited, while a low P-factor keeps sediment in transport longer. Note that a high P-factor does not necessarily mean high sedimentation; sedimentation depends on the amount of sediment in transport and thus indirectly also on e.g. the K-factor. If erodibility is low, there may be little sediment in transport and little sediment deposited, even if sedimentation potential P is high.

27

Chapter 2

Unravelling Late Pleistocene and Holocene landscape dynamics

Landscapes in SE Spain have developed in response to tectonics, climate fluctuations and, more recently, human activity. Fluvial and colluvial sediments in the valleys reflect a complex interplay between landscape forming processes. Investigating these sediment archives, we reconstructed landscape evolution for the Upper Guadalentín Basin, SE Spain, placing recent erosion processes in a landscape evolution context. Palaeo-lake sediments dated between ~17 and ~13.8 ka form evidence for a Late Glacial lake. Differences in relative height above the floodplain and age between the river terraces of parts of the Guadalentín river indicate that they have not been in equilibrium in the Late Quaternary. Deposition of river terraces along the upstream part of the river is recorded at ~13 and ~9.5 ka, whereas no evidence of deposition is found for that period along the lower part of the river. There, episodes of sedimentation occur at ~7.5–5 ka, ~3.4, ~1.6, ~0.7 and ~0.4 ka. This discrepancy is explained by the palaeo-lake and its influence on erosion and sedimentation processes through base level changes. We propose a schematic model of Late Pleistocene and Holocene landscape evolution. Correlation of erosion and sedimentation episodes with climate change and human impact is discussed. There is strong evidence that climate was not the main driver of landscape processes. We suggest that internal dynamics and local processes are more important drivers for landscape dynamics in the Upper Guadalentín Basin than external and regional factors.

2.1. Introduction

Landscapes in south-eastern Spain have developed in response to tectonics, climate fluctuations and, more recently, human activity. Fluvial and colluvial sediments are found in the form of river terraces and pediments. Studying these sediments reveals complex sequences of erosion and deposition varying in time and space (e.g. Temme *et al.*, 2008). Driving forces of sedimentation and erosion can be external (e.g. tectonics, climate) or internal (e.g. complex response; Schumm, 1981) and can have a regional or more local character. By correlating episodes of sedimentation and erosion to past climate fluctuations and human impact on the land, insight can be gained into the relative influence of both factors on landscape dynamics (Faust *et al.*, 2004; Gellis *et al.*, 2004; Houben *et al.*, 2009). We used a multi-scale system-approach (Veldkamp *et al.*, 2001; Temme *et al.*, 2008) to reconstruct dynamic landscape formation and evaluate its most important agents in the semi-arid region of the Guadalentín Basin in SE Spain.

Research in this area has focussed on current processes such as gully dynamics as a result of intense rainstorms (Vandekerckhove *et al.*, 2000; Bull *et al.*, 2000), channel morphology (Hooke and Mant, 2000; Hooke *et al.*, 2005), hillslope erosion (Cammeraat, 2004; Bracken and Kirkby, 2005), the impact of land cover and land use (Kirkby *et al.*, 2002) on erosion dynamics and land degradation and desertification (Onate and Peco, 2005; Van Wesemael *et al.*, 2006). These recent processes have not, up to now, been placed in the larger context of landscape dynamics. However, this is necessary if the objective is to get insight in longer term process dynamics which may have time-lags of thousands of years between cause and effect (e.g. Temme and Veldkamp, 2009). Appropriate time-scales for such a study would range from 0.1 to 10 ka, i.e. between recent erosion processes (years–decades) and landscape evolution (10–1000 ka). Processes of Holocene erosion and sedimentation in the context of natural climate fluctuations and/or human influences are described for the Lower Guadalentín river (Calmel-Avila, 2000; Silva *et al.*, 2008), forming a reference for our study on the Upper Guadalentín river and the Lorca Basin.

The objectives of this chapter are 1) to get insight into Late Pleistocene and Holocene landscape development in the study area, in particular sedimentation and erosion dynamics and to develop a schematic model for these processes; and 2) to determine which drivers have been and still are most important for landscape formation and whether they have a local or regional character; and 3) to assess the relative importance of natural versus human influence on erosion and deposition processes over time.

2.2. Study area

The Guadalentín Basin (~3300 km^2) is located in Murcia Province, south-east Spain. Our study area is restricted to the upper part of the Guadalentín river, upstream of the city of Lorca (Fig. 2.1; UTM 30N 614800; 4171000). Research is conducted along this stretch of the river and along three of its tributaries: the Rambla Torrealvilla and Rambla Estrecho ('rambla' meaning gully or ephemeral river in Spanish), draining the Lorca Basin, and the Velez river, one of the rivers upstream of the 'Puentes' reservoir. Additionally, observations are available from north of the Puentes reservoir along small ramblas draining directly into the reservoir.

General characteristics of the study area are described in section 1.7. Geologically, the area is located in the Betic Cordillera, an NE–SW oriented alpine orogenic belt, resulting from the ongoing convergence of the African and Iberian plates. The Lorca-Alhama Fault (LAF) is located at one side of the active graben known as the Guadalentín Depression (Fig 2.1b). The LAF formed from the Late Neogene to the present as part of the Eastern Betic Shear Zone (EBSZ; Silva *et al.*, 2008). Left-lateral slip (8–20 km) is recorded from the Messinian to the present (Silva *et al.*, 1997), as well as significant tectonic uplift of ≥ 0.08 m ky^{-1} during the Quaternary (Silva *et al.*, 2003). The Lorca Basin is a Neogene intramontane depression (Thrana and Talbot, 2006). Dominant rock types are limestones and dolomite, marl, sandstone, conglomerates and calcarenite, while some schists and phyllites occur (IGME, 1981; Geel and Roep, 1998).

Late Pleistocene and Holocene landscape evolution has been studied relatively sparsely for the Guadalentín Basin. Schütt (2006) made three corings in an alluvial fan in the north-western part of the Guadalentín Basin. Using radiocarbon dating on charcoal pieces and chemical analysis of the sediments, Schütt (2006) made a first reconstruction of local environmental conditions from the Late Glacial to recent times. Benito and Thorndycraft (2005) and Benito *et al.* (2008, 2010) reconstructed the magnitude and frequency of palaeo-floods using geological evidence such as slackwater flood deposits and silt or scour lines for the Rio Guadalentín, upstream of the Valdeinfierno reservoir. Calmel-Avila (2000) identified phases of erosion and sedimentation over the past 10 ka for the lower Guadalentín (near Librilla), and analyzed the role of natural and human induced processes. Silva *et al.* (2008) analysed in detail the aggradation and dissection phases of the Lorca Fan; i.e. the alluvial fan on which Lorca is situated and which forms the transition from our study area to the Guadalentín Depression (Fig 2.1b). For surrounding basins in SE Spain, studies covering Quaternary landscape evolution include Harvey *et al.* (1999; Cabo de Gata ranges); Mather *et al.* (2002; Sorbas Basin); Schulte (2002; Vera Basin); Schoorl and Veldkamp (2003; Malaga Basin); and Schulte *et al.* (2008; River Aguas).
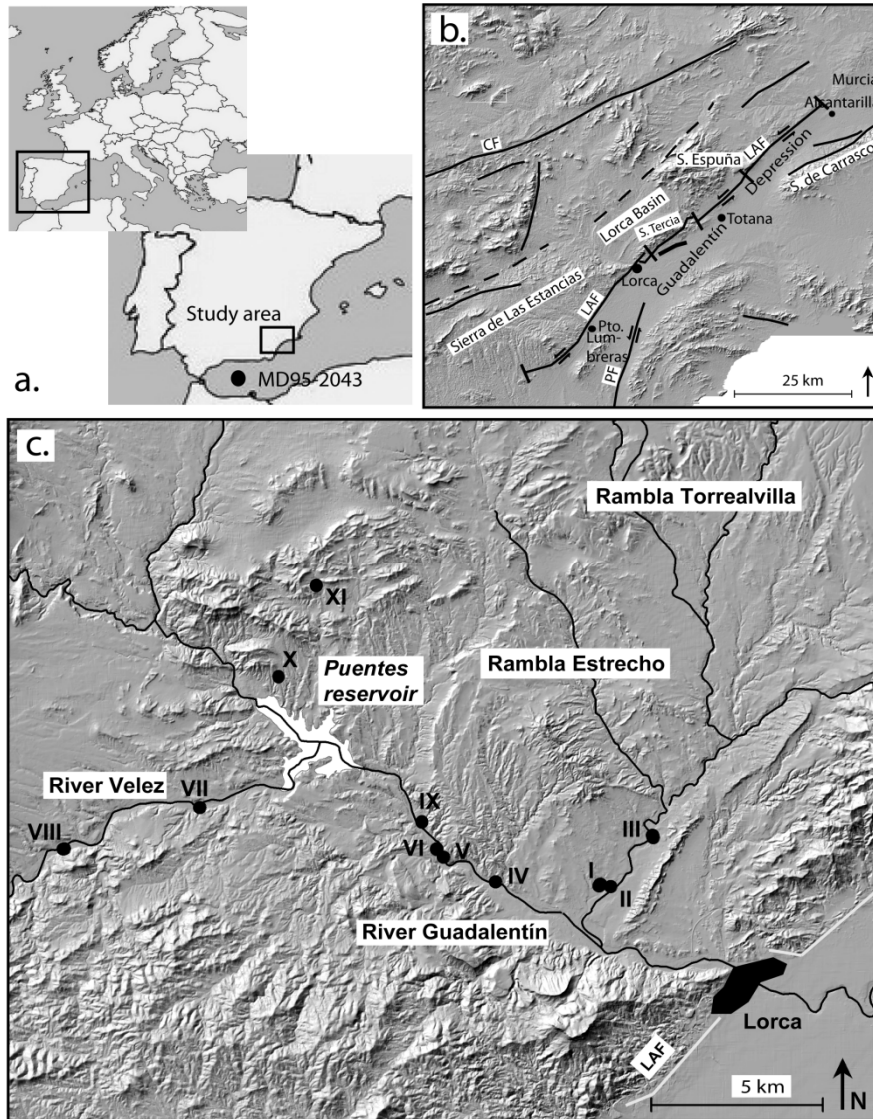
Fig. 2.1. Location of study area with a). Location in Spain; b). Geological setting of the Lorca region; LAF=Lorca-Alhama Fault; CF=Carrascoy Fault; PF=Palomares Fault and c). Upper Guadalentín Basin; Black dots indicate OSL/Radiocarbon sampling sites. White lines are faults.

2.2.1. Palaeo-climate in SE Spain

Terrestrial records of palaeo-climate in the region are based on fragmented pollen analyses (Jalut *et al.*, 2000; Zazo *et al.*, 2008; Jalut *et al.*, 2009; Carrión *et al.*, 2010). Two marine cores are available from the Alboran Sea; core ODP-977A (Martrat *et al.*, 2004) and core MD95-2043 (Cacho *et al.*, 2001; Fig 2.1a). Retrieved from this latter core (Cacho *et al.*, 2001; Cacho, 2006), sea surface temperature (SST) fluctuations can be used as a proxy for moisture regime. Although not confirmed and under debate, Mediterranean geomorphic change may have responded more to change in precipitation than in temperature (Bridgland and Westaway, 2008; Zielhofer *et al.*, 2008).

Already from the onset of the Holocene, SE Spain experienced a semi-arid Mediterranean climate (Jalut *et al.*, 2000; Zazo *et al.*, 2008), and Pantaleon-Cano *et al.* (2003) deduce four main phases: i) from 18 000–15 000 cal y BP, the area was relatively warm and humid with deciduous and evergreen *Quercus* and *Pinus* vegetation; ii) between 15 000–7 000 cal y BP, the pollen record shows a decrease in arboreal pollen and an increase in steppe-type plant species. At Padul, a clear climatic amelioration is recorded at 13 000 y BP (Pons and Reille, 1988), which can also be seen in the SST reconstruction; iii) the Holocene Climatic Optimum lasted from ~7000 to ~5000 cal y BP with a reduction of steppe type plant species and an increase of shrubs and arboreal pollen. This phase is recognised by Carrión *et al.* (2010) as the mesophytic optimum / xerophytic minimum with lowest fire activity and (local) high lake levels; and iv) from 5000 cal y BP, a radical change is recognised which marked the onset of the definite installation of steppe vegetation (Zazo *et al.*, 2008), also displaying increased fire activity (Carrión *et al.*, 2010). This radical change is not well visible in the reconstructed SST, although a drop in SST is visible slightly earlier (around 6 ka).

2.2.2. Human occupation in SE Spain and Lorca

Human occupation of SE Spain started as early as at least 7.5 ka BP. However, the impact of this early occupation on the land in terms of erosion is limited. Therefore, the occupation history since Roman times is outlined here. In 209 BC, Romans invaded SE Spain at Carthago Nova (modern Cartagena; Orejas and Sánchez-Palencia, 2002). Lorca functioned as a regional agricultural and craft market (Pérez Asensio, 2007). More than 45 large or medium-sized rural sites and many small villages have been identified in the municipality of Lorca (Orejas and Sánchez-Palencia, 2002). From the 3rd century AD, population was spread over the country mainly in large rural *villae rusticae* (Pujante Martínez, 2002). The rural areas comprised of arable fields, often irrigated and mostly in the valleys, some vineyards and olive groves, a vast area of pastoral land on the slopes bordering the Guadalentín valley and residual and degraded forest on the higher slopes of the Sierra Espuña and Carrascoy (Calmel-Avila, 1998). In Roman as well as in Arabic times, irrigation schemes were widely improved and enlarged (López-Bermúdez *et al.*, 2002).

With the decline of the Roman Empire around ~350 AD, intensity of agriculture as well as maintenance of its structures decreased.

Arab rule started in 713 AD in the Lorca area. Villages were prominently situated on fluvial terraces or near springs (Pujante Martínez, 2002). Vita-Finzi (1969) reports Arab irrigation works underlying 8 m of alluvium in the Guadalentín valley. Population grew, especially in the 9th to 13th centuries, and agriculture intensified with the development of irrigation techniques (Calmel-Avila, 1998). Contrary to the Roman period, when only the best lands were used, in the Arab period an exploding population had to be fed (Calmel-Avila, 1998). New territories were put in cultivation. Remarkably, the increased population pressure did not result in increased erosion, according to Calmel-Avila (1998). She attributes this to the more skilled agricultural techniques used. In 1244 Lorca was recaptured by Christians and located on the frontier with the Arab territory. Because of insecurity, rural population decreased dramatically from 18 to 2.5 habitants per km^2 (Calmel-Avila, 1998). During the 13th and 14th centuries, the territory of Lorca was virtually free of agriculture and nearly uninhabited, except for a small area surrounding the town (López-Bermúdez *et al.*, 2002). Livestock breeding was more flexible than agriculture. In an effort to repopulate the area, locals were allowed to cut every tree except when it carried fruits, resulting in heavy deforestation in the nearby Sierra the Carrascoy (Calmel-Avila, 1998). This social-political and economical crisis lasted from the 13th to 15th centuries. During the 16th and 17th centuries, a slow expansion of agriculture occurred, mainly in the valley close to Lorca town and on the nearby hillslopes (López-Bermúdez *et al.*, 2002). The 18th century marked a change in land use around Lorca with mostly dryland farming (cereals) and an increase in population (López-Bermúdez *et al.*, 2002). These authors further describe the land use changes over the last centuries in the Guadalentín Basin, which are of less importance for the present chapter.

2.3. Methods

2.3.1. Fieldwork

An inventory of sediments was made along the Guadalentín river and three of its tributaries: the Velez river, Rambla Torrealvilla and Rambla Estrecho (Fig. 2.1c). Presence of gravel layers, imbrication and stratification, colluvial deposits overlying gravel layers, and thickness of the gravel layers were investigated. If visible, the base of the gravel layer was recorded using a GPS (Garmin eTrex Legend); if not, its top was recorded.

2.3.2. Reconstruction of floodplain profiles

To calculate the relative height of river terrace levels, the floodplain of the river was reconstructed by smoothing a trendline through the distance–height profiles of the rivers (Fig. 2.2). For the Guadalentín and Velez rivers, an exponential trendline fitted best (Eq. 2.1), while for the Ramblas Torrealvilla and Estrecho, polynomial smoothing was applied (Eq. 2.2).

$$H = a \cdot e^{(b \cdot D)} \qquad\qquad\qquad \text{Eq. 2.1}$$

$$H = c \cdot D^2 + d \cdot D + e \qquad\qquad\qquad \text{Eq. 2.2}$$

With H = (absolute) height (m); D = distance along the floodplain (km) from a zero-point which was chosen at the upstream edge of the city of Lorca; and a to e river-specific regression constants. Parameter values given in Fig. 2.2 are valid for D between 0 and 12.5 km for the Guadalentín river and D between 15.8 and 25 km for the Velez river. Between 12.5 and 15.8 km, the height of the Guadalentín/Velez river is not recorded because of the presence of the reservoir. The two profile lines would connect at an angle, suggesting a geological barrier (bedrock step), possibly where the Puentes reservoir dam is located.
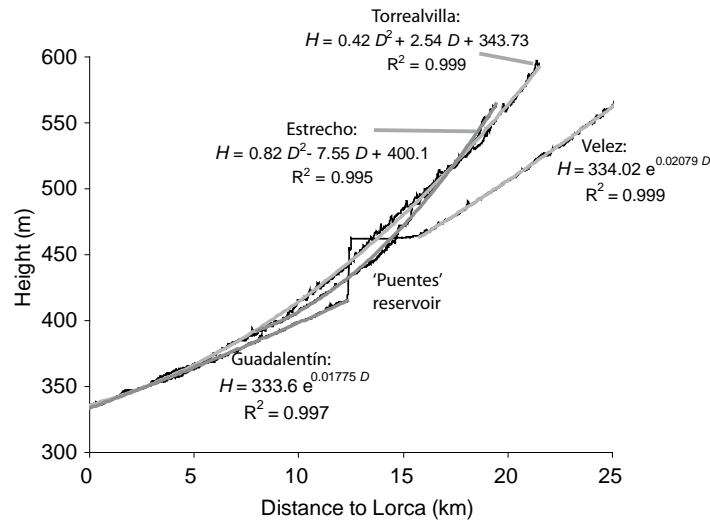

Fig. 2.2. Height profiles of reconstructed floodplains of the Guadalentín river, Velez river and Ramblas Torrealvilla and Estrecho. Parameters and correlation coefficients are indicated for the trend lines (grey lines).

2.3.3. Chronological control

To determine the timing and deduce rates of sediment deposition, sediment samples were taken for Optically Stimulated Luminescence (OSL) dating. In addition, charcoal fragments encountered in the terrace sediments were sampled for AMS radiocarbon dating. A total of 26 dating samples were taken at 11 locations (Fig. 2.1). For some of these locations, both OSL and radiocarbon dating could be applied, offering the opportunity to check the consistency of dating results obtained by the two independent methods.

Optically Stimulated Luminescence (OSL) dating
The OSL signal of quartz grains is erased upon light exposure and builds up after burial due to ionizing radiation from the surrounding sediments and a small contribution from cosmic rays. Thereby the method determines the time of deposition and burial of the sediments, provided that light exposure prior to burial is sufficient to reset the OSL signal of at least part of the grains (e.g. Wallinga, 2002; Rittenour, 2008). To obtain an OSL age, two quantities need to be determined: i) the amount of ionizing radiation received by the sample since the last exposure to light; the equivalent dose (D_e, Gy); and ii) the millennial radiation dose the sample is exposed to in its natural environment; the dose rate (DR, Gy ka^{-1}). The age is then obtained through (Eq. 2.3):

$$Age \ (ka) = \ D_e \ /DR \qquad \text{Eq. 2.3}$$

Thirteen OSL dating samples were taken at five sites (Figs. 2.1 and 2.3) from coarser parts of the sediments. Sand-sized grains are preferred for analysis as this allows detection of heterogeneous bleaching of the sediments (e.g. Duller, 2008). Metal cores (diameter ~10 cm; length ~50 cm) were hammered into the sediment; sealed and transported to the laboratory. Outer parts were removed under subdued orange light and used for dose rate determination, while inner parts were used for determination of the equivalent dose. Detailed information on applied procedures and OSL properties of the samples is provided in the Appendix to this chapter (p. 56-64).
Single-aliquot equivalent dose distributions of all samples showed significant scatter, likely due to limited light exposure during fluvial transport. Taking the mean value would result in OSL ages that overestimate the burial age. To overcome this problem, we applied the Finite Mixture Model of Roberts *et al.* (2000), using an overdispersion parameter of 10% (based on Rodnight *et al.*, 2005), and selecting the number of components with the lowest BIC value. We assume the lowest component to reflect the burial dose, apart from sample NCL-2108074 where the lowest component only contained some rogue low outliers.

For this sample the second component was used. Based on the equivalent-dose distribution, the percentage of single-aliquot equivalent dose estimates attributed to the lowest component, and the consistency of OSL dates at a site, we provide an estimate of the validity of each OSL age.

Radiocarbon dating
Charcoal fragments were radiocarbon dated using the Accelerator Mass Spectrometer (AMS) at the Centre for Isotope Research, University of Groningen, the Netherlands (Gottdang *et al.*, 1995). Conversion of ^{14}C years BP to calibrated years BP was done using the IntCal04 calibration curve (Reimer *et al.*, 2004) and the WinCal25 calibration program.

2.4. Results

We found three types of sediments in the study area; river terrace sediments, slope deposits and lake sediments. These are described below, followed by the results of OSL- and radiocarbon dating. Finally, for some of the sites, sedimentation rates are derived.

2.4.1. River terrace sediments

Correlation of relative heights above the floodplain for observation points with gravel resulted in several river terrace levels along the Guadalentín and Velez rivers as well as along the Ramblas Torrealvilla and Estrecho (Figs. 2.4 and 2.5; Table 2.1). Within the same terrace level, stratigraphical and spatial correlation was based on sediment characteristics such as stoniness, texture, colour and strata-transitions (see Fig. 2.5 for an example of three profiles along the Rambla Torrealvilla). Observation points were correlated (lines in Fig. 2.4) when they had a distinct river terrace morphology, i.e. stratified gravel with overlying finer sediments for the lower terraces (Fig. 2.5) and distinct gravel bands in between other material for the higher terrace levels. In the Guadalentín river and the Rambla Torrealvilla, some observations of gravel ('higher terrace deposits' in Fig. 2.4) could not be correlated to form one distinct level. For the Velez river, even more observations are encountered that do not form a distinct level ('other gravel' in Fig. 2.4).
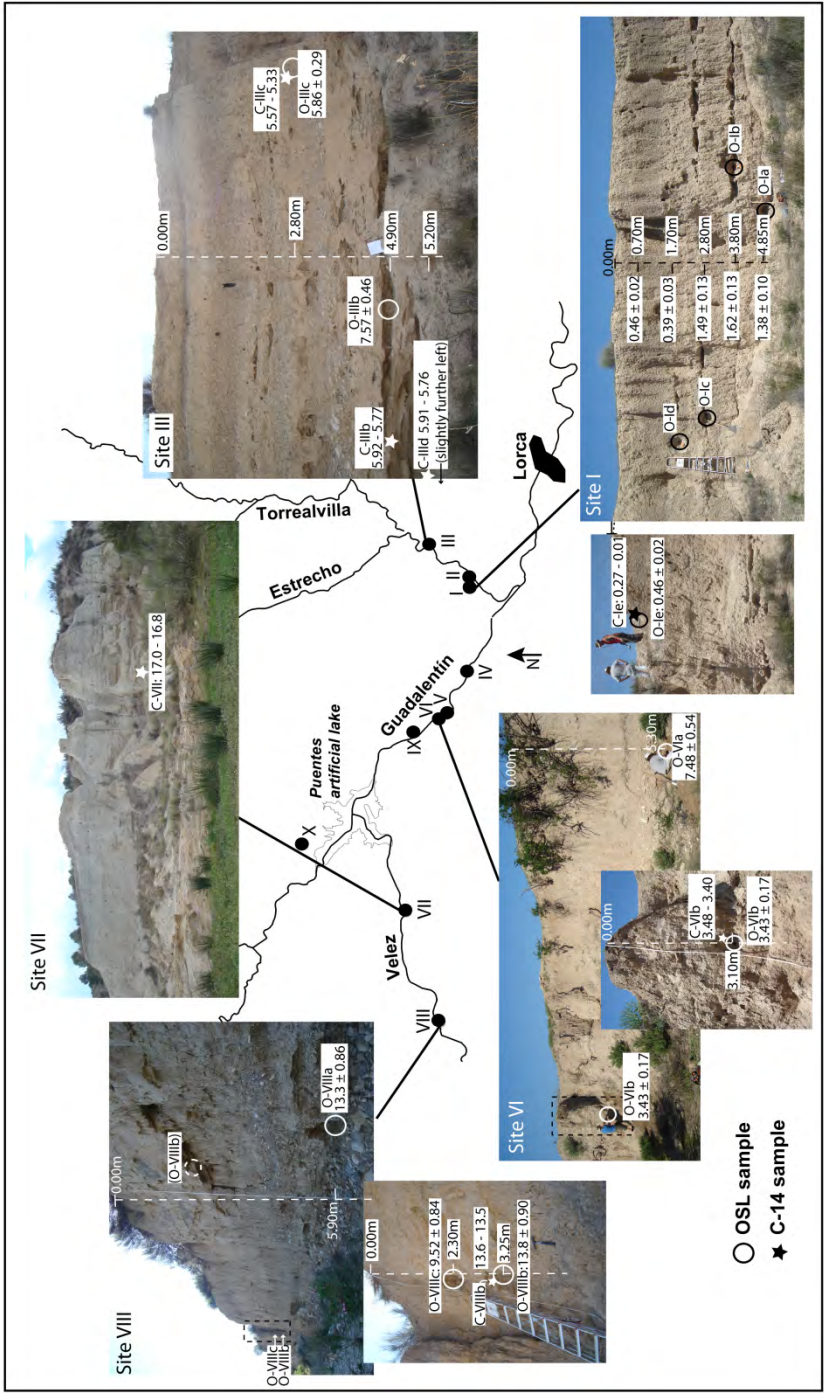
Fig. 2.3. Sampling sites for OSL and radiocarbon dating; outcrops shown for sites I, III, VI, VII and VIII. Samples codes explained in text and given in Tables 2 and 3. Ages are given in ka (OSL) and cal ka BP (AMS).
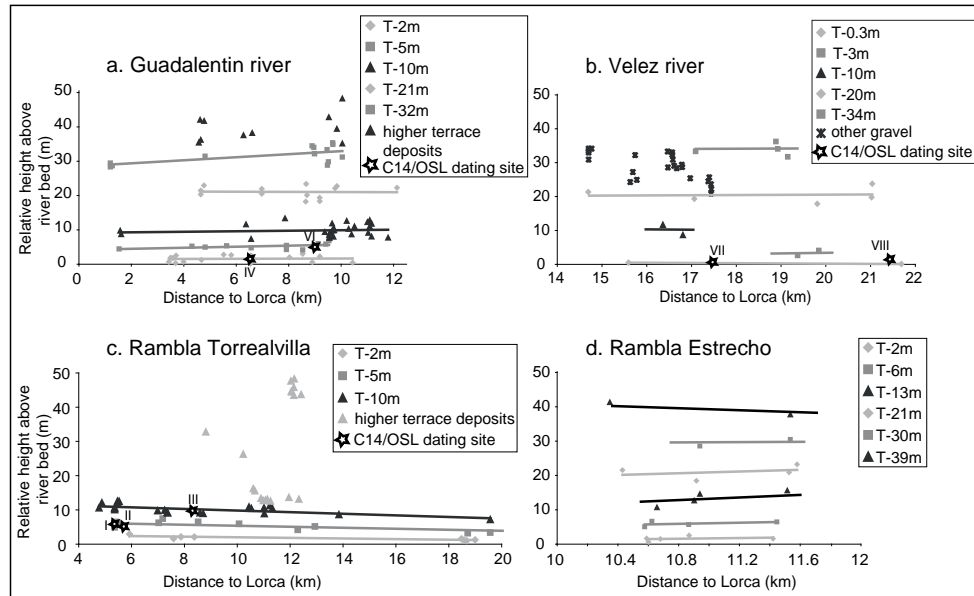
Fig. 2.4. River terrace levels: relative heights (m) above floodplain for the a). Guadalentín river, b). Velez river, c). Rambla Torrealvilla and d). Rambla Estrecho. Note differences in scale of x-axis. Sampling sites for radiocarbon/OSL dating indicated with star and roman numbers. Terrace levels are labelled after their average relative height (see Table 2.1).

Average heights of the river terraces (Table 2.1) correlate well between the Guadalentín river and Ramblas Torrealvilla and Estrecho, but not for the Velez river. In general, the higher levels show steps of approximately 10 m vertical distance between each level. The lower levels do not follow this trend.

Table 2.1. Average relative height (m) above floodplain of river terrace layers for the Guadalentín river and three tributaries (the Velez river, Rambla Torrealvila and Rambla Estrecho)

Guadalentín river	Velez river	Rambla Torrealvilla	Rambla Estrecho
2	0.3	2	2
5	3	5	6
10	10	10	13
21	20	-	21
32	34	-	30
-	-	-	39

River terrace levels are named after their relative height, where the stretch of the river will be indicated if applicable; i.e. T-2m (Rambla Torrealvilla) for the 2 m terrace level of the Rambla Torrealvilla. Profiles of the lowest terrace level (T-2m) consist completely of

coarse-grained, fluvial material. Profiles belonging to the T-5m (Rambla Torrealvilla) all show a succession of coarse gravel layers, finer, non-layered strata, coarse gravel and again finer, non-layered sediments (Fig. 2.5). Profiles belonging to T-10m (Rambla Torrealvilla) also show an alternation of coarse and fine fluvial strata and colluvial sediments. The profiles encountered directly north of the Puentes reservoir are small and located in protected positions related to narrow reaches between bedrock outcrops. They show fluviatile and slope deposits directly over marl bedrock, with in one case sands and coarse subrounded gravels over stratified marl, and course, imbricated, clast supported gravel, overtopped with sandy and silty slope deposits in the other profile.
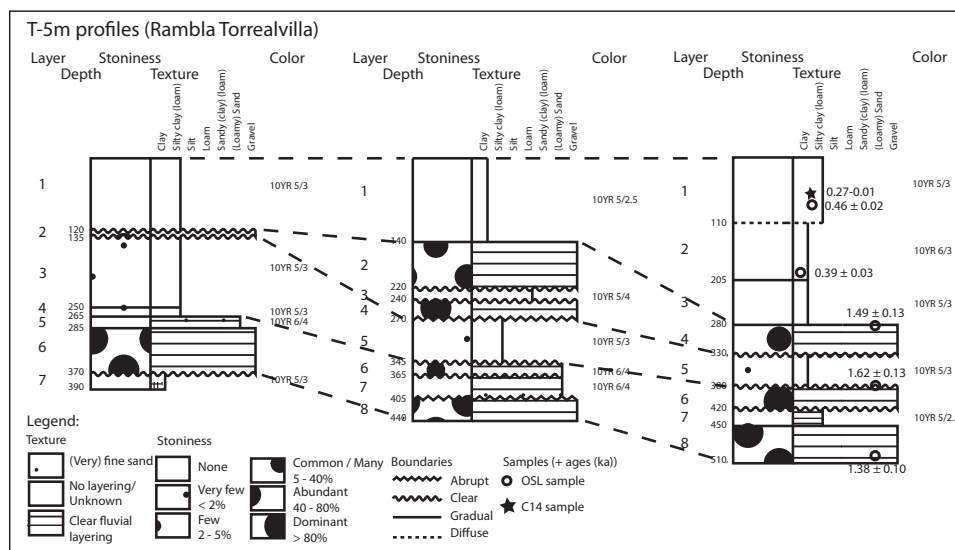
Fig. 2.5. Example of schematic profile descriptions for three profiles of terrace level T-5m (Ramble Torrealvilla) with sediment layers, depth (cm), stoniness, texture and colour. OSL and radiocarbon sampling location and ages (ka) are indicated.

2.4.2. Lake and delta sediments

Along the Guadalentín river, from about 10 km upstream of Lorca, finely laminated sediments are encountered (Fig. 2.6a,b), deposited directly on top of coarse gravels (Fig. 2.6g). Layers consisting of remnants of carbonate-coated roots or stems occur in these laminated sediments (Fig. 2.6e). Upstream along the Velez river, thick packages of gravel are found as well as finely layered deposits consisting of very fine silty to coarser sand and gravel material (Fig 2.6e). At one side, ridges are found with flat tops consisting of layered carbonate accumulations standing out in the present landscape (Fig. 2.6d,f). Two levels of these ridges are observed, at ~470 and ~490 m above sea level. The 490-m contour line (grey line in Fig. 2.6a) indicates the highest level. Supposed margins of a lake

(i.e. not including related deltas) are sketched. The southern and eastern margins are derived from lake sediments and layered carbonate accumulations (solid line). The western margin is obscured by the modern Puentes reservoir, while the northern margin could not be established well (dashed line in Fig. 2.6a). Combined with the 490-m contour line, an impression of the size of the lake and possible delta-sediments (e.g. photo 2.6e) is pictured.

2.4.3. Dating results

Results from OSL and radiocarbon dating are given in Tables 2.2 and 2.3. Ages are consistent in the sense that they increase with depth within each profile. Between profiles, sediments from higher terrace levels are older than those of lower terrace levels. Where radiocarbon and OSL samples overlap, ages show similar values for most sites and samples. For site III, OSL sample O-IIIb (NCL-2108073) yields a ~1.5 ka greater age than underlying radiocarbon ages. There are two possible reasons for this: i) the percentage of 'well-bleached' grains may be too low to allow accurate dating of this sample using small aliquots in combination with the Finite Mixture Model. ii) The dose rate experienced by the sample during burial may be underestimated because it was sampled just centimetres below a lithological transition. The overlying, finer grained, unit will have a higher radionuclide concentration, and its contribution to the dose rate was not taken into account. Possibly the age discrepancy is caused by a combination of these two phenomena.

Based on luminescence-dating characteristics (mostly equivalent-dose distribution) and internal consistency of results from a single section, a validity mark is given to all OSL ages. Most samples are valued to be 'Likely OK', but some are 'Questionable'. This applies especially to samples where the FMM equivalent-dose estimate is based on few aliquots, or in the case of sample O-IIIb, due to its location close to a lithological transition.
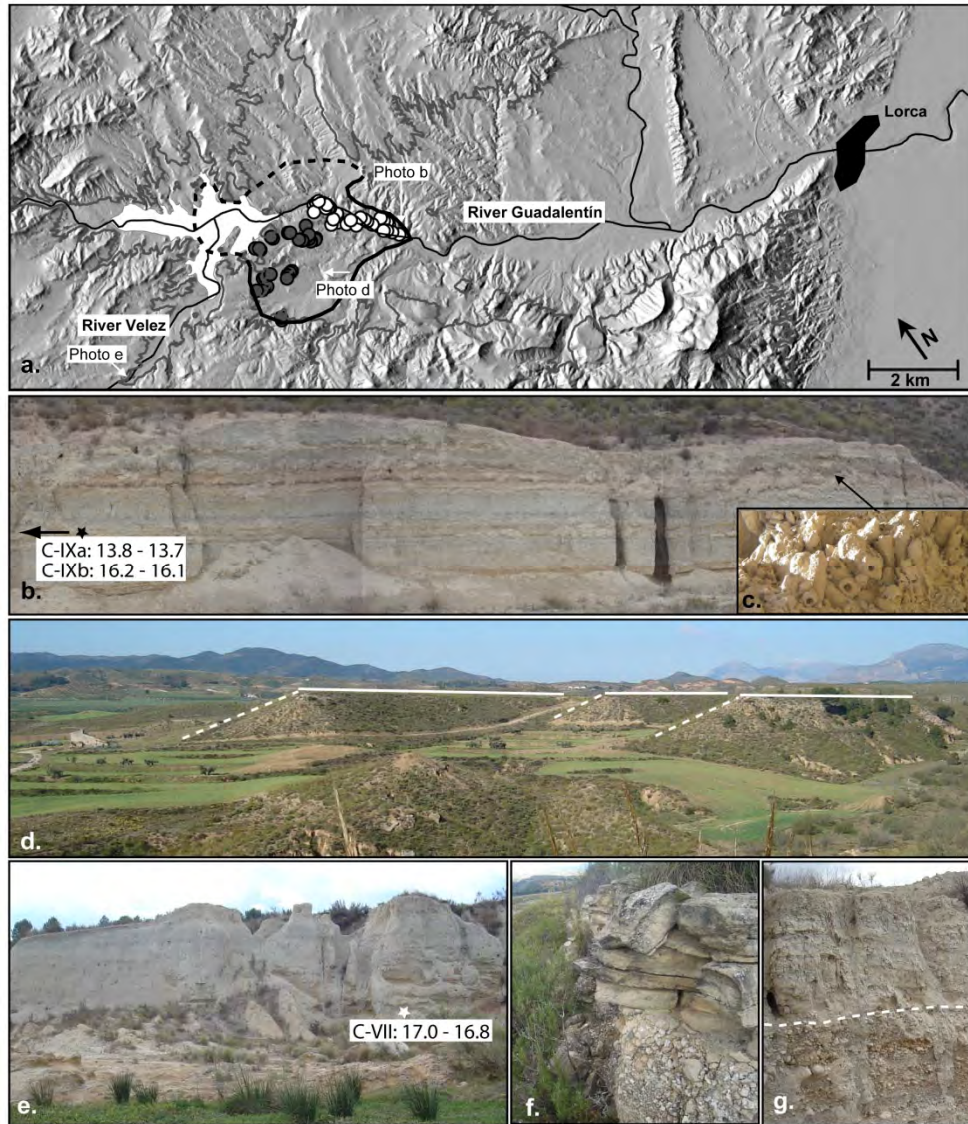
Fig. 2.6. Illustrations of lake and delta sediments. a) Location of lake sediments (white dots) and carbonate-topped ridges (black dots); supposed lake margins indicated with black line; 490m-contour line in grey. b) Close-up of finely laminated lake sediments; location indicated on a). c) Detail of root remnants coated with carbonate. d) Flat-topped ridges with layered carbonate accumulations on top (Photo towards W as indicated on a). e) Deposit of fine to coarse sediment, correlated to the onset of the lake; location indicated on a). f) Close-up of carbonate accumulations covering the ridges; and g) Boundary between lake sediments (upper) and terrace sediments (lower).

In the Rambla Torrealvilla, T-5m is sampled at two locations (sites I and II). Site I gives ages of 1.6–0.4 ka, and site II gives an age of 3.4 ka for a piece of carbon found halfway the profile. Ages for T-10m (Rambla Torrealvilla) are 7.6–5.6 ka (Site III). Ages of T-5m in the Guadalentín river coincide with both levels of the Rambla Torrealvilla at 7.5–3.4 ka (Site VI). T-2m of the Guadalentín (Site IV) is distinctly younger (0.7 ka) than T-5m of the same river. Ages for the Velez river are older than those of the other rivers, ranging from 13.8–9.5 ka for T-3m (Site VIII) and 17 ka for a charcoal fragment found at the bottom of finely layered sediment (Fig. 2.4). Ages for the laminated lake sediments are 16 and 13.8 ka (Fig. 2.6).

Table 2.2. Results of radiocarbon dating with calibrated ages (1σ)

Sample code	Sample name	River/ Rambla	Terrace level	Depth (cm)	Age BP (ka BP)	Calibrated age (ka BP)
GrA-40384	C-Ie	Torrealvilla	T-5m	30	0.14 ± 0.025	0.27 – 0.01
GrA-40390	C-II	Torrealvilla	T-5m	300	3.20 ± 0.03	3.44 – 3.39
GrA-40389	C-IIIc	Torrealvilla	T-10m	280	4.70 ± 0.03	5.57 – 5.33
GrA-40388	C-IIIb	Torrealvilla	T-10m	490	5.12 ± 0.03	5.92 – 5.77
GrA-40385	C-IIId	Torrealvilla	T-10m	520	5.10 ± 0.03	5.91 – 5.76
GrA-40682	C-IIIa	Torrealvilla	T-10m	730	5.77 ± 0.07	6.65 – 6.50
GrA-40391	C-VIb	Guadalentín	T-5m	300	3.24 ± 0.03	3.48 – 3.40
GrA-40516	C-VII	Velez	-	-	14.19 ± 0.05	17.00 – 16.80
GrA-40684	C-VIIIb	Velez	T-3m	325	11.70 ± 0.06	13.62 – 13.47
GrA-45170	C-IXa	Guadalentín	-	-	11.91 ± 0.06	13.82 – 13.73
GrA-45452	C-IXb	Guadalentín	-	-	13.58 ± 0.07	16.24 – 16.06
GrN-25452	C-X	N of Puentes	-	350	1.98 ± 0.06	2.00 – 1.87
GrN-26176	C-XI	N of Puentes	-	150	0.65 ± 0.035	0.66 – 0.56

Table 2.3. Results of OSL dating with validity estimates (see Section 2.3.3. and appendix for explanation)

Sample code (NCL-)	Sample name	River/ Rambla[a]	Terrace level	Depth (cm)	Equivalent dose (Gy)	Dose rate (Gy ka^{-1})	Age (ka)	Validity[b]
2108071	O-Ie	T	T-5m	110	0.89 ± 0.03	1.95 ± 0.07	0.46 ± 0.02	1
2108070	O-Id	T	T-5m	280	0.54 ± 0.03	1.38 ± 0.05	0.39 ± 0.03	1
2108069	O-Ic	T	T-5m	330	1.38 ± 0.10	0.93 ± 0.04	1.49 ± 0.13	2
2108068	O-Ib	T	T-5m	420	1.32 ± 0.08	0.81 ± 0.04	1.62 ± 0.13	1
2108067	O-Ia	T	T-5m	510	2.58 ± 0.17	1.87 ± 0.06	1.38 ± 0.10	2
2108074	O-IIIc	T	T-10m	280	8.78 ± 0.26	1.31 ± 0.05	5.86 ± 0.29	1
2108073	O-IIIb	T	T-10m	490	6.67 ± 0.27	0.88 ± 0.04	7.57 ± 0.46	2
2108078	O-IV	G	T-2m	270	1.06 ± 0.09	1.49 ± 0.05	0.71 ± 0.07	2
2108076	O-VIb	G	T-5m	310	7.09 ± 0.25	2.07 ± 0.07	3.43 ± 0.17	1
2108075	O-Via	G	T-5m	530	9.81 ±0.62	1.31 ± 0.05	7.48 ± 0.54	2
2108081	O-VIIIc	V	T-3m	230	31.10 ± 2.58	3.27 ± 0.10	9.52 ± 0.84	2
2108080	O-VIIIb	V	T-3m	325	39.19 ± 2.26	2.84 ±0.09	13.81 ± 0.90	1
2108079	O-VIIIa	V	T-3m	590	30.17 ± 1.69	2.27 ± 0.07	13.29 ± 0.86	1

[a] T = Torrealvilla; G = Guadalentín; V = Velez
[b] 1 = Likely OK; 2 = Questionable

2.4.4. Sedimentation rates

As there are four sites with vertical sequences of ages (sites I, III, VI and VIII), each site representing a different terrace level, we can estimate minimum sedimentation rates for these levels (Fig. 2.7). For most sites, rapid deposition of part of the profile, followed by a phase of non-deposition at that specific site with subsequent reactivation of rapid deposition is observed (sites I, VI and VIII in Fig. 2.7). For site XI, fast, high energy fluviatile processes deposited the coarse material, followed by slower slope deposits consisting of charcoal-rich silty material. For site III, sedimentation rates are estimated at 0.42 cm y^{-1} for the dated part (730–280 cm) based on the radiocarbon ages, although also on this site it is probable that deposition occurred in phases. Consequently, given rates are minimum rates not accounting for discontinuous or erosional phases.
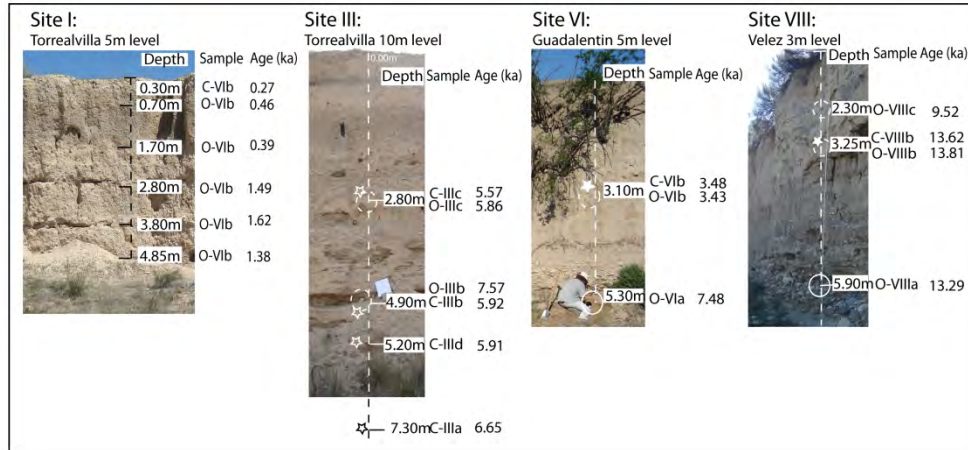
Fig. 2.7. Ages and depths of sampled sediments for sites I, III, VI and VIII.

2.5. Discussion

2.5.1. River terrace deposition

As can be deduced from Table 2.1, the higher terrace levels of the Guadalentín river and its tributaries show a vertical distance of approximately 10 m between each level. No colluvium was found on top of the gravel layers, while it was found on the lower terraces. Without further data (e.g. age estimates), we tentatively interpret these levels as 'full cycle' river terraces, being formed during a full cycle of glacial + interglacial (Schoorl and Veldkamp, 2003; Bridgland and Westaway, 2008). The terrace levels lower than 10 m are not 'full cycle' terraces, as evidenced by their sedimentary architecture (e.g. close relative positions, which are also not equally divided; Table 2.1). Colluvium is found on top of the coarse gravels and, more importantly, their ages suggest that they are Late Pleistocene (Velez river) to Holocene (Guadalentín river and Ramblas Torrealvilla and Estrecho).

Most profiles of the younger terraces show a succession of coarse gravel layers, finer, non-layered strata, coarse gravel and again finer, non-layered sediments. The finer strata are probably overbank deposits and/or colluvium. The two layers of coarse material could point to an overall reactivation of the fluvial system during terrace development, but could also be attributed to lateral displacement of the riverbed inside its floodplain, thus representing a diachronic layer (point bar structures were encountered). As noted before, fluvial terrace formation occurred in phases of rapid sedimentation, followed by periods of quiescence at that particular location and subsequent reactivation of sedimentation in later phases. We assume that sedimentation and possibly erosion during the 'quiet' phase continued in other parts of the floodplain. This is evidenced by

deposition of T-5m in the Rambla Torrealvilla, which started at ~3.4 ka at one side of the river, while ages of the same terrace level at the other side of the river start at ~1.6 ka.

Differences in thickness of the strata can be due to local differences at the time of deposition (e.g. various flow-velocities and associated transport capacities in inner or outer curve of gully for fluvial deposits or landscape position and distance to source area for colluvium) or local differences following deposition (e.g. re-erosion of sediments in erosion-prone spots and conservation of protected sediments).

In the Velez river, two phases at around 13 and 9.5 ka deposited the T-3m sediments. Afterwards, incision of this terrace level occurred except for a 0.3 m level that is not dated. The present deposition in the riverbed is associated with the lake level and sediment fill of the modern Puentes reservoir dam.

For the Guadalentín river, deposition of T-5m sediments first occurred around 7.5 ka with reactivation around 3.4 ka. Deposition possibly continued as the dated sample (O-VIb) is located halfway the terrace level, with incision afterwards. The next terrace level (T-2m) is dated at ~0.7 ka. Current incision is visible in the present riverbed and probably influenced by the modern Puentes dam, which retains the river's sediments.

For the Rambla Torrealvilla, no information is available from before ~6.6 ka, when T-10m sediments started to be deposited. Deposition of this level occurred from 6.6 to ~4.8 ka (see Section 2.4.3). Deposition of T-5m started at ~3.4 ka at one location (site II). At the other side of the modern riverbed (site I), deposition of this terrace level occurred in two phases at ~1.6 and ~0.4 ka. The non-dated T-2m level that only occurs at some locations is assumed to be a present phenomenon, representing floodplain morphology. Present incision is visible in the current riverbed. Sediments directly north of the Puentes reservoir (Sites X and XI) were deposited around 2.0 and 0.6 ka.

2.5.2. Influence of palaeo-lake and delta

The finely laminated sediments (Fig. 2.6b) were interpreted as sediments deposited in standing water, at the bottom of a lake. The lake is probably formed as a consequence of sudden blockage of the Guadalentín river. Although the blocking agent is not visible anymore, a possibility is mass movement of saturated marly sediments from a side valley, blocking the Guadalentín river. A relict of such a mudflow, visible as a ridge in the present landscape, is present downstream of the lake sediments. As there are many faults in the area, it is conceivable that a major earthquake could trigger such mass movement. As a result of the blockage, local base level would rise abruptly. At the distal end of the lake, at the inlet of the Velez river, a delta was built. Sequences of coarsening upward gravels and finer sediments provide evidence for such delta built-up with fluctuating water levels. The latter are also deduced from remnants of carbonate-coated roots or stems at the lake bottom (Fig. 2.6c; Mount and Cohen, 1984), indicating that the lake dried out completely at least several times. At the shallow edges and fringes of the lake, calcite precipitated, forming layered carbonate accumulations that were encountered around

the lake margins on the top of flat ridges. Similar features have been described for palaeo-lakes in the Dead Sea Basin (Bartov *et al.*, 2007; Waldmann *et al.*, 2009; Abu Ghazleh and Kempe, 2009).

The age of the lake sediments is measured on very small amounts of charcoal, giving Last Glacial Maximum (LGM) ages of ~16.2 and ~13.8 ka. The finely layered sediments found upstream along the Velez river (Fig. 2.6e) are interpreted to belong to the onset of the lake existence, when the Velez river deposited its finer sediments as a result of the sudden base level rise. Their age of 17–16.8 ka indeed corresponds to the lake sediment ages.

Differences in relative height above the floodplain (Table 2.1) and age (Tables 2.2 and 2.3) between the terraces of the Velez and Guadalentín rivers indicate that they have not been in equilibrium at least for some time. T-3m (Velez river) is dated at 13.3 ka at its base (sample O-VIIIab), while the oldest age for the Guadalentín terrace level is 7.5 ka. This discrepancy can be explained by the presence of the palaeo-lake and its influence on erosion and sedimentation processes.

Timing of the onset of the lake is around or slightly earlier than ~17 ka. An estimate for the time of disappearance of the lake can be derived from the river terrace levels of the Velez river. A relatively large vertical distance is observed in the Velez river between T-10m and the subsequent T-3m sediments. We interpret this vertical distance to be the result of blockage failure, causing a base level lowering for the Velez river and subsequent fast and deep incision. Thus, the palaeo-lake can be placed between 17–13.8 ka. However, the lower part of T-3m (Velez river) consisting of coarse gravels and dated at ~13.3 ka (Fig. 2.3) could also be a remnant of the delta of the lake, on top of which T-3m was deposited and into which the river later incised.

Processes of erosion and sedimentation for the Guadalentín and Velez rivers were interrupted by the palaeo-lake. As we do not know exactly what caused the blockage of the Guadalentín river, we do not know its nature or the way it eventually failed (e.g. sudden collapse or gradual removal). We presume that, while upstream a delta was being built and sediments accumulated in lower parts of the lake, some clean water spilled over or through the blockage, causing incision downstream. After failure, the upstream effects are the rapid incision described before, while downstream the effect is increased sediment loads as the accumulated lake sediments are gradually, but incompletely, removed. Lake sediments were only partly removed, as they can be encountered at present on many locations. Transport-limited sediment redistribution depending on water availability in the river in this semi-arid area probably played an important role in the removal of lake sediments.

2.5.3. Synthesis: landscape reconstruction

As Schumm (1981) suggested, it may not be possible to explain certain features of a landscape within the concepts of erosion cyclicity or dynamic equilibrium. Especially the more recent deposits may be the result of complex response inherent to erosional development of a landscape. Moreover, erosional/depositional phases need not be in phase. From our results, it is clear that the Upper Guadalentín river displays complex response. In the following, we unravel the complex set of processes that formed the landscape of the Upper Guadalentín Basin from the Late Glacial to present times. We propose a schematic model of sedimentation phases, based on fieldwork findings and age estimations (Fig. 2.8).

Schematic model of landscape development
In Fig. 2.8a–e, a schematic model of landscape development is sketched for the last ~17 ka. Figs. 2.8a–c display the processes of erosion and deposition for the Guadalentín study area. Solid lines and arrows indicate dated episodes of deposition, dashed lines indicate probable processes of erosion or deposition (undated).
Ages of the lake sediments give evidence of its existence between ~17–13.8 ka, indicated in Fig. 2.8 with vertical lines. While T-3m (Velez river) is deposited at ~13 and ~9.5 ka, no evidence for deposition is found for the Guadalentín river and Rambla Torrealvilla at that time. In the Velez river, furthermore, no younger terrace sediments are found, except for the T-0.3m level. This can be attributed to the influence of the palaeo-lake on erosion and sedimentation processes after its disappearance: i) downstream (Guadalentín river): removal of lake sediments and increased sediment loads (complex response in Fig. 2.8b); and ii) upstream (Velez river): adjustment to lowered base level after failure of the blockage.
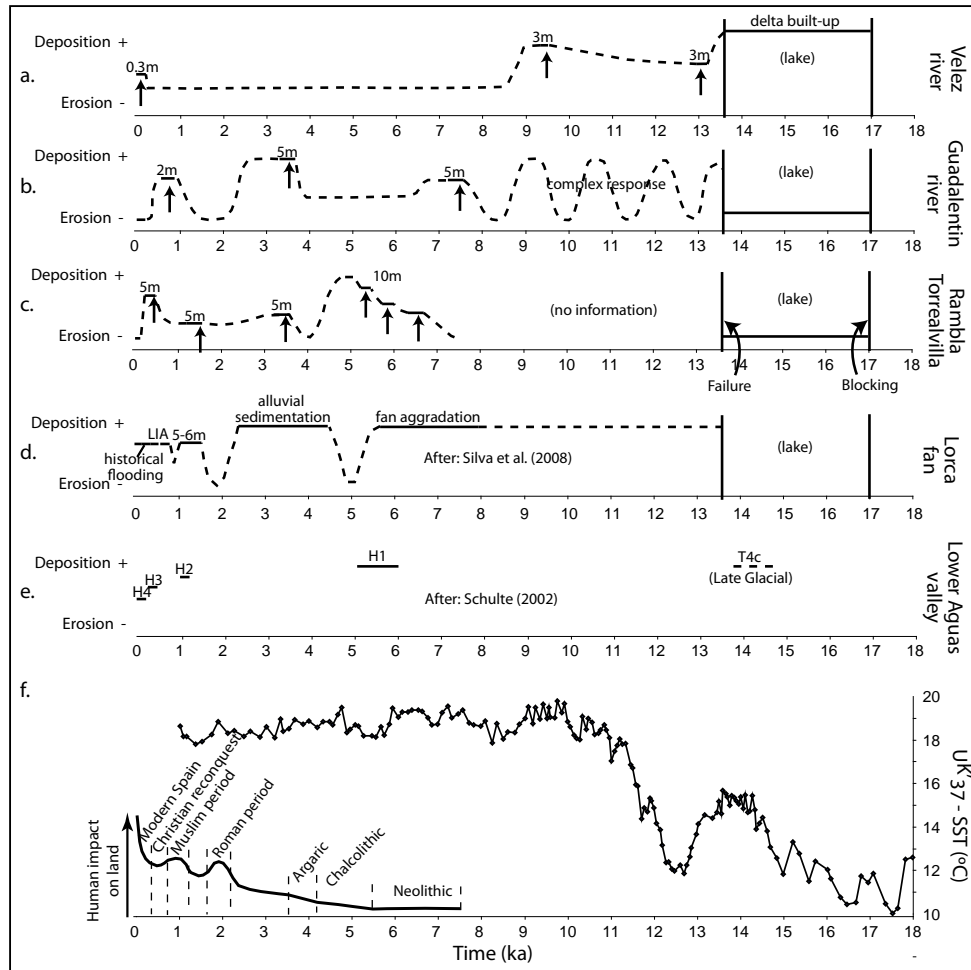
Fig. 2.8. Schematic model of deposition episodes (solid lines) and possible erosion (dashed lines). Arrows indicate dated pulses of deposition. a–c). Schematic model for the Upper Guadalentín Basin with a) Velez River; b) Guadalentín river, part downstream of the palaeolake, and; c) Rambla Torrealvilla. d) Schematic model for the Lorca fan, as described by Silva et al. (2008); e) Deposition episodes as described for the lower Aguas valley, based on Schulte (2002); and f) Sea surface temperature fluctuations, data from marine core MD95-2043 (Alboran Sea; Cacho et al., 2001; Cacho, 2006) and visualisation of human impact on land, based on literature review (Section 2.2.2).

Regarding the younger terraces, most remarkable is their absence in the Velez river. For the Guadalentín river and Rambla Torrealvilla, dated episodes of sedimentation in some cases coincide, for others deposition is asynchronous. Start of deposition of T-5m (Guadalentín river) and T-10m (Rambla Torrealvilla) occurs at the same time. Continued deposition is dated for T-10m (Rambla Torrealvilla), while it is not for the Guadalentín

river. However, it is still possible that deposition continued in the latter as well. The next dated pulse of sedimentation also coincides in time (~3.4 ka), but not in terrace level. While in the Guadalentín river, this is renewed sedimentation of T-5m, in the Rambla Torrealvilla this belongs to a new terrace level (T-5m instead of T-10m). Sedimentation on the other side of the river floodplain for the same terrace level is dated at ~1.6 and ~0.4 ka. Meanwhile, in the Guadalentín river an age of ~0.7 ka for a new terrace level (T-2m) is found. This suggests that, while deposition is occurring at similar times, they constitute different terrace levels. Thus, episodes of erosion that occur in between terrace level aggradation phases do not coincide between the Guadalentín river and the Rambla Torrealvilla.

Overall we can conclude that i) the influence of the Late Glacial palaeo-lake on deposition and erosion processes both upstream and downstream is evident; and for the younger terraces that ii) episodes of deposition seem to coincide in time, but iii) episodes of erosion in between terrace level aggradation phases do not coincide and neither do terrace levels and iv) no evidence of deposition is found for the Velez river.

Correlation with climate fluctuations and/or human impact

With the schematic model in mind, we can question whether the drivers of river dynamics for the Upper Guadalentín Basin are internal and local, such as river damming or possibly also external and regional, such as climate fluctuations or human impact.

In Fig. 2.8f, fluctuations in SST (Cacho *et al.*, 2001; Cacho, 2006) are given as proxy for moisture regime (Section 2.1) and a visualisation of human impact on the land is sketched, based on literature research (Section 2.2). Remarkably, the significant increase of SST (i.e. transition from arid to humid conditions) at the transition from Pleistocene to Holocene does not result in deposition of sediment, evidenced by the absence of sediments dated between 12.5–10 ka. The removal of lake sediments after blockage failure overruled this important climate shift for the Upper Guadalentín river. For the Rambla Torrealvilla, located outside the direct influence-zone of the palaeo-lake, no sediments of such age are encountered. Possibly, the subsiding hinterland did not supply enough sediment for large scale deposition or deposits are covered by the next level deposits (the relatively thick T-10m level).

Deposition of the T-5m level (Guadalentín river) and T-10m level (Rambla Torrealvilla) can tentatively be correlated to the Holocene Climatic Optimum around 5–7 ka (Pantaleon-Cano *et al.*, 2003; Zazo *et al.*, 2008; Carrión *et al.*, 2010). This period of increased humidity interrupted a general trend of aridification that started at the onset of the Holocene (Jalut *et al.*, 2000). The higher humidity and rainfall triggered erosion of the accumulated soil (Knox, 1972). Although the percentage of shrubs and trees increased, vegetation cover was possibly not enough to prevent erosion during rainstorms, as Jalut *et al.* (2000) indicate that climate in SE Spain was semi-arid with dry periods of 3–10 months per year throughout the Holocene. However, as mentioned before, this period is not well visible in the SST fluctuations (Fig. 2.8f).

The sedimentation pulse at ~3.4 ka cannot be correlated to known climate fluctuations or human impact, but may be triggered by a still unknown climatic or human driver. The two later phases of deposition of T-5m in the Rambla Torrealvilla can be correlated to periods of decreased human impact on the land (lower graph in Fig 2.8b): the period after the Roman occupation and the period of Christian rule after Moorish occupation, respectively. The consequences of farmland abandonment on erosion in modern times are widely studied with varying results in different environments (García-Ruiz, 2010). On weak lithologies (e.g. marl) and with scarce and irregular rainfall, increased erosion after land abandonment is observed (e.g. Lesschen *et al.*, 2007). Also, failure of formerly maintained agricultural terraces accelerated erosion after the Romans resp. the Moors left (see Lesschen *et al.*, 2008 for a modern analogue of this process).

Thus, we can correlate some of the episodes of deposition to climate fluctuation (Holocene Climatic Optimum) and human impact (decrease of impact after Roman and Moorish occupation). On the other hand, we have strong evidence that climate was not the main driver of erosion and deposition processes. This is reflected by i) the absence of Late Glacial – Holocene transition sediments caused by the influence of the palaeo-lake; ii) the asynchrony of erosion episodes between the Guadalentín river and the Rambla Torrealvilla and iii) the absence of younger terraces in the Velez river. If climate would have been the most important driver, synchronous and spatially homogeneous deposition and erosion episodes should be expected. Thus, we suggest that internal river dynamics and local processes were more important drivers for the evolution of the Upper Guadalentín Basin than external and regional factors.

Regional correlation
In Fig. 2.8d,e similar sketches as those in Fig. 2.8a–c are given, reconstructed for the Lorca fan, directly bordering our study area, based on Silva *et al.* (2008) and for the Antas/Aguas Basin (Schulte, 2002), located to the south of our study area.
Silva *et al.* (2008) studied the Holocene evolution of the Lorca fan, that forms the transition of the Upper Guadalentín river to the large graben system known as the Guadalentín depression, thus directly bordering our study area. They report early Holocene alluvial sedimentation from ~7.9–7.7 ka, with possible older sedimentation as the dated palaeosols overlie a ~5 m thick, undated, sedimentary sequence. With our findings of the palaeo-lake, we can correlate the earliest phase (before ~7.9–7.7 ka) of the Lorca fan aggradation to the failure of the palaeo-lake dam. Subsequently, the Guadalentín river gradually and incompletely removed accumulated lake sediments. These sediments have been (partly) deposited on the Lorca fan. Aggradation of the fan surface continued and possibly increased during the Holocene Climatic Optimum (Fig. 2.8d) and ceased slightly before ~5.4 ka with incision during Neolithic and Chalcolithic periods. For the latter period, no sedimentation phases were observed in the Upper Guadalentín Basin. Renewed aggradation of the Lorca fan started ~3.1 ka, generating a +8–

9 m terrace level at mid-fan locations (not sketched in Fig 2.8a). This aggradation is not described for the apex location, which is closest to our study area. We cannot correlate this aggradation phase to what we found for the Upper Guadalentín river, suggesting that this aggradation phase is the result of internal fan dynamics rather than a regional, climate driven, phenomenon. Alluvial sedimentation was significant between ~4.5 and 2 ka at the apex location, which correlates with renewed deposition of our T-5m sediments in the Guadalentín river. The fan surface stabilized in Roman times (~2.1 ka), after which cut-and-fill episodes generated several terrace levels. The +5–6 m level developed between ~1.7–1.0 ka, i.e. from Roman to early Muslim times. This can be correlated to the first deposition phase of our T-5m (Rambla Torrealvilla) terrace sediments which we associated with abandonment after Roman occupation. Calmel-Avila (2000), slightly more downstream, recognizes a Holocene terrace of 0.8–0.6 ka, and relates it to the onset of the Little Ice Age. Our T-2m level in the Guadalentín river coincides with this level. Further deposition episodes at the Lorca fan location are by historical flooding (Silva *et al.*, 2008).

Schulte (2002) and Schulte *et al.* (2008) extensively describe terrace sequences of the lower Aguas river and Antas river, located to the south of the Guadalentín Basin. Various levels for the Holocene terraces of the lower Aguas are reported; generally between 4.5 and 1 m, comprising 3 to 4 different terrace levels. As no erosion phases are described, only the reported deposition phases are sketched in Fig. 2.8e. Schulte's (2002) H1 (~4.5 m) has a Chalcolithic (~5 ka) age along the Aguas river and a pre-Neolithic (~6 ka) for the Antas river. These ages coincide with those of our T-5m (Guadalentín) and T-10m (Rambla Torrealvilla) sediments. Terrace level H2 (~3 m) in the Aguas river has ages ranging from 1040 y BP to the 16th century with much younger overbank deposits and is correlated with post-Roman increased slope erosion (Schulte, 2002). This age falls in between our ~1.6 and ~0.7 ka ages for the T-5m (Rambla Torrealvilla) and T-2m (Guadalentín river) levels, so correlation is not obvious. Interestingly, Schulte (2002) also found an age difference between lower, older gravel deposits and overlying, finer and younger deposits within one terrace level. Schulte's (2002) H3 terrace (~2 m) has an age of 0.4 ka, coinciding with the second deposition phase of our T-5m level in the Rambla Torrealvilla. Schulte (2002) correlates this with either Little Ice Age climatic fluctuations or the Christian reconquest, the expulsion of the Muslims, transition from small to large agricultural plots and abandonment and collapse of irrigation systems. The youngest terraces of the Aguas river (H4 at ~1.5 m) comprise small remnants deposited along the modern riverbed and date to the 20th century. This can be correlated to our T-2m deposits in the Rambla Torrealvilla, comprising gravel remnants along the modern riverbed.

Although the deposits in the two basins (Upper Guadalentín and Lower Aguas) may seem to correlate well, caution should be taken. As Candy *et al.* (2004) stress, there is a strong need to properly understand the main controls on terrace aggradation and incision, before attempting regional correlation. Thus, we should be careful to regionally correlate terrace levels in an area where local circumstances (e.g. our palaeo-lake or river capture events in the Aguas Basin; Harvey and Wells, 1987) have had a large impact on river

dynamics and depositional processes. Furthermore, contrasting to Schulte (2002), we suggest internal river dynamics and local drivers to be more important than external drivers (i.e. climate and human influence). In line with these considerations, we refrain from attempting to correlate our results to an even wider area such as the Spanish Mediterranean coastal basins or the entire Mediterranean Basin.

2.6. Conclusions

In this chapter, we investigated sediment archives of the Upper Guadalentín Basin with the aim of reconstructing Late Pleistocene and Holocene landscape dynamics. Dated episodes of river terrace deposition occur at ~14; from ~7.5–5, possibly lasting to 3.4; ~1.6, ~0.7 and ~0.4 ka BP. Palaeo-lake sediments were dated Late Glacial (~17 to ~13.8 ka). This lake probably formed as the result of sudden blocking of the Guadalentín river, as the finely laminated sediment directly overlie coarse riverbed gravels.

From our proposed schematic model of landscape development it is clear that the studied rivers are not in equilibrium, evidenced by their out-of-phase sedimentation pattern. We hypothesize this to be due to the palaeo-lake, influencing erosion and deposition processes during and (long) after its disappearance. After the blockage failed, accumulated sediments were gradually and incompletely removed by complex response processes. These processes even overruled the significant climate shift of the transition from Late Glacial to Holocene. Further correlation of deposition phases to climate fluctuations was difficult to establish, probably because the river system is still adapting to the disappearance of the palaeo-lake and thus, internal river dynamics are more important than regional climate fluctuations. A tentative correlation of the younger deposits to human impact after the Roman and Moorish occupation respectively is made, although also here internal river dynamics can not be excluded. In line with Candy *et al.* (2004), we stress the importance of understanding the main controls on sedimentation processes before attempting a regional correlation.

The Upper Guadalentín Basin, from our results, seems to be an a-typical river system, evidenced by the a-synchronous behaviour of its rivers, where local processes and internal river dynamics play a more important role than external drivers such as climate fluctuation or human impact.

Appendix Chapter 2

Our chronology partly relies on optically stimulated luminescence (OSL) dating results of sand-sized quartz grains from the fluvial deposits. In this appendix some additional information on measurement procedures and results is provided.

Measurement procedure

All luminescence measurements were made on a Risø TL/OSL-DA-20 TL/OSL reader (Bøtter-Jensen et al., 2003). This machine is equipped with an internal Sr/Y source delivering a dose rate of ~0.11 Gy s^{-1} to quartz grains at the sample position. The machine is equipped with an array of blue diodes (470 nm, ~35 mW cm^{-2}) for stimulation.

The Single-Aliquot Regenerative dose (SAR) procedure was used for equivalent-dose estimation. The preheat temperature was selected based on a preheat plateau test and thermal-transfer test. Preheat plateau tests showed acceptable recycling ratios over a wide range of preheat temperatures, but scatter in single-aliquot equivalent dose estimates prevented selection of a suitable preheat temperature from the data. Thermal transfer tests (following Wallinga et al., 2010) showed that no thermally transferred OSL signal was induced for preheats up to 200°C. Based on these results we selected a preheat temperature of 180°C (for 10 s) for all subsequent measurements. The adopted procedure is detailed in Table A1; data was accepted for analysis if it passed the rejection criteria detailed in Table A2.

Table A1. The SAR procedure

Step	Action	Measured
1	Regenerative beta dose	
2	10s preheat 180 °C	
3	20s blue stimulation at 125 °C	L_n, L_i
4	Fixed test beta dose	
5	Cutheat 180 °C	
6	20s blue stimulation at 125 °C	T_n, T_i
7	40s blue bleaching with blue diodes at 190 °C	
8	Repeat step 1-7 for number of regenerative doses	
Extra 1	Repeat cycle 1-7 with additional IR measurement at 30 °C prior to step 3	
Extra 2	Beta dose of 50 Gy, followed by LM-OSL	

Table A2. Applied thresholds for accepting data analysis

Test	Ideal case	Accepted if
1 – Recycling test	$(L_5/T_5) / (L_1/T_1) = 1$	$0.9 < (L_5/T_5) / L_1/T_1) < 1.1$
2 – Recuperation test	$(L_4/T_4) / L_1/T_1) = 0$	$(L_4/T_4) / L_1/T_1) < 0.1$
3 – Feldspar test	$IR_e/T_e = 0$, $T_e/T_5 = 1$	$IR_e/T_e < 0.2$ or $T_e/T_5 > 0.9$

OSL properties

The samples showed relatively low luminescence sensitivity. The OSL signal was dominated by the fast OSL component which is most suitable for dating (e.g. Wintle and Murray, 2006). Shinedown curves of the Natural, Regenerative and Test doses were of similar shape (Fig. A1). With the adopted procedure, a given dose could be accurately recovered (Fig. A2).
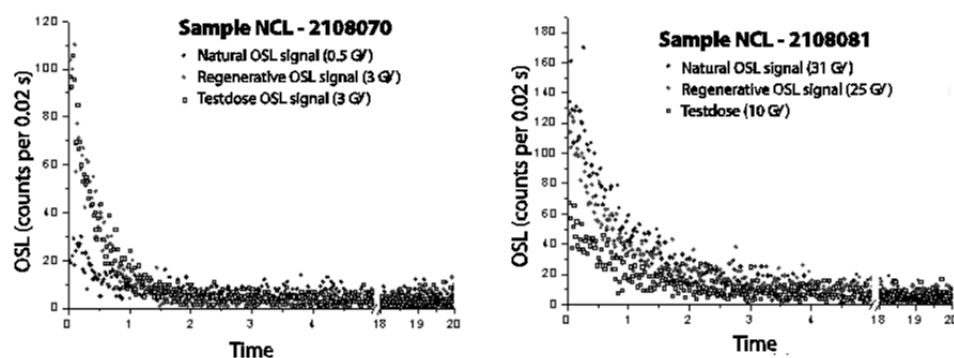

Fig. A1. OSL responses of aliquots from a young sample (left; NCL – 2108070) and an old sample (right; NCL – 2108081).

55
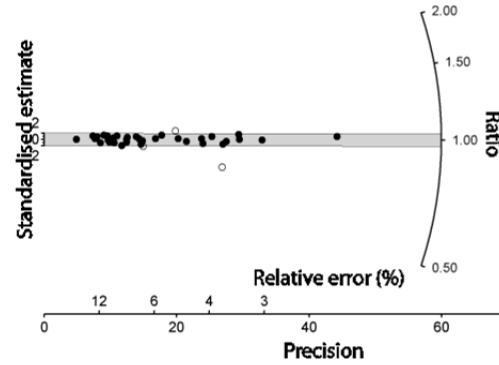
Fig. A2. Radial plot of dose-recovery ratios obtained for given laboratory dose, delivered after bleaching natural aliquots for 2 * 300s with blue diodes at 30°C. Given doses were 5, 10, 20 or 30 Gy, depending on the expected natural dose.

Equivalent-dose distributions

For the equivalent-dose samples we sieved the sediment from the inner parts of the tubes to obtain grains in size range 180–212 μm for samples NCL-2108067, -68, -70 and -71, and 212–250 μm for all other samples. Quartz grains were obtained by chemical treatment with HCL, H_2O_2, and concentrated HF. Finally this fraction was rinsed with HCl, and sieved again to discard any remaining feldspar grains. Tests with infrared stimulation indicated that no feldspars remained in the refined extracts. Equivalent doses were measured on small aliquots (centre 2 mm covered with grains) using the Single-Aliquot Regenarative dose (SAR) procedure (Murray and Wintle, 2003). A relatively low preheat and cutheat of 180°C was used to prevent overestimation of the equivalent dose due to thermal transfer (e.g. Wallinga et al., 2010). Following Ballarini et al. (2007) we applied an early background approach to select the OSL signal that is most light sensitive, and thus most likely to be reset during fluvial transport. Integration intervals used were the first 0.8 s for the initial signal, and the subsequent interval of 0.8–1.6 s for the background. Data was accepted for analysis if the recycling ratio was within 10% from unity, and recuperation was below 10%. With the adopted procedure, a laboratory dose could be accurately recovered (dose recovery ratio 1.00 ± 0.02; n = 38) and recycling was near perfect (1.01 ± 0.01; n = 390).

Single-aliquot dose distributions showed significant scatter, likely caused by incomplete resetting of the OSL signal of part of the grains prior to deposition and burial. In Fig. A2 dose distributions are shown for all samples; the blue shading denotes the equivalent dose obtained through application of the Finite Mixture Model (Roberts et al., 2000) which was used for age calculation.

For comparison we also calculated equivalent doses by taking the sample mean after iterative removal of outliers (those single-aliquot estimates removed more than two standard deviations from the sample mean). These estimates are shown by the grey lines in Fig. A2.

Dose rate estimation

Dose rates were determined from the outer parts of the samples. This material was dried, ashed and then cast in wax pucks for measurement of radionuclide activity concentrations using a broad energy gamma-ray spectrometer (e.g. Murray et al., 1987). Because water and organic material absorb part of the environmental radiation, assumptions need to be made about their average values during burial. We assumed that both water and organic contents at the time of sampling were representative of the time-average values. We applied a minimum water content of 3%, and a large relative uncertainty on the water content of 50% to account for past variations.

Dose rates were estimated based on high-resolution gamma-ray spectroscopy. Assumptions made and resulting dose rates are outlined in Tables A3 and A4.

Table A3. Measured and used water and organic contents of the OSL dating samples

Sample Code (NCL-)	Depth (m)	Burial assump-tion	Grain size range		Water content		Organic content	
			Lower (µm)	Upper (µm)	Measured	Used	Measured	Used
2108067	4.85	Gradual	180	212	4.33	4.33 ± 2.17	2.05	2.05 ± 0.41
2108068	3.77	Gradual	180	212	0.47	3.00 ± 1.50	0.76	0.76 ± 0.15
2108069	2.80	Gradual	212	250	0.70	3.00 ± 1.50	0.46	0.46 ± 0.09
2108070	1.70	Instant	180	212	2.21	3.00 ± 1.50	1.68	1.68 ± 0.34
2108071	0.70	Instant	180	212	4.24	4.24 ± 2.12	4.59	4.59 ± 0.92
2108072	1.00	Instant	212	250	0.47	3.00 ± 1.50	0.34	0.34 ± 0.07
2108073	5.50	Instant	212	250	1.16	3.00 ± 1.50	0.73	0.73 ± 0.15
2108074	3.85	Instant	212	250	1.21	3.00 ± 1.50	1.78	1.78 ± 0.36
2108075	5.30	Gradual	212	250	0.72	3.00 ± 1.50	1.20	1.20 ± 0.24
2108076	3.07	Gradual	212	250	3.23	3.23 ± 1.62	4.01	4.01 ± 0.80
2108077	1.24	Instant	212	250	1.22	3.00 ± 1.50	1.02	1.02 ± 0.20
2108078	2.70	Instant	212	250	1.00	3.00 ± 1.50	0.87	0.87 ± 0.17
2108079	6.90	Instant	212	250	1.14	3.00 ± 1.50	1.77	1.77 ± 0.35
2108080	3.25	Instant	212	250	1.36	3.00 ± 1.50	1.35	1.35 ± 0.27
2108081	2.30	Instant	212	250	2.05	3.00 ± 1.50	2.17	2.17 ± 0.43

Table A4. Radionuclide concentrations and resulting dose rates for the OSL dating samples

Sample Code (NCL-)	Radionuclide concentrations (Bq kg^{-1})			Dose rates (Gy ka^{-1})				
	U	Th	K-40	Internal alpha	External beta	gamma	Cosmic	Total
2108067	25.06 ± 0.18	20.58 ± 0.39	338 ± 3	0.06 ± 0.03	1.01 ± 0.05	0.63 ± 0.03	0.17 ± 0.01	1.87 ± 0.06
2108068	18.37 ± 0.19	5.89 ± 0.28	69 ± 3	0.06 ± 0.03	0.33 ± 0.02	0.25 ± 0.01	0.17 ± 0.01	0.81 ± 0.04
2108069	18.76 ± 0.25	6.62 ± 0.23	83 ± 4	0.06 ± 0.03	0.38 ± 0.02	0.29 ± 0.02	0.19 ± 0.01	0.93 ± 0.04
2108070	22.81 ± 0.24	13.85 ± 0.42	207 ± 4	0.06 ± 0.03	0.70 ± 0.03	0.45 ± 0.2	0.17 ± 0.01	1.38 ± 0.05
2108071	26.67 ± 0.24	22.11 ± 0.54	382 ± 5	0.06 ± 0.03	1.08 ± 0.05	0.61 ± 0.03	0.20 ± 0.01	1.95 ± 0.07
2108072	20.14 ± 0.23	3.92 ± 0.18	50 ± 3	0.06 ± 0.03	0.29 ± 0.01	0.21 ± 0.01	0.19 ± 0.01	0.75 ± 0.04
2108073	19.39 ± 0.22	80.3 ± 0.52	97 ± 3	0.06 ± 0.03	0.41 ± 0.02	0.30 ± 0.02	0.11 ± 0.01	0.88 ± 0.04
2108074	23.18 ± 0.26	13.42 ± 0.46	197 ± 4	0.06 ± 0.03	0.67 ± 0.03	0.44 ± 0.02	0.13 ± 0.01	1.31 ± 0.05
2108075	17.03 ± 0.21	13.66 ± 0.40	224 ± 4	0.06 ± 0.03	0.68 ± 0.03	0.41 ± 0.02	0.16 ± 0.01	1.31 ± 0.05
2108076	26.27 ± 0.23	25.61 ± 0.70	375 ± 16	0.06 ± 0.03	1.11 ± 0.06	0.71 ± 0.03	0.19 ± 0.01	2.07 ± 0.07
2108077	21.82 ± 0.24	16.68 ± 0.41	249 ± 5	0.06 ± 0.03	0.77 ± 0.04	0.48 ± 0.03	0.19 ± 0.01	1.51 ± 0.05
2108078	23.96 ± 0.26	15.37 ± 0.43	227 ± 4	0.06 ± 0.03	0.77 ± 0.03	0.51 ± 0.02	0.15 ± 0.01	1.49 ± 0.05
2108079	22.51 ± 0.23	27.89 ± 0.55	449 ± 5	0.06 ± 0.03	1.30 ± 0.06	0.81 ± 0.03	0.10 ± 0.00	2.27 ± 0.07
2108080	30.35 ± 0.35	33.71 ± 0.80	532 ± 7	0.06 ± 0.03	1.60 ± 0.07	1.03 ± 0.04	0.14 ± 0.01	2.84 ± 0.09
2108081	34.26 ± 0.26	44.30 ± 0.70	642 ± 6	0.06 ± 0.03	1.86 ± 0.08	1.19 ± 0.05	0.16 ± 0.01	3.27 ± 0.10

OSL ages

Table A5 lists equivalent doses, dose rates and resulting ages for all samples. In addition the table shows information on the number of aliquots passing the rejection criteria of Table A2, and results of the Finite Mixture Modelling exercise (number of components, component used for analysis, percentage of single aliquot results attributed to the selected component). Finally, the table indicates the validity estimate, based on the equivalent dose distribution, the finite mixture model results and the stratigraphic consistency of OSL results.

Table A5. OSL dating results, including details on Finite Mixture Model results

Sample Code (NCL-)	Loca-tion[a]	Depth (m)	Equivalent dose (Gy)	Dose rate (Gy ka⁻¹)	Age (ka)	Ali-quots	Finite Mixture Model			Validity[b]
							Comp.	Used	Attr. (%)	
2108067	T Ia	4.85	2.58 ± 0.17	1.87 ± 0.06	1.38 ± 0.10	27	6	1	14	2
2108068	T Ib	3.77	1.32 ± 0.08	0.81 ± 0.04	1.62 ± 0.13	23	6	1	18	1
2108069	T Ic	2.80	1.38 ± 0.10	0.93 ± 0.04	1.49 ± 0.13	15	5	1	20	2
2108070	T Id	1.70	0.54 ± 0.03	1.38 ± 0.05	0.39 ± 0.03	20	6	1	30	1
2108071	T Ie	0.70	0.89 ± 0.03	1.95 ± 0.07	0.46 ± 0.02	38	6	1	37	1
2108072	T IIa	1.00	0.54 ± 0.04	0.75 ± 0.04	0.72 ± 0.06	17	6	1	18	3
2108073	T IIb	5.50	6.67 ± 0.27	0.88 ± 0.04	7.57 ± 0.46	34	6	1	31	2
2108074	T IIc	3.85	7.65 ± 0.26	1.31 ± 0.05	5.86 ± 0.29	37	3	2	67	1
2108075	G Ia	5.30	9.81 ± 0.62	1.31 ± 0.05	7.48 ± 0.54	24	5	1	17	2
2108076	G Ib	3.07	7.09 ± 0.25	2.07 ± 0.07	3.43 ± 0.17	23	3	2	78	1
2108077	G II	1.24	0.95 ± 0.05	1.51 ± 0.05	0.63 ± 0.04	29	6	1	21	1
2108078	G III	2.70	1.06 ± 0.09	1.49 ± 0.05	0.71 ± 0.07	16	5	1	17	2
2108079	V Ia	6.90	30.2 ± 1.7	2.27 ± 0.07	13.29 ± 0.86	31	2	1	23	1
2108080	V Ib	3.25	39.2 ± 2.3	2.84 ± 0.09	13.81 ± 0.90	27	2	1	59	1
2108081	V Ic	2.30	31.1 ± 2.6	3.27 ± 0.10	9.52 ± 0.84	29	3	1	23	2

[a] T = Torrealvilla; G = Guadalentín; V = Velez
[b] 1 = Likely OK; 2 = Questionable; 3 = Doubtful

Fig. A3. Radial plots of equivalent dose distributions. Sample equivalent doses obtained through the Finite Mixture Model (blue) and through an iterative removal of outliers procedure (grey) are shown (cont. on next page).
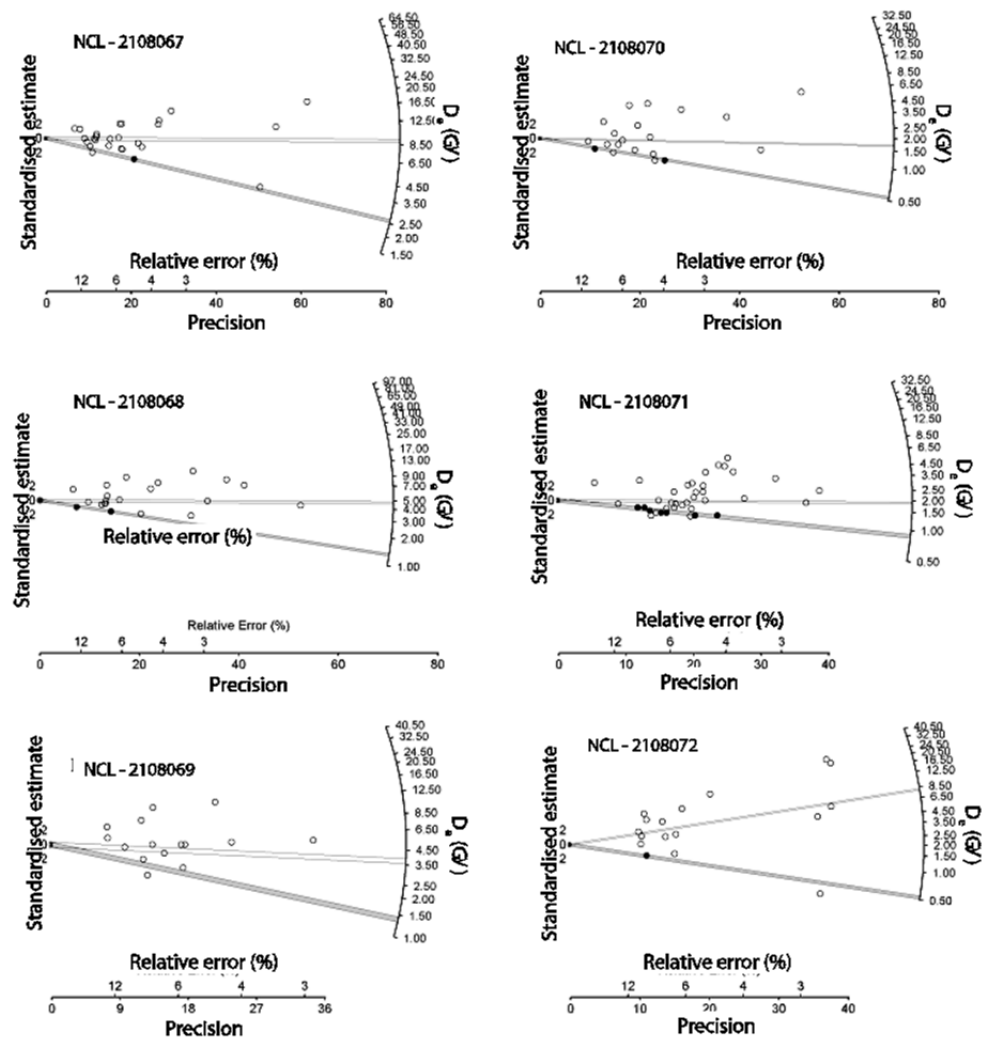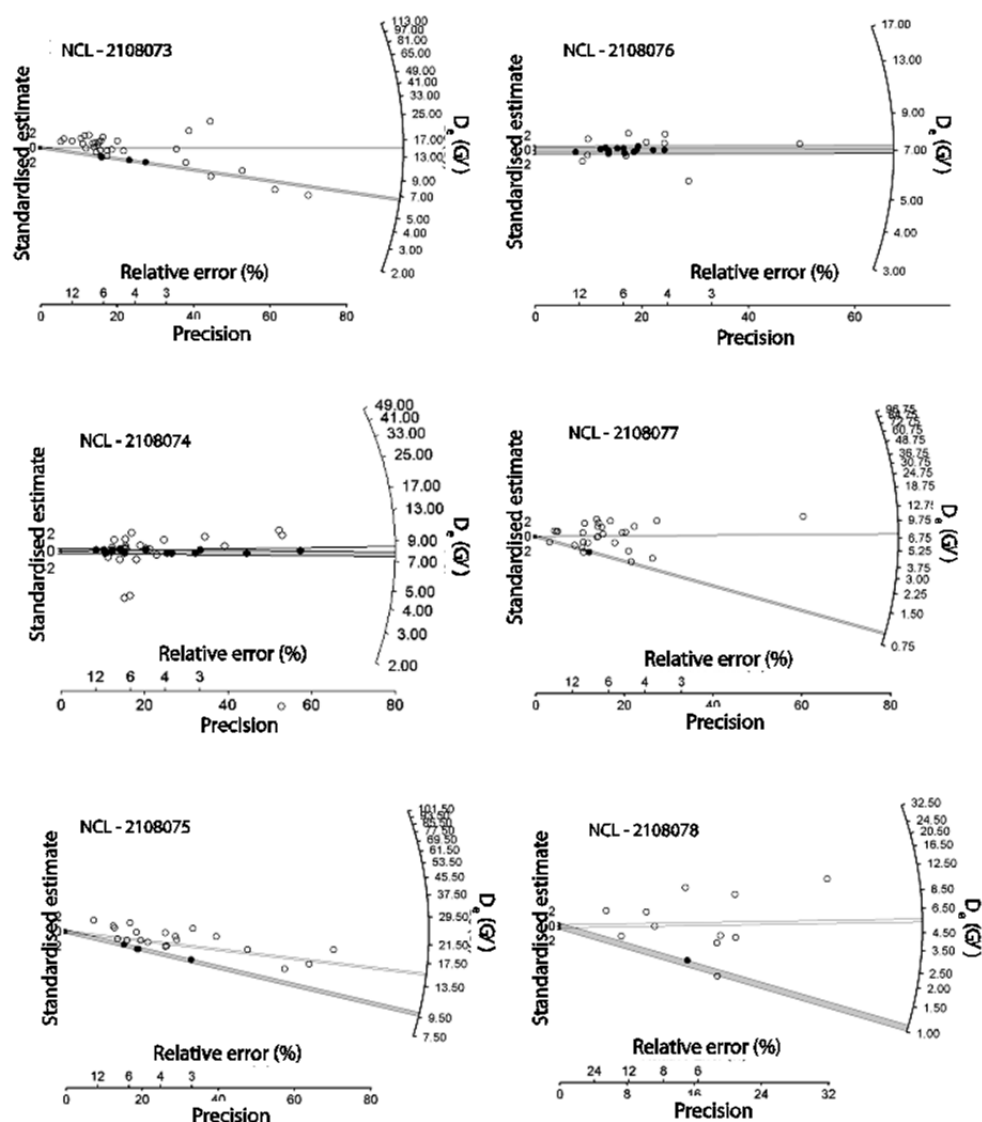
Fig. A3. Radial plots of equivalent dose distributions. Sample equivalent doses obtained through the Finite Mixture Model (blue) and through an iterative removal of outliers procedure (grey) are shown.

Chapter 3

Modelling sediment dynamics due to hillslope – river interactions: incorporating fluvial behaviour in landscape evolution model LAPSUS

Landscape evolution models (LEMs) simulate the three-dimensional development of landscapes over time. Different LEMs have different foci, e.g. erosional behaviour, river dynamics, the fluvial domain, hillslopes or a combination. LEM LAPSUS is a relatively simple cellular model that has had a hillslope focus. Our aim was to incorporate fluvial behaviour in LAPSUS without changing the model equations. The model should be able to reproduce alternating aggradation and incision in the floodplains of catchments, depending on simulated conditions. Testing was done using an artificial DEM and the ability for fluvial simulation was also demonstrated for a real landscape (Torrealvilla catchment, SE Spain). Model equations to calculate sediment dynamics and water routing were similar for both hillslope and fluvial conditions, but different parameter values were used for these domains based on annual discharge. Erodibility and 'sedimentability' factors K and P were changed between cold (little vegetation; high erodibility) and warm conditions (more vegetation, lower erodibility). Results show that the adapted parameters reproduced alternating aggradation - due to divergent flow in the floodplain and sediment supply under cold conditions - and incision due to reduced sediment supply and resulting clean water erosion during simulated warm conditions. The simulated results can be explained by interactions between hillslopes and floodplains, as the former provide the sediments that are deposited in the latter. Similar behaviour was demonstrated when using the real DEM.

3.1. Introduction

Landscape evolution models (LEMs) predict or simulate the three-dimensional development of landscapes over time (Kirkby, 1971; Ahnert, 1976) and are increasingly used to assess sediment dynamics over various time-scales (e.g. Murray and Paola, 1994; Coulthard, 2001; Pelletier, 2004; Thomas *et al.*, 2007; Temme and Veldkamp, 2009). These models can be used to simulate observed processes and erosion or sedimentation rates in various landscapes and over different time-scales. Their strength lies in the ability to provide improved insights into the mechanisms that control catchment behaviour and response, by improved quantitative description and inclusion of various interacting processes (Tucker and Hancock, 2010). Some LEMs are designed to simulate mainly river processes and apply to stretches of rivers, either in isolation (e.g. Murray and Paola, 1994, 1997, 2003; Coulthard and Wiel, 2006), or within a landscape (Nicholas and Quine, 2007; Thomas *et al.*, 2007). Models that include coupled systems of hillslope and fluvial processes include e.g. CAESAR (Coulthard *et al.*, 2002), SIBERIA (Willgoose *et al.*, 1991a, b), CHILD (Tucker and Bras, 2000) and others, reviewed recently by Tucker and Hancock (2010). LEMs have primarily focussed on erosional landscapes. However, according to Willgoose (2005) the ability to model storage bodies within a basin (e.g. terraces, floodplains) is poorly developed. This chapter focuses on adding such ability to LEM LAPSUS (LAndscape ProcesS modelling at mUlti-dimensions and Scales; Schoorl *et al.*, 2000, 2002), while maintaining its simplicity. LAPSUS has so far focused on erosional landscapes. The LAPSUS model is briefly compared to some other LEMs to decide in which way LAPSUS can be best adapted.

The LAPSUS model is a cellular model with relatively simple process descriptions and input requirements (see section 3.2.1 for details). It was initially developed to simulate hillslope erosion and deposition on a catchment scale. The model operates on annual time-scales, with sinks as non-spurious features (Temme *et al.*, 2006).

LEMs CAESAR (Coulthard *et al.*, 2002) and SIBERIA (Willgoose *et al.*, 1991a, b) are similar to LAPSUS in that they are cellular, display self-organised behaviour and use a DEM as landscape representation. Differences are in process descriptions, detail, input requirements and time-scales.

An important difference between different LEMs is the flow routing algorithm used. CAESAR uses a scanning or flow-sweeping routine (Van De Wiel *et al.*, 2007) and calculates flow depths and velocities. SIBERIA uses the D8 routing algorithm (Hancock *et al.*, 2010), which moves all water from one cell to its lowest neighbouring cell. LAPSUS uses a multiple flow routing algorithm that, depending on convergence factor p, routes water to multiple (e.g. all) lower neighbouring cells.

CAESAR uses a mixed-sediment-size formula which includes shear velocity and a ratio of sediment to water density. Bed load is distributed proportionally to local bed slope, while suspended load is routed according to flow velocity. SIBERIA uses different equations for

hillslope and fluvial sediment dynamics. The latter is an advective function similar to that used in LAPSUS for whole-landscape activity, although other parameter values are used. The former is a diffusive equation, to be able to correctly capture hillslope morphology (Hancock *et al.*, 2002). LAPSUS uses the multiple flow algorithm with low values for convergence factor *p* to simulate water routing on hillslopes.

Furthermore, CAESAR simulates individual storm events, distinguishes between different grain size classes (nine ranges), and uses layers of sediment allowing for armouring effects. LAPSUS and SIBERIA, on the other hand, operate on annual basis and do not use different grain sizes. Although the first (CAESAR) is more sophisticated, input requirements are higher (e.g. hourly rainfall time series, spatial information about grain size distributions) and run time increases.

Summarizing, there is a lack of models that use annual time steps, that assesses the coupled hillslope–river system with little input requirements to make it generally (i.e. worldwide) applicable.

In this paper we developed, tested and demonstrate the ability of LEM LAPSUS to simulate sediment dynamics for coupled hillslope–river systems without adding new process equations.

Our objective is to enhance fluvial behaviour in the originally hillslope-focussed LAPSUS model, while keeping the existing model structure and avoiding new equations and parameters. Fluvial behaviour is defined in this study as: (1) the floodplain should be able to consist of multiple (neighbouring) cells, (2) the model should be able to reproduce alternating aggradation and incision behaviour in the river floodplain over centennial temporal extents, depending on simulated warm/wet or cold/dry conditions. We explore the parameter settings for which the model displays the desired behaviour using different scenarios. In this model development phase it is not yet our objective to reproduce 'real world' situations. Hence, we use an artificial DEM to assess the model's performance. However, the model should be able to display the desired behaviour also when applied to a real DEM (Torrealvilla catchment, SE Spain). Evaluation is done on qualitative (i.e. displayed behaviour) rather than quantitative criteria (i.e. absolute or measured values) (Van De Wiel *et al.*, 2011).

3.2. Methods

The LAPSUS model structure is described in section 1.8. Here the adaptations to the model to incorporate fluvial behaviour are described. This is followed by the input data used in this study, the methods to evaluate the output and finally the methods for sensitivity analyses to parameters and DEM resolution.

3.2.1. Model adaptations

To mimic both hillslope and fluvial behaviour with the same formulation (Eqs. 1.8 – 1.11), we need a criterion to distinguish between hillslopes, hillslope–fluvial transitional environments and channels, whose extents may change over time as the landscape evolves. This distinction was based on discharge Q (Eq. 1.8). Initial runs showed that in the test setup, hillslopes had discharges typically lower than ~50 m (per cell (m^2) and in one time step (y)), while the channel had discharges higher than ~150 m, so threshold values were set at 50 and 150. Parameter values on hillslopes were set to differ from those in channels. In hillslope-fluvial transitional areas parameter values were changed linearly between hillslope values and channel values. Note that the threshold discharge values may differ for different catchments, resolutions and climatic regimes, and consequently should be assessed in advance for each study separately.

Parameters that were changed as a function of environment are the discharge and gradient exponents in Eq. 1.8 (m and n), and convergence factor p (Eq. 1.7). In addition, input parameters that are changed as a function of climatic regime (cold and dry or warm and wet; section 3.2.3) are erosion and sedimentation parameters K and P.

The effects of changing these parameters were evaluated both separately and in combination. Parameter values for the different scenarios are given in Table 3.1.

- A: this basic scenario has default values for K, P and p, but differentiates for m and n between hillslope and river conditions. Values for m and n are based on Kirkby (1971, 1987).
- B: the multiple flow routing factor, convergence-factor p, has been set to zero for river conditions. This means that water is distributed evenly over all lower neighbouring cells, resulting in divergent flow in the river. This is expected to mimic widening of river flow over its floodplain. With this scenario we aim to test whether setting $p = 0$ for the floodplain makes floodplain aggradation possible.
- C: erodibility and sedimentability (K and P-factors) were set 100 times lower for warm and wet conditions than for cold and dry conditions. We expect lower erodibility in warm and wet periods than in cold and dry periods because of thicker vegetation cover which prevents erosion. In an erosional situation, increasing K (all else being equal) increases the detachment capacity D (Eq. 1.10), which results in a decrease in term h. In Eq. 1.9 this eventually leads to an increased amount of sediment that will be transported (S), i.e. more erosion. This scenario evaluates the effect of climate on erosion and deposition dynamics through vegetation cover, but without the effect of $p = 0$ as described in scenario B. We expect more erosion to occur under warm and wet conditions than under cold and dry conditions in this scenario.

- D: scenario D combines scenarios B and C: combined effects of low convergence factor *p* for fluvial conditions and lower *K* and *P* factors for warm and wet conditions.

In this model development phase it is not our intention to simulate real conditions (such as glacials–interglacials). Instead, we aim at simulating the desired behaviour (aggradation or incision) in the floodplain depending on simulated cold or warm conditions. Also note that variations in climate as well as vegetation (represented by parameters *K* and *P*) take place at the same moment in this model setup. This means that there is no time-lag between vegetation (re)growth after climate amelioration.

Table 3.1. Parameter settings for all scenarios (changes in bold)

	Parameter				
	m	*n*	*p*-factor	*K*-factor	*P*-factor
Scenario A (basic: default parameter settings					
hillslope	0.5	1	2	0.0003	0.0003
river	2	3	2	0.0003	0.0003
Scenario B (*p*-factor varies between hillslope and river)					
hillslope	0.5	1	2	0.0003	0.0003
river	2	3	**0**	0.0003	0.0003
Scenario C (*K/P*-factors vary between cold and warm conditions)					
Cold and dry conditions					
hillslope	0.5	1	2	0.0003	0.0003
river	2	3	2	0.0003	0.0003
Warm and wet conditions					
hillslope	0.5	1	2	**0.000003**	**0.000003**
river	2	3	2	**0.000003**	**0.000003**
Scenario D (combine scenarios B and C)					
Cold and dry conditions					
hillslope	0.5	1	2	0.0003	0.0003
river	2	3	**0**	0.0003	0.0003
Warm and wet conditions					
hillslope	0.5	1	2	**0.000003**	**0.000003**
river	2	3	**0**	**0.000003**	**0.000003**

3.2.2. Input data

For model development and evaluation we used an artificial DEM as input. This DEM was kept as simple as possible, consisting of an upstream area that is ten times steeper (~5%) than the almost flat (~0.5%) floodplain. Elevation ranges between 175.8 and 300 m. The resolution is 20 m and the width measures 2100 m and the length 6000 m long (12.6 km²; 105 x 300 cells), whereby the floodplain is twice as long as the upstream area (Fig. 3.1). To avoid possible edge effects at the bottom of the DEM in our results, we ignored the lowest 50 cells of the DEM in our analysis.
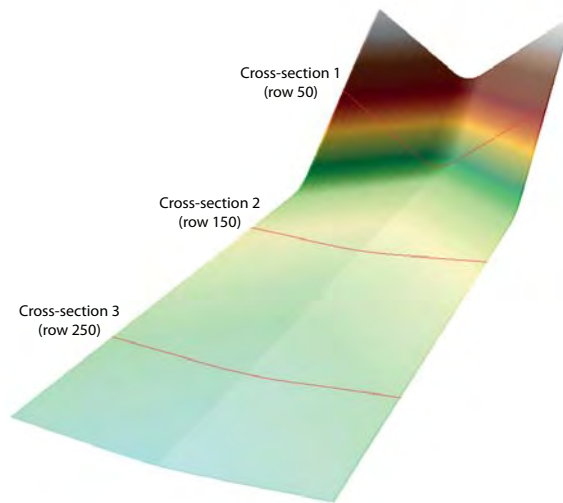

Fig. 3.1. DEM used for model simulations. Red lines indicate positions of cross-sections.

A spatially uniform time series of effective rainfall (rainfall minus infiltration and evapotranspiration) was used for input. Here 150 mm y^{-1} was taken for cold and dry conditions and 300 mm y^{-1} for warm and wet conditions (Fig. 3.2). These values are based on Veldkamp and van Dijke (2000) who used similar values for a simulation of the fluvial terrace stratigraphy of the Meuse river. Although we use values for NW European conditions here, the model is not restricted to these conditions. We alternated between cold/dry and warm/wet conditions every 500 years. Two cycles were simulated, resulting in a total runtime of 2000 years. This choice of alternating between parameter settings every 500 years allows that the model stabilizes and that the effects of the various settings are substantial while keeping model runtime reasonable. Time step (*dt*) used is one year.
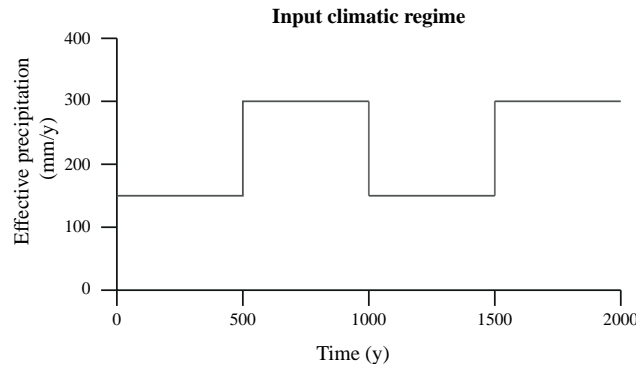
Fig. 3.2. *Input climatic regime for model simulations. High effective precipitation (300 mm y^{-1}) represents warm and wet conditions, low effective precipitation (150 mm y^{-1}) reflects cold and dry conditions.*

3.2.3. Output evaluation methods

To evaluate the effects of the different model settings we used DEM cross-sections and spatially averaged criteria. Three cross-sections were made (Fig. 3.1), for which we differentiated between the entire cross-section and its floodplain part, which was set at between 700 and 1400 m (where the left edge of the catchment in Fig 3.1 is zero, the right edge is 2100 m). Evaluation criteria were mean erosion, mean deposition, and net elevation change and discharge (*Q*) over the cross-section and its floodplain-part.

3.2.4. Sensitivity analysis and resolution effects for best scenario

For the best scenario (i.e. the one that results in the best simulated alternating aggradation and incision pattern for the floodplain) a sensitivity analysis was performed to find out how sensitive the model is to small changes in the input parameter values. Parameter values were changed by -/+5, -/+10, -/+15 and -/+20 %. Each parameter was changed separately for each run. For example only the value of *p* for hillslope was changed, others were kept constant, also *p*-river. For parameter *p*-river (with initial value zero), the same absolute changes as for *p*-hillslope were applied, i.e. a change of +5% resulted in a value of 0.1, +10% a value of 0.2 etc. This approach resulted in 80 separate model runs. Outcomes were compared to the original results by evaluating individual periods of simulated behaviour: aggradation in the first 500 years; incision from 500 to 1000 years, again aggradation from 1000 to 1500 years and finally incision for the last 500 years. A score of 1 was given for each consecutive period in which the desired behaviour was displayed and a score of 0 if the desired behaviour was not displayed.

These individual scores were then combined in a lumped score, with 4.00 being the best lumped score, in which the desired simulated behaviour is displayed in each consecutive time period. Explanation of these scores is given in Table 3.2.

Table 3.2. Scores and interpretation of sensitivity analysis

Individual score	Lumped score	Explanation: modelled behaviour[a]
1111	4.00	Aggradation – incision – aggradation - incision[b]
1110	3.75	Aggradation – incision – aggradation – *aggradation*
1101	3.50	Aggradation – incision – *incision* – incision
1011	3.25	Aggradation – *aggradation* – aggradation – incision
1010	2.50	Aggradation – *aggradation* – aggradation – *aggradation*
0111	2.25	*Incision* – incision – aggradation – incision
0101	2.00	*Incision* – incision – *incision* - incision

[a] Modelled behaviour that deviates from desired behaviour is given in italics.
[b] Desired behaviour

Finally, the effects of DEM resolution were assessed by changing the initial resolution of 20 m to resolutions of 10 m, 50 m and 100 m respectively using bilinear resampling in ArcGIS. This ensured that DEM extent could be kept at 2100 x 6000 m. Very small resolutions of e.g. 1 m were not evaluated as the LAPSUS model has been developed for larger catchments and often involves long (e.g. millennial) time-scales. Using fine resolution would involve conceptual drawbacks in the equations used in the present model and would therefore need a separate model parameterisation which is beyond the scope of the objectives of the present chapter. Parameter settings and threshold values of scenario D were used (see Table 3.1).

3.2.5. Testing for a real landscape – SE Spain

Model behaviour for different parameter settings was tested using an artificial DEM. However, to ensure that the new functionality of the adapted model are not related to the unrealistic properties of such an artificial DEM, we applied the described model changes to a real DEM, located in SE Spain, in the Guadalentín Basin, Murcia Province (UTM 30 N 614800; 4171000). The Torrealvilla catchment is ~250 km^2 and elevation ranges between ~360 and ~1525 m (Fig. 3.3). In this section, we only test whether there are differences in outcome between the basic scenario (A) and the best tested scenario (D) for this catchment. It was not our aim to calibrate model parameters for this area in detail yet (but see chapter 4) so parameter settings and input rainfall are the same as described above (Table 3.1 and Fig. 3.2), except for the threshold values for discharge to differentiate between hillslope, transitional and fluvial conditions. These were set at 5000 and 10000 m respectively, based on preliminary runs which showed that these values were appropriate for locations of channels.

The input DEM is a reconstructed palaeo-DEM in which the altitude of the river was increased with about 10m, to correspond with the height level where remnants of a (palaeo) river terrace have been found (chapter 2).
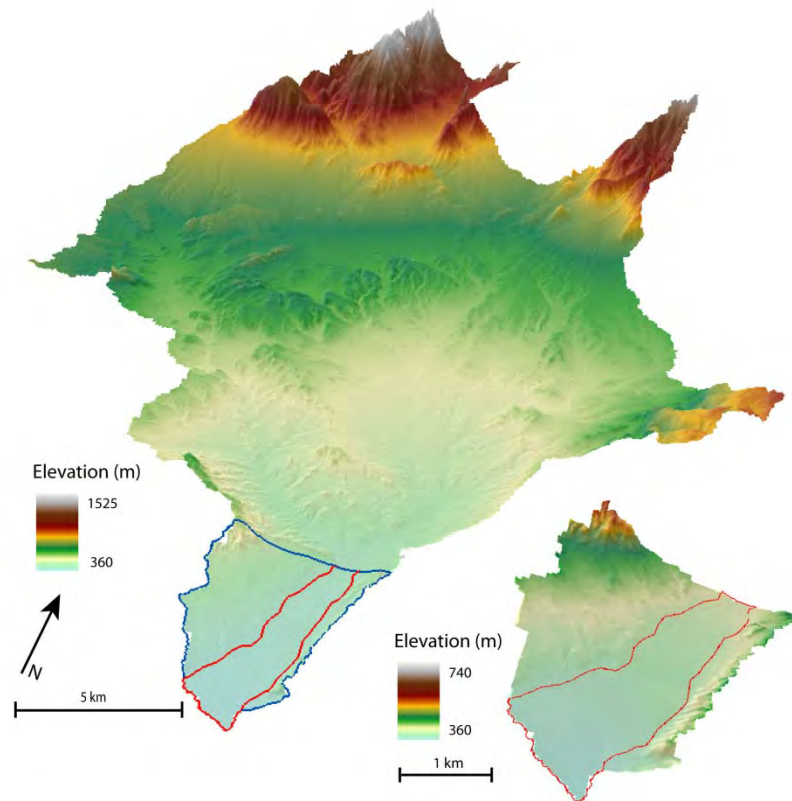
Fig. 3.3. DEM of the Torrealvilla catchment in SE Spain and zoom to lower part of the catchment (delineated by blue line) and floodplain area (delineated by red line).

3.3. Results

Results of the model scenarios are presented in section 3.3.1. Sensitivity analysis results are given in section 3.3.2 and resolution analysis results in section 3.3.3. Finally, results for the application to the real SE Spanish catchment are given in section 3.3.4.

3.3.1. Results for model adaptations

Results for the entire DEM for scenarios A-D are shown in Fig. 3.4. All scenarios show erosion in the upper part and deposition in the transitional zone between the steeper and flatter slopes. Generally, erosion and deposition increases over time. However, we are most interested in the downstream area where the floodplain is located. For scenarios A and C results show continuously increasing erosion over time in the lowest area, where the effect of cold/dry or warm/wet conditions in scenario C results in less erosion in warm/wet periods compared to scenario A (Table 3.3). For scenario B continuous deposition is simulated. For scenario D deposition is simulated from 0 to 500 y, erosion increases from 500 y until 1000 y, then decreases slightly until 1500 y and increases slightly again until 2000 y.

Results for the lowest cross-section are given in Table 3.3 and Fig 3.5. The left half of Table 3.3 gives erosion and deposition values for the entire cross-section, while the right half zooms in on the floodplain part of the cross-section. These results are evaluated in terms of aggradation and incision behaviour in the two right columns. Scenarios A and C display continuous erosion in the floodplain section (see also Figs. 3.5a and c), although in scenario C the effect of cold/dry or warm/wet conditions (low K and P factors representing vegetation cover and preventing erosion) leads to hardly any erosion during warm and wet periods (i.e. t = 500–1000 y and t = 1500–2000 y). The effect of changing convergence parameter p from two to zero in scenario B causes continuous deposition. Clearly visible from Fig. 3.5d and from Table 3.3 is the alternation of aggradation and incision in scenario D. Thus, the combined effect of setting low K and P factors in warm and wet periods (scenario C) and imposing divergent flow in the river (scenario B) results in the desired behaviour (scenario D).
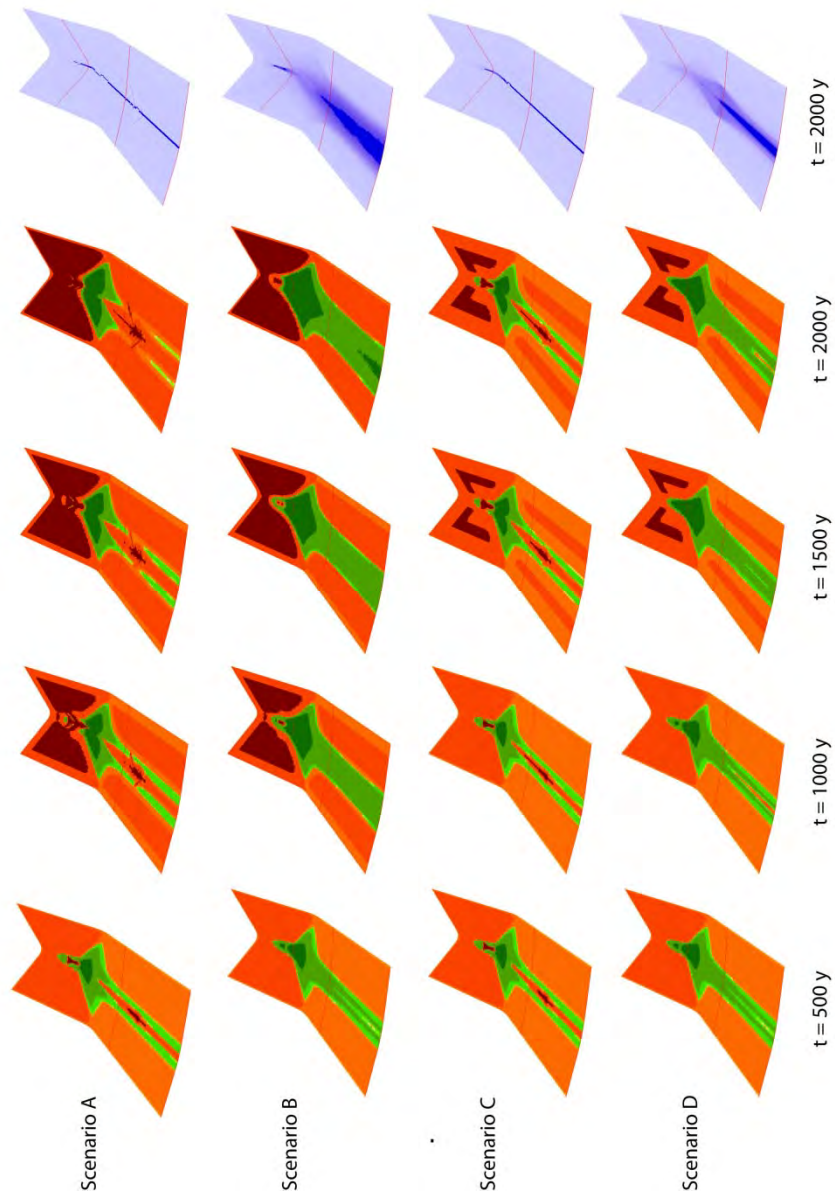
Fig. 3.4. Changes in elevation for scenarios A-D for time steps 500, 1000, 1500 and 2000 y. Orange to red colors are erosion, light to dark green colours are deposition. Note that time series show cumulative erosion / deposition patterns. Right column: discharge at t = 2000 y for scenarios A – D; darker blue is more water.

Table 3.3. Scores and interpretation of sensitivity analysis

Time (y)	Total (m²)			Floodplain (x = 700–1400 m)				
	Erosion	Deposition	Net	Erosion	Deposition	Net	Aggradation	Incision
Scenario A								
500	-81.2	9.3	-71.8	-22.1	9.3	-12.7	no	yes
1000	-122.7	8.0	-114.7	-32.0	8.0	-23.9	no	yes
1500	-81.0	0.0	-81.0	-24.3	0.0	-24.3	no	yes
2000	-123.0	0.2	-122.9	-37.4	0.1	-37.3	no	yes
Scenario B								
500	-63.6	32.5	-31.1	-4.5	32.5	28.0	yes	no
1000	-91.2	217.9	126.7	-1.3	215.6	214.3	yes	no
1500	-54.0	101.0	47.0	0.0	94.4	94.4	yes	no
2000	-77.3	188.5	111.2	0.0	156.4	156.4	yes	no
Scenario C								
500	-81.2	9.3	-71.8	-22.1	9.3	-12.7	no	yes
1000	-5.0	2.0	-3.0	-2.5	2.0	-0.5	no	yes
1500	-78.7	3.3	-75.4	-20.1	3.3	-16.8	no	yes
2000	-5.1	0.0	-5.1	-2.6	0.0	-2.6	no	yes
Scenario D								
500	-63.6	32.5	-31.1	-4.5	32.5	28.0	yes	no
1000	-12.6	0.7	-11.8	-10.0	0.7	-9.3	no	yes
1500	-61.3	51.7	-9.6	-2.8	51.7	48.9	yes	no
2000	-16.3	0.3	-16.0	-13.8	0.3	-13.5	no	yes
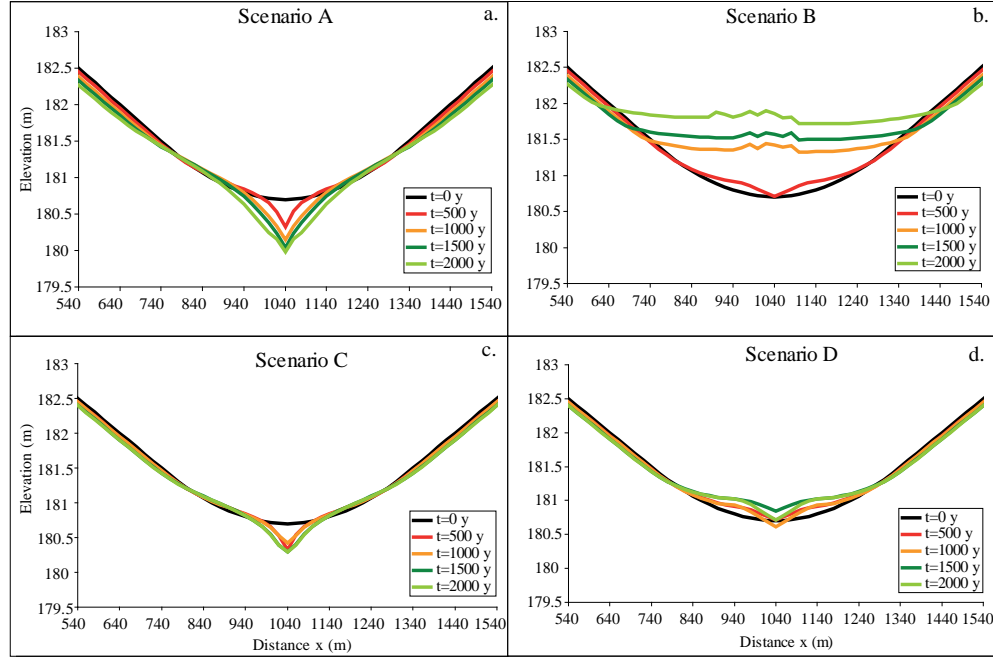
Fig. 3.5. Elevation difference at t= 500, 1000, 1500 and 2000 y for scenarios A-D for floodplain of cross-section 3.

3.3.2. Results from sensitivity analysis

A maximum score of 4 was obtained for all different values of *P* and *K*, which does not mean that the model is not sensitive to these parameter values, see Fig. 3.6. In terms of incising and aggrading behaviour, sensitivity for these two parameters was low. Sensitivity of sedimentability factor *P* increased when values were changed more than -20% during cold and dry conditions. In this case, more deposition was simulated in the floodplain at the location of the cross-section. This is further discussed in section 3.4. Changing *P* with -20% during warm and wet periods resulted in less erosion at the cross-section.

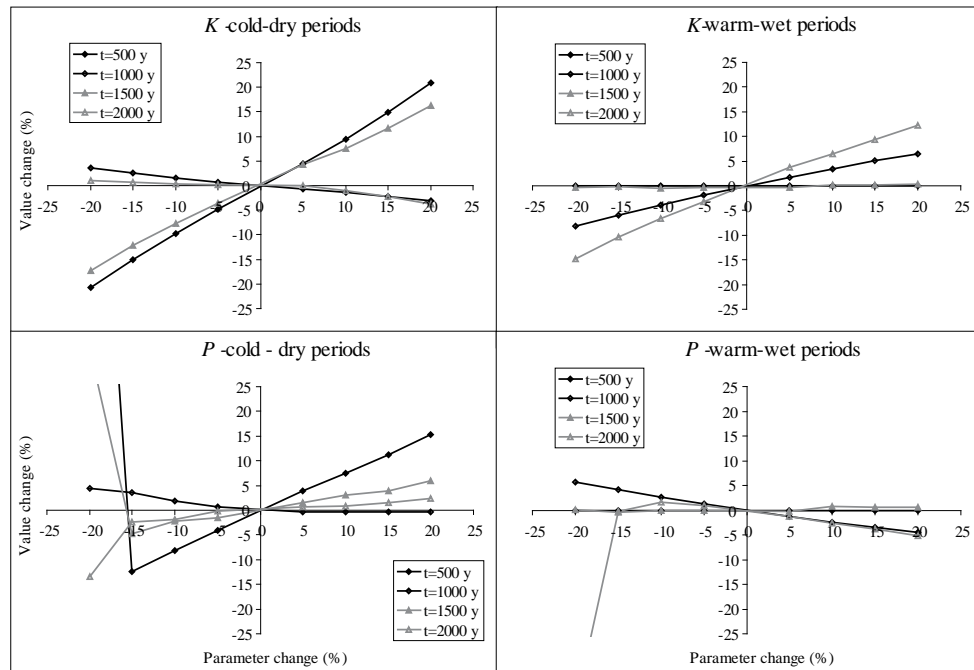*Fig. 3.6. Results of sensitivity analysis for parameters K and P. Values on the y-axis are percentage change of net floodplain erosion / deposition relative to the original amount of net floodplain erosion / deposition of scenario D.*

Sensitivity for *p*-hillslope was also low with maximum scores for all runs (Fig. 3.7). For *p*-river, and for discharge and gradient exponents *m* and *n*, sensitivity was much higher and maximum scores were not always achieved (Fig. 3.7).

Scores for *p*-river are low for negative changes and maximum for positive changes, except for the largest maximum change of +20%. In the case of *p*-river, negative changes result in negative values of *p*, meaning that water, while still flowing to lower neighbouring cells, preferentially flowed to the highest of its lower neighbouring cell, resulting in simulated continuous aggradation. Changing *p*-river to 0.4 (+20%), concentrates water, resulting in erosion (score 3.25 or 1101, see Fig. 3.7 and Table 3.2). Patterns for *m* and *n* are similar but opposite: scores for *m*-hillslope and *n*-river are maximum for positive changes (increasing values), while scores for *m*-river and *n*-hillslope are maximum for negative changes (decreasing values), except for the largest change of -20%. Vice versa, scores are low for *m*-river and *n*-hillslope for positive changes and for *m*-hillslope and *n*-river for negative changes.

Summarizing, sensitivity analysis of scenario D shows that the model is not very sensitive to changes in parameters *K*, *P* and *p*-hillslope, but highly sensitive to changes in *m*, *n* and *p*-river.
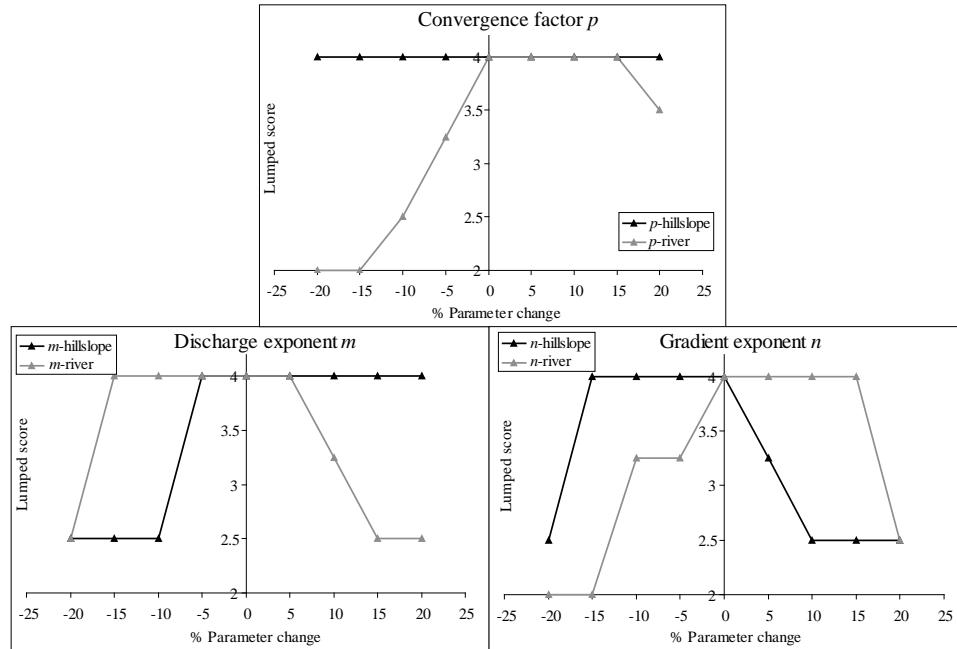
Fig. 3.7. Lumped scores of sensitivity analysis for parameters p, m and n. For explanation of scores, see Table 3.2.

3.3.3. DEM resolution effects

DEM resolution was changed from the original 20 m to 10 m, 50 m and 100 m. Results for the floodplain part of the lowest cross-section are given in Table 3.4. Scores are the same as used for the sensitivity analysis (Table 3.2). Fig. 3.8 shows simulated discharge for the different resolution runs (note difference in scale of Y axes). For the 10-m resolution DEM almost continuous incision is simulated. Amounts of discharge Q are much higher than for the 20-m resolution. For coarser 50-m resolutions scores are better, but for 100-m resolution, continuous aggradation in the floodplain is simulated. These effects are further discussed in section 3.4.

Table 3.4. Erosion and deposition results (in m²) for resolution analysis of the floodplain at cross-section 3

Time (y)	Erosion	Deposition	Net
10m			
500	-32.0	13.1	-18.9
1000	-2.4	0.0	-2.4
1500	-7.5	8.5	1.0
2000	-2.0	0.1	-2.0
Individual score	0111		
Lumped score	2.25		
20m			
500	-4.5	32.5	28.0
1000	-10.1	0.7	-9.3
1500	-2.8	51.7	48.9
2000	-13.8	0.3	-13.5
Individual score	1111		
Lumped score	4		
50m			
500	-5.6	47.8	42.2
1000	-8.2	2.4	-5.8
1500	-3.2	47.1	44.0
2000	-6.1	6.5	0.4
Individual score	1110		
Lumped score	3.75		
100m			
500	-16.5	86.3	69.8
1000	-2.8	18.4	15.6
1500	-3.1	108.8	105.8
2000	-7.9	23.2	15.4
Individual score	1010		
Lumped score	2.50		
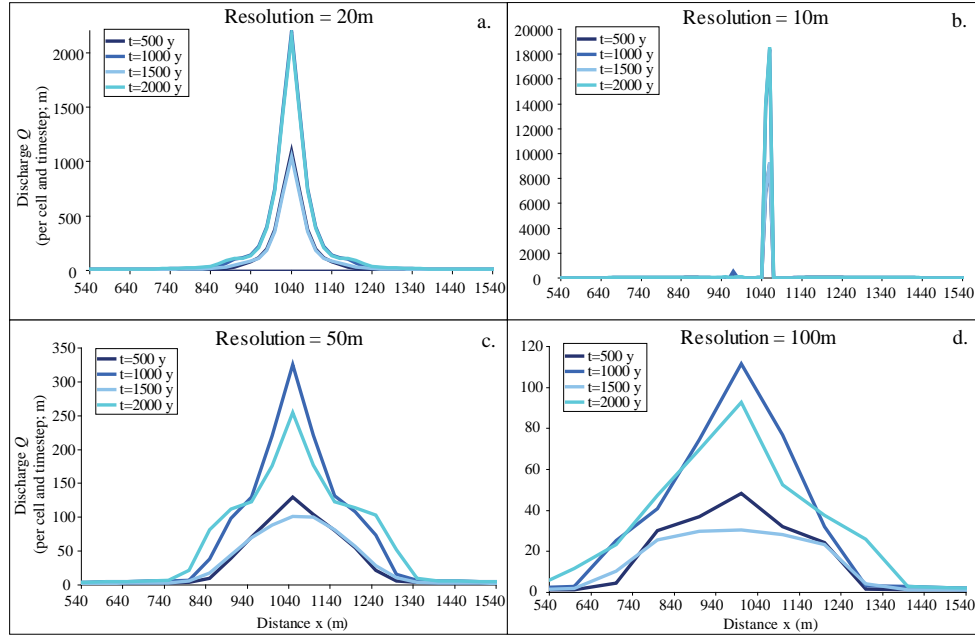
Fig. 3.8. Discharge at time steps t = 500, 1000, 1500 and 2000 y for different resolution runs. Note difference in scale of axes.

3.3.4. Application to a real landscape – SE Spain

In Fig. 3.9 and Table 3.5 results are given for the application of the basic scenario (A) and the best model scenario (D) to a real landscape; Torrealvilla catchment in SE Spain. Net erosion is simulated for the entire area as well as for the lower area of the Torrealvilla catchment (Fig. 3.3). However, if we zoom in on the floodplain in the lower area, scenario D results in alternating aggradation and incision, while scenario A only shows aggradation.

Table 3.5. Erosion and deposition at time steps t = 500, 1000, 1500 and 2000 y for Torrealvilla catchment (SE Spain) for scenarios A and D

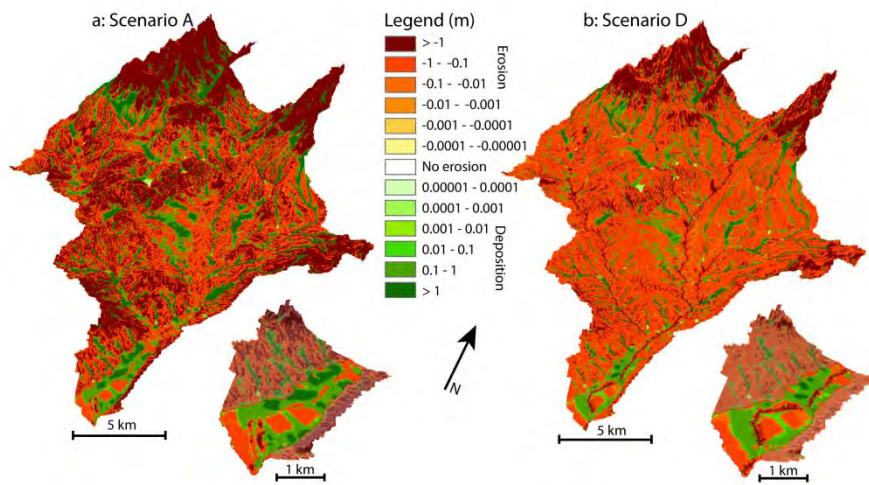| Time (y)	Net erosion or deposition (· 10⁶ m³)			
	Entire area	Lower area	Floodplain	
Scenario A				
500	-33.45	-0.68	0.36	Aggradation
1000	-60.32	-1.21	0.60	Aggradation
1500	-43.49	-0.97	0.19	Aggradation
2000	-63.32	-1.51	0.29	Aggradation
Scenario D				
500	-38.95	-0.86	0.17	Aggradation
1000	-6.16	-0.14	-0.04	Incision
1500	-34.57	-1.05	0.05	Aggradation
2000	-6.77	-0.14	-0.04	Incision

Fig. 3.9. Simulated cumulative erosion and deposition for the Torrealvilla catchment for scenarios A and D at time t = 2000 y. Inset is lower part of the catchment with floodplain.

3.4. Discussion

3.4.1. Modelling results

We used an artificial DEM to test whether we could simulate fluvial incision-aggradation cycles in an idealized setting. This implies that we did not calibrate our results to measured or observed values. This is reflected in the methods for evaluating the output and the sensitivity analysis, i.e. we evaluated only on the basis of simulated aggradation and incision behaviour, not on the basis of absolute values or detailed patterns (Van De Wiel *et al.*, 2011).

Model scenario D is the only scenario that displays the desired behaviour. The combined effect of divergent flow in the floodplain ($p = 0$) and different values of erodibility and sedimentability (K and P parameters) for cold-dry and warm-wet conditions produced alternating aggradation (cold and dry conditions) and incision (warm and wet conditions) in the floodplain. Incision is due to the effect of clean water: low erodibility during warm and wet periods results in clean water coming from the hillslopes, which erodes the river valley. During cold and dry periods, the combined effect of sediment coming from the hillslopes and divergent flow in the floodplain results in deposition and aggradation of the floodplain. Note that we did not model river meandering or avulsion (see Fig. 3.4), and that changes in flow patterns in the floodplain result only from the behaviour simulated through Eqs. 1.8 – 1.11.

Parameter settings and DEM configuration co-determine these results. The hillslopes adjacent to the river floodplain and the steeper hinterland are necessary to provide sediment for deposition in the floodplain during cold and dry conditions. If the sediment produced on the adjacent hillslopes is ignored in the model, the river carries too much water (or too little sediment) and will erode, even in cold periods. Therefore, the model settings described in this chapter will not work for purely fluvial reaches (e.g. Murray and Paola, 1994, 1997), but they successfully simulate the interaction of hillslopes and fluvial processes (Van De Wiel *et al.*, 2011).

Sediment delivery ratios (SDR = (total erosion – total deposition) / total erosion) were calculated for the entire catchment. Scenario A gives SDRs around 0.30 for all time periods, whereas scenario D gives low SDRs (0.01) for the cold, dry periods and high SDRs (0.60) for the warm, humid periods. This indicates that in the former, sediment is stored in the catchment, while during warm, humid periods more sediment is transported out of the catchment. These results for the entire catchment support the results for the lowest cross-section (Table 3.3) where deposition (storage) occurs during cold, dry periods and erosion is dominant during warm, humid periods.

The combined effect of vegetation and climate is responsible for fluvial behaviour through its effect on water and sediment supply. This allows the model to be used for a broader range of studies, such as the effects of land use changes upstream on fluvial behaviour downstream or the effects of climate variability and their combination (in

many different forms). Also, the effect of introducing for example a time-lag between vegetation (re)growth after climate amelioration can be evaluated, which may lead to different response in terms of erosion and deposition (e.g. Vandenberghe, 2008).

Not all deposition is necessarily the result of changes in climate or vegetation, but can be intrinsic to the landscape system, i.e. complex-response (Schumm, 1981). The adapted LAPSUS model is not necessarily climate driven, which provides possibilities to explore modelling complex-response type of processes. For example sediment pulses that migrate downslope and are deposited on a flatter area and subsequently (partly) removed by erosion without changing climate. In the current model setup, these pulses and their partial erosion need to be 'regulated' by the erodibility and sedimentability parameters. These can be temporally varied in the model. If these parameters would also be spatially variable, this could mimic weak sediments that are easily erodible and provide a pulse of sediment.

In this chapter, we were looking for model settings for which the desired behaviour of alternating aggradation and incision could be simulated in the catchment. During aggradation phases, sediments are retained in the catchment and supply of these sediments to the outlet is delayed. This is in line with, and by looking at the catchment also complementary to, modelled irregularities and out-of-phase sediment supply at the catchment outlet (e.g. Wainwright, 2006).

3.4.2. Application to a real-world DEM

Simulations for a real DEM of a landscape in SE Spain also displayed the required alternation of aggradation and incision in the floodplain area. Although net aggradation is calculated in scenario D for the floodplain for t = 0–500 y, an erosion channel is formed (Fig. 3.9b). This is similar to observed behaviour in the test-DEM (Fig. 3.5d). From t = 500 to 1000 y, in the test-DEM this channel is deepened, causing (net) incision. For the Torrealvilla DEM, different behaviour was observed; the channel is filled with sediments eroded from its sides. Also, erosion occurs on different locations during t = 500-1000 y than during the previous period, eventually resulting in net incision for the floodplain area. These results show the difference between an idealized, symmetrical test-DEM and a real-world DEM with spatially variable response. Thus, depending on the objective of the study, the adapted LAPSUS model needs calibration if used for a specific real world catchment. In the tested area in SE Spain, an evaluation and interpretation of sediment archives suggests that complex-response processes are important (chapter 2). Calibration of the adapted LAPSUS model for this area, for which landscape evolution data are available, is shown in chapter 4. An advantage of the LAPSUS model, having relatively few input parameters compared to other LEMs, is its applicability to unknown and/or remote areas for which few data are usually available to calibrate the model.

3.4.3. Sensitivity analysis effects

Sensitivity analysis of scenario D shows that the model is less sensitive to changes in parameters *K*, *P* and *p*-hillslope, than to changes in *m*, *n* and *p*-river. Sensitivity of sedimentability factor *P* increased at low (-20%) values for cold and dry periods. Lower *P* values mean that sediment is kept in transport longer. This results in redistribution of eroded sediment from the steeper hillslopes over larger and lower areas down the floodplain than for higher *P* values. This effect is noticed at the location of the cross-section at *P*-values of -20%. Additional simulations with changes of -17, -18 and -19% and differences between spatial erosion and deposition maps showed that sediments from the steeper upstream slopes are redeposited gradually lower on the floodplain. Total net erosion for the entire DEM showed a threshold between -18 and -19% change; apparently *P* values are so low that sediments can not be deposited in the catchment anymore and they are delivered as sediment output out of the catchment.

For decreased *m*-hillslope or increased *n*-hillslope values, continued deposition was simulated while erosion was expected during cold and dry periods. Decreasing *m*-hillslope and increasing *n*-hillslope values both result in decrease of transport capacity (*C* in Eq. 1.8) for the hillslope, resulting in less erosion on the hillslopes. This subsequently gives less deposition next to the floodplain, which allows water to spread over a larger area (i.e. the floodplain is wider), as its width is less limited by deposited sediments that were eroded from the adjacent hillslopes. However, if the same amount of water is spread over a wider area, values of *Q* decrease, which decreases transport capacity in the floodplain environment, which leads to deposition of sediment. Conversely, if *m*-river values are increased or *n*-river values are decreased, transport capacity of the river increases, which leads to more erosion in the river. However, the opposite is simulated. This is due to the influence of the steep hinterland slopes, where indeed more material is transported and less deposited than in the original settings of scenario D. However, due to much lower slopes in the floodplain area, the transported material is deposited again directly and river water is forced to flow around the deposited material. This reduces the transport capacity due to lower *Q* which reduces erosion. If values of *n*-river are decreased up to -15 and -20%, continued erosion is simulated. In this case, transport capacity is large enough to start eroding and creating a channel. Once a channel is created, all water will concentrate there, even if *p* is zero because there is only one lower neighbour cell. This increases transport capacity and erosion even more, resulting in more erosion of the channel, etc. The channel formation started low in the DEM, where the least material of the fan is deposited. Subsequently, the channel was seen to be growing upwards, due to the process described above.

This analysis shows that because of interaction between the processes of erosion, deposition and water distribution the effects of changing model parameters are not always straightforward and that the spatial (catchment) dimension is important to consider in understanding the model behaviour.

3.4.4. Effects of DEM resolution

There is a large effect of DEM resolution on the model's fluvial behaviour (Table 3.4). DEM resolution effects are to be expected for every spatial model and have been described for the LAPSUS model previously (Schoorl *et al.*, 2000, Claessens *et al.*, 2005, Temme *et al.*, 2011). Although methods exist to possibly overcome this problem (Stark and Stark, 2001), it is beyond the scope of this chapter to include and evaluate these. In general, when the model is applied any catchment, the resolution should be chosen beforehand (based on various reasons, see Van De Wiel *et al.*, 2011) and kept the same throughout the study.

For 10-m resolution (instead of the original 20m), the effect of smaller cell size is that distribution of water (multiple flow, Eq. 1.7) is calculated more frequently which results in higher values of Q for these cells (Fig. 3.8b). Consequently, this leads to higher transport capacities (Eq. 1.8). If values of erodibility (K) are kept the same, then this leads to more erosion. Erodibility factor K should therefore be scaled with resolution, as suggested already by Schoorl *et al.* (2000). Important here, when higher values of Q are calculated, threshold values for fluvial behaviour will be exceeded for more cells, resulting in more cells behaving as rivers compared to the simulations at 20 m resolution. When these thresholds are not also scaled with resolution, two contradictory effects occur. On the one hand, in the (larger) fluvial environment convergence factor $p = 0$ will lead to distribution of flow over more cells, leading to lower values of Q in individual cells and lower transport capacity. On the other hand, the values for Q increase calculated transport capacity quadratic as $m = 2$ (Eq. 1.8). Apparently, the second effect overrules the first (erosion is simulated, Table 3.4). Additionally, as soon as a channel is created by erosion, the spreading effect of $p = 0$ is lost, as there is only one lower neighbouring cell.

If resolution is increased, the opposite effect is observed: only few cells have Q values high enough to exceed the threshold for fluvial behaviour. This stresses that model performance depends on discharge values and that threshold values to distinguish between hillslope and fluvial behaviour are scale dependent and should be adapted for DEMs with different resolutions. Threshold values $Q1$ and $Q2$ can be adapted to the resolution, so that approximately the same area is designated as hillslope / transitional / fluvial. The corresponding threshold values are plotted for each resolution in Fig. 3.10.

If these threshold values are used in the runs with different resolutions, the 10-m resolution run shows continued incision; the 50-m resolution run shows the desired aggradation – incision – aggradation – incision behaviour but with less incision than the 20m results; and the 100-m resolution run shows continued aggradation.
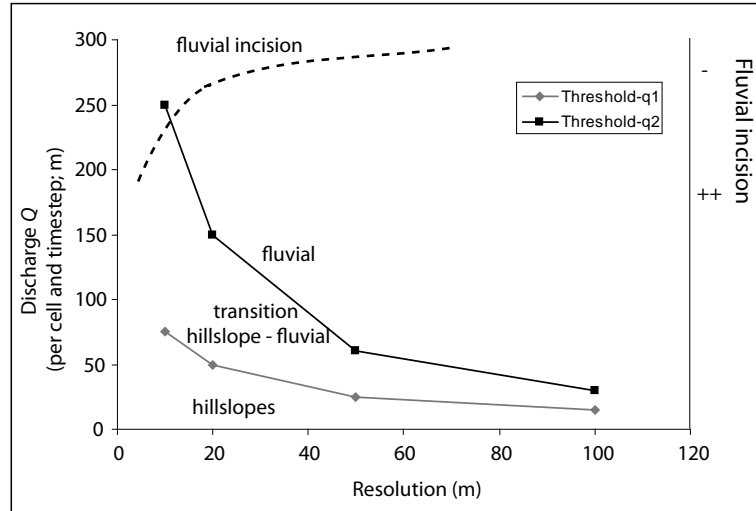
Fig. 3.10. Threshold values for discharge Q (left y-axis) varying with resolution based on areas designated to be hillslopes, transition or fluvial environments. Above certain high Q values, fluvial incision (right y-axis) may occur.

This shows that not only threshold values for hillslope, transition and fluvial environment are important. Probably, erodibility (*K*-factor) values for the 100-m resolution runs were too high, resulting in aggradation. For the 10-m resolution runs, the effect of quadratic increased transport capacities in the fluvial domain overrules the effect of spreading water due to *p* = 0. This effect is indicated as 'fluvial incision' in Fig. 3.10. Independent of resolution, this effect will occur if catchments become larger and Q values increase. A model using these equations (section 1.8) and settings (i.e. *m* = 2, *n* = 3) is therefore restricted to relatively small catchments with small rivers or, if modelling larger catchments, coarser resolution. Prediction or calculation at which values of Q this fluvial incision effect occurs is difficult, and depends on many factors, including erodibility factor *K* and redistribution of sediments which influences water redistribution patterns. Also, if it does not start in the first time step, it may occur in later time steps.

3.4.5. Model adaptations

In this chapter it was our objective to keep to the existing LAPSUS model structure, its annual time-scale, limited input requirements and computational efficiency. Until now, the LAPSUS model was used in predominantly hillslope environments (e.g. Buis and Veldkamp, 2008, Temme and Veldkamp, 2009). To make the model better suited for modelling catchments that include both hillslopes and floodplains, we distinguished hillslopes from floodplains by assigning a unique set of parameter values to each environment. The transition from distributed flow on hillslopes to concentrated flow in channels is acknowledged to be problematic (Tucker and Hancock, 2010). Willgoose *et al.* (1991b) introduced a channel initiation function in their SIBERIA landscape evolution

model, which made the distinction between channels and hillslopes explicit, but at the cost of introducing new and poorly constrained parameters (Tucker and Hancock, 2010). In the adapted LAPSUS model, the transition from hillslope to fluvial conditions is also explicitly modelled, but the same equations are used for the three domains (hillslopes; transition hillslope–fluvial; and fluvial), albeit with different parameter values for m, n and p. The parameters discharge exponent m and gradient exponent n mainly determine the transport capacity (Eq. 1.8); the convergence factor p determines the spatial distribution of water (Eq. 1.7). For the transition zone, in this study a simple linear relation between hillslope parameter values and fluvial parameter values was used. Other hillslope–channel transitions are imaginable but require additional calibration.

Simple hillslope-based equations can be used to model fluvial behaviour to a certain extent, as shown in this paper. However, the model does not simulate this behaviour without hillslopes, i.e. for pure river stretches. To achieve this, it is probably necessary to add new rules and equations for routing (river) water. However, modelling pure river stretches is beyond the scope of this chapter.

We chose discharge to distinguish between hillslope and fluvial conditions and parameter settings, as rivers typically carry more water than hillslopes. Another choice could have been for example transport capacity. Here discharge was a logical choice, because LAPSUS is based on discharge (Eq. 1.8) and values for m and n are available in the literature (see Fig. 3.1 in Kirkby, 1987) for both fluvial and hillslope processes. Although values for m and n are available, there is no information that links these parameters to absolute values for Q, hence the necessity to calibrate the threshold values.

In LAPSUS, a multiple flow algorithm is used to route the kinematic wave (Eq. 1.8), which provides a means to approximate a time-varying, two dimensional flow field and avoids problems related to kinematic wave solutions (Tucker and Hancock, 2010). The values used for convergence factor p in the multiple flow algorithm can be controversial. Theoretically, water concentrates in rivers which implies a high p-factor (steepest descent) for rivers. In their river-model, Murray and Paola (1994, 1997) use multiple-flow routing with a p-factor of 0.5. Using the same value in our model does not result in the desired behaviour, because different equations are used to calculate sediment transport. Murray and Paola (1994, 1997) use a constant that ensures that elevation changes by at most a few percent of the mean elevation difference between cells in each time step, thus preventing deep erosion. In this study, we have set the p-factor to zero for fluvial behaviour. This mimics the behaviour of diverging (river) water over a flat floodplain, because it makes it easy for (river) water to spread out over multiple neighbouring cells. Thus, this simulates a diffusion-wave approximation, in which both gravity and pressure gradients drive water flow.

3.5. Conclusions

We adapted parameter settings of landscape evolution model LAPSUS to model fluvial processes in addition to existing hillslope processes. A spatially explicit distinction between the two environments (hillslopes and fluvial) is made, based on discharge (Q). The combined effect of adapting discharge exponent m, gradient exponent n and convergence factor p for hillslope/fluvial conditions and different values for erodibility K and sedimentability P for two climatic regimes resulted in the desired simulated behaviour of alternating aggradation in cold and dry conditions and incision in warm and wet conditions. During cold-dry climate, rainfall is lower and erodibility values are relatively high, representing little vegetation. The simulated aggradation is due to divergent flow in the floodplain and sediment supply during simulated cold-dry conditions, and simulated incision is due to reduced sediment supply and resulting clean water erosion during simulated warm-wet periods. These results were also obtained when applying the successful model scenario to a real-world DEM of a catchment in SE Spain.

The simulated behaviour is an interaction of hillslope and fluvial processes in the sense that the hillslopes adjacent to the river floodplain are necessary to provide the sediment that is deposited in the floodplain during cold periods. The river itself does not carry enough sediment, resulting in concentration of water in and erosion of the floodplain. The model is sensitive to values of discharge and gradient exponents m and n. The spatially interacting processes of erosion, deposition and water distribution determine model behaviour. Resolution analysis shows that especially values of discharge (Q) are affected and that the effect of setting convergence factor $p = 0$ for fluvial environments is overruled by the effect of setting discharge exponent $m = 2$. Due to the latter effect, transport capacities increase and continuous fluvial erosion is simulated. A model using these equations and settings is therefore restricted to relatively small catchments with small rivers or, if modelling larger catchments, coarser resolution. Threshold values of discharge Q that were used to distinguish between hillslope and fluvial behaviour should be calibrated for each DEM.

The adapted landscape evolution model LAPSUS simulates sediment dynamics as a result of the coupled hillslope-fluvial system interactions. This allowed us to gain insight in the processes and conditions under which observed sediment bodies are deposited in natural catchments, especially if other process that can be included in LAPSUS are activated such as for example tillage erosion, landsliding or vegetation effects.

Chapter 4

Did tillage erosion play a role in millennial scale landscape development? – an evaluation in SE Spain using LEM LAPSUS

Landscape evolution models (LEMs) quantitatively simulate processes of sedimentation and erosion on millennial time-scales. An important aspect of human impact on erosion is sediment redistribution due to agriculture. In this chapter we aim to analyse the potential contribution of tillage erosion to landscape development using a LEM. The model is separately calibrated for: i) water erosion processes only and ii) water plus tillage erosion processes. It is applied to the ~250 km2 Torrealvilla study area, SE Spain. We were able to simulate alternating sequences of incision and aggradation. Generally, model results show that tillage erosion adds to deposition in the lower floodplain area, but neither water erosion alone nor water plus tillage erosion together could exactly reproduce the observed amounts of erosion and sedimentation for the case study area. This implies that other processes not included in the model and / or input and model assumptions and uncertainties play a role. In addition, scale effects are apparent: on hillslopes, tillage importantly contributes to erosion and fills local depressions. On the catchment scale, sediments from tillage erosion eventually reach the floodplain area. Here they contribute to aggradation, but to a lesser extent than on hillslopes, also depending on the connectivity within the catchment. This is the first time that tillage erosion is explicitly included in a LEM on a millennial time-scale and the large catchment scale.

4.1. Introduction

Landscape evolution models (LEMs) quantitatively simulate the geomorphic evolution of landscapes over time. They have been tested using hypothetical data and applied to simulate the evolution of actual landscapes (e.g. Coulthard and Macklin, 2001, Hancock *et al.*, 2008a, b, Hancock, 2009, Temme and Veldkamp, 2009, Hancock and Coulthard, 2011, Hancock *et al.*, 2011). Because most geomorphic processes are slow, experiments and real-time observation are rarely undertaken. LEMs provide tools to evaluate the effects of these processes (Tucker, 2009). Topographic change or sediment redistribution can be calculated in a LEM as the effect of one or more processes, such as water erosion, landsliding, tillage and creep that can be described in the model with geomorphic transport laws. Recent reviews of LEMs can be found in Coulthard (2001), Willgoose (2005) and Tucker and Hancock (2010). LEMs are commonly used to reproduce, in retrospect, landscape morphology observed today (Temme *et al.*, in press). Important limitations for these kinds of studies include uncertainty about the initial state of the landscape and equifinality – the notion that the current landscape can result from different starting landscapes and processes. To constrain the initial state, remnants of sediment bodies, for example river terraces, can provide information about the palaeo landscape (Tucker, 2009). As Govers *et al.* (2006) state, simulation models can provide additional information on the time-scale and way in which landscapes respond.

In this respect, an important question that can be studied with LEMs, relates to the drivers of geomorphic processes. An example is the question whether climate or human impact has been more important in shaping landscapes (Verstraeten *et al.*, 2009). Generally, it is believed that human pressure increased erosion rates (e.g. Hooke, 2000a, Syvitski *et al.*, 2005, Knox, 2006). Most studies focussing on human impacts base calculations of erosion rates on field monitoring for the short, human time-scales, and on sediment archives or cosmogenic nuclides analysis for the longer, natural, time-scales (e.g. Kirchner *et al.*, 2001, Gellis *et al.*, 2004, Arnaud-Fassetta *et al.*, 2006). The analysis of cosmogenic nuclides, however, leads to estimates of net temporal landscape change (Walling and Quine, 1991, Quine *et al.*, 1997), so that sequences of erosion and deposition over time are not included. On decadal time-scales, this might not form a limitation, but on longer (millennial) time-scales, erosion and deposition sequences become relevant to understanding landscape evolution.

An important aspect of human impact on erosion is sediment redistribution due to agriculture - tillage erosion. In a modelling study on effects of tillage erosion at field scale and decadal time-scales, Govers *et al.* (1996) found that the impact of tillage should be taken into account in landscape evolution studies in addition to the impact of water erosion. Only a few LEMs currently include tillage erosion as a geomorphic process (WATEM/SEDEM, Van Oost *et al.*, 2000, Van Rompaey *et al.*, 2001, Verstraeten *et al.*, 2002;

SPEROS, Van Oost *et al.*, 2003, 2005; SORET, De Alba *et al.*, 2004; and LAPSUS, Schoorl *et al.*, 2004). Studies that use these models mostly focus on the tillage process itself and on short (contemporary) time-scales and small spatial scales (e.g.Van Oost *et al.*, 2000, Heuvelink *et al.*, 2006). LAPSUS (Schoorl *et al.*, 2000, 2002) is a landscape evolution model that addresses long time-scales (millennia). The original model simulates erosion and deposition by overland flow, while other processes, including tillage erosion, can optionally be activated. The model was modified to include fluvial interaction at the catchment scale (chapter 3).

Until now, the effects and relative contribution of tillage erosion (in addition to erosion by water) to sediment redistribution have not been studied on a millennial time-scale and spatial catchment scale using a LEM. It is important to be able to separate these two processes and simulate them individually (Van De Wiel *et al.*, 2011) in order to quantitatively address the issue of natural or human induced erosion.

In this chapter we analyse the potential contribution of tillage erosion to observed erosion–sedimentation–erosion sequences for an entire catchment and on millennial time-scales using LEM LAPSUS. First, the sensitivity of LAPSUS outputs to changes in its parameters is measured using a Monte Carlo set-up. Then the model is separately calibrated for i) water erosion processes only and ii) water plus tillage erosion processes.

4.2. Study area

For our analyses and to evaluate simulation results, we use the Torrealvilla case study area; a ~250 km^2 catchment in SE Spain where dated remnants of river terraces are used to reconstruct several past landscape stages (chapter 2). The Torrealvilla catchment is located in Murcia Province, SE Spain (Fig. 4.1; UTM 30N 614800; 4171000). Altitudes in the catchment range from ~350 to ~1525 meter above sea level. General characteristics are described in section 1.7. Fig. 4.1 shows the study area with indication of the floodplain area as used in this chapter.
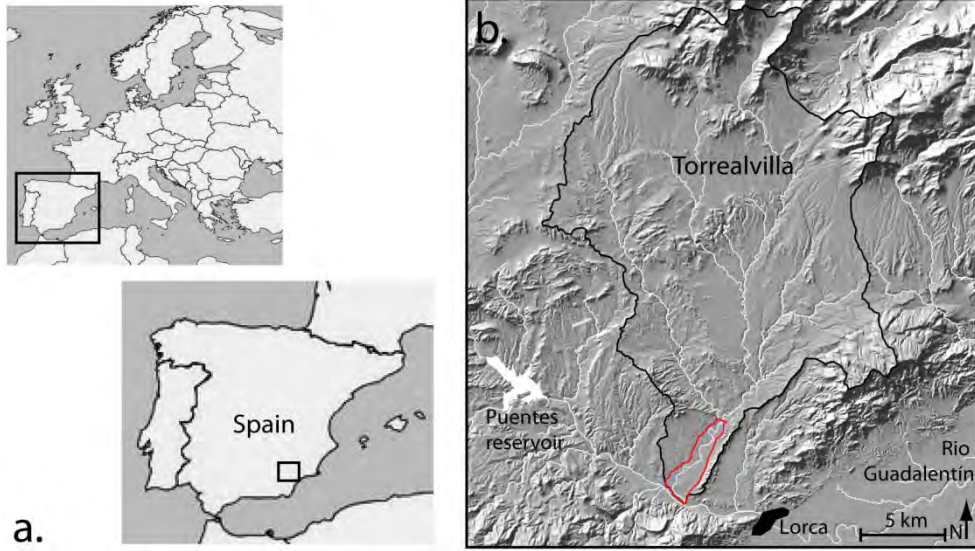
Fig. 4.1. Location of the study area: Torrealvilla catchment with indication of floodplain area (red line).

4.3. Methodology

4.3.1. LAPSUS model

The landscape evolution model LAPSUS (LAndscape ProcesS modelling at mUlti-dimensions and Scales) is described in section 1.8. In chapter 3, adaptations to the original model are described, which allow better representation of fluvial behaviour in the model. This enables simulation of alternating aggradation and incision of a river floodplain, in which the river can occupy multiple neighbouring cells. This adapted version of the model is used here, with the water erosion and deposition processes and, when and where relevant, the tillage erosion process activated. The main input is a Digital Elevation Model (DEM) which is described in section 4.5.2. In all runs, a time step of 10 y and spatial resolution of 30 m are used.

In LAPSUS, tillage erosion can be simulated as a separate process, calculated with a diffusion-type equation (Govers *et al.*, 1994) (Eq. 4.1), assuming a linear relation between soil flux (S_{till}; m³ a⁻¹) and slope:

$$S_{till} = c_{till} \cdot H \cdot \Lambda \hspace{4cm} \text{Eq. 4.1}$$

With c_{till} (m² a⁻¹) a tillage transport coefficient and *H* (m) the ploughing depth.

Eq. 4.1 is used to calculate the tillage translocation within tilled areas. In order to also account for the off-site effects of tillage, it is assumed that cultivation increases erodibility *K* (Eq. 1.10) and decreases the sedimentability *P* (Eq. 1.11) of the tilled areas (e.g.Veihe, 2002). Therefore, we have changed the *K* and *P* values for the tilled cells, now termed *K-till* and *P-till,* when and where tillage was performed.

4.3.2. Input data

Precipitation data
Average annual rainfall data (1951 – 1980) from four stations located in the area (Navarro Hervás, 1991) were used to derive a linear relation between elevation and mean annual precipitation (R^2 = 0.78, mean = 370mm). Effective rainfall (precipitation minus infiltration and evaporation) is much lower. López-Bermúdez (1990) calculated for the Segura Basin, of which the Torrealvilla is a subcatchment, that the mean evapotranspiration is ~92% of the mean annual rainfall and that two-third of the basin receives less than 20mm of effective rainfall (~5.3% of average annual rainfall). Because the Torrealvilla catchment is located in the southern and driest part of the Segura Basin, an effective rainfall of 5% of the average annual precipitation is assumed in this chapter. The resulting effective rainfall map (Fig. 4.2) is used as input.
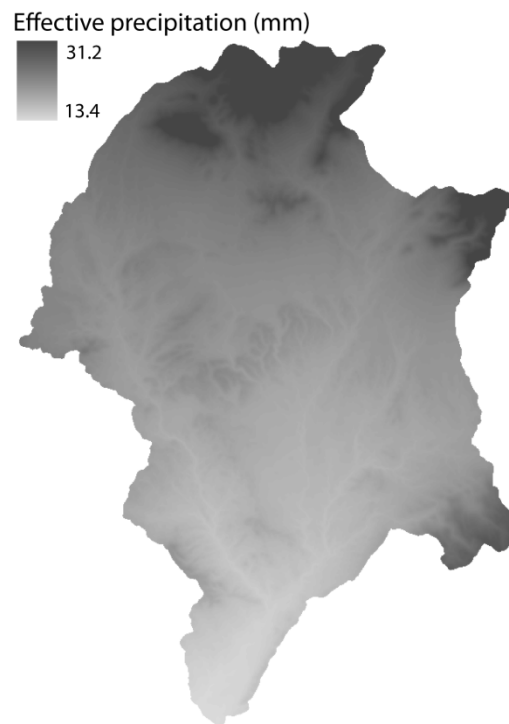

Fig. 4.2.Input effective precipitation (5% of average annual precipitation), linear interpolation with elevation.

Qualitative information about variations in palaeo-precipitation for SE Spain and the Western Mediterranean is abundant (e.g. Jalut *et al.*, 2000, Magny *et al.*, 2002, Pantaleon-Cano *et al.*, 2003, Carrión *et al.*, 2010). Quantitative palaeo-precipitation estimates, however, are rare. From a marine core in the Alboran Sea (ODP 976) Martín-Puertas *et al.* (2010) retrieved the Mg/Al ratio as an indicator of Iberian riverine input into the Alboran basin, which have been associated with changes in precipitation (Fig. 4.3a; grey line). Combourieu Nebout *et al.* (2009) quantitatively reconstructed palaeo-precipitation for the last 25000 y, based on the ODP 976 pollen record. This record is too long and, for the last 5000 y, too coarse to be used for this study.
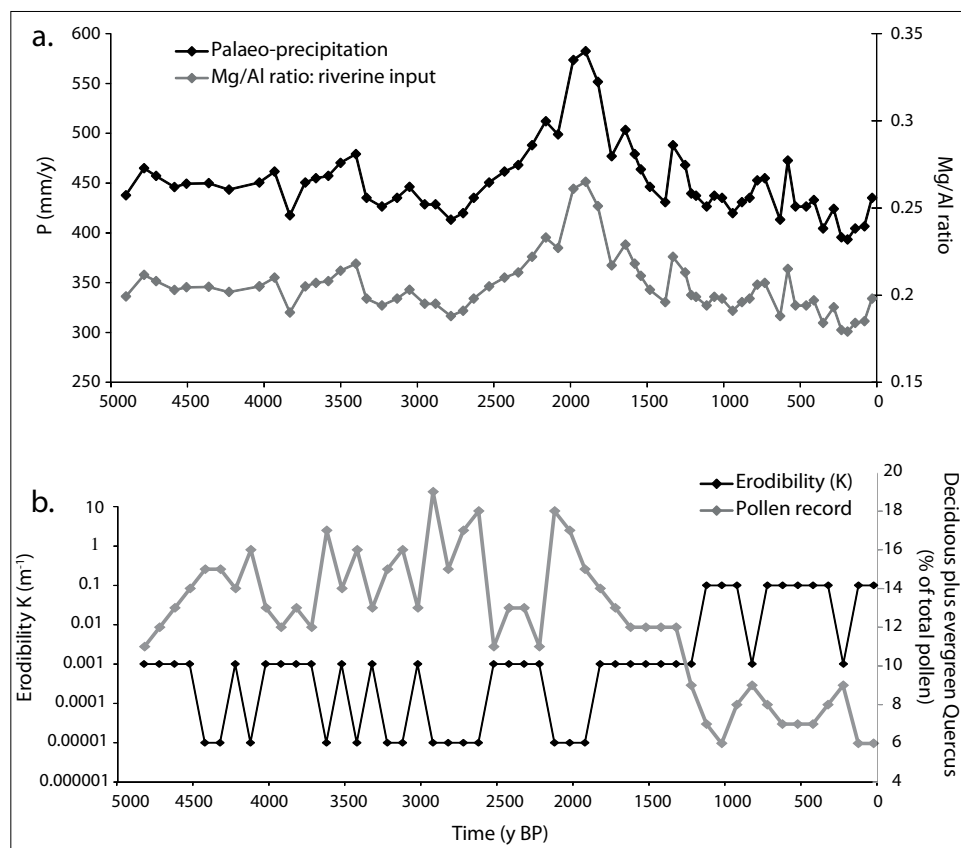
Fig. 4.3. a). Mg/Al ratio as indicator of Iberian riverine inputs, from marine core ODP 976 (Alboran Sea; Martín-Puertas et al., 2010); grey line and right y-axis) and input palaeo-precipitation scheme (black line and left y-axis) and b). Palaeo-vegetation record: percentage pollen of deciduous plus evergreen Quercus; from Baza sequence (Carrion et al., 2007); grey line and right y-axis) and input time-series of erodibility K representing variation in vegetation cover due to climate change (black line and left y-axis). Note that the value of K was changed step-wise (section 4.5.1), the K shown here is an example value.

In the reconstructed precipitation anomaly of Combourieu Nebout *et al.* (2009), a peak of ~300 mm y^{-1} occurs around 3000 y BP. We assumed that this peak correlates with the peak in riverine input (Martín-Puertas *et al.*, 2010), although the peak in the latter occurs later. This peak value of the Mg/Al ratio (0.265) is correlated with 300 mm more rainfall than at present, giving a ratio between yearly rainfall and Mg/Al ratio of 2530. The youngest value for Mg/Al ratio (0.198) is related to current rainfall (370 mm y^{-1}), giving a lower ratio between yearly rainfall and Mg/Al ratio of 1870. The average of these two ratios (2200) is used to convert all Mg/Al ratio values to palaeo rainfall values.

The resulting palaeo-precipitation time-series (Fig. 4.3a, black line) is used as input in this chapter. The peak from ~2500 to ~2000 y BP represents the so called Iberian Roman Humid Period, recognised by among others Martín-Puertas *et al.* (2008).

Vegetation and land use data

Variations in vegetation over time are split into two parts: (i) change in vegetation cover due to climate change (Fig. 4.3b; grey line), reflected in higher and lower erodibility (*K*) and sedimentability (*P*) values (Fig. 4.3b; black line); and (ii) change in land use due to human activity. The latter are used as input for tillage erosion simulations.

For the first – change in vegetation cover due to climate change – we assume the same trends over the entire catchment, hence no spatial variability in vegetation change is assumed. Deciduous and evergreen *Quercus* pollen were supposed to represent a (Mediterranean) forest type of vegetation. To convert the pollen values (Carrion *et al.*, 2007) to values for *K*, two rules were applied: (i) if pollen values of deciduous plus evergreen *Quercus* exceeded 15%, vegetation cover was assumed to be thick enough to protect the soil from erosion and input *K* values were divided by 100. (ii) If these pollen values decreased below 8%, input *K* values were multiplied by 100 and *P* values were divided by 100. This is because sedimentability is assumed to be higher (easier) under vegetation and, conversely, sediment is entrained longer when vegetation is absent. The amplitude of the changes (times 100 and divided by 100) are based on earlier experience with the model parameters *K* and *P* (Temme *et al.*, 2009).

For the second – change in vegetation due to human activity - agriculture, and thus tillage erosion, is assumed to have occurred in areas where archaeological remains have been found. The most important periods of human impact on the land for SE Spain and the Torrealvilla area in particular are summarized in chapter 2. Fig. 4.4 shows maps for locations of tillage erosion for three time-frames: the Roman period (~2000 to ~1600 y BP; Fig. 4.4a), the Arab period (~1200 to ~700 y BP; Fig. 4.4b); and the modern areas of agriculture (Fig. 4.4c), based on cereal cultivation of the CORINE land use map (EEA, 2000).
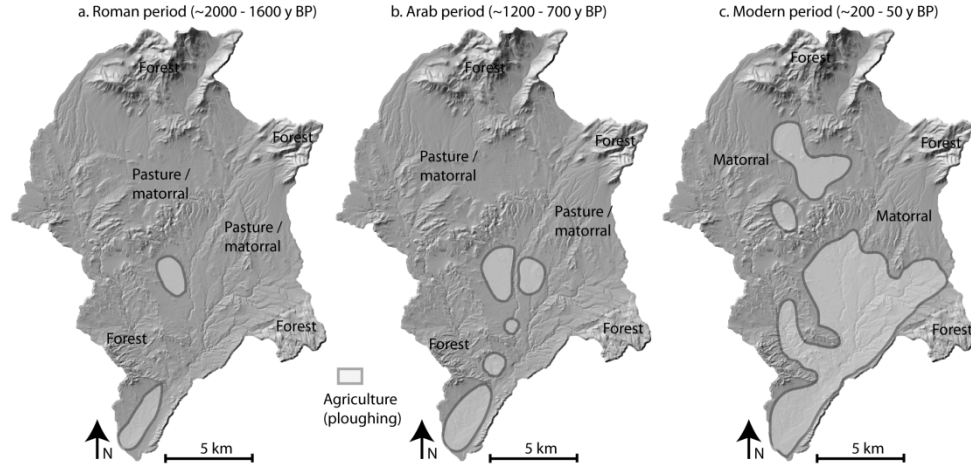
Fig. 4.4. Areas with agriculture in the Roman (a), Arab (b) and Modern (c) periods. Ploughing is assumed to have taken place in these areas. These maps are used as model input..

Values for ploughing depth (H, Eq. 4.1) were set to 0.10 m during Roman times (White, 1967), 0.20 m during Arabic times (Eiroa Rodriguez, 2011) and 0.40 m during modern times (Moret *et al.*, 2007). Values for c_{till}, K-till and P-till were determined during model calibration. For simplicity, we assumed that soil depth does not limit erosion in the entire catchment. This might not be true for the higher, rocky outcrops in the northern part of the catchment.

4.3.3. Overview of methodology

In chapter 3 the LAPSUS model was adapted to include fluvial processes. In that development phase, parameter values were chosen based on expert judgment and results were evaluated in a qualitative way, using an artificial DEM. In the present chapter, the main aim is to calibrate the adapted LAPSUS model for the Torrealvilla catchment. Fig. 4.5 shows an overview of the methodology followed in this chapter, divided in a sensitivity analysis phase and a model calibration phase. In the first part, the sensitivity of the adapted LAPSUS parameters was evaluated (see section 4.4), so that only the most sensitive model parameters would be included in the second part. The second phase is the actual model calibration. The focus of this chapter is on the second part (see section 4.5), in which model results are compared to observed erosion and aggradation sequences in the Torrealvilla study area.
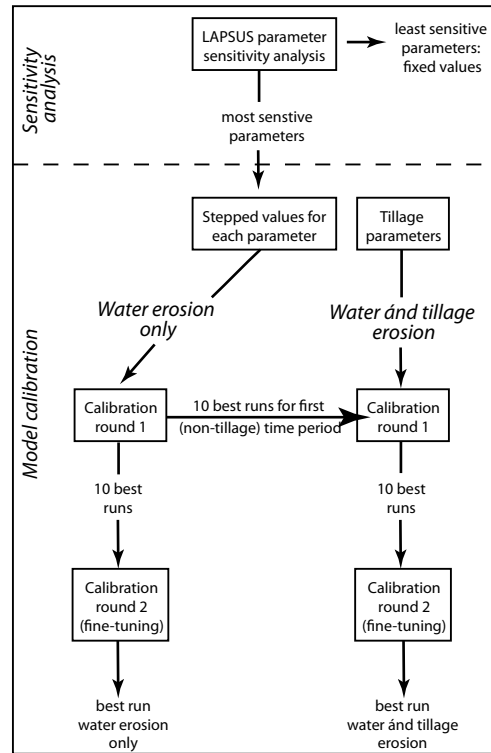
Fig. 4.5. Scheme of methodology.

4.4. Sensitivity of LAPSUS parameters

To quantitatively evaluate the sensitivity of the adapted LAPSUS parameters, a Monte Carlo approach was used. For all runs, temporal extent was 500 y in order to keep runtime reasonable and rainfall was kept constant.

In each run, one parameter was kept constant at the mean value of its distribution, while all other parameters were varied randomly. These parameters had a value between a maximum and a minimum value, chosen so that a wide range of probable values was covered (Table 4.1). Distributions of randomly generated parameters are uniform, thus each value between the minimum and maximum is equally likely to be selected. This approach was used for each parameter separately (N = 5000; meaning N = 500 for each parameter). Simulated average elevation change for the floodplain area was used as model output variable. SPSS (PASW Statistics 19) was used for the analyses. Histograms of the outcomes were analyzed. In this analysis, a smaller variance of the outcome points to a larger influence of the parameter on model results.

Table 4.1. Mean, minimum and maximum values of LAPSUS parameters used in sensitivity analysis

Parameter	Mean	Minimum	Maximum
m-slope	1.05	0.1	2
m-river	2.25	1.5	3
n-slope	1.05	0.1	2
n-river	2.25	1.5	3
p-slope	3.00	1	5
p-river	1.00	0	2
Threshold Q1*	255	10	500
Threshold Q2*	1050	100	2000
K	0.005	0.000001	0.01
P	0.005	0.000001	0.01

* Extra constraint: Threshold Q2 > Threshold Q1

4.4.1. Sensitivity analysis results

Table 4.2 shows the results of the histogram analysis. The results indicate that four parameters most influence the outcome: *m*-river, *n*-river, *n*-slope and *m*-slope. The variance of the outcome (mean elevation change in the floodplain) is smallest for the these parameters.

Table 4.2. Results of histogram analysis

Constant parameter	Mean	St. Error	Variance	N
m-slope	0.40	0.051	1.27	493
m-river	0.11	0.055	1.51	494
n-slope	0.41	0.062	1.89	488
n-river	0.28	0.064	2.03	490
p-slope	0.22	0.074	2.65	487
p-river	0.22	0.073	2.63	490
Threshold Q1*	0.24	0.076	2.82	488
Threshold Q2*	0.30	0.076	2.82	489
K	0.26	0.076	2.81	491
P	0.24	0.070	2.41	488

4.5. Water and tillage erosion in the Torrealvilla catchment

The LAPSUS model was calibrated against observed erosion – deposition – erosion sequences in the floodplain area of the study site. To evaluate the possible influence of tillage erosion, the model was calibrated separately for (i) only water erosion processes and (ii) water erosion and tillage erosion processes combined.

4.5.1. Calibration procedure

Calibration of the model on the Torrealvilla catchment was performed in a step-wise procedure (see Fig. 4.5). Parameters that had little influence on the model outcome, were given constant values. Values for thresholds $Q1$ and $Q2$ were set $225 \cdot 10^3$ m^3 y^{-1} and $450 \cdot 10^3$ m^3 y^{-1} respectively based on preliminary runs for water distribution, which showed that areas (cells) with values above threshold $Q2$ would be considered as rivers and areas (cells) with values less than threshold $Q1$ would be hillslopes. Values for convergence factor p were set to 2 for hillslopes and 0 for rivers, based on chapter 3.

The four parameters that have most influence on model outcome were varied in steps (Table 4.3). Erodibility factor K and sedimentability factor P were also varied, based on earlier experience with the model (e.g. Schoorl *et al.*, 2002, Temme *et al.*, 2009, Temme and Veldkamp, 2009). Values used for the six parameters in the first calibration round are shown in Table 4.3, giving a total of 256 possible combinations for water erosion processes only.

Because tillage erosion does not start before the second time period (from 1500 y BP), it does not affect the first time period (4800 – 1500 y BP; see Table 4.4). Therefore, the ten best parameter sets after calibration with water erosion for the first time period (4800 – 1500 y BP) were taken as a start for the water plus tillage erosion calibration (see Fig. 4.5). In the calibration of water plus tillage erosion, three tillage parameters were varied in steps, giving a total of 180 parameter sets (Table 4.3).

In the second calibration round for water erosion, additional values for *m-* and *n-slope* (value of 1.00) and P (value of 0.001) were introduced to the parameter sets. This was based on the results of the best 10 runs for the first calibration round, which suggested that for these parameters, performance gains were possible.

Table 4.3. Values used for the first round of model calibration for water erosion and for water plus tillage erosion processes

Parameter	Values			
Water erosion parameters				
m-slope	0.50	1.50		
m-river	1.50	2.00	2.50	3.00
n-slope	0.50	1.50		
n-river	1.50	2.00	2.50	3.00
K	0.0001	0.01		
P	0.0001	0.01		
Tillage parameters				
c_{till}	0.05	0.5		
K-till	1	10	100	
P-till	0.001	0.001	0.01	

4.5.2. Evaluation criteria and data

Calibration results were evaluated both qualitatively and quantitatively. In chapter 2, three main phases of incision and aggradation were recognised. Here, evaluation focuses on the lower floodplain area (~4.35 km^2; see Fig. 4.1) because data (ages and terrace remnants) are from this area. For qualitative calibration, model simulations should display a sequence of first incision, then aggradation and finally incision again (see Table 4.4). In order to be able to quantitatively compare model simulations and landscape dynamics, volumes and average elevation changes were calculated. For this purpose, a palaeoDEM was constructed for each incision and aggradation phase:

-   As a starting landscape, a palaeoDEM with infilled valleys up to the highest terrace level was constructed, which was estimated to have an age of ~4800 y BP based on a sequence of dated sediments.
-   Little information is available about the extent of subsequent incision. We assumed that incision occurred as a V-shaped, elongated trench to the depth of the current stream, where the lowest dated sediments were found. This palaeoDEM represents the landscape at ~1500 y BP.
-   For the next aggradation phase, which ended ~400 y BP, a palaeoDEM with infilled valleys up to the next (lower) terrace level was constructed.
-   The final erosion phase ended at current times and the present DEM was used.

In Table 4.4, the calculated average elevation change and volumes of aggradation or incision in the floodplain area are given. These values are used to quantitatively evaluate model simulations in each time period.

Table 4.4. Average reconstructed elevation change and volumes of aggradation or incision at the end of the time period for the floodplain area calculated from constructed palaeoDEMs

Time period (y BP)	Process	Average elevation change (m)	Floodplain volume ($\cdot 10^6 \, m^3$)
4800 – 1500	Incision	-4.56	-19.8
1500 – 400	Aggradation	1.50	6.5
400 - 50	Incision	-1.09	-4.7

4.5.3. Results for water erosion only

Calibration for water erosion only resulted in six runs that showed the correct process sequence: incision during the first period (4800 – 1500 y BP), aggradation during the second period (1500 – 400 y BP) and incision from 400 y BP until present. However, eroded and deposited volumes were much smaller than those estimated from the palaeoDEMs (results not shown). Subsequently, each time period was evaluated separately. In Fig. 4.6a the average elevation change of the floodplain over time is shown for the ten best simulations for all time periods. Fig. 4.6b shows the ten best simulations of the second calibration round for water erosion processes only (no tillage).
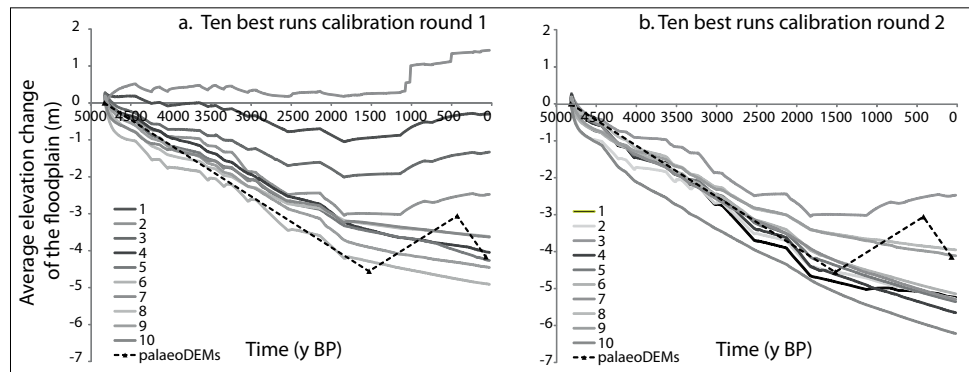

Fig. 4.6. Average elevation change of the floodplain area over time for the ten best runs of the first (a) and the second (b) calibration round for water erosion only.

4.5.4. Results for water plus tillage erosion

When calibrated using any of the best ten runs for the first time period, adding tillage erosion during the second and the third time periods resulted in increased deposition (or decreased erosion) compared with model runs without tillage erosion (Table 4.5). Thus tillage erosion adds to deposition in the floodplain in the model set-up used in this study.

Table 4.5. Average elevation change of the floodplain area (m) for the ten best runs of water erosion only and the same ten runs with tillage erosion (best run for each)

Time period	Average elevation change (m)	
(y BP)	*Water erosion*	*Water + tillage erosion*
4800 – 1500	-4.09	-3.80
1500 – 400	-0.34	-0.23
400 - 50	-0.13	-0.11

The average elevation change of the floodplain for all simulations with tillage is shown in Fig. 4.7a. Fig. 4.7b shows the best ten simulations with tillage; for comparison, it also shows the best run without tillage. All of the runs with tillage in Fig. 7b start with the set of parameters that gave the best simulation without tillage and add the tillage option. For the water runs that simulated erosion correctly for the first time period, the activation of tillage erosion did not yield a strong enough increase in deposition.

When the aggradation (second time period) of the best water and best tillage runs are compared, tillage almost doubles (factor 1.8) the simulated average floodplain elevation change. However, as can be seen in Fig. 4.7b, the simulated amounts of floodplain incision and aggradation are not the same as those measured from the palaeoDEMs.
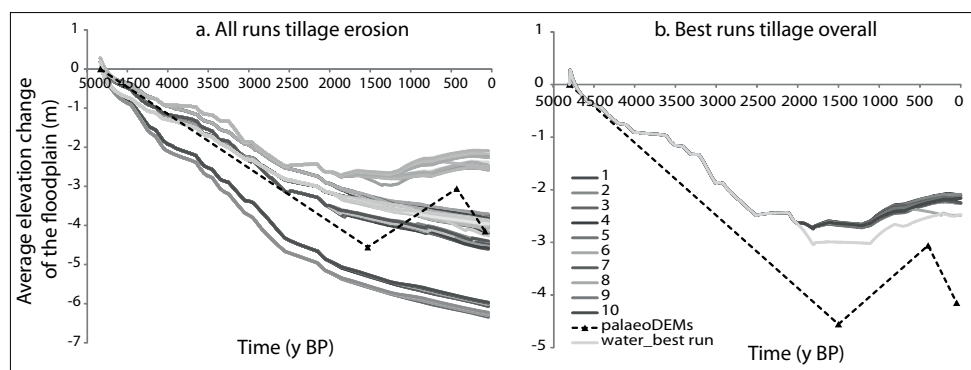

Fig. 4.7.Average elevation change of the floodplain area over time for a). all runs; and b). the ten best runs for all time periods for water plus tillage erosion.

4.6. Discussion

4.6.1. Case study results and assumptions

As shown in Fig. 4.6, a major result is that the observed sequence of processes (erosion – aggradation – erosion) was simulated correctly by the model. The results show that tillage erosion, being a high frequency (each year), but slow and low impact process, has a considerable impact in terms of sediment accumulation in the floodplain. However, individual runs show that neither water erosion alone, nor water plus tillage erosion processes could exactly reproduce the reconstructed volumes of eroded, deposited, and again eroded sediments. This implies that other processes, not included in the model, could have played an important role, such as lateral erosion or landsliding, including undercutting of steep gully side walls (Hooke, 2000b), or the effects of land use change processes other than tillage. In this chapter, we focussed on tillage as a major human influence on erosion and deposition dynamics. However, other human impacts could have played a role, in particular land use change (e.g. Kosmas *et al.*, 1997, Coulthard and Macklin, 2001, Lang, 2003, Bakker *et al.*, 2008) such as deforestation and burning on steep slopes (Descroix and Gautier, 2002) with related changes in *K* and *P* values. In addition, grazing might have led to degraded vegetation cover and increased *K* values (e.g. Carrión *et al.*, 2010). These processes have not been modelled explicitly, although changes are partly included in the palaeo-vegetation record, which is based on pollen data.

Alternatively, individual extreme events could have been important. As the model uses average annual precipitation as input, such events are not accounted for in this chapter. The effect of extreme events could either be increased erosion in gullies (Hooke and Mant, 2000, Valentin *et al.*, 2005) or increased deposition of eroded material in the floodplain (e.g. Kirchner *et al.*, 2001, Tomkins *et al.*, 2007) or both, depending on event and catchment characteristics (for example vegetation) at the time of the event (Tucker and Bras, 2000). We consider the effect of individual extreme events on topography over longer time-scales a topic of continuing interest.

An independent source of longer term measurements of erosion rates is not available for the Torrealvilla catchment itself. However, the nearby Puentes reservoir (Fig. 4.1), which was built in 1884 has received an average of 2.12 t ha^{-1} y^{-1} of sediments over the last 100 y (De Vente, 2009). Our simulation results for the entire Torrealvilla catchment show erosion rates between 20.5 t ha^{-1} y^{-1} for the last 100 y and 11.2 t ha^{-1} y^{-1} for the entire 4750 years. The Torrealvilla catchment (~250 km^2) is about one-quarter the size of the ~992 km^2 Puentes catchment, and would therefore be expected to have higher erosion rates (Hooke, 2000b). The simulated values are still somewhat high but at least of similar magnitude as the observations. Estimates of sedimentation rates from other reservoirs in SE Spain range from 1.5 to 26.2 t ha^{-1} y^{-1} (De Vente, 2009).

Qualitative evaluation

We can further evaluate, qualitatively, the best simulation with only water erosion. Fig. 4.8 shows profiles of a cross-section from the palaeoDEMs in the lower part of the floodplain area. This shows that from 4800 – 1500 y BP, the model simulates incision, although only for part of the cross-section; from 1500 – 400 y BP, partial infilling of the formerly eroded volume is simulated; from 400 – 50 y BP model simulations show little change, while erosion is expected, based on the palaeoDEM reconstructions. Thus, for two of the three time periods, model simulations qualitatively show the expected erosion and sedimentation dynamics when averaging over the entire floodplain area, as well as on the cross section scale.

None of the simulations could reproduce erosion in the last time period (t = 400 – 50 y BP). As mentioned before, this might be attributed to the lack of relevant processes in the model, especially lateral erosion or valley widening.
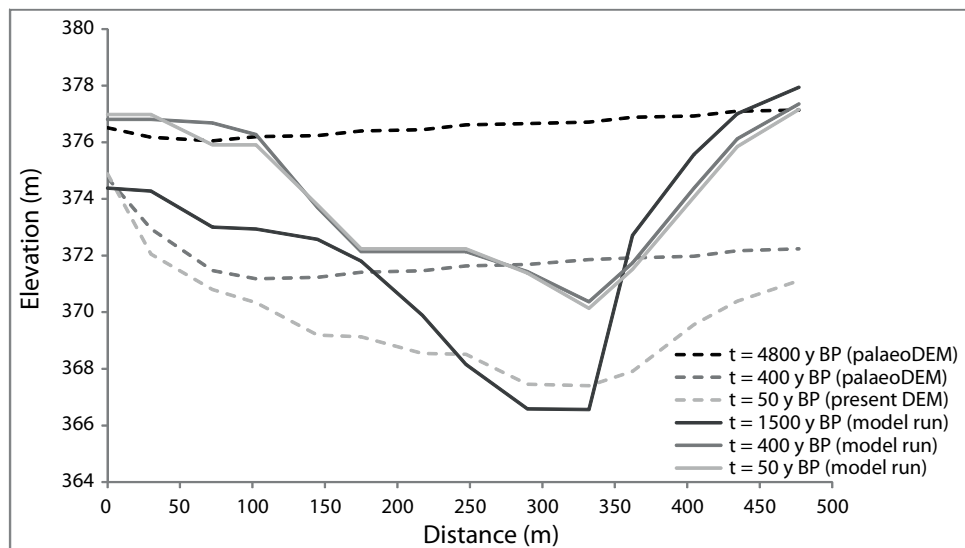
Fig. 4.8.Cross-section profile of best run for water erosion only; model output is given in solid lines, dashed lines are cross-sections derived from palaeoDEMs for comparison.

The case study results are inherently context dependent, inasmuch as they are restricted to the local topography, DEM resolution, temporal resolution, quality of proxy data used for time series input and so forth. For example, values for palaeo-vegetation (erodibility factor *K*) were difficult to estimate, because the parameter is a model- and scale-specific, lumped factor. The same applies to the *K* and *P* values used for the tilled areas. The use of other proxies might lead to different model results. Another source of uncertainty is the reconstructed palaeoDEMs, which we used to estimate the eroded and deposited sediment volumes in the floodplain area. This is a common problem if past topography is

used (e.g. Coulthard *et al.*, 2002, Tucker, 2009) and no simple solution exists. However, although these input issues need to be addressed for each case study area individually, our method of using a LEM and incorporating tillage erosion is valid for any area.

4.6.2. Model limitations

The LAPSUS model features some limitations that might be assessed in future studies. As already mentioned, not all processes that might be relevant in the field, are included in the model, most importantly lateral erosion or valley widening (Hooke, 2000b). The model has a landslide module, which was not activated in the present chapter, that could prevent gully side walls from becoming oversteepened.

Furthermore, there is no explicit feedback in the model between vegetation (in terms of erodibility factor *K*) and the water balance (Claessens *et al.*, 2009). For example, less vegetation could lead to less infiltration and increased runoff; these processes are not coupled in the model. Thus, transport capacity (Eq. 1.8) is not altered with vegetation.

Work is in progress to keep track of spatial and temporal dynamics of erodibility and sedimentability. For example, easily eroded material could be deposited downstream, where it still would be easily erodible. However, the current model version does not keep track of these dynamics and the deposited material is assigned the erodibility of the location (cell) where it was deposited. In a partial solution to this problem that could be used in LAPSUS, another LEM - CAESAR - incorporates and keeps track of different grain sizes (Coulthard and Van De Wiel, 2007).

Finally, in chapter 3 the LAPSUS model was adapted to incorporate fluvial behaviour. The adaptation defines cells as hillslope, river or a transition between the two. In the current model versions, the threshold discharge values are simply based on the locations in the field where streams start. They are, however, spatially dynamic in the model, for example as a gully erodes headward, its cells may also become river cells. Other methodologies to derive the threshold values and locations that are more sophisticated or widely applicable could be developed in future research.

4.6.3. Methodology

For reasons of modelling time, a full optimisation was not performed, although many parameter combinations were included in the calibration procedure. Thus, the best combination of parameter values for calibration may have been missed. However, it was not the objective of the chapter to obtain a best fit for the palaeo-sediment dynamics. Rather, the palaeo-sediment data enabled us to explore model performance and to analyse the potential contribution of tillage erosion in the evolution of the case study catchment.

Simulation studies on the effect of tillage erosion have previously concluded that the impact of tillage should be taken into account in landscape evolution studies in addition to water erosion (e.g. Govers *et al.*, 1996). However, the simulation results for the Torrealvilla case study area indicate that our procedure for incorporating tillage erosion could not entirely account for the observed aggradation in the floodplain area. This apparent contradiction should be viewed in the context of spatial scale. Studies that focussed on tillage erosion, were conducted on the field or hillslope scale (Govers *et al.*, 1996, Van Oost *et al.*, 2000). The Torrealvilla catchment, however, is a large (~250 km²) catchment. In our analysis, we focus on the lower floodplain area. Tillage erosion as it is represented in the LAPSUS model directly affects the tilled slopes and sediments fill local depressions. Eventually, these sediments reach the floodplain area, but in an indirect way and depending on connectivity within the larger catchment and possible changes in sediment storage within the catchment (Trimble, 1981, 1983). Thus, the simulation results suggest that tillage erosion is less important on the (large) catchment scale than on individual hillslopes. This is a novel result that may add to our understanding of landscape evolution over a range of scales.

In our model assumptions, no base level change or tectonics were included. The simulation results show a sequence of alternating erosion and sedimentation, which is thus possible without tectonics as external driver. The simulated process alternation is due to changes in rainfall and, more importantly, vegetation. These changes in vegetation, based on pollen records, can be natural or human induced (for example deforestation, grazing, etc.). In this respect, the model does not distinguish between the two. However, we included tillage as a separate, obviously human, process, including changes in vegetation for the cultivated (tilled) areas.

Many authors have attempted to relate erosion and sedimentation dynamics to either natural or human causes or both (Hooke, 2000a, Hooke, 2006, Knox, 2006, Fuchs, 2007, Dearing *et al.*, 2008, Houben *et al.*, 2009). Quantification, if included, is usually done on the basis of dated sediment archives and is therefore fragmented in time, or consists of only net values (e.g. Quine *et al.*, 1997). In those cases, sequences of alternating erosion and sedimentation are not assessed. However, landscape evolution over longer time-scales (millennia) is clearly influenced by such cycles. Modelling over longer time spans attempts to stretch the quantification of erosion and sedimentation dynamics over the entire time period involved (e.g. Coulthard and Macklin, 2001, Coulthard *et al.*, 2005, Verstraeten and Prosser, 2008, Temme and Veldkamp, 2009). A dynamic landscape evolution model such as LAPSUS, including complex response feedbacks is needed to capture the sequences of alternating erosion and sedimentation processes.

4.7. Conclusions

In this chapter, we analysed the potential contribution of tillage erosion to observed erosion and sedimentation dynamics on a millennial time-scale. Using the dynamic landscape evolution model LAPSUS we were able to simulate an alternating sequence of erosion – aggradation – erosion, that is important on longer (millennial) time-scales. We explicitly included tillage as a separate process and evaluated model simulations with or without tillage erosion. Generally, model results for the ~250 km^2 Torrealvilla case study catchment show that tillage erosion adds to deposition in the lower floodplain area during periods of occupation. However neither water erosion nor water plus tillage erosion could exactly reproduce the observed amounts of erosion and sedimentation for the case study area. This implies that other processes, not included in the model, play a role, or that input assumptions and uncertainties, such as reconstructed palaeoDEMs and vegetation reconstructions, are incorrect. Simulation studies that focussed on tillage erosion on the field or hillslope scale conclude that tillage erosion is an important process. The apparent contradiction with the present simulation results indicates a scale effect; on hillslopes, tillage significantly contributes to erosion and fills local depression. On the catchment scale, sediments from tillage erosion eventually reach the floodplain area, where they contribute to aggradation, but to a lesser extent than on hillslopes, also depending on the connectivity within the catchment.

This is the first time that tillage erosion has been explicitly included in a landscape evolution model on a millennial time-scale and large catchment scale. Further research on the same time-scale in other areas is needed to refine the procedure. Also, further investigations on the effects of spatial configuration and connectivity would be interesting.

Chapter 5

Exploring effects of rainfall intensity and duration on soil erosion at the catchment scale using OpenLISEM

In semi-arid areas high-intensity rainfall events are often held responsible for the most soil erosion. Long-term landscape evolution models usually use average annual rainfall as input, making the evaluation of single events impossible. Event-based soil erosion models are better suited for this purpose, but cannot be used to simulate longer time-scales and are usually applied to plots or small catchments. In this chapter, the OpenLISEM event-based erosion model was applied to the medium sized (~50 km²) Prado catchment in SE Spain. Our aim was to (i) test the model's performance for medium sized catchments; (ii) test the ability to simulate four selected typical Mediterranean rainfall events of different magnitude, and (iii) explore the relative contribution of these different storms to soil erosion using scenarios of future climate variability.

Due to large differences in the hydrologic response between storms of different magnitudes, each event needed to be calibrated separately. The relation between rainfall event characteristics and the calibration factors may help in determining optimal calibration values. Scenario calculations show that, although ~50 % of soil erosion occurs as a result of high frequency, low intensity rainfall events, large magnitude, low frequency events potentially contribute significantly to total soil erosion. The results illustrate the need to incorporate temporal variability in rainfall magnitude-frequency distributions in landscape evolution models.

5.1. Introduction

Erosion and deposition are important processes that shape the landscape over time. Simulating landscape evolution over long time-scales is often done using Landscape Evolution Models (LEMs, e.g. Coulthard, 2001, Tucker and Hancock, 2010) in which erosion and sedimentation processes form the core of the model. Over shorter time-scales, erosion and deposition are simulated with event-based models, that can be process-based or empirical. Many event-based models exist and have been compared in various reviews (e.g. Jetten *et al.*, 1999, 2003, Merritt *et al.*, 2003, Jetten and Favis-Mortlock, 2006). Spatial scales that are assessed vary widely from catchment to hillslope and plot, with event-based models usually being applied to smaller catchments than landscape evolution models.

In semi-arid areas highest soil erosion rates have been observed as a result of single high intensity but low frequency rainfall events. Although exceptions exist (Coulthard *et al.*, 2002), most landscape evolution models use average annual rainfall as input, making the evaluation of single events impossible. Event-based models are better suited for this purpose.

In semi-arid South-East Spain, total rainfall is generally low (~300 mm y^{-1}), but very variable and unevenly distributed over the year with rainfall events occurring mainly in spring and autumn (Navarro Hervás, 1991, Bracken *et al.*, 2008). Future soil erosion depends, among other factors, on temporal rainfall patterns and therefore will be affected by climate variability. Projections of climate variability generally predict a decrease in precipitation in the subtropics, but an increase in rainfall intensity and longer periods between rainfall events (Christensen *et al.*, 2007, Meehl *et al.*, 2007, Giorgi and Lionello, 2008). Given the relative importance of extreme rainfall events for erosion and sediment export, simulation studies are required to assess the implications of climate change for soil erosion.

The Limburg Soil Erosion Model (LISEM) is a physically based model simulating water erosion during and immediately after a rainfall event (De Roo *et al.*, 1996a, b). Model principles are detailed in section 1.8. Although initially developed for an area in the south of The Netherlands, LISEM has been applied world-wide (e.g. Jetten *et al.*, 1996, Hessel *et al.*, 2003, Boer and Puigdefábregas, 2005, Hessel *et al.*, 2006, Vigiak *et al.*, 2006). LISEM was designed to simulate agricultural catchments of sizes ranging from 1 ha up to ~10 km^2 (De Roo and Jetten, 1999). Consequently, scales that are modelled are mostly small catchments (45 and 69 ha, De Roo and Jetten, 1999; 2 km^2, Hessel *et al.*, 2003; 2 and 5.7 km^2 Hessel *et al.*, 2006; 2.9 km^2, Takken *et al.*, 1999).

It is our objective in this chapter, as a first step towards including event information into LEMs, to apply an event-based model to a medium sized catchment and evaluate its performance for simulating rainfall events of different magnitudes and to assess the contribution of rainfall events of different magnitude and frequency to total annual soil loss.

In this chapter, a new open source version of LISEM (OpenLISEM[1]) is applied to the ~50 km[2] Prado catchment, located in SE Spain. One of the reasons for the development of OpenLISEM was the ability to deal with larger areas: technically there is no catchment size limit, but the cell size and time step must remain small (< 1 ha and < 1 min) because of certain model principles (see section 1.8). Our specific aims were i) to test the performance of the OpenLISEM model for simulating erosion and deposition in a relatively large catchment; ii) to test the model's ability to simulate storms of different magnitudes of rainfall intensity and duration; and (iii) to explore the relative contribution of the different magnitude storms to erosion using scenarios of possible future climate variability.

5.2. Research area

The study was conducted in the semi-arid region of South-East Spain. The research area and its general characteristics have been described in section 1.7. The Prado catchment forms a tributary of the Rambla Torrealvilla, upper Guadalentín river, upstream of the town of Lorca in Murcia Province (Fig. 5.1; UTM 30N 614800; 4171000).

Several erosion related studies have been carried out in the study area, e.g. during the EU funded MEDALUS projects (Bull *et al.*, 1999; Hooke and Mant, 2000; Kirkby and Bull, 2000; Bracken and Kirkby, 2005; Hooke *et al.*, 2005; Kirkby *et al.*, 2005; Hooke, 2007). Shannon *et al.*(2002) modelled sediment transport for the nearby, but lithologically different, Nogalte catchment. Boer and Puigdefábregas (2005) applied LISEM to a nearby small catchment in Almeria province, South-East Spain, to assess the effects of vegetation patterns on erosion.

---

[1] Please find OpenLISEM at: <u>http://sourceforge.net/projects/lisem/</u>
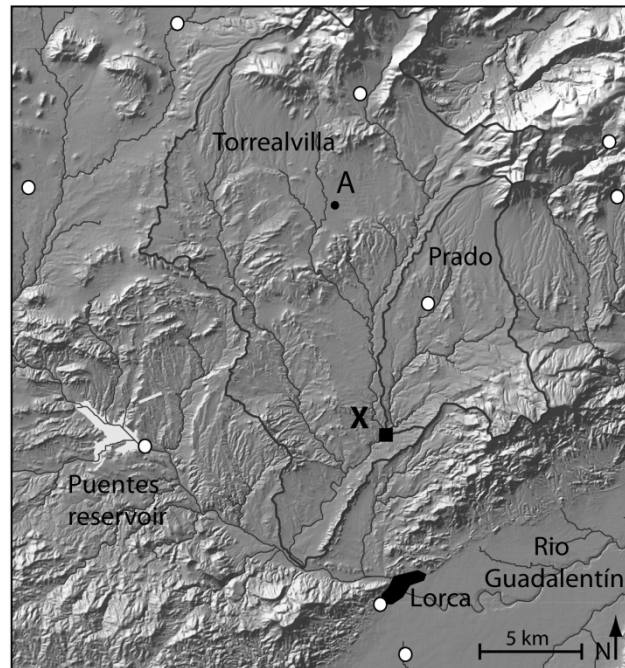
Fig. 5.1. Prado catchment. X = location of discharge and rainfall measurement devices at Prado outlet; A = Alhagüeces rainfall station; white dots are other rainfall stations used for this study.
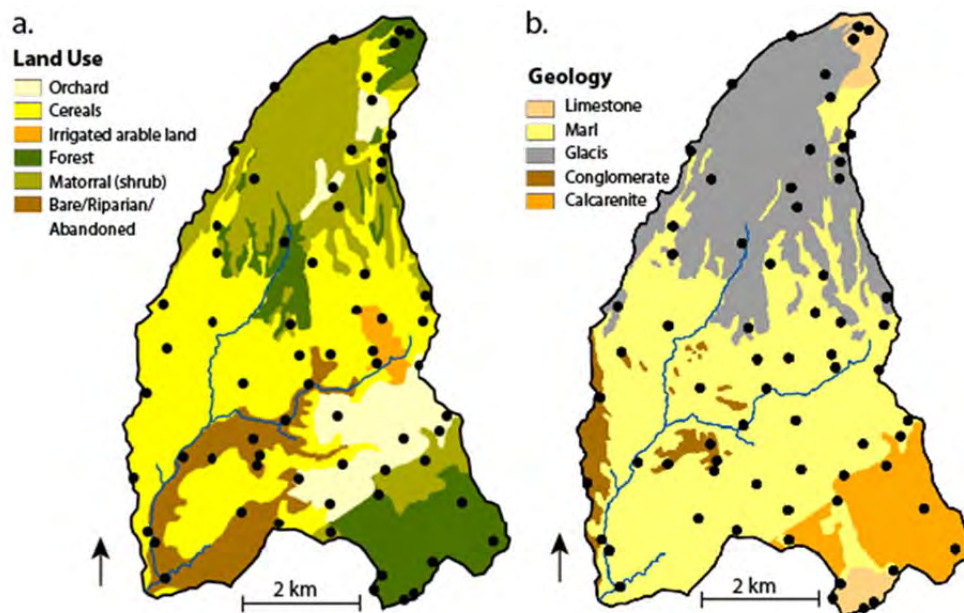

Fig. 5.2. CORINE Land use map (a) and geological map (b) of the Prado catchment with major ramblas indicated. Black dots are measurement and sampling locations.

112

5.3. Methods

5.3.1. OpenLISEM model

The OpenLISEM model is a physically based runoff and soil erosion model, based on the original Limburg Soil Erosion Model (LISEM) (De Roo *et al.*, 1996a; Jetten and De Roo, 2001). It simulates runoff and erosion during and immediately after a rainfall event. The model is described and model equations are given in section 1.8.

Such an event-based model is a logical choice for the study area in South-East Spain where rainfall mainly occurs in separate events. Moreover, OpenLISEM gives spatial output for each time step of all hydrological and erosion variables, which allows us to not only evaluate discharge and sediment at the outlet, but also to assess erosion and sedimentation patterns.
Maps with a cell size of 20 m were used and the calculation time step *dt* was set to 15 s. The channel option of OpenLISEM is used in this chapter to represent the permanent gullies occurring in the area.

5.3.2. Input parameters

Input parameters for OpenLISEM were measured in April and September / October 2009. We used a land use map based on the CORINE 2000 land cover classification (EEA, 2000), in which the original 44 CORINE land cover classes were aggregated to a total of 6 (Fig. 5.2a). The geological map (scale 1:50 000; IGME, 1981) was aggregated to 5 classes (Fig 5.2b); for example all types of marls (sandy, clayey, with silica, etc.) were grouped together. Based on these two maps, a total of 67 locations were visited for sampling and measurements (Fig. 5.2), of which 52 locations provided useful data for parameters based on the geological map and 56 for parameters based on the land use map. At each location, the following parameters were measured or sampled:

- Leaf area index (*LAI*): Area of representative plant leaf divided by estimated total number of leaves of each species and amount of that species (e.g. number of trees) on a representative specified surface (e.g. 5 x 5 m plot). Total *LAI* is the sum of the *LAI*s of all species.
- Vegetation cover (fraction): estimated vegetated cover within one square metre; average of three estimates per measurement site;
- Vegetation height: measured with measuring tape; average height of each species per measurement site;
- Random roughness: standard deviation of micro-relief, measured in the field with a pinboard (Wagner and Yu, 1991; Jester and Klik, 2005)

- Stone cover (fraction): estimated area covered by stones within one square metre; average of three estimations per measurement site;
- Saturated soil moisture content (or porosity; θ_s): Ring samples (100 cc) were taken in the field. They were saturated by putting them in water for a minimum of three days and weighed afterwards (W_{sat}). After oven-drying them for at least 24h at 105 °C, they were weighed again (W_{dry}) Saturated moisture content was calculated using Eq 5.1:

$$\theta_s = \frac{W_{sat} - W_{dry}}{V \cdot \rho_{water}}$$

Eq. 5.1

With V the volume of soil sample (m^3) and ρ_{water} water density (kg m^{-3}).

- Initial soil moisture content: field measurements with hand-held TDR (Time Domain Reflectometry) device (Trime TDR probe, IMKO, Ettlingen, Germany); average of at least three measurements per measurement site;
- Soil cohesion: Pocket vane tester (Eijkelkamp Agrisearch Equipment, The Netherlands) measurements; average of three measurements per measurement site.
- Texture (*D50*): soil samples from the upper 5 cm were analysed using a laser particle sizer (A22-c-version; Fritsch GmbH) at the Laboratory of Sediment Analysis, Free University, Amsterdam.

Other parameters were derived from literature, such as aggregate stability (López-Bermudez *et al.*, 1996; Cammeraat and Imeson, 1998), soil water tension at the wetting front (Regalado *et al.*, 2005) and root cohesion (Cammeraat *et al.*, 2005; De Baets *et al.*, 2007; De Baets *et al.*, 2008a, b; Pollen-Bankhead *et al.*, 2009). Conversion of point measurement averages to maps was done on basis of the geology and land use map classes.

5.3.3. Rainfall data analysis and input

Rainfall and discharge data for the period 1997 – 2006, measured during the EU MEDALUS projects (Brandt and Thornes, 1996) by the University of Leeds and others at the confluence of the Rambla de Prado and the Rambla Torrealvilla (indicated with X in Fig. 5.1) were used in this study. These data were kindly provided by Prof. M. J. Kirkby (University of Leeds). Part of this record was used in earlier studies (e.g. Bracken and Kirkby, 2005; Bracken *et al.*, 2008). Rainfall was measured using a Casella 0.2 mm tipping bucket rain gauge, recording rainfall every minute.

This ten-year rainfall record was analysed. Consecutive rainfall was considered a rainfall event if the following criteria were met: >2.4 mm h^{-1} intensity at some stage during the event; and <60 min time between recorded rainfall, i.e. if there was no additional rainfall for over an hour, the event was considered to have ended. This is relatively short

compared to other studies, for example Bracken *et al.* (2008) use 12 hours between rainfall events due to antecedent moisture and drying of the soil. However, as openLISEM simulates separate events, the initial moisture is specified beforehand. Furthermore, events must have >5 mm total rainfall and >30min total duration. This resulted in a selection of 94 rainfall events recorded between 1997 – 2006.

Classification of events is, depending on the objective of the study, done using different characteristics (Kunkel et al., 1999) and often total amount of precipitation or maximum precipitation intensity are used to characterise Mediterranean precipitation events (e.g. Martínez-Casasnovas et al., 2002), disregarding the importance of rainfall duration which is often reported to have an important effect on the hydrological response. Therefore, here, we classified the events according to a combination of three event characteristics: maximum precipitation intensity (Pmax; mm h^{-1}), total precipitation (Ptot; mm) and total duration (T; min). Classification was based on the ratio (Pmax * Ptot) / T, which combines three of the most important event characteristics (Bracken et al., 2008). This ratio is hereafter called 'Event Index' or EVI. A high EVI represents an intense rain storm of short duration and high peak intensity, while a low EVI indicates events with low intensities but long duration. Based on the EVI, four rainfall events of different intensity and duration were selected from the 1997 – 2006 record and further used in this chapter (18 June 1997 as extreme event; 17 October 2003; 29 September 1997 and 9 December 2003).

Rainfall events in Mediterranean areas in general and also in the study area are recognised to have spatially and temporally heterogeneous patterns (Bull *et al.*, 1999; Bracken and Kirkby, 2005; Kirkby *et al.*, 2005). Detailed (i.e. rainfall intensity) measurements were available from the Prado outlet station only (X in Fig 5.1b). Daily totals are available from nine stations nearby (Fig. 5.1b). These totals were spatially interpolated using Inverse Distance squared Weighted interpolation (e.g. Webster and Oliver, 2007) in ArcGIS for each event separately and classified in classes of 1mm difference in rainfall (Fig. 5.3). Total rainfall amounts of each class were then related to the measured total rainfall at the Prado outlet station. This coefficient was used to recalculate the detailed rainfall intensity for each class. These spatially heterogeneous rainfall time series were used as input for the OpenLISEM model.
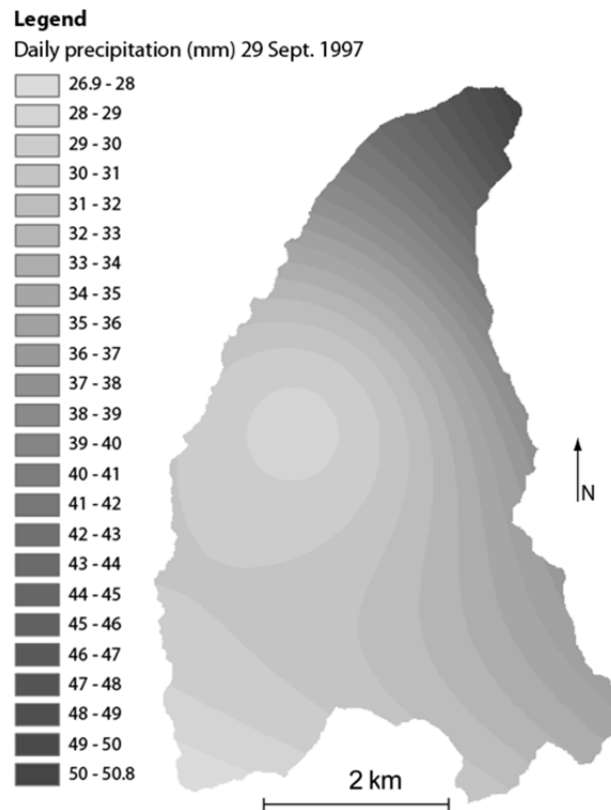
Fig. 5.3. Example of spatial rainfall distribution; Inverse Distance Weighted interpolated daily precipitation (mm) for 29 September 1997.

5.3.4. Calibration data, methods and evaluation

Calibration of OpenLISEM was done using discharge data measured at the outlet of the Prado catchment (X in Fig. 5.1b) where also the detailed rainfall was recorded. The model was calibrated for four selected rainfall events with distinct rainfall characteristics. Water height was measured using a Metrolog logging system with a Druck pressure transducer (PTX 530-1521). Stage recordings were converted to flow velocity and discharge using Manning's equation as described by Bull *et al.* (1999) for the same location, using the same parameters.

Unfortunately, no sediment concentration data is available for the period 1997 – 2006. However, estimates were made of sediment concentration at the Prado outlet during a rainfall event on the 28th September 2009, to be used for comparison with model predictions. Detailed (5-min interval) rainfall data of this event are available from a

station ~10 km north of the Prado outlet (Alhagüeces; UTM 4188000, 612550; A in Fig. 5.1b). Recordings of hourly rainfall from two other nearby stations (Lorca, ~6.5 km south of Prado; 4.7 mm and Zarzadilla de Ramos, ~15 km north of Prado; 0.7 mm) indicate that the event was not equally intense at all locations. Therefore, we scaled the detailed information of the Alhagüeces station to the Prado outlet location, using the hourly observations of the two other stations. If distance to Prado is plotted against total rainfall (mm) for these three stations, a linear relation with r^2 = 0.90 is obtained. From this relation, total rainfall for the Prado outlet calculated at 3.8 mm; ratio between this amount and that recorded at Alhagüeces station (2.8 mm) is 1.35. This ratio was used to scale the detailed 5-min rainfall from the Alhagüeces station to the Prado outlet location. At the Prado outlet, measurements were carried out to estimate water and sediment discharge during the event. For water discharge, flow velocity measurements were done at straight, uniform sections where width and depth of the stream were measured. For sediment concentration, water samples were taken and oven-dried at 105 °C to calculate sediment concentration.

Calibration results of OpenLISEM were evaluated using the Nash-Sutcliffe model efficiency coefficient (Nash and Sutcliffe, 1970). Calibration for discharge was done on peak discharge, total discharge and timing of the hydrograph and peak discharge. Parameters used for calibration were saturated hydraulic conductivity (K_{sat}) and Manning's n (n) for both slopes and channels. Initial values for K_{sat} were derived from literature for nearby areas (Table 5.1). A multiplication factor for K_{sat} was used for model calibration. In this way, relative differences between K_{sat} values between land use classes were not affected by calibration. For timing of the hydrograph, Manning's n values were tuned from an initial value of 0.01 with steps of 0.0005 and within the range 0.0005 – 0.10. As water discharge and sediment concentration data were only available for two moments during the 28 September 2009 rainfall event, calibration for this event was rather difficult due to data limitations. Therefore, we used the relation between Event Index (EVI) and the calibrated K_{sat} multiplication factors of the selected 1997 – 2006 rainfall events to estimate an appropriate K_{sat} multiplication factor for the 28 September 2009 event. Thereafter, sediment calibration for the 2009 event was done using a multiplication factor for texture (*D50*) data to ensure that simulated values are in the same range of those measured for the 2009 event. Subsequently, this *D50* multiplication factor was also used for the selected 1997 – 2006 events.

Table 5.1. Initial values for saturated hydraulic conductivity (K_{sat}; mm h^{-1}) per land use type with literature reference and the area and land use the values were measured in

Land use	K_{sat} (mm h^{-1})	Reference	Area – Land use - Geology
Orchard	38.9	Martinez-Fernandez *et al.* (1995)	El Ardal, Murcia – almonds – Quaternary deposits (marl)
Cereals	65.9	Martinez-Fernandez *et al.* (1995); Lopez-Bermudez *et al.* (1996)	El Ardal, Murcia – cereals – Quaternary deposits
Irrigated arable land	91.8	Martinez-Fernandez *et al.* (1995)	El Ardal, Murcia – cultivated land – Quaternary deposits
Forest	112.4	De Wit (2001)	Alqueria, Murcia – Forest - Limestone
Matorral (Shrub)	104.8	Martinez-Fernandez *et al.* (1995) Lopez-Bermudez *et al.* (1996); De Wit (2001)	El Ardal & Alqueria, Murcia – shrubland – Limestone & conglomerates
Bare / Riparian / Abandoned	47.2	Martinez-Fernandez *et al.* (1995)	El Ardal, Murcia – shrubland with bare soil – Quaternary deposits

5.3.5. Scenario analysis of different magnitude rainfall event series

To evaluate the effects of different magnitude rainfall events on discharge and soil loss, several model scenarios were calculated. Each scenario includes increasingly more extreme events but similar total annual rainfall, as such reflecting a range of possible future climate scenarios for the coming century. A base scenario was deduced from the ten-year 1997 – 2006 rainfall record, in which three events of magnitude similar to that of the 17 October 2003 event occurred; 32 smaller events, similar to the 29 September 1997 event; 47 events similar to the lowest magnitude event of 9 December 2003, and 1 extreme event (18 June 1997). The base scenario consists of all of these events together (Table 5.2). Scenario A does not contain an extreme event and more low magnitude events. Scenario B contains two extreme events in ten years, scenario C five, while in scenario D almost all precipitation occurs as extreme events. Total sediment loss of each of the different rainfall scenarios is calculated by adding up the simulated sediment losses of all rainfall events in each scenario.

Table 5.2. Calculation of base scenario and settings for scenarios A, B, C and D

Scenario	Base			A	B	C	D
	Ptotal – event (mm)	No. of events / 10 y	Ptotal – acc. (mm) for 10 y	No. of events / 10 y	No. of events / 10 y	No. of events / 10 y	No. of events / 10 y
18 June 1997	62.8	1	62.8	0	2	5	26
17 Oct 2003	32	3	96	2	3	11	20
29 Sept 1997	19.4	32	620.8	30	31	24	9
9 Dec 2003	43.3	47	2035.1	50	46	39	9
Total		83	2815	82 (2811[a])	82 (2815[a])	79 (2820[a])	64 (2837[a])

[a.] Total precipitation summed over ten years (mm)

5.4. Results

5.4.1. Field measurements of input data

Results from measured field parameters per land use and geology class are given in Tables 5.3 and 5.4 respectively. Values are averages of all measurements in each land use or geology class.

Table 5.3. Average values of measured field parameters per land use class; st. dev given between brackets

	Orchard (n = 8)	Cereals (n = 13	Irrigated arable land (n = 3)	Forest (n = 11)	Matorral (Shrub) (n = 13)	Bare / Riparian / Abandoned (n = 8)
Leaf Area Index ($m^2 \, m^{-2}$)	1.59 (1.35)	0.71 (0.57)	2.67 (0.00)	4.78 (2.25)	1.26 (1.42)	0.47 (0.30)
Plant cover (fraction)	0.32 (0.11)	0.60 (0.17)	0.93 (0.05)	0.57 (0.18)	0.55 (0.20)	0.21 (0.14)
Vegetation height (m)	2.6 (0.7)	0.5 (0.2)	0.4 (0.1)	6.1 (2.6)	1.4 (0.7)	0.5 (0.2)
Random roughness (cm)	1.55 (0.67)	1.21 (0.56)	1.27 (0.56)	1.50 (0.77)	1.12 (0.64)	0.62 (0.28)
Soil cohesion (kPa)	29.8 (12.8)	17.6 (11.5)	30.0 (8.0)	34.5 (10.6)	43.3 (8.6)	33.1 (9.9)
Porosity ($cm^3 \, cm^{-3}$)	0.57 (0.11)	0.48 (0.04)	0.40(0.16)	0.52 (0.06)	0.52 (0.05)	0.45 (0.06)
Initial soil moisture content ($cm^3 \, cm^{-3}$)	0.09 (0.04)	0.16 (0.09)	0.12 (0.11)	0.12 (0.05)	0.20 (0.08)	0.23 (0.10)

Table 5.4. Average values of measured field parameters per geology class; st. dev given between brackets

	Limestone (n = 5)	Marl (n = 23)	Glacis (n = 14)	Conglomerate (n = 6)	Calcarenite (n = 4)
Median texture (µm)	29.4 (10.1)	38.6 (24.5)	110.9 (155.3)	87.2 (42.5)	32.3 (23.6)
Stone cover (fraction)	0.75 (0.15)	0.16 (0.29)	0.59 (0.26)	0.43 (0.39)	0.84 (0.14)

5.4.2. Event Index (EVI)

To test the model's ability to simulate storms of different magnitudes of rainfall intensity and duration, four events were selected for which sufficient discharge measurements were available. The selected events have distinct event characteristics, as shown in Table 5.5 (total and maximum precipitation and event duration), resulting in different Event Indices (EVIs). The maximum event (highest EVI) that occurred between 1997 – 2006 was on 18 June 1997 and resulted also in the maximum peak and total discharge. The selected event from 1997 – 2006 with the lowest intensity as indicated by the EVI occurred on the 9th December 2003, which was reflected also in the lowest hydrological response.

Table 5.5. Event characteristics for the four selected events from the 1997-2006 period, and the 28 September 2009 event

	18 June 1997	17 Oct 2003	29 Sept 1997	9 Dec 2003	28 Sept 2009
Total rainfall (mm)	62.8	32.0	19.4	43.3	16.8
Max intensity (mm h^{-1})[a]	171.2	117.4	46.1	15.4	18.2
Total duration (min)	65	110	145	710	370
Peak discharge (l s^{-1})[b]	13070	2989	920	466	-
Total discharge (m^3)[b]	31422	14920	3508	3217	-
Event Index (EVI)	165.4	34.2	6.2	0.9	0.8

[a] Maximum average intensity over a 5-min interval
[b] Not given for the 28 Sept 2009 event, as only two discharge measurements are available

5.4.3. Calibration results

In Table 5.6, calibrated multiplication factors for K_{sat} and Manning's n values for both slopes and channels are given for the four selected events. As can be seen, each event had to be calibrated separately, i.e. it was not possible to obtain good calibration results for all selected events with one calibration data set. The calibrated multiplication factors for K_{sat} show a decreasing trend from the highest to the lowest magnitude rainfall event, indicating that intense rainfall events need higher K_{sat} values to give good calibration results for measured discharge than the lower magnitude events. Values of Manning's n, which mainly affect the timing of the hydrologic response, differ between the events.

This reflects differences in slope and channel roughness in time. Manning's n values for channels are higher than those for slopes, reflecting obstacles in the channels, such as small earth dams constraining water flow. Calculated model efficiencies (Nash and Sutcliffe, 1970) for discharge are considered to be good (18 June 1997 event) to reasonable (9 Dec 2003 and 17 Oct 2003 events). For the 29 Sept 1997 event, model efficiency is low. This is due to the more complex shape of the measured hydrograph (Fig. 5.4c), with a long tail of discharge. Simulated results either had good timing of the discharge peak, but very limited tail; or the simulated discharge lasted long, but the peak was too high and too late. This is reflected in the different values for Manning's n for slopes and channels. With the K_{sat} dataset used, it was not possible to simulate a rapid, but relatively low peak and a long discharge tail.

Table 5.6. Calibration results: K_{sat} multiplication factor, Manning's n values and discharge model efficiency for each event

Rainfall event	K_{sat} multiplication factor	Manning's n slopes	Manning's n channels	Discharge model efficiency
18 June 1997	1.43	0.06	0.06	0.72
17 Oct 2003	0.63	0.04	0.06	0.43
29 Sept 1997	0.18	0.02	0.09	0.18
9 Dec 2003	0.08	0.035	0.06	0.51

5.4.4. Simulation results for the Prado catchment

A summary of simulation results of OpenLISEM for the Prado catchment are given in Table 5.7. Fig. 5.4 shows the measured and simulated hydrographs at the outlet for the four selected events. The discharge – rainfall ratios show that only between 0.2 and 1.1 % of rainfall is measured as discharge at the outlet. Simulated sediment delivery ratios are also low, except for the extreme event (18 June 1997). This suggests that most eroded sediment is deposited in the catchment before reaching the outlet. Table 5.7 shows that during the extreme event of 18 June 1997 about 15 times more sediment was exported from the catchment than simulated for the other events.
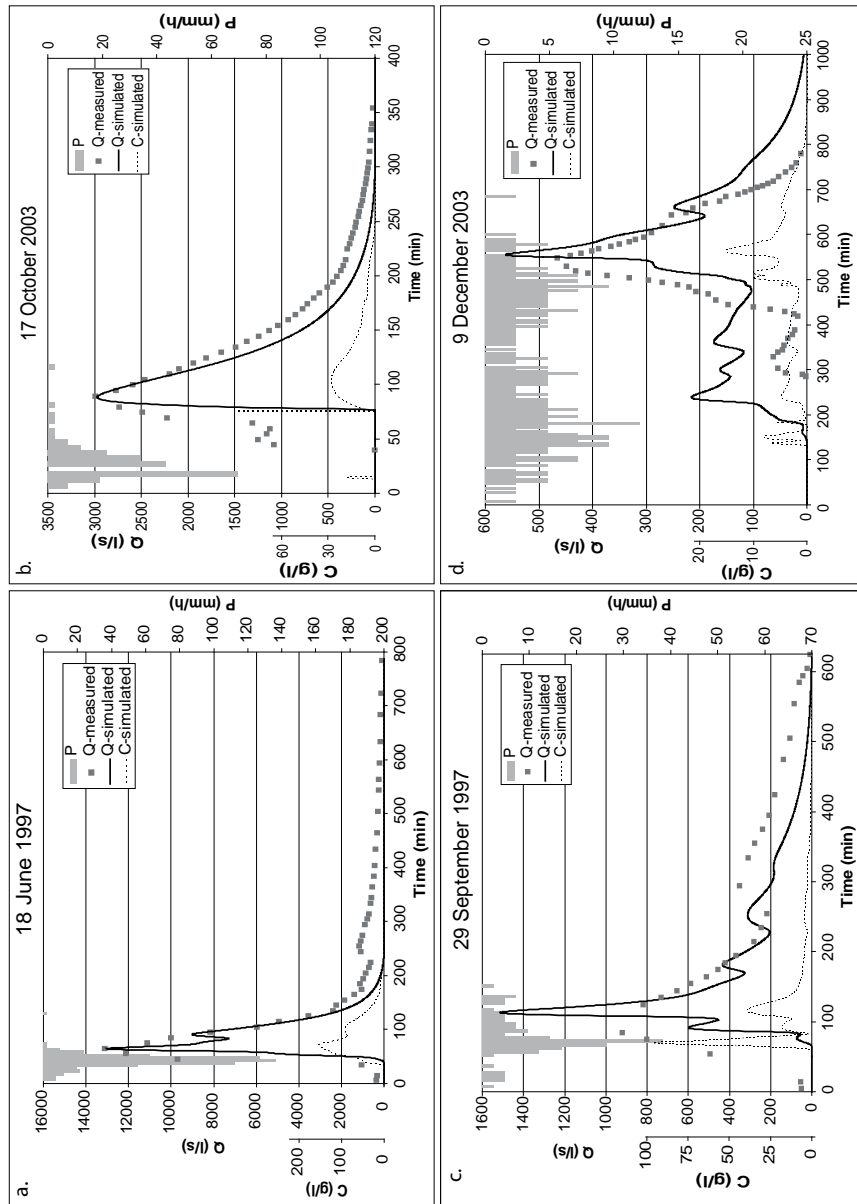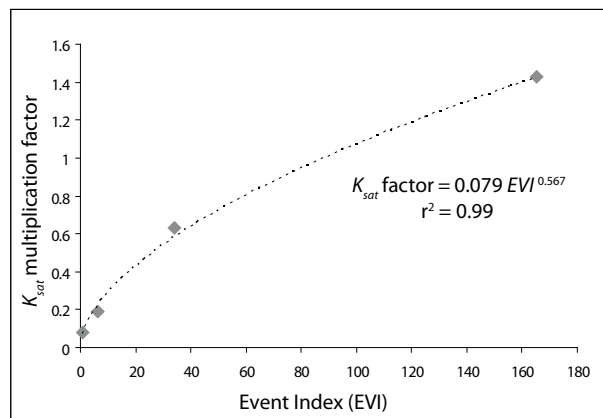
Fig. 5.4. Precipitation (P, right axis), discharge (Q, 2nd left axis) and sediment concentration (C, 1st left axis) at the Prado outlet for four events: 18 June 1997 (a), 17 Oct 2003 (b), 29 Sept 1997 (c) and 9 Dec 2003 (d). Note differences in scales of axes between the four events.

Table 5.7. Summary of simulation results for the four selected events and the 28th September 2009 event

	18 June 1997	17 Oct 2003	29 Sept 1997	9 Dec 2003	28 Sept 2009
Discharge/Rainfall (%)	1.12	0.59	0.68	0.31	0.17
Total detachment (ton)[a]	21254	9634	7482	7702	3579
Total deposition (ton)[a]	17277	9069	7220	7483	3351
Total soil loss at outlet (ton)[b]	3609.1	191.0	87.4	35.3	3.1
Average soil loss (ton ha^{-1})	0.68	0.036	0.016	$6.6 \cdot 10^{-3}$	$0.58 \cdot 10^{-3}$
SDR (%)[c]	17.0	1.98	1.17	0.46	0.09

[a] Summed detachment/deposition of the entire catchment
[b] Detachment minus deposition as measured at the outlet location
[c] Sediment Delivery Ratio = Total soil loss at the outlet / Total detachment

The relation between the calibrated K_{sat} multiplication factors of the four selected events and their Event Indices (EVIs) can be described by a power function (r^2 = 0.99; Fig. 5.5). Using this relation, a K_{sat} multiplication factor of 0.07 can be calculated for the 28 September 2009 event (EVI = 0.8), for which real calibration was not possible due to lack of discharge data. Calibrated values of Manning's n were 0.03 for the slopes and 0.05 for the channels. Simulation results for the 28 September 2009 events are shown in Fig. 5.6. For this event, sediment loads were measured, and calibration was done using a multiplication factor for median texture (*D50*). A multiplication factor of 0.8 gave best results. This multiplication factor of 0.8 for *D50* was also used for the rainfall event of 1997 – 2006. The simulated hydrograph is reasonable, although the simulated discharge tail is somewhat low (Fig. 5.6). Similarly, the simulated sediment concentration tail is also low and the peak is earlier than measured, but values are in the correct order of magnitude.

Fig. 5.5. Relation between calibrated K_{sat} multiplication factors and Event Indices (EVIs) for the four selected events.
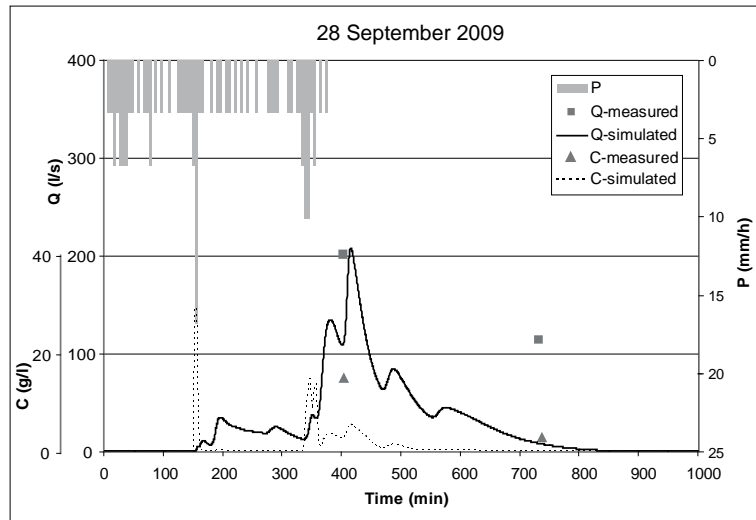
Fig. 5.6. Precipitation (P, right axis), discharge (Q, 2nd left axis) and sediment concentration (C, 1st left axis) at the Prado outlet for the 28 September 2009 event.

Fig. 5.7 shows the simulated spatial pattern of net total soil loss for the four simulated events in the period 1997 – 2006. Strikingly, erosion and sedimentation are simulated to occur almost exclusively in the area with land use type 'Bare / Riparian / Abandoned'. Although land use class 'Orchards' has a lower K_{sat} value than land use class 'Bare / Riparian / Abandoned', no erosion is simulated for land use class 'Orchards'. This is due to the low initial moisture content (Table 5.2) of this land use class compared to that of 'Bare / Riparian / Abandoned. K_{sat} and initial moisture content together determine the effective infiltration rate, which explains why less overland flow and less erosion is simulated for land use class 'Orchards'. As expected, absolute erosion and deposition increase with increasing event magnitude. Sediment transport also becomes more efficient as reflected by the increasing SDR with increasing event magnitude (EVI).
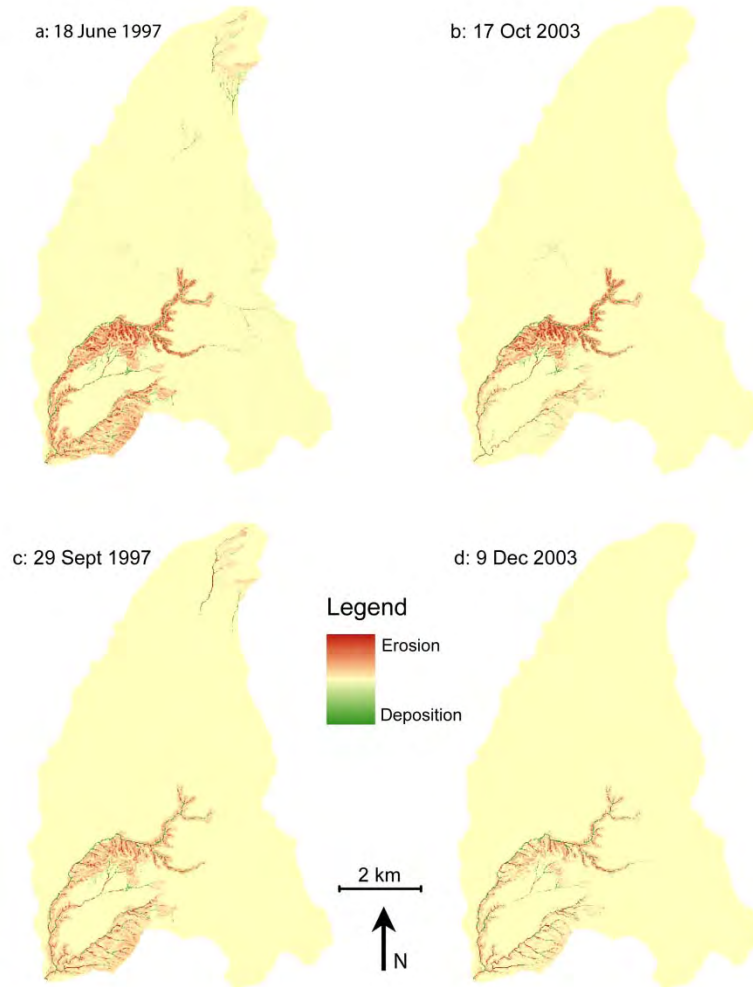
Fig. 5.7. Simulated spatial pattern of net total soil loss for the Prado catchment: (a) 18 June 1997, EVI = 165.4; (b) 17 October 2003, EVI = 34.2; (c) 29 September 1997, EVI = 6.2; and (d) 9 December 2003, EVI = 0.9.

5.4.6. Results of scenario analysis of different magnitude rainfall event series

Fig. 5.8 shows results from the scenario calculations. Simulated erosion for the four selected events is summed according to settings given in Table 5.2 and plotted for each scenario with relative contributions from the different magnitude events. The base scenario calculations show that one extreme event causes 42% of total erosion. On the other hand, all small events together cause 51% of total erosion, indicating that, assuming the scenario is representative for longer time spans, about half of the total erosion occurs

during low intensity long duration and high frequency events. Scenario A gives a 45% reduction in erosion due to the absence of the one extreme event. Scenario B results in ~1.5 times more erosion than in the base scenario. In this scenario, two extreme events constitute 60% of total erosion. Scenario C even has 5 extreme events in 10 years, which increases the erosion to almost three times the amount of the base scenario. In this scenario, the extreme events constitute 11% of total rainfall, but cause 76% of total erosion. For scenario D, being an extreme scenario with almost all rainfall occurring in large events, 95% of total erosion is due to extreme events. In this scenario, the 26 instead in one extreme event in the base scenario, results in 11.4 times higher total erosion, compared to the base scenario. The smaller magnitude events contribute significantly to erosion in the base scenario (51%), while their contribution is very small in scenario D (1.3%).
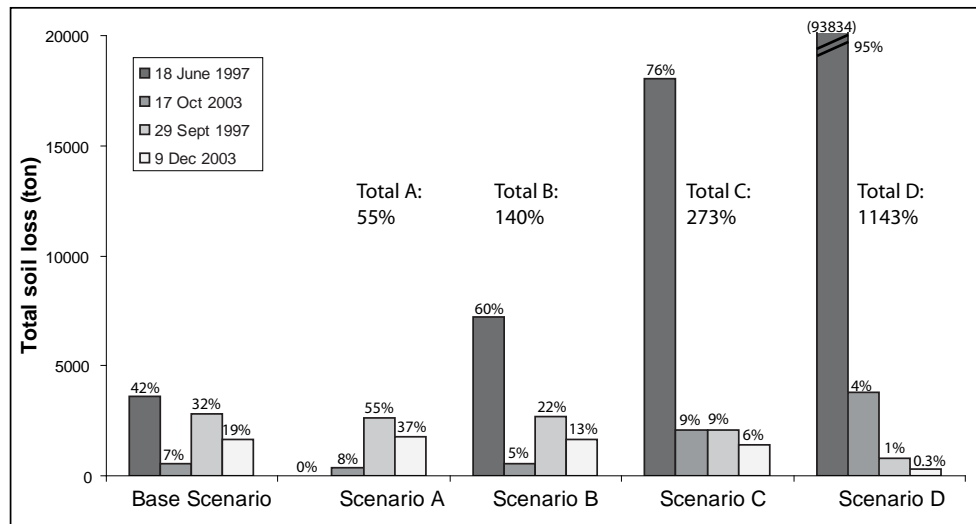
Fig. 5.8 Total soil loss (tons) at the outlet for the four scenarios with relative contribution per event-type. Total percentages are relative to the base scenario; percentages given for each event-type are contributions of total erosion of that scenario (i.e. they sum to 100% for each scenario).

5.5. Discussion

5.5.1. Model calibration

Calibration of the model was a challenge with the available data and features some important drawbacks. Most importantly, lack of detailed sediment data for the 1997 – 2006 events posed a problem for sediment calibration. A multiplication factor for median texture ($D50$) was used to calibrate simulated sediment on the 2009 event and the same

multiplication factor was subsequently used for the selected 1997 – 2006 events. Detailed rainfall data (i.e. 5-min rainfall intensity) for the period 1997 – 2006 was available from only one station at the Prado catchment outlet. Daily precipitation was available from nine stations in the surrounding area, which provided extra information about the spatial distribution of the rainfall events. However, storm movement could influence timing of flow, which is not represented in the input precipitation data. Furthermore, we used the same soil, topography and vegetation parameter values as input for all events. However, especially crop related parameter values may change substantially throughout the year. This was not accounted for in this study, but is known to be of importance (e.g. Nearing *et al.*, 2005).

We chose to use literature values as initial values for saturated hydraulic conductivity (K_{sat}) and to calibrate using a multiplication factor. A disadvantage of this method is that the proportion between K_{sat} values of different land use types is always equal. This may lead to dominance of one land use type on the simulated hydrograph, which indeed is the case in this study (see further discussion below). Another option was to calibrate K_{sat} values for each land use type individually, without setting predetermined values. An advantage would be that for each event, it is possible to tune the K_{sat} values of each land use type individually, which may lead to better reproduction of the measured hydrograph (as preliminary runs using this calibration method proved). For example, the 29 September 1997 event which has a complicated hydrograph and a low model efficiency of 0.18, could be reproduced better using this method. The disadvantage of the latter method is that it lacks an empirical basis and many possible combinations of K_{sat} values for the different land use types could lead to good model results, which makes it difficult to determine the optimal configuration. This is the reason why we chose to use initial values and calibrate using a multiplication factor. Because of data availablility, the K_{sat} values used are based on land use types, not on geology or soil type (Stolte *et al.*, 1996; 2003).

Calibration results lead to good to reasonable agreements between measured and modelled discharge, except for the 29 September 1997 event. Together with the fact that each event had to be calibrated separately, this illustrates a model shortcoming, which may be due to model structure or detail and quality of input data.

This was not considered a main problem in this study as our main aim was to explore the behaviour of events of different magnitude and their relevance for long term landscape development.

In our simulations, initial soil moisture content was predefined. K_{sat} is one of the most sensitive model parameters (De Roo *et al.*, 1996b). Preliminary investigations showed that when using K_{sat} as calibration parameter, initial soil moisture content affected model outcomes only slightly. In other studies, where K_{sat} was predefined, initial soil moisture content did influence model results (Castillo *et al.*, 2003). This is because the patterns for

porosity and initial moisture are similar to those of K_{sat}, and the model eventually combines all to a calibrated infiltration rate. Which of these parameters are used for calibration is then of less importance.

In this study, each rainfall event needed to be calibrated separately. Because of a lack of sediment yield data we could not calibrate or validate on sediment load for most events. Validation is not possible without a larger and more detailed dataset of discharge and, particularly, sediment concentration. These difficulties for calibration can have various explanations. First, the necessity of separate calibration for events of different magnitudes was also found by others (Hessel *et al.*, 2003; 2007) and may be explained by the fact that infiltration rates are dependent on rainfall intensity, as was demonstrated by rainfall simulation experiments (Paige *et al.*, 2002; Karssenberg, 2006; Stone *et al.*, 2008) and studies on natural rainfall variability (Yu *et al.*, 1997; Léonard *et al.*, 2006). A higher K_{sat} was measured when rainfall intensity was higher for the same soil. Reasons for this effect include disturbance of the soil surface by large raindrops during high intensity storms which keeps splashed particles in suspension and prevents formation of depositional crusts; greater ponding at high intensities leading to a larger surface area for infiltration (Burt, 1998) and more of the pore system being included in the infiltration process, so that the apparent K_{sat} is higher. This is in accordance with our results, in which higher K_{sat} values are needed for events of larger magnitudes. Secondly, there may be errors and oversimplifications in the model structure and equations which make that not all process interactions are accurately represented. Finally, a reason for poor calibration and validation results may be the lack of detail in input data of soil, vegetation and topography.

The relation between the calibrated multiplication factor for K_{sat} and EVI, although based only on four calibrated events, seems to be promising. This relation might help in predicting which values of K_{sat} are optimal to calibrate an event if its characteristics are known. Hessel *et al.* (2007) use a similar relation between the K_{sat} multiplication factor and maximum intensity. However, if not EVI but only maximum intensity is included in the relation in this study, the K_{sat} factor for the 28 September 2009 event would be too high, resulting in too little simulated discharge and erosion. Therefore, we conclude that not only maximum intensity, but the combined effect of maximum intensity, total precipitation and event duration represents an event better.

The difference in timing of the runoff between the simulated events resulted in different values for Manning's n. This can be due to obstacles and or vegetation in the channels. In the field, it was observed that some parts of the channels are fully vegetated, while other stretches are bare. This strongly influences the velocity of the waterflow in the channels, reflected in the different values of Manning's n.

For practical reasons (e.g. run time and data availability), we used a resolution of 20m for all runs. It should be kept in mind that the results are scale dependent and new calibration will be required when different resolutions are used (Hessel, 2005).

5.5.2. Simulation results

Simulated rainfall / discharge ratios and SDR are low, which is not surprising for a relatively large and dry catchment such as Prado, and similar results were found in the nearby Mula basin (Bathurst *et al.*, 1996). A large part of the eroded material re-deposits in the catchment before reaching the outlet, at least during one event. These sediments may be re-mobilised during a next event, resulting in a wave of sediment through the catchment as was also observed by Puigdefabregas *et al.*, (1999). The evaluation of individual rainfall events is therefore an important simplification, which needs to be taken into account when looking at the long-term effect of a sequence of events. The effect of a high intensity event is not the same when it is preceded by several low intensity events or by another high intensity event. Runoff and sediment connectivity is an important concept in many semi-arid catchments, as has been stressed and discussed in detail by various authors (Puigdefabregas *et al.*, 1999; Kirkby *et al.*, 2002; 2005; Hooke, 2003; Bracken and Croke, 2007; Bracken *et al.*, 2008). In terms of runoff connectivity the simulated runoff shows that part of the runoff infiltrates before reaching the channels, and that most of the runoff reaching the channels originates from the area immediately adjacent to the channels (which is reflected in the erosion; see Fig. 5.7). This is in accordance with field observations.

As stated before, calibration of sediment concentration was hampered by lack of data. However, the order of magnitude of measured sediment concentrations was correctly simulated by the model. Also, simulated sediment concentrations are in the range of measured values in similar (semi) arid areas (Alexandrov *et al.*, 2003; Boix-Fayos *et al.*, 2007).

Strikingly, the OpenLISEM model predicts erosion to occur almost exclusively in an area with land use class 'Bare / Riparian / Abandoned' (Fig. 5.7), situated around the channels close to the catchment outlet. The reason for this is the predefined configuration of K_{sat} values (and using a multiplication factor for calibration). Apparently, K_{sat} of this one land use type dominates and determines the simulated hydrograph. Although the area with land use type 'Bare / Riparian / Abandoned' (Fig. 5.2a) is prone to erosion, and certainly more erosion is likely to occur there than for example in the forested areas, the spatial pattern of simulated erosion and deposition maps seems not very reliable (Takken *et al.* 1999; Hessel *et al.* 2003) This illustrates that an accurate prediction of sediment yield at the catchment scale not necessarily implies that the spatial pattern of sediment sources and sinks is also accurately predicted. The large effect of K_{sat} was also observed by Hessel *et al.* (2007). As values of K_{sat} can differ over a range of values and are spatially and temporally heterogeneous in the field (e.g. Woolhiser *et al.*, 1996; Muñoz-Carpena *et al.*, 2002), using them in the model for larger areas (i.e. modelling of a medium-sized catchment such as the Prado) features some drawbacks as shown in this study. The

simulated maps should therefore certainly not be used for prediction purposes. For prediction purposes it is advisable to model smaller areas with more detailed input data and spatial information on erosion prone areas for model calibration (Takken *et al.,* 1999).

Although the spatial pattern of simulated erosion and deposition seems not to reflect reality, the average amounts of erosion that are simulated for the entire catchment (Table 5.7), are in the order of magnitude of measured values in South-East Spain (Boix-Fayos *et al.*, 2005; 2007). In this sense, we feel confident that on average, the model predictions are in the right order of magnitude and that they can be used for evaluation of the climate variability scenarios.

5.5.3. Scenario analysis

Scenario calculations for the base scenario show that about half (51%) of total erosion is caused by all small events in a period of ten years. However, one extreme event is responsible for 42% of total erosion, and if the number of extreme events is increased, total erosion increases dramatically. The impact of large magnitude events is therefore potentially very large, which is confirmed by other research in South-East Spain (e.g. Puigdefabregas *et al.*, 1996; Cammeraat, 2004; Boix-Fayos *et al.*, 2005), the Mediterranean in general (e.g. Gonzalez-Hidalgo *et al.*, 2007) and other areas listed in (Boardman, 2006). The scenarios in this study have been chosen to explore and demonstrate the consequences of different temporal rainfall series. In these scenarios the 18 June 1997, being the largest event in the data-series, is treated as an extreme rainfall storm. However, it should be noted that much larger events have occurred in the past (Alonso-Sarría *et al.*, 2002; López-Bermúdez *et al.*, 2002) for which we do not have the required data for simulation.
These scenario calculations are a lumped sum of different sets of different magnitude events over 10 years. What we could not assess with these scenarios is a temporal effect of e.g. large magnitude events on a landscape. For instance, two large events that occur within one year have another effect than if the second event would occur five years after the first. Or, put differently, several subsequent small events leave lots of sediments ready to be washed out by one large event (Puigdefabregas *et al.*, 1999). These dynamics are not included in our scenario calculations.

Our results show that events, especially when they are of large magnitude (i.e. high EVI), are important agents in shaping the landscape. However, as indicated in the introduction, such extreme rainfall events are often not accounted for in long term landscape evolution modeling (with exceptions, e.g. Gonzalez-Hidalgo *et al.*, 2007; Buis and Veldkamp, 2008). We suggest therefore that temporal rainfall variability and extreme events should be taken into account in long-term erosion modelling in semi-arid regions. If incorporated in a LEM, the temporal effects of different magnitude events as discussed above could also be assessed.

5.6. Conclusions

Until now, the event-based erosion model LISEM has been applied to small catchments up to a few square kilometres in size. Our results show that, for a medium sized catchment (~50 km^2), the model can simulate storms of different magnitude, but for each event a separate calibration set is needed. The power relation (r^2 = 0.99) between calibrated K_{sat} multiplication factor and Event Index (EVI) helped in determining which values of K_{sat} are optimal for calibration if the event characteristics (maximum and total precipitation and event duration) are known. Using initial literature values of K_{sat} and a multiplication factor for calibration resulted in one land use dominating the simulated hydrograph, resulting in simulated erosion being concentrated in one area and unreliable spatial maps of simulated erosion and deposition. However, average values of erosion for the entire catchment are in the order of measured values in SE Spain. This confirms the need for spatially explicit calibration and validation of model results.

Although the contribution of many small magnitude events is about half of total erosion in the base scenario, the contribution of one extreme event constitutes 42% of total erosion. Thus, although occurring infrequently, high magnitude events potentially contribute much more to total soil loss than lower magnitude events, even though the number of lower magnitude events is much larger. This has consequences for longer-term landscape evolution modelling, in which usually average annual precipitation is used as input for erosion equations. This does not reflect the potentially large influence of single events. Because the calculated scenarios in this study are a lumped sum of the erosion caused by different events, we could not evaluate interactions between subsequent events. Incorporating the results of event based erosion models in landscape evolution models would make this kind of evaluation possible.

Chapter 6

Exploring the role of rainfall variability and extreme events in long-term landscape evolution

An obvious time-scale gap exists between a single rainfall event and long term landscape development. In this study the event- and physically based OpenLISEM soil erosion model was compared to the landscape evolution model LAPSUS, deliberately extending and shortening the time-scales for which each model was developed. Calibration of OpenLISEM using average erosion rates derived from long-term simulations with LAPSUS and, vice versa, calibration of LAPSUS on event-scale did not give satisfactory results. This suggests that the gap between the different time-scales of both models is too large to be bridged directly. However, calibration of LAPSUS on annual basis using the summed OpenLISEM erosion and deposition values for each year resulted in a good reproduction of these values by LAPSUS. Subsequently, the erosion effects of rainfall variability, climate and land use change were explored on a centennial time-scale. Results show non-linear behaviour between rainfall input and simulated net erosion. Simulated net erosion for increased rainfall erosivity was compared to rainfall variability, showing that mean annual net erosion of up to 15% increased erosivity is not significantly different from annual mean net erosion of the original simulations. Single events must be very high and/or frequent to leave a signal in the landscape that is beyond the scope of natural rainfall variability. Scenarios of human impact show that land use changes can have a potentially larger effect on erosion dynamics than climate variability and change. This is the first time that an event-based erosion model and a landscape evolution model were calibrated for the same area and compared in terms of erosion and deposition dynamics.

6.1. Introduction

There is an obvious gap in time-scales between runoff and erosion during a storm event and the landscape evolution of a catchment (Tucker and Hancock, 2010). Due to the episodic nature of extreme events, sediment-yield measurements can greatly underestimate or overestimate long-term average sediment fluxes, for instance by including or missing such an event in the measurement period (Kirchner *et al.*, 2001, Vanacker *et al.*, 2007). Distinct sets of data and models are available for events and landscape evolution. On the one hand, many models have been developed that focus on storm events. These models simulate runoff and erosion as the result of a distinct event and are either empirical or physically-based (see for reviews e.g. Jetten *et al.*, 1999, Merritt *et al.*, 2003, Aksoy and Kavvas, 2005). On the other hand, landscape evolution models (LEMs) focus on simulating long-term development of a landscape as a result of one or more geomorphic processes (see for reviews e.g. Coulthard, 2001, Willgoose, 2005, Tucker and Hancock, 2010). Physically based erosion models feature more processes and more complex process descriptions compared to LEMs. The reductionist approach (Leeder, 2011, Van De Wiel *et al.*, 2011) aims to include as many processes as feasible, assuming that this will result in enhanced realism in the simulations. However, it also increases the models' complexity and simulation uncertainty. Jetten *et al.* (2003) conclude that the more complex, physically based models do not necessarily perform better than lumped, regression-based models, mainly because the effects of input errors increase with increasing model complexity. On the other hand, the synthesist approach aims to keep the model as simple as possible, by removing as many processes as possible or merging their formulations in as few equations as possible, while still maintaining realistic simulations (Paola, 2011, Van De Wiel *et al.*, 2011). Most LEMs are of this latter type, partly due to their aim to simulate long and often past time periods for which few input data are available.

Low frequency, high magnitude rainfall events seem to contribute disproportionally to total erosion, especially in semi-arid areas (e.g. Brunsden and Thornes, 1979, Hooke and Mant, 2000, González-Hidalgo *et al.*, 2009, 2010), due to, among others, scale-dependent connectivity for water and sediment (Lesschen *et al.*, 2009, Kirkby, 2010a). For example, the landscape changing impact of an extreme cyclone event is described by Page *et al.* (1994) in relation to a 93-year record using a sediment budget approach. However, Jacobson *et al.* (1989) for example conclude that present-day catastrophic events, although effective in modifying the landscape in some parts of their study area (Appalachian Mountains), have not yet erased much of the legacy of previous Quaternary climates. These contradictory examples indicate that there is no consensus about the impact of events on long-term (centennial to millennial scale) landscape development.
Similarly, the relative geomorphic significance of climate variability as opposed to mean climate is not well known. Tucker and Bras (2000) use the landscape evolution model CHILD and a stochastic approach to model the effects of rainfall variability, concluding

that in some circumstances, precipitation variability may be more significant than total precipitation and that climate variability should therefore be considered in landscape evolution modelling. Snyder (2003) evaluate the importance of events in bedrock river incision, stating that through application of surface process models to well-constrained field settings, we can begin to bridge the gap between our understanding of erosion driven by individual floods that are part of a stochastic distribution of events, and our understanding of erosion rates over geologic time-scales.

This study aims to bridge the time-scale gap between events and landscape evolution by (i) comparing two different models; an event-based erosion model and a landscape evolution model; and by (ii) quantitatively evaluating the effects of rainfall variability and extreme events on long-term landscape evolution. Both models have been calibrated to a catchment in semi-arid SE Spain (chapters 4 and 5). In the present study, both models were calibrated using a nine-year rainfall record. Models from both extremes (in time-scales) have not before been compared. After this comparison, rainfall variability was introduced by randomly selecting sequences of different rainfall years and evaluating the simulated erosion. Finally, the effects of introducing extreme rainfall events and of land use change were explored.

6.2. Case study area

The study was conducted in the semi-arid region of South-East Spain. The research area and its general characteristics are described in section 1.7. The Prado catchment forms a tributary of the Rambla Torrealvilla, upper Guadalentín river, upstream of the town of Lorca in Murcia Province (Fig. 6.1; UTM 30N 614800; 4171000).
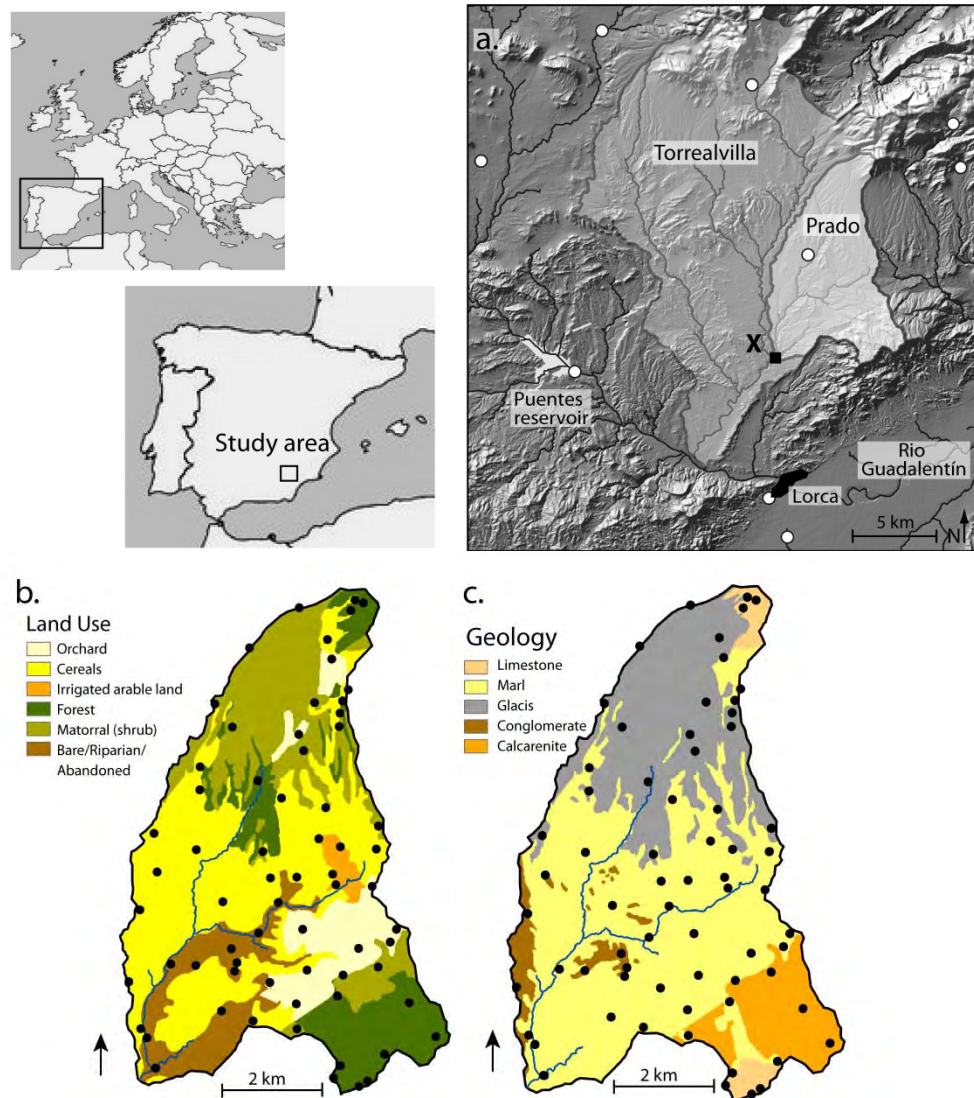
Fig. 6.1. Location of the study area in SE Spain; a) with Prado and Torrealvilla catchments indicated. X = location of discharge and rainfall measurement devices at Prado outlet; white dots are other rainfall stations used for this study; b). CORINE land use map and c). geology map of the Prado catchment with major ramblas indicated. Black dots are measurement and sampling locations for OpenLISEM input parameters.

6.3. Methodology

In this study we use two different types of models: the event-based, spatially explicit erosion model OpenLISEM (De Roo *et al.*, 1996, Jetten and De Roo, 2001), and the long-term landscape evolution model LAPSUS (Schoorl *et al.*, 2000, 2002). First, input data are given

(section 6.3.1). Both models have been calibrated separately in earlier studies: OpenLISEM has been calibrated for the Prado catchment for four typical Mediterranean events of different magnitude (chapter 5). LAPSUS has been calibrated for the Torreavilla catchment, of which the Prado is a sub-catchment (see Fig. 6.1b), on a total of 4750 years, based on dated accumulated sediments in the floodplain area (see chapters 2 and 4). In the present study, each model was calibrated on the results of the other, i.e. the LAPSUS model was calibrated using the OpenLISEM event results and the OpenLISEM model was calibrated using the long-term LAPSUS results. This is explained in section 6.3.2. Finally in section 6.3.3, using the calibrated LAPSUS model, the effects of different sequences of rainfall variability were evaluated, as well as the effects of some examples of climate change, the impact of events on long-term erosion and the effects of land use changes were explored.

Model descriptions are given in section 1.8. For this study, time steps of the OpenLISEM and LAPSUS models were 15 s. and one year or one event respectively. Spatial resolution of both models was 20 m.

6.3.1. Input data

Rainfall data

Detailed rainfall data for the period 1997–2006 have been measured during the EU MEDALUS projects (Brandt and Thornes, 1996) by the University of Leeds and others at the outlet of the Prado catchment (Fig. 6.1a). These data were kindly provided by Prof. M. J. Kirkby and co-workers (University of Leeds). Part of this record was used in earlier studies (e.g. Bracken and Kirkby, 2005, Bracken *et al.*, 2008) and the same record was used in chapter 5 in which the OpenLISEM model was calibrated. Rainfall was measured using a Casella 0.2 mm tipping bucket rain gauge, recording rainfall every minute.

This nine-year rainfall record was analysed. Consecutive rainfall was considered a rainfall event if the following criteria were met:
- larger than 2.4 mm h^{-1} intensity at some stage during the event
- less than 60 min time between recorded rainfall, i.e. if there was no additional rainfall for over an hour, the event was considered to have ended
- more than 30 min total duration
- more than 5 mm total rainfall.

This resulted in a selection of 110 rainfall events recorded between 1997–2006.

These events were ranked according to a combination of three characteristics: maximum precipitation intensity (P_{max}; mm h^{-1}), total precipitation (P_{tot}; mm) and total duration (T; min). Ranking was based on the 'Event Index' EVI: the ratio (P_{max} * P_{tot}) / T, because total or maximum precipitation intensity alone does not sufficiently reflect the variability in Mediterranean rainfall events (see chapter 5). A high EVI represents an intense rain storm of short duration and high peak intensity, while a low EVI indicates events with low intensities but long duration.

OpenLISEM rainfall input data

Detailed (e.g. 5-min resolution) rainfall input data is required for the OpenLISEM model. Rainfall events in Mediterranean areas in general and also in the study area are recognised to have spatially and temporally heterogeneous patterns (Bull et al., 1999; Bracken and Kirkby, 2005; Kirkby et al., 2005). Detailed measurements of rainfall intensity were available from the Prado outlet station only (see location X in Fig 6.1a). In chapter 5 daily total rainfall data from nine nearby stations were used to calibrate four selected events of different magnitudes. These data were not available for the entire 1997–2006 period. To incorporate spatial distribution of rainfall over the catchment and to be able to use this for the entire period, we used the average daily total rainfall of the four events and interpolated them using Inverse Distance squared Weighted interpolation (e.g. Webster and Oliver, 2007) in ArcGIS. The resulting pattern of relative rainfall intensity (Fig. 6.2) was used to calculate spatial patterns of rainfall for all events by multiplying it by the measured total amount of precipitation for each event. The resulting spatially heterogeneous rainfall time series were used as input for the OpenLISEM model.
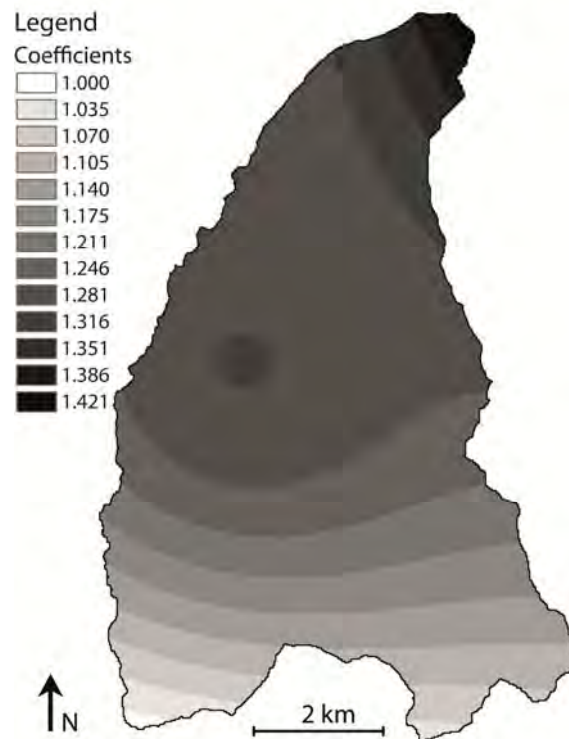

Fig. 6.2. Spatial distribution of rainfall pattern, coefficients indicated were used to calculate rainfall totals and intensities relative to those measured at the outlet (lower left corner).

LAPSUS rainfall input data

LAPSUS requires effective rainfall maps (i.e. precipitation minus evapotranspiration and infiltration) as input data. These maps need to include a spatial representation of (only) rainfall that contributes to runoff. To be able to create these maps, at least some idea of spatially distributed infiltration is needed. In this study, we used saturated hydraulic conductivity, which varies spatially with land use.

Table 6.1. Characteristics of the four calibrated events

Rainfall event	Total rainfall (mm)	Maximum intensity (mm h^{-1})	Duration (min)	Event Index (EVI)	Discharge/rainfall ratio (%)[a]
18 June 1997	61.4	194.4	65	183.6	0.972
17 Oct 2003	26.9	92.1	110	23.5	1.009
29 Sept 1997	19.7	47.7	145	6.5	0.278
9 Dec 2003	49.0	17.1	625	1.4	0.119

[a] Non-spatially distributed, average discharge/rainfall ratio for the entire catchment

In Table 6.1 the characteristics of the four selected events are given. Discharge/rainfall ratios were calculated for the selected events by dividing the measured rainfall by the measured discharge for each event. These low ratios suggest that most precipitation infiltrates and hence does not contribute to runoff and erosion. However, these ratios are average values for the entire catchment, without spatial distribution. Runoff decreases with increasing infiltration and saturated hydraulic conductivity. A spatially distributed infiltration factor was therefore calculated by multiplying the discharge/rainfall ratio of each event by the reciprocal of the saturated hydraulic conductivity iteratively until the average of the entire catchment equals the average discharge/rainfall ratio. Ten iterations were sufficient. Finally, the resulting map for each event (Fig. 6.3a) was multiplied by the spatial rainfall distribution (Fig. 6.2) to obtain the spatially distributed effective rainfall map for each event that was used as input for LAPSUS (Fig. 6.3b).
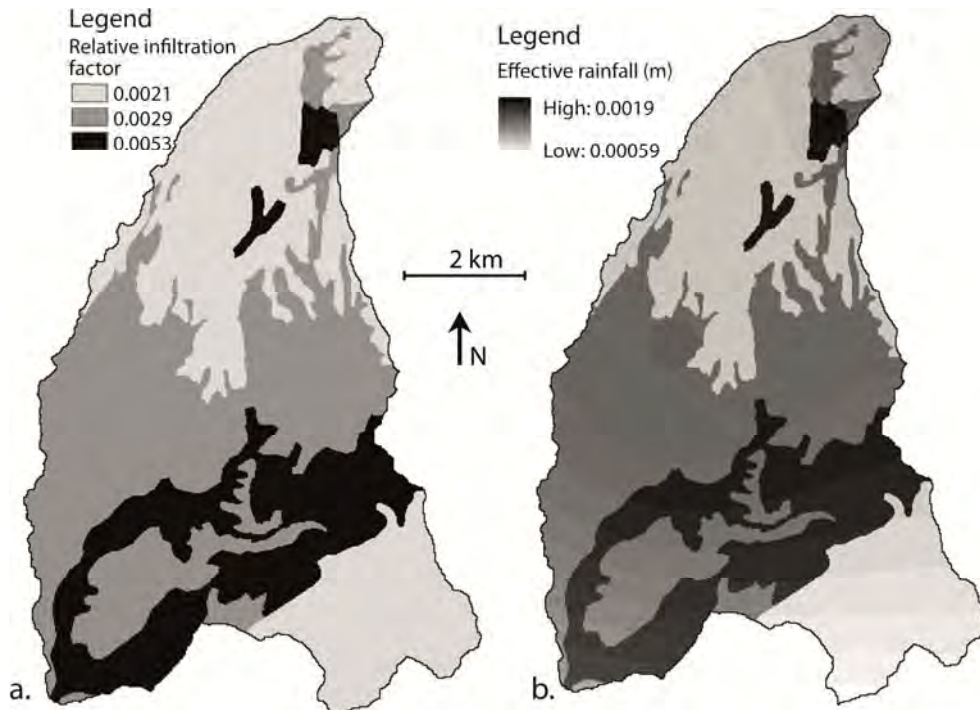
Fig. 6.3. a) Relative infiltration factor based on hydraulic saturated conductivity, spatially distributed based on land use, example for year 1997-1998 ; b) Effective rainfall, calculated by multiplying Figs. 6.2 and 6.3a; example for year 1997-1998.

Unfortunately, discharge data were not available for all events in the period 1997–2006 due to occasional equipment failure. However, discharge/rainfall ratios are needed to calculate the effective rainfall input for LAPSUS as described above. We used the close linear relation between EVI and discharge/rainfall ratio of three of the calibrated events (r^2 = 0.997) to derive discharge/rainfall ratios for all events. The extreme event of 18 June 1997 was not included, because it is exceptional in the rainfall record and the other rainfall events are more like the three selected events. Subsequently spatially distributed effective rainfall maps for all events were calculated using the same procedure as described above.

Table 6.2 gives an overview of the 1997-2006 rainfall record. As can be seen, the average rainfall that occurred in events (based on the criteria mentioned in section 6.3.1) is 165 mm y^{-1}, which is ~62% of the average annual rainfall over 1951–1980 of five neighbouring stations (Navarro Hervás, 1991). The discharge/rainfall ratios in Table 6.2 are the average of the discharge/rainfall ratios of all events of that year.

Table 6.2. Annual rainfall from Prado rainfall record 1997 – 2006 and average annual discharge/rainfall ratios used as input data for LAPSUS

Year	Total rainfall (mm y^{-1})	Rainfall of events (mm y^{-1})	% of total rainfall	Discharge/rainfall ratio (%)[a]
1997-1998	388.8	273.0	70.2	0.308
1998-1999	248.0	186.2	75.1	0.141
1999-2000	170.4	60.4	35.4	0.328
2000-2001	234.0	172.2	73.6	0.216
2001-2002	291.8	169.0	57.9	0.101
2002-2003	257.8	174.4	67.6	0.267
2003-2004	365.4	264.0	72.2	0.179
2004-2005	195.6	94.8	48.5	0.238
2005-2006	155.6	91.8	59.0	0.100
Mean	*256.4*	*165.1*	*62.2*	*0.209*

[a] Mean discharge/rainfall ratio of all events of each year

OpenLISEM input parameters

As described in chapter 5, sampling of OpenLISEM input parameters has been carried out in the Prado catchment (Fig. 6.1bc). Sampling locations were based on the CORINE 2000 land cover classification (EEA, 2000), in which the original 44 CORINE land cover classes were aggregated to a total of 6 (Fig. 6.1b) and on the geological map (scale 1:50 000; (IGME, 1981) which was aggregated to 5 classes (Fig. 6.1c). For details on sampling and measurement methods we refer to chapter 5. Resulting input parameter values for the OpenLISEM model are given in Tables 6.3 and 6.4. Values for aggregate stability, soil water tension at the wetting front and saturated hydraulic conductivity are based on literature.

Table 6.3. OpenLISEM input parameters values based on land use class

	Orchard (n=8)	Cereals (n=13)	Irrigated arable land (n=3)	Forest (n=11)	Matorral (shrub) (n=13)	Bare/ Riparian/ Abandoned (n=8)
Leaf Area Index (m^2 m^{-2})	1.59	0.71	2.67	4.78	1.26	0.47
Plant cover (fractions)	0.32	0.60	0.93	0.57	0.55	0.21
Vegetation height (m)	2.6	0.5	0.4	6.1	1.4	0.5
Random roughness (cm)	1.55	1.21	1.27	1.50	1.12	0.62
Soil cohesion (kPa)	29.8	17.6	30.0	34.5	43.3	33.1
Root cohesion (kPa)	3.1	3.4	2.8	5.9	8.3	0.0
Porosity (cm^3 cm^{-3})	0.57	0.48	0.40	0.52	0.52	0.45
Initial soil moisture content (cm^3 cm^{-3})	0.09	0.16	0.12	0.12	0.20	0.23
Aggregate stability[a] (-)	28	15	15	80	54	45
Soil water tension at the wetting front[a] (cm)	15	11	11	6	10	7
Saturated hydraulic conductivity[a] (mm h^{-1})	38.9	65.9	91.8	112.4	104.8	47.2

[a] These parameter values are derived from literature and were not measured in the field.

Table 6.4. OpenLISEM input parameters values based on geology class

	Limestone (n=5)	Marl (n=23)	Glacis (n=14)	Conglomerate (n=6)	Calcarenite (n=4)
Median texture (μm)	29.4	38.6	110.9	87.2	32.3
Stone cover (fraction)	0.75	0.16	0.59	0.43	0.84
Soil depth (m)	22.5	100.0	19.0	21.5	11.0

LAPSUS input parameters

Input data for the LAPSUS model, besides the main inputs DEM and rainfall, consist of a soil depth map and maps for the parameters erodibility (*K*) and sedimentation potential (*P*). The soil depth map is based on the geology map, see Table 6.4. In this study discharge exponent *m* = 1.6, slope exponent *n* = 1.6 and convergence factor *p* = 2 were used, based on earlier experience with hillslope domains (Temme and Veldkamp, 2009, Temme *et al.*, 2011a).

Erodibility *K* is related to plant cover and soil cohesion, while sedimentation potential *P* includes the effects of plant cover, random roughness and soil texture. These characteristics vary with land use type. Land use types were grouped for LAPSUS: land use types orchard and bare/riparian/abandoned (see Fig. 6.1) were taken together, representing 'open cultivation'; cereals and irrigated arable land represent 'closed cultivation' and forest and matorral represent 'semi-natural vegetation'. Different relative values for *K* and *P* for these three land use types were used: 0.1 for open

cultivation, 0.01 for closed cultivation and 0.001 for semi-natural vegetation. Note that absolute values for *K* and *P* are derived during calibration (see section 6.3.2). A relative high erodibility for open cultivation is due to low plant cover and cohesion (see Table 6.3). Plant cover for closed cultivation and semi-natural vegetation is about equal, but cohesion for the latter is higher, leading to lower erodibility. For sediment potential, texture is important and because semi-natural vegetation occurs mainly on glacis and conglomerate (see Table 6.4), sediment potential is lower (meaning earlier deposition) than for cultivation.

6.3.2. Model calibration

To be able to compare the OpenLISEM event-based soil erosion model and the LAPSUS landscape evolution model, we took both models out of their 'comfort zones' regarding the time-scales for which they were developed. For this purpose, both models were calibrated using results of the other:

- OpenLISEM was calibrated using average erosion rates, derived from long-term (4750 years) simulations of erosion and deposition dynamics with the LAPSUS model;
- LAPSUS was calibrated using results from OpenLISEM simulation results for 110 events in a 9-year period.

OpenLISEM calibration using four selected events

Because the spatial distribution of input rainfall was slightly different from that used in chapter 5, OpenLISEM was calibrated again for the four selected events. Calibration was done on the discharge hydrograph at the outlet. Model Efficiency (Nash and Sutcliffe, 1970) on the discharge were calculated for each event. It was not possible to calibrate all 110 events, because of lack of data on hydrographs. Therefore, all events were first assigned as one of the types of the four calibrated events based on their EVIs (type 1 = 18 June 1997; type 2 = 17 Oct 2003; type 3 = 29 Sept 1997 and type 4 = 9 Dec 2003). The Manning's n value of each of the four event types was used in the simulations of all events of its type. The relation between the K_{sat} multiplication factor and EVI of the calibrated events was used to calculate an appropriate K_{sat} multiplication factor for each of the 110 events. As the type 1 (extreme) event only occurred once in the 1997-2006 record (i.e. on 18 June 1997), we focussed on the relation between the K_{sat} multiplication factor and EVI for the other three calibrated events, which was linear (r^2 = 0.995; see Fig. 6.4).

OpenLISEM calibration using LAPSUS results

In chapter 4, the LAPSUS model was calibrated on long-term erosion and deposition dynamics (4750 year) for the Torrealvilla catchment, of which the Prado catchment is a sub-catchment. The results of that study were recalculated to derive total erosion, total deposition and net erosion for the Prado catchment for a nine-year period, by calculating the average annual erosion and deposition for the Prado sub-catchment and multiplying

by nine. To calibrate the OpenLISEM model we took the 1997-2006 rainfall event record and varied the K_{sat} multiplication factor until all events in this nine-year period together produced the amounts simulated by the LAPSUS. Note that in this calibration all events have the same K_{sat} multiplication factor, unlike in the calibration of OpenLISEM for the four selected events.

LAPSUS calibration using OpenLISEM results
The LAPSUS model was calibrated using the OpenLISEM results on an annual basis. OpenLISEM results were summed per year. Parameters erodibility *K* and sedimentation potential *P* were used for calibration. In an initial calibration round, values between extremes of 100, 10, 1, ..., 10^{-9}, 10^{-10} were explored, keeping the relative values between land uses intact as described in section 6.3.1. In a second calibration round, best values from the initial round were varied, for example 0.01, 0.02, 0.03 etc., until the best combination was found. Runtime for calibration was nine years. Calibration results were compared to three criteria: total erosion, total deposition and net erosion for each of the nine years. Calibration aimed at minimizing the summed residuals for these 27 criteria (i.e. 3 criteria for 9 years).
For comparison with OpenLISEM outputs, the LAPSUS results, initially given in m^3, were converted to tons using a density of 1.37 kg m^{-3}, based on measurements in similar areas in SE Spain (Quine et al., 1999, Nachtergaele et al., 2001). Note that an important difference between summed OpenLISEM simulations and LAPSUS simulations is that OpenLISEM uses the same start DEM for each simulation, while LAPSUS updates the DEM between time steps.

6.3.3. Analysis of rainfall variability and scenarios of land use and climate change

Using the calibrated LAPSUS model, we evaluated the effects of rainfall variability and some examples of climate and land use change for a 99-year period. For rainfall variability analysis, the 1997-2006 record was assumed to be representative for a 99yr sequence, so no trend in rainfall variability was assumed. First, the 1997-2006 annual rainfall (Table 6.2) sequence was repeated 11x. Then, the order of years was changed randomly, keeping the frequency of the 9 years constant (i.e. all nine years occurred 11 times). Fifty realisations were simulated.
In addition, two more extreme cases were simulated: a sequence of 11x the highest year (1997-1998); followed by 11x the one but highest year, etc.; and vice versa: 11x the lowest year (1999-2000), followed by 11x the one but lowest year, etc.

IPCC climate change predictions for the Mediterranean and for Spain predict less or equal total rainfall but with increased rainfall intensity (Castro *et al.*, 2005, Christensen *et al.*, 2007, Meehl *et al.*, 2007). To evaluate the effects of such climate change predictions in terms of erosion and sedimentation, two different sets of scenarios were developed. In

LAPSUS rainfall intensity is not included, but erosivity, i.e. the discharge/rainfall ratio can be increased, which results in more erosive events while total rainfall is kept equal. In a first set of scenarios, erosivity of all events was increased by increasing the discharge/rainfall ratio by 10, 15, 20, 25 and 30% for each year. The same 50 simulations were run and results were compared to the results from rainfall variability with the original erosivity. In a second set of scenarios the impact of extreme events was evaluated. The erosivity of the 18 June 1997 event (the most extreme event of the 1997-2006 record) was increased by multiplying its discharge/rainfall ratio by ten. The effects of incorporating such an extreme event were evaluated for different frequencies: once in 99 years at different times, twice in a row at different times and 11 times (each 9 years).

Finally the effects of some examples of land use change were explored. The relative infiltration, erodibility and sedimentation potential factors of semi-natural vegetation (mainly shrub and forest) were changed to those of open cultivation (see Fig. 6.3a) to imitate deforestation. We simulated different scenarios: first, deforestation for the entire 99 years was simulated. Second, 10 years of deforestation were simulated, after which the natural vegetation was supposed to have reappeared. In addition, effects of reforestation were explored by converting the entire catchment to forest.

6.4. Results

6.4.1. OpenLISEM calibration and simulation results

In Table 6.5 an overview of characteristics of the four selected events and the calibration results are given. Model Efficiencies (Nash and Sutcliffe, 1970) were generally satisfactory, except for the 29 September 1997 event. This was also the case in chapter 5 and is due to the more complicated form of the measured hydrograph with a relatively low peak and long tail of discharge that OpenLISEM has difficulties to simulate.

Table 6.5. OpenLISEM calibration results for the four selected events

Events	18 June 1997	17 Oct 2003	29 Sept 1997	9 Dec 2003
K_{sat} multiplication factor	1.46	0.36	0.17	0.09
Manning's N (slopes)	0.055	0.09	0.02	0.025
Manning's N (channels)	0.055	0.055	0.08	0.11
Discharge Model Efficiency	0.76	0.81	0.31	0.61
Total erosion (tons)	18063	7711	8329	6609
Total deposition (tons)	12500	6247	7771	6417
Net erosion (tons)	5563	1464	558	192
SDR (%)[a]	30.8	19.0	6.7	2.9

[a] SDR = Sediment Delivery Ratio = Net erosion / Total erosion * 100%

In chapter 5 a power relation was found between the K_{sat} multiplication factor and the Event Index (EVI) for the four calibrated events. However, the 18 June 1997 event is an exception in the 1997-2006 record and the other events in the record are more similar to the three lower events (i.e. 17 Oct 2003, 29 Sept 1997 and 9 Dec 2003). Therefore, the linear relation between the K_{sat} multiplication factor and the Event Index for the three lower magnitude events (Fig. 6.4) is used in this study to calculate K_{sat} multiplication factors for all other events.
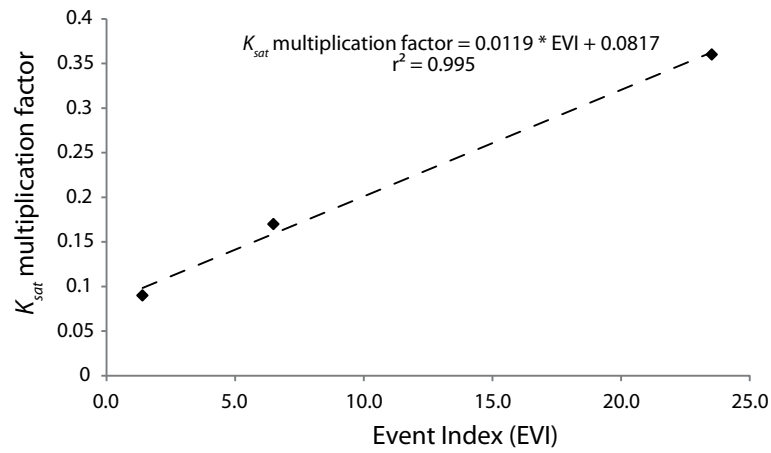

Fig. 6.4. Relation between K_{sat} multiplication factor and Event Indices (EVIs) for three of the four selected events.

In Table 6.6, the summed results for OpenLISEM event simulations are given per year (1997-2006).

Table 6.6. Simulation results for OpenLISEM, sum of events per year, including mean and totals for entire 9-year period

Year	Total no. of events[a]	No. of erosive events[b]	Total erosion (·10³ ton)	Total deposition (·10³ ton)	Net erosion (·10³ ton)	SDR (%)
1997-1998	18	9	124.8	107.7	17.1	13.7
1998-1999	12	4	80.2	69.6	10.6	13.2
1999-2000	10	0	3.9	3.9	0.0	0.0
2000-2001	13	4	93.5	82.0	11.5	12.3
2001-2002	17	3	53.3	48.9	4.4	8.3
2002-2003	12	1	22.6	17.3	5.3	23.6
2003-2004	16	7	78.6	70.7	7.9	10.1
2004-2005	12	2	20.1	17.9	2.2	10.9
2005-2006	9	1	19.9	18.4	1.6	7.8
Mean	13.2	3.4	55.2	48.5	6.7	11.1
Total	119	31	497	436	60.6	12.2[c]

[a] According to the criteria explained in section 6.3.1

[b] An erosive events is defined as an event that produced net erosion

[c] This is the SDR calculated from the total values: summed net erosion / summed total erosion * 100%

6.4.2. OpenLISEM calibration on the LAPSUS long-term results

Table 6.7 shows the overall results of calibrating OpenLISEM to the LAPSUS results, derived from the long-term (4750 years) calibration (chapter 4). Best results were obtained using a K_{sat} multiplication factor of 0.35 for all events. This resulted in an overall fit of 102.3 % (average percentage of LAPSUS results for total erosion, total deposition and net erosion). Fig. 6.5 reveals that, when using these calibration settings, only few events contribute to total net erosion. Most events do not produce any runoff or erosion. The 18 June 1997 event constitutes 92.1 % of total net erosion.

Table 6.7. OpenLISEM calibration results over 9 years on long-term LAPSUS results

Model	Total erosion (·10³ ton)		Total deposition (·10³ ton)		Net erosion (·10³ ton)		SDR (%)
LAPSUS	478.6		231.9		246.7		51.5
OpenLISEM[a]	474.0	99.1%	221.9	95.7%	252.1	102.2%	53.2

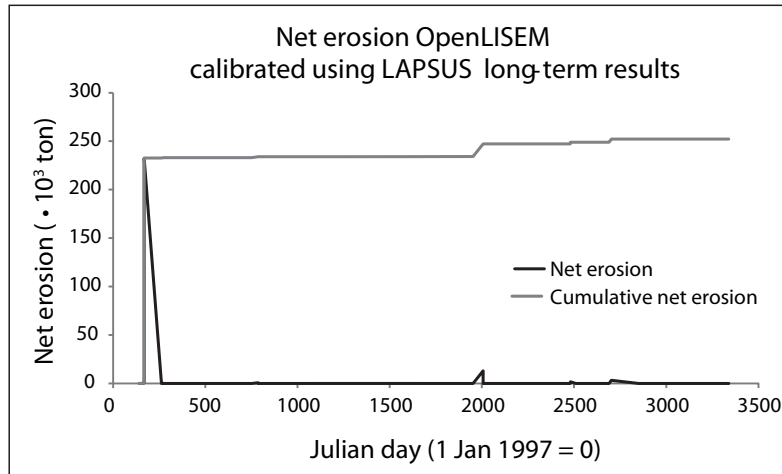[a] Left value: · 10³ tons; right value: % of LAPSUS result

Fig. 6.5. Net erosion as simulated by OpenLISEM – calibrated using LAPSUS long-term results.

6.4.3. LAPSUS calibration on OpenLISEM results

Table 6.8 shows the results of the LAPSUS calibration for annual erosion and deposition. Simulated amounts of total erosion, total deposition and net deposition are given. Model efficiency for total erosion and deposition is low (0.29 and 0.12), but for net erosion it is satisfactory (0.50). The best calibration for LAPSUS on an annual basis resulted in *K* values of 0.8, 0.09 and 0.02 for closed cultivation, open cultivation and semi-natural vegetation respectively and *P* values of 0.0005, 0.5 and 0.1 for the same land uses. In Fig. 6.6 calibrated LAPSUS and summed OpenLISEM results are compared on an annual basis. This shows that results of LAPSUS and OpenLISEM summed results are generally close. For three years, net erosion is slightly underpredicted by LAPSUS compared to OpenLISEM (1998-1999, 2000-2001 and 2001-2002), but the temporal pattern of net erosion is closely simulated.

Table 6.8: LAPSUS calibration results for annual calibration using OpenLISEM summed results

Year	Total erosion (·10³ ton)	Total deposition (·10³ ton)	Net erosion (·10³ ton)	SDR (%)
1997-1998	125.4	106.5	19.0	15.1
1998-1999	70.1	68.9	1.2	1.7
1999-2000	39.0	38.5	0.5	0.0
2000-2001	58.0	53.7	4.2	7.3
2001-2002	38.0	36.8	1.2	3.1
2002-2003	59.6	55.2	4.4	7.4
2003-2004	65.4	57.6	7.8	11.9
2004-2005	42.0	39.0	3.0	7.1
2005-2006	25.0	24.4	0.6	2.5
Mean	58.1	53.4	4.6	6.2
Total	523	481	41.8	8.0[a]

[a] This is the SDR calculated from the total values: summed net erosion / summed total erosion * 100%
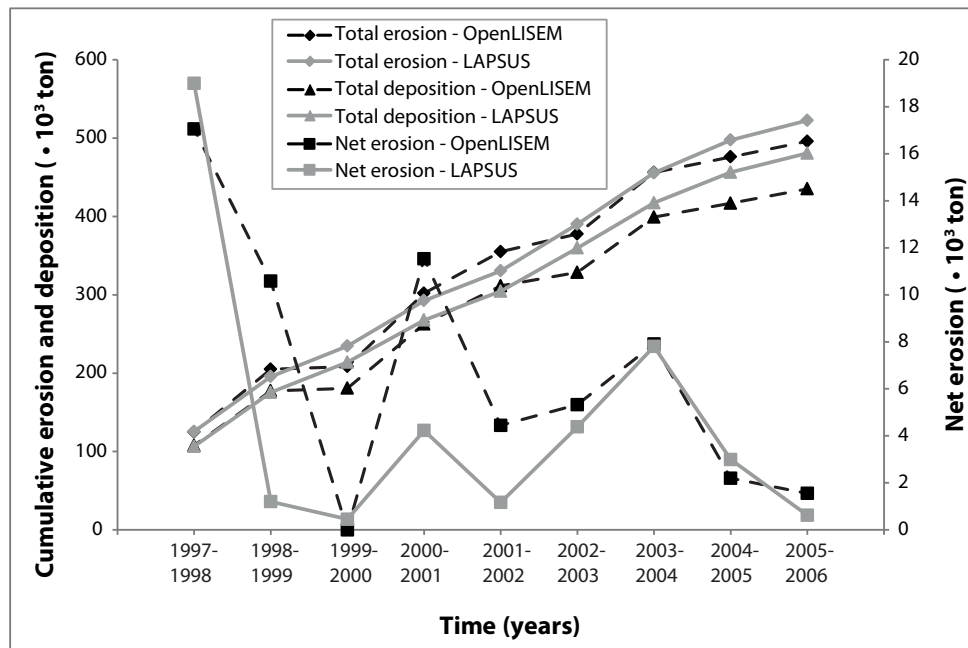

Fig. 6.6. Comparing calibrated LAPSUS and summed OpenLISEM results on annual basis

6.4.4. Results for long-term rainfall variability and climate and land use change scenarios

Fig. 6.7 shows cumulative net erosion for 50 randomly selected sequences of rainfall variability over 99 years. As can be seen, some sequences result in high cumulative net erosion. Mean annual net erosion of the 50 runs was $4.87 \cdot 10^3$ ton, while results range from $3.36 \cdot 10^3$ to $9.64 \cdot 10^3$ ton mean annual net erosion. For comparison, erosion was also simulated for 99 years with average annual rainfall as input for each year, which resulted in mean net annual erosion of $4.92 \cdot 10^3$ ton. Simulating the 1997-2006 record (Table 6.2) repeated 11x, resulted in relatively high mean annual net erosion ($7.12 \cdot 10^3$ ton). Two more extreme cases (highest and lowest in Fig. 6.7) show the erosional response to rainfall sequences starting with 11x the highest rainfall year, followed by 11x the one-but-highest year etc. and starting with 11x the lowest rainfall year, followed by 11x the one-but-lowest rainfall year etc., ending with 11x the highest rainfall years, respectively.
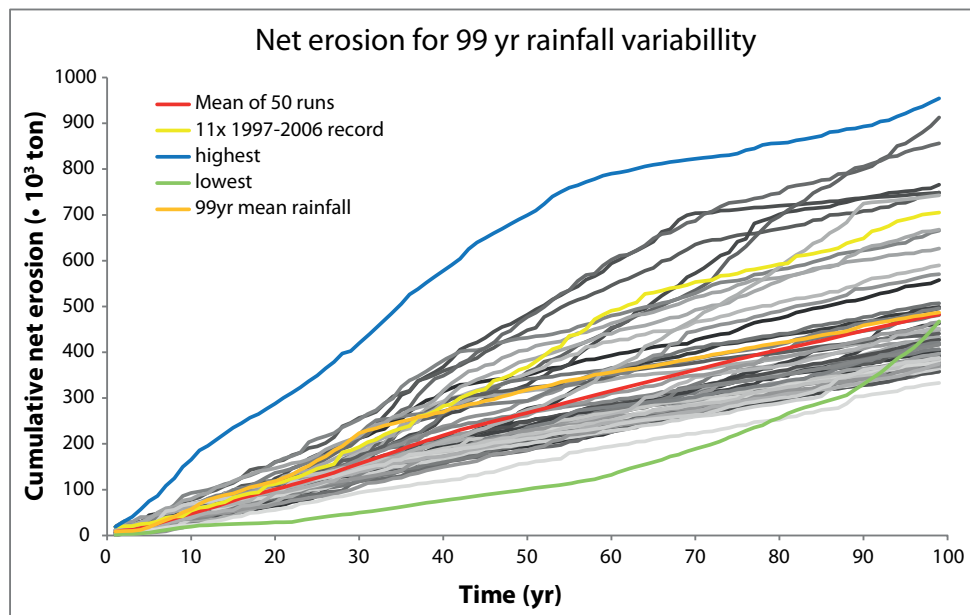

Fig. 6.7. Cumulative net erosion for 50 simulations of randomly selected sequences of rainfall variability over 99 years (in grey). In red the average of the 50 simulations; in yellow 11x 1997-2006 sequence ; in blue and green the extreme sequences of 11x highest, then 11x one but highest etc. (blue) and 11x lowest, 11x one but lowest etc.; in orange 99yr using the mean average rainfall as input.

In line with IPCC climate predictions of equal total precipitation but higher intensity events, the effects of increased rainfall erosivity were explored. Fig. 6.8 shows the results of scenarios in which the erosivity of all events was increased by 10, 15, 20, 25 and 30%. Fig. 6.8b shows boxplots of cumulative net erosion after 99 years of simulation for the original set of 50 simulations and for the increased sensitivity scenarios. The original set of 50 simulations was compared to the sets with increased erosivity in a paired-samples t-test. Cumulative net erosion after 99 years simulation was significantly different ($p < 0.05$) for 20, 25 and 30% increased erosivity, while for 15% increased erosivity the significance level p was 0.053. When comparing the individual simulations, in the case of 10% increased erosivity, 68% of the 50 simulations had a larger mean than the mean of the corresponding original simulation, for 15, 20, 25 and 30% increased erosivity, this was 74, 76, 82 and 90% respectively.

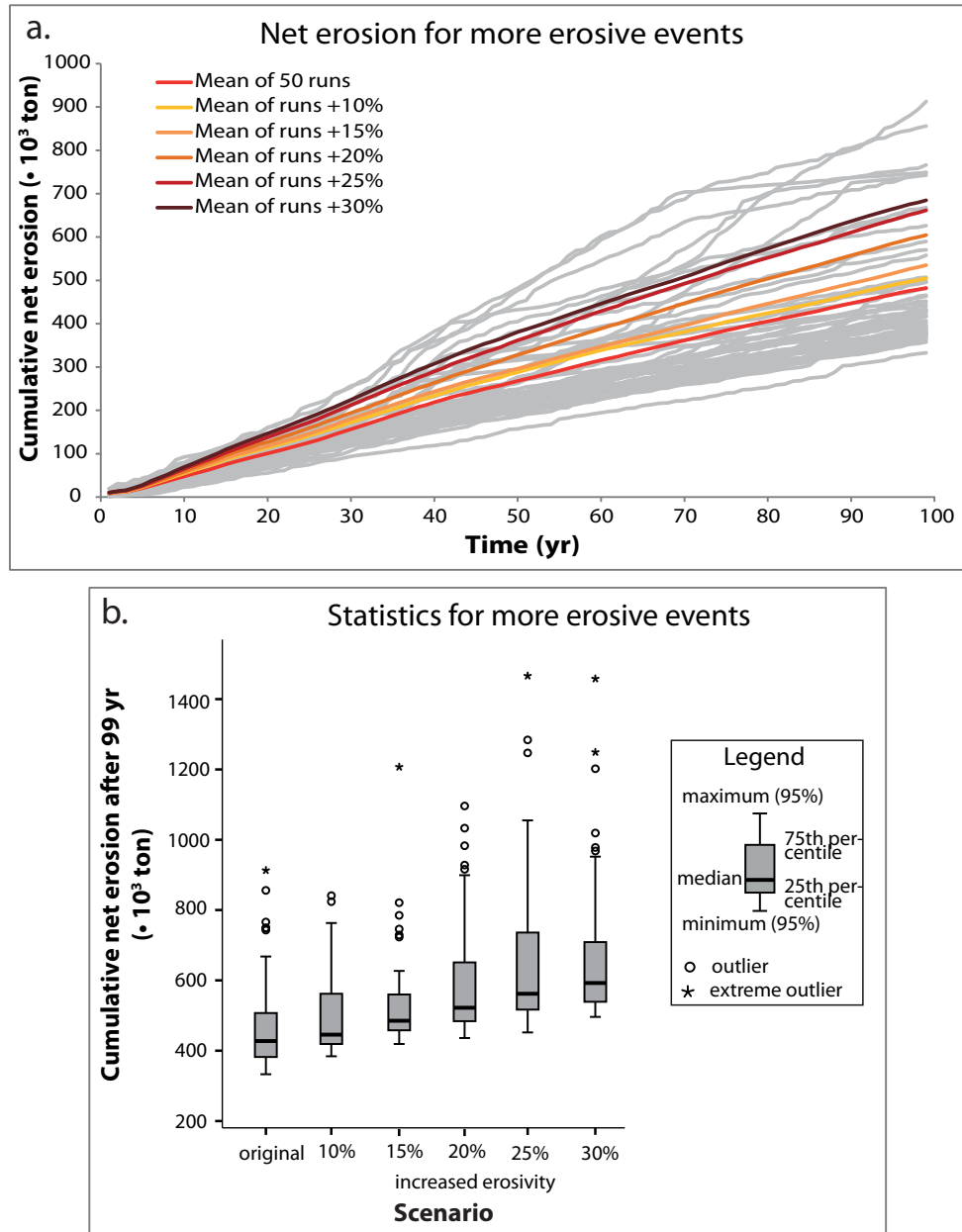*Fig. 6.8. a). Mean of cumulative net erosion over 99 years of 50 simulation for increased erosivity for all events keeping the same total rainfall amounts. For readability, the mean is given instead of all individual simulation. The cumulative net erosion for rainfall variability (see also Fig. 6.7) is given in grey for comparison; b). Boxplots for original and increased sensitivity scenarios.*

In the analysis of climate change effects the erosivity of the highest magnitude event in the 1997-2006 record (18 June 1997), was increased tenfold (Fig. 6.9). The frequency of occurrence of such an increased erosivity, high magnitude event was varied (once, twice and 11x in 99 years), as well as its timing. For comparison with the original set of 50 runs (Fig. 6.7), the rainfall sequence with resulting net erosion closest to the mean was used as input for simulations with increased erosivity events. An extreme event of ten times the erosivity of the 18 June 1997 event produces significantly more erosion than the original run if it occurs every 9 years (blue line). However, it does not lead to cumulative net erosion higher than that simulated for rainfall variability (in grey). Net erosion increases once an extreme event occurs, but its effect can be eliminated a few decades later. The same may happen when an extreme event occurs twice in a row (e.g. occurrence at times t = 5 and 6).
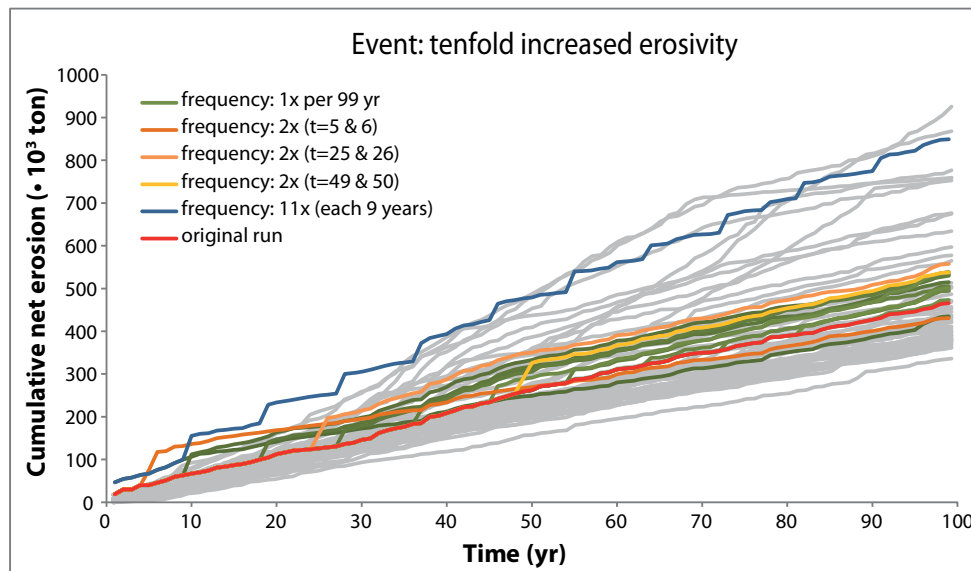

Fig. 6.9. Cumulative net erosion for climate change scenarios with more erosive extreme events, in which the erosivity of the 18 June 1997 event was increased tenfold. Different frequencies of such an event were simulated. The cumulative net erosion for rainfall variability (see also Fig. 6.7) is given in grey for comparison.

In Fig. 6.10, cumulative net erosion as a result of three scenarios of land use change is shown. Net erosion increases significantly if the areas of semi-natural vegetation (matorral and forest) are converted to open cultivation, using those values of relative infiltration and erodibility (*K*) and sedimentation potential (*P*) factors for the entire 99 years. If deforestation is simulated for only ten years, after which the vegetation is supposed to have returned, simulated net erosion is only somewhat higher than the original run.

Alternatively, in a scenario of reforestation, in which the entire catchment is converted to semi-natural vegetation, simulated erosion is significantly lower than in the original simulations.
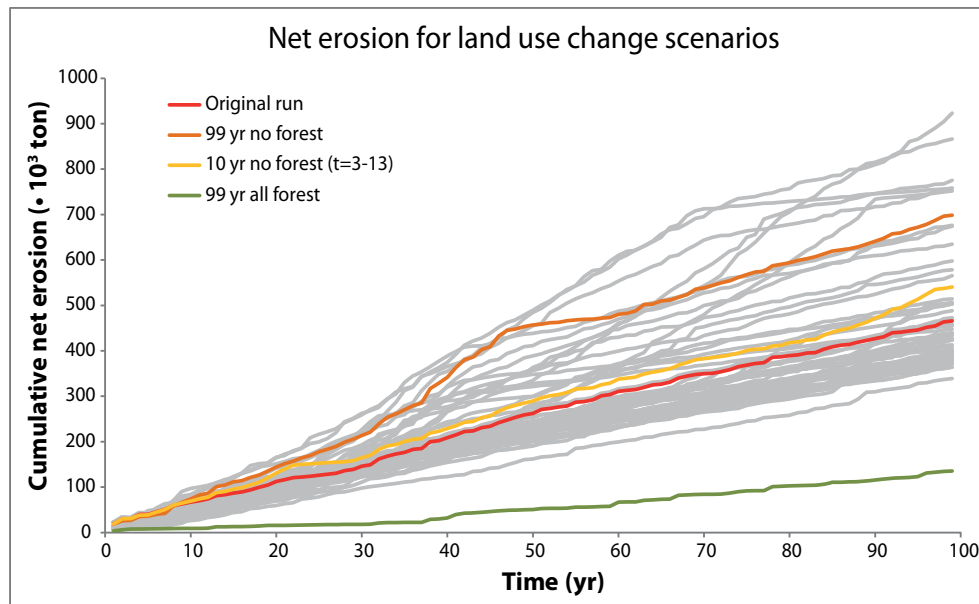

Fig. 6.10. Cumulative net erosion for three examples of land use change. For comparison, in grey the cumulative net erosion for rainfall variability (see also Figs. 6.7, 6.8 and 6.9).

6.5. Discussion

6.5.1. Model comparison

Comparing two different types of models is, to some extent, comparing apples and oranges, or, as Kirkby (2010) states: 'it is always a non-trivial matter to show that models on different [time] scales are compatible'. In the present study, where OpenLISEM and LAPSUS have clearly different intended time-scales, it was not our aim to obtain the same results from both models (as in, for example Temme *et al.* (2011b)). Instead, we deliberately took both models out of their 'comfort zones', i.e. the time-scales for which they were developed and calibrated them on 'uncomfortable' time-scales with the aim to bridge the time-scale gap between events and landscape evolution.

Comparing totals of erosion and deposition (compare Tables 6.6, 6.7 and 6.8) for the two different calibrations, total erosion over 9 years is similar, but there is a large difference for total deposition and consequently also for net erosion (61 $\cdot 10^3$ ton for OpenLISEM summed events versus 247 $\cdot 10^3$ ton for LAPSUS 9-year long-term average). This difference

may be explained by the fact that during the 4750 year record that was used to calibrate LAPSUS, it is probable that larger events than those of the 1997-2006 record occurred, which added to the higher net erosion (Kirchner *et al.*, 2001, Tomkins *et al.*, 2007, Meyer *et al.*, 2010). Evidence of such extreme events in the area over the last millennia are described by e.g. Machado *et al.* (2011), Benito *et al.* (2008, 2010).

Results from calibrating the OpenLISEM model to the long-term LAPSUS results (Fig. 6.5) show that only the most extreme event of the 1997-2006 record would contribute significantly to runoff and erosion. Measured hydrographs of lower magnitude events, however, indicate that these also contributed to runoff and erosion. Calibration was done using a fixed K_{sat} multiplication factor. Results might improve if a variable K_{sat} multiplication factor would be used. However, this was considered beyond the scope of this paper. If the calibrated LAPSUS model is run on an event basis, it underpredicts deposition, thereby overpredicting net erosion, especially for the smaller events (for example the 29 Sept 1997 and 9 Dec 2003 events). This is due to the relatively large amount of runoff that infiltrates in OpenLISEM, but not in LAPSUS and partly to the difference in time step: OpenLISEM uses many time steps to simulate one event, creating possibilities to deposit sediment that has been eroded in a previous time step. LAPSUS, on the other hand, was forced to simulate the erosion and deposition of one event in one time step, which does not allow for such redeposition of previously eroded sediment. Overall, the comparison of these two models shows that an event-based model such as OpenLISEM might be too complex in terms of input parameters and calibration requirements to simulate longer term (decadal) erosion and deposition dynamics. Also, the OpenLISEM model could benefit from improvements to the spatial description of sediment deposition, so that a realistic output DEM can be simulated and the model can be used to simulate sequences of events. On the other hand, a landscape evolution model such as LAPSUS does not include enough hydrological detail to correctly simulate individual events that occur in semi-arid areas such as SE Spain. LAPSUS could benefit from incorporating a dynamic infiltration procedure (Calvo-Cases *et al.*, 2003, Buis and Veldkamp, 2008). Due to the absence of re-infiltration, small events simulated in LAPSUS have connectivity, for instance between hillslopes and channels, whereas in reality in semi-arid areas this connectivity is probably low during low magnitude events.

6.5.2. Rainfall variability and sequencing: non-linearity and self-organization

According to Kirkby (2010) the contribution of each storm is part of the distribution of magnitudes and frequencies in the longer term and data from an erosion plot or small catchment can only provide a meaningful average erosion rate if the runoff and sediment response is analysed, storm by storm, and the results of this analysis used to calibrate the site record against a longer term distribution of storm sizes and intensities. We do so deductively (as opposed to empirically) in this study by calibrating the longer-term

LAPSUS model with 'observations' of individual events (simulated by OpenLISEM in this study).

The simulated variability in net erosion due to different sequencing of rainfall years shows a perhaps surprising pattern (grey lines in Fig. 6.7); they do not vary around a central mean and most simulated sequences hardly show any variation over time, whereas some show a sudden increase in net erosion. This can be explained by non-linear and self-organising behaviour within the catchment, i.e. there is not necessarily a linear relation between higher rainfall (e.g. in year 1997-1998) and high net erosion and even low rainfall can produce high net erosion (e.g. Coulthard and Van De Wiel, 2007, Van De Wiel and Coulthard, 2010). This is illustrated in Fig. 6.11a, which shows the net erosion over time for the extended 1997-2006 record and the simulation in which average annual rainfall was used as input for every time step.

Even with constant rainfall input, net erosion in the catchment varies, especially in the first few decades when the catchment is adjusting to the initial conditions (Coulthard *et al.*, 1999). However, the amplitude of erosion peaks are clearly smaller than those where rainfall variability was included. In the simulation with the 1997-2006 sequence as input rainfall, the highest peaks do correspond to peaks in erosion, but their magnitude differs (compare e.g. t = 64 and t = 73) and high peaks in erosion occur in response to small peaks in rainfall (e.g. at t = 58).

Comparing the 50 simulations of rainfall variability to the simulation in which mean annual rainfall was used as input (orange line, Fig. 6.7), mean annual net erosion for the latter is about equal to the mean of the 50 simulations with rainfall variability. However, 68% of the 50 simulations result in lower annual net erosion and 32% show higher annual net erosion than the annual net erosion if average annual rainfall was used as input. This suggests that, at least in the modelled catchment and using this particular rainfall data, average annual rainfall reflects erosion dynamics in a similar way as annually variable rainfall data. Thus, average annual rainfall could be appropriate as input for a landscape evolution model such as LAPSUS, especially on the longer (centennial – millennial) time-scales (Hancock, 2010). On shorter (decadal – centennial) time-scales, variability in rainfall seems to be important. Moreover, if average annual rainfall is used as input, information about the range of net erosion due to different sequencing of variability (Fig. 6.7) is lacking.
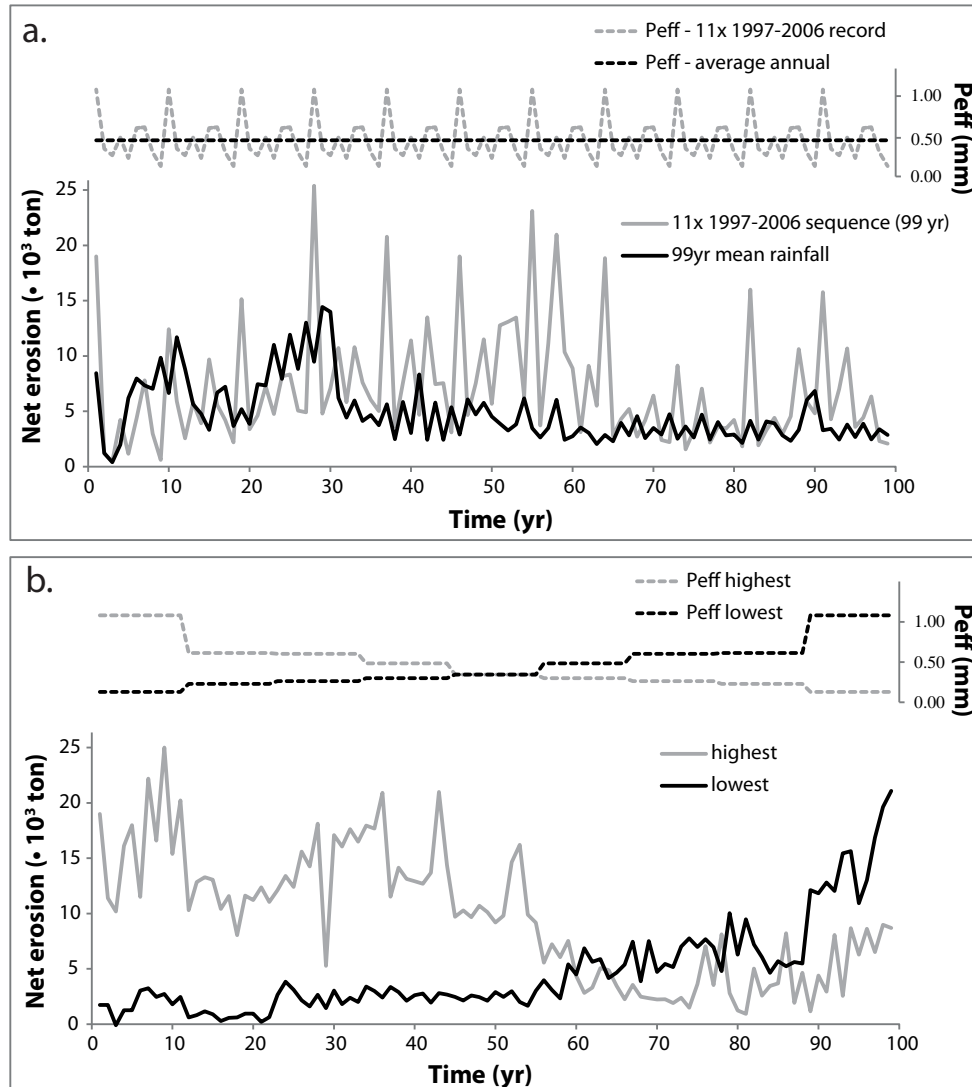
Fig. 6.11. Input effective precipitation (Peff; upper graphs) and net erosion (lower graphs) over time for a). 11x the 1997-2006 record (grey lines) and average annual rainfall (black lines) and b). the highest (grey lines) and lowest (black lines) rainfall variability scenarios.

Interestingly, the highest and lowest simulations of rainfall variability (blue and green lines in Fig. 6.7) do not result in equal cumulative net erosion. Fig. 6.11b shows effective rainfall input and net erosion per year for both sequences. Both sequences show a trend of higher net erosion in response to higher effective rainfall. However, when effective rainfall is increasing (black line in Fig. 6.11b), net erosion in response to higher rainfall is lower than net erosion in response to the same rainfall when effective rainfall is decreasing (grey line in Fig. 6.11b), or in other words, the net erosion lines in Fig 6.11b are

not each other's mirrors, as is the case for input rainfall. An explanation for this behaviour might be that the higher rainfall at the start of the simulation increases connectivity (e.g. gullying) in the catchment, which would increase the erosional effectiveness for the lower rainfall (e.g. Nachtergaele *et al.*, 2002).

Another interesting feature of Fig. 6.7 is the apparent convergence of some simulations after about 60-70 years. Before this time, all simulations show increasing net erosion. Data shows that for the converging simulations, total erosion per time step, while depending on rainfall, remains similar, but that total deposition per time step increases, resulting in lower net erosion. Apparently, sediments were transported out of the catchment more effectively in the first few decades. A decrease in connectivity between hillslopes and channels or within the channels might have caused the increased deposition. The LAPSUS model is sensitive for landscape patterns (e.g. DEM configuration). Topographic feedback, local sediment storage and (dis)connectivity within the landscape, which is changing over time, seem to be important processes determining landscape response. While this paper focussed on the temporal erosion and deposition dynamics, additional research into the spatial erosion dynamics over time could increase insight in this subject. Continuous simulations models (as opposed to event-based models) such as LEM LAPSUS are capable of simulating these landscape processes, patterns and responses over time, which in turn might increase insight in landscape dynamics.

6.5.3. Scenarios of climate and land use change

From the rainfall variability and sequencing analysis (Fig. 6.7) and the scenarios for increased erosivity (Figs. 6.8 and 6.9) results showed that mean annual net erosion was not significantly different from the effects of natural rainfall variability for simulations in which the erosivity was increased up to 15%. Semi-arid areas may be relatively less sensitive to changes in erosivity, because of high natural rainfall variability. Similarly, single events must be very high and/or frequent if they are to leave a signal in the landscape that is beyond the scope of natural rainfall variability (Fig. 6.9; (Jerolmack and Paola, 2010). These findings correlate with those of Tucker and Bras (2000), who found that arid, poorly vegetated catchments showed less sensitivity to changes in rainfall variability than humid, vegetated catchments. Note that for these rainfall variability scenarios, we have not included specific trends, for example alternations of wetter or drier decennia, except for the highest and lowest sequences (Figs. 6.7 and 6.11).
In this study we changed the erosivity of rainfall events, keeping total rainfall amount equal, in line with climate change predictions (Castro *et al.*, 2005, Christensen *et al.*, 2007, Meehl *et al.*, 2007).

An interesting future research topic would be to further quantitatively investigate the effects of increased or decreased erosivity and rainfall amount, separately and in combination, thus quantifying the relative importance of each.

Scenarios of human impact should be seen as model explorations, not as exact and reliable predictions. Nevertheless, they do indicate a trend and show that land use change can have a large impact on erosion dynamics and that this impact can be larger than climate variability and change. The simulated trends correspond to findings by e.g. Bakker *et al.* (2008), that erosion and sedimentation have decreased in areas where de-intensification of land use practices occurred. In a study on the impact of land use and climate change in the Holocene, Ward *et al.* (2009) found a three times increase in sediment yield due to conversion of forest to agricultural land, while rainfall erosivity increased by only 3% in the same time period. In his review on the effects of land uses on soil erosion in Spain, García-Ruiz (2010) states that due to the expansion of cereal cultivation, episodes of extensive soil erosion occurred, whereas farmland abandonment resulted in a reduction of erosion due to vegetation recolonization. Alternatively, these results indicate that the combined effect of climate and land cover change might indeed have a larger impact than climate alone. This is, for example, the case in glacial – interglacial cycles when not only climate but as a result also vegetation cover changes (e.g. Knox, 1972, Vandenberghe, 2008).

6.6. Conclusions

By comparing an event-based soil erosion model (OpenLISEM) and a landscape evolution model (LAPSUS), we conclude that the gap between their different time-scales is too large to be bridged directly. The OpenLISEM model was calibrated using the average 9-year erosion and deposition, derived from the long-term (4750 year) simulations with the LAPSUS model. Results showed that only the highest magnitude event would contribute to erosion. Conversely, the LAPSUS model was calibrated on the four individual events, resulting in underprediction of total deposition and consequent overprediction of net erosion. When calibrating the LAPSUS model on annual basis using the summed OpenLISEM erosion and deposition for each year, results showed a good reproduction of these values by LAPSUS. Thus, when keeping to the time-scale that the model was originally intended for (here: years in LAPSUS), but calibrating the model using simulation results from the event-based model, short-term variability could successfully be introduced in longer-term modelling of landscape development.

Using this catchment and this particular rainfall record, average annual rainfall and rainfall variability resulted in comparable net erosion over centennial time-scales. This suggests that average annual rainfall might be used in landscape evolution over longer time-scales (centuries – millennia). Over shorter time-scales (decades – centuries) rainfall variability seems important. Moreover, when using average annual rainfall, variation in

erosional response to different sequencing of rainfall variability cannot be assessed. Non-linear behaviour is evident: non-varying, average annual rainfall as input results in peaks in simulated net erosion. Also, variability in rainfall as input does not necessarily lead to a corresponding peak in simulated erosion and peaks occur at points in time when no rainfall peak occurs.

Simulated net erosion for increased rainfall erosivity (with equal total rainfall) was compared to rainfall variability, showing that mean annual net erosion of up to 15% increased erosivity is not significantly different from annual mean net erosion of the original simulations. Semi-arid areas may be relatively less sensitive to changes in erosivity, because of high natural rainfall variability. Similarly, single events must be very high and/or frequent if they are to leave a signal in the landscape that is beyond the scope of natural rainfall variability. Scenarios of human impact, although they should be seen as model explorations, show that land use changes can have a large effect on erosion dynamics, larger than climate variability and change, especially for reforestation.

This is the first time that an event-based and landscape evolution model were calibrated for the same area and compared in terms of erosion and deposition dynamics. Landscape evolution models such as LAPSUS have the advantage over event-based models that they are capable of simulating landscape dynamics on a continuous basis over long time-scales, which allows evaluation of topographic feedback mechanisms, temporally changing (dis)connectivity and local sediment storage and non-linear, self-organizing behaviour. This study has shown that these feedback mechanisms are important in landscape erosion and deposition dynamics and catchment evolution.

Chapter 7

Synthesis

7.1. Introduction

Soil erosion has been mentioned to be one of the most serious problems for our society (Pimentel, 2006, Banwart, 2011), especially in semi-arid areas where land degradation can lead to desertification (e.g. Kefi *et al.*, 2007). Although erosion can be affected to a large degree by the direct or indirect effects of human impact (e.g. Hooke, 2000b, Wilkinson, 2005), it is a natural process of landscape evolution. Rates of erosion are important for our understanding of landform development (Parsons *et al.*, 2004) and to estimate the role of human impact on erosional processes, knowledge of natural erosion rates is required. The latter are difficult to obtain for recent times, because it is difficult to find locations that have never been influenced by human activity. Therefore, natural or background erosion rates are usually estimated for prehistoric and often longer time-scales using for instance cosmogenic nuclides (e.g. Vanacker *et al.*, 2007) or dated sediment bodies.

Landscape evolution is driven by sequences of discrete events which have a frequency distribution varying in space and time (Tucker and Bras, 2000). However, there is a gap in time-scales of a discrete event (hours up to days) and the time-scale of landscape evolution (millennia; Fig. 1.1).

Thus, in erosion research, spatial and temporal scales as well as research methods differ. On the one hand research is performed on plot-slope-small catchment scale, for event based change, on 'human' time-scales (Fresco and Kroonenberg, 1992, Kroonenberg, 2006) and conducting field experiments. On the other hand, the landscape regional scale is assessed, for decadal change, on time-scales of landscape evolution (Quaternary) and using landscape evolution models as tools.

This thesis aimed to bridge the gap between these two contrasting approaches with focus on the time-scale gap between rainfall events and landscape evolution and the relative contribution of human activity to natural erosion. Tools of both approaches (i.e. field measurements and modelling on different time-scales) are combined.

In this chapter, the main findings of the previous chapters are combined and discussed. The research questions are addressed within three themes related to this thesis that were introduced in chapter 1: section 7.2 discusses human-induced versus natural erosion dynamics; in section 7.3 the time-scale gap between events and landscape evolution is addressed, and section 7.4 discusses modelling as a research tool for geomorphology and landscape dynamics. In section 7.5 implications of the research are discussed in a broader context. Finally, in section 7.6 general conclusions of this thesis are drawn and ideas for future research are indicated.

7.2. The human imprint on the erosional landscape

Before a conclusion can be reached about the relative contribution of natural and/or human factors on a landscape, it is important to assess the overall functioning of the landscape system in terms of processes and triggers of landscape dynamics. This should be done at a relatively large spatial scale, so that large-scale processes that influence erosion dynamics of a (sub)catchment, are incorporated in the analysis. In chapter 2, such an analysis is done for the Upper Guadalentín Basin and a schematic model of landscape evolution is proposed (section 2.5.3; Fig. 2.8). By mapping and dating sediment bodies along several river stretches, insight was gained in the processes and drivers of erosional and depositional dynamics in the area. The advantage of analysing a larger area is evident for example from our explanation of the sedimentation dynamics of the Lorca fan (Silva *et al.*, 2008). These were found to be due to sediment pulses resulting from erosion of lake sediments after collapse of the palaeo-dam (Fig. 2.8). From the analysis in chapter 2, it is clear that a Late Glacial palaeo-lake influenced erosion and sedimentation dynamics in the Upper Guadalentín Basin during its existence and (long) after its disappearance. This indicates that a time-lag between driver and effect of several millennia may exist (Temme and Veldkamp, 2009). Another conclusion is that the Upper Guadalentín rivers are not in equilibrium, evidenced by their out-of-phase sedimentation pattern. Chapter 2 tentatively and qualitatively correlates the deposits of the Torrealvilla catchment to climate and human impact, based on sediment ages. However, there is strong evidence that climate was not the main driver of erosion and deposition in the area (most notably the absence of Late Glacial – Holocene transition sedimentation and the asynchrony of erosion episodes between the Guadalentín river and Rambla Torrealvilla). Therefore, it is concluded in chapter 1 that internal river dynamics (e.g. complex response; Schumm, 1981) and local processes (e.g. local base changes due to palaeo- and historic lake formation and disruption) are more important drivers for the area than external and regional factors.

7.2.1. Modelling human impact on erosion

In many (modelling) studies, the impact of human changes to the land has been evaluated in terms of erosion, notably through land use changes such as de- or reforestation or land abandonment (e.g. Boix-Fayos *et al.*, 2008, Cantón *et al.*, 2011). These studies are mostly done on small spatial scales and for short, contemporary time-scales. Studies that evaluate the influence of human activity on erosion for long-term (millennial) time-scales in the past are mostly qualitative, for example correlating episodes of increased erosion to periods of increased human impact (e.g. chapter 2, Schulte, 2002, Knox, 2006, De Moor *et al.*, 2008). Quantitative evaluation of erosion due to human activity over long time-scales is rare (Peeters *et al.*, 2008, Wainwright and Millington, 2010, Temme *et al.*,

2011b). One of the most important forms of human impact on the landscape is through agriculture (Hooke, 2000a). In chapter 4, the effects of tillage erosion on long-term landscape development were evaluated quantitatively using landscape evolution model LAPSUS. Results in Fig. 4.7 show that, despite being a high frequency (yearly), but slow and low impact process, tillage erosion has a considerable impact in terms of sediment accumulation in the floodplain area of the catchment, adding almost 20% compared to simulations without tillage erosion. However, water erosion remains the most important process (Peeters *et al.*, 2008), opposed to findings by Van Oost *et al.* (2000, 2005) who conclude that for the last decades tillage was the dominant process. This apparent paradox should be viewed in the context of scale: the direct, on-site impact of tillage is important on (tilled) hillslopes. However, in chapter 4 simulation was performed at the catchment scale and calibration and results focused on the lower floodplain area. Due to changes in erodibility, sedimentation potential and water balance in the tilled areas and indirect changes in transport-capacity off-site, tilled sediments eventually reach the floodplain area, but in an indirect way and depending on connectivity and (temporal) storage in the catchment.

Chapter 4 focused on quantifying the contribution of tillage erosion to total erosion. Other human induced processes such as land use change or grazing were not included. In chapter 6, these forms of human impact were explored in land use change scenarios (Fig. 6.9). Results indicate that for the Prado subcatchment, deforestation and especially reforestation might impact erosion to a large extent. Another possibly important process is that of abandonment of agricultural terraces, for instance after the Roman period. Field abandonment in SE Spain has been shown to accelerate (gully) erosion due to crust formation and slow vegetation recovery (e.g. Lesschen *et al.*, 2008, García-Ruiz, 2010). The effect of terrace failure has been simulated by Lesschen *et al.* (2009) using the LAPSUS model, but for short, contemporary periods. It would be interesting to include the effects of abandonment and terrace failure in a long term simulation and quantify how these processes contribute to erosion and deposition at the catchment scale (e.g. Claessens *et al.*, 2009). Doing so, insight can be gained in the time-lag between cessation of cultivation activities and its effect on erosion and sedimentation dynamics on the catchment spatial scale.

7.2.2. Problems in human versus natural erosion research

Two problems related to natural or human-induced erosion were identified in the introduction (section 1.2), i.e. that the onset of anthropogenic influence frequently predates historical records (Wilkinson, 2005) and that undisturbed areas where natural rates can be assessed are difficult to find (Gellis *et al.*, 2004). In this section, problems related to human versus natural erosion research encountered in this thesis are discussed.

In chapter 2 dated sediment bodies were used to reconstruct erosion and deposition dynamics for the study area that were then correlated to human and/or natural processes. Both OSL and radiocarbon dating was used. Where possible, results of the two methods were compared and indeed confirmed each other (Fig. 2.3; Fuchs and Lang, 2009). Still, uncertainties related to age determination exist (Tables 2.2 and 2.3). For the radiocarbon dates, pieces of charcoal were used. Although in the field these charcoal pieces were estimated to be *in situ* within the sediment, there might be a time-lag between their formation, transportation and actual incorporation into the sediment (Fuchs *et al.*, 2010). Ideally, high-resolution sampling (e.g. Fuchs and Buerkert, 2008) on many locations throughout the catchment should be carried out. As shown in chapter 2, stratigraphic sampling for OSL dating was carried out on several locations. OSL and radiocarbon sampling on more locations, especially in the upstream part of the Torrealvilla catchment would have given a more complete spatial and temporal picture of sediment dynamics. However, practical (preservation, financial) restrictions make this unfeasible for many studies and for this thesis research.

Furthermore, there might be a time-lag between the trigger of (accelerated) erosion or deposition and its effect (e.g. Temme and Veldkamp, 2009). This implies that a direct link in time between a dated sediment and a cause should perhaps not be made. Such a time-lag is probably different for each specific area and quantifying it is not easy, although simulation using a landscape evolution model (LEM) might be helpful as suggested in the previous section (Tebbens and Veldkamp, 2000, Tebbens *et al.*, 2000).

In chapter 4, important input data for long-term simulations were the palaeo-precipitation and –vegetation time series (Fig. 4.3). However, quantitative data, especially for precipitation, are not easily available. Evaluation of different plausible palaeo-precipitation data might help improving the insight in the potential variation of natural processes. This in turn might improve insight in the relative contribution of tillage erosion. Furthermore, quantification of the on-site waterbalance and erodibility for different areas (e.g. natural vegetation, tilled fields, cropped fields) is difficult for appropriate spatial and temporal scales. Also, soil depth and production through weathering, changes in erodibility due to different soil horizons or saprolite are important factors for which data is also scarce, especially for long (past) time-scales. Quantification of uncertainty in the output due to variation in input values would add to the insight of these factors on simulated erosion rates.

7.3. Linking events to landscape evolution

The obvious time-scale gap between runoff and erosion as a result of one storm event on the one hand and landscape evolution on the other hand (Tucker and Hancock, 2010) was assessed in this thesis. Two types of models were first calibrated for the study area individually. In chapter 4 the landscape evolution model LAPSUS was calibrated for the

Torrealvilla area over almost 5000 years using reconstructed palaeoDEMs (Hoffmann *et al.*, 2010). In chapter 5, the event- and physically based OpenLISEM model was calibrated for the Prado catchment for four typical Mediterranean storms of different magnitudes and frequencies. In chapter 6, these two models were compared. In this section, results from the mentioned chapters are compared and discussed.

7.3.1. Different estimates for erosion rates

An important research question was how different magnitude storms contribute to total erosion (Question 2b, section 1.5). Total erosion as calculated in chapters 4, 5 and 6 is compared. In chapter 5 a base scenario was created, deduced from the 1997-2006 rainfall record. Events in this record were compared to the four calibrated events based on their Event Index (EVI) and a frequency of each event type was calculated (Table 5.2). The net erosion of each event was multiplied by its frequency, leading to a calculated total of 8.6 $\cdot 10^3$ ton net erosion for the 1997-2006 period. In chapter 6 all events were simulated individually using the OpenLISEM model. Because calibration data for all events were not available, the relation between the K_{sat} multiplication factor and the Event Index (EVI) was used to derive an appropriate K_{sat} multiplication factor for each event. Summing the simulated net erosion for all events results in a total of 60.6 $\cdot 10^3$ tons of net erosion for the period 1997-2006. In chapter 4, the LAPSUS model was calibrated on long-term erosion and deposition dynamics (4750 year) for the Torrealvilla catchment. The simulated net erosion was recalculated in chapter 6 to derive net erosion for the Prado catchment for a nine-year period by calculating the average yearly erosion and deposition and multiplying by nine. This resulted in a total of 246.7 $\cdot 10^3$ ton net erosion for a nine-year period. There is a large discrepancy between these three values. The discrepancy between the latter two (60.6 $\cdot 10^3$ and 246.7 $\cdot 10^3$ ton) was attributed to the probable occurrence of much larger events during the 4750 years simulation than occurred in the 1997-2006 period, which influenced the average erosion rate (e.g. Kirchner *et al.*, 2001, Tomkins *et al.*, 2007, Meyer *et al.*, 2010). Evidence for such extreme events in the Guadalentín area have been described (e.g. Benito *et al.*, 2008, 2010, Machado *et al.*, 2011) and can be seen by comparing input rainfall data (Fig. 4.3 and Table 6.2). The discrepancy between the first two (60.6 $\cdot 10^3$ and 8.6 $\cdot 10^3$ ton) must be attributed to the way the totals were calculated or simulated. In chapter 6, all events were simulated and some events produced relatively large amounts of erosion, even if they had a low Event Index and would be expected to have a less erosive character. This indicates, as discussed in chapter 5, that each event should be calibrated separately (Hessel *et al.*, 2003, 2007) and that the relation between the K_{sat} multiplication factor and EVI is possibly not suitable to predict an appropriate K_{sat} multiplication factor for each event. Another factor that may influence simulation results is the temporal and spatial variability in soil and vegetation input parameters such as vegetation cover or LAI. These input parameters were kept

equal for each simulated event, whereas in reality these parameters may change throughout the year.

Estimates of sedimentation rates over longer time-scales are available from reservoirs in SE Spain and range from 1.5 to 26.2 ton ha^{-1} y^{-1} (De Vente, 2009). The Puentes reservoir, located ~10 km from the Torrealvilla area, received an average of 2.12 ton ha^{-1} y^{-1} of sediments over the last 100 y. The three calculated values for net erosion of the Prado catchment convert to 5.2, 1.3 and 0.2 ton ha^{-1} y^{-1} respectively. The ~50 km^2 Prado catchment is about 20 times smaller than the ~990 km^2 Puentes catchment and would therefore be expected to have higher erosion rates. Boix-Fayos *et al.* (2005) reviewed erosion rates from SE Spain on different scales. For catchments, these authors found field measured rates between ~2 and ~4 ton ha^{-1} y^{-1}, while rates measured on plots and hillslopes are usually lower. From this comparison the calculated amounts are in the right order of magnitude, but the lowest value (8.6 ·10^3 ton or 0.2 ton ha^{-1} y^{-1}) seems very low and more confidence is given to the other two estimated values. However, as Cantón *et al.* (2011) rightly state, caution should be exercised in comparing measurements based on different methodologies and temporal or spatial scales (Boix-Fayos *et al.*, 2007). Results of measured erosion rates in SE Spain show a high variability, which are mainly related to spatial and temporal scale of measurements, disturbance and inadequate representation of natural conditions (e.g. continuity, connectivity and heterogeneity of natural systems) and complex ecosystem interactions (Cantón *et al.*, 2011, Nadal-Romero *et al.*, 2011, Vanmaercke *et al.*, 2011).

7.3.2. Contribution of (extreme) events

Related to the variation in total net erosion is the variation in the contribution of an extreme event to total erosion. As calculated in the base scenario in chapter 5, the single largest event contributed 42% to total erosion, while the lower magnitude events together caused 51% of total erosion (Fig. 5.8). In chapter 6, the OpenLISEM model was calibrated to the LAPSUS long-term results from chapter 4. This resulted in the largest event contributing 92.1% to total erosion (Fig. 6.5). However, one (fixed) K_{sat} multiplication factor for all events was used, whereas chapter 5 showed that different calibration parameter sets were needed for events of different magnitudes. The highest event as simulated with OpenLISEM in chapter 6 caused 16.3% of total erosion. According to the yearly LAPSUS simulations (Table 6.8), the first year, which includes the highest event, contributed 45.5% to total (nine-year) erosion. In their review of daily soil erosion of the Western Mediterranean, Gonzalez-Hidalgo *et al.* (2007) found that for each year, the three highest daily erosion events (ranked by magnitude) represent more than 50% of annual soil erosion. The one highest daily erosion event caused more than 25% of total soil loss, while in some extreme situations this one highest magnitude event caused more than 50% of total erosion (Gonzalez-Hidalgo *et al.*, 2007). In the OpenLISEM simulations of

chapter 6, the largest three events of the nine-year period cause 42.1% of total erosion, which correlates well with the findings of Gonzalez-Hidalgo *et al.* (2007). Thus, (extreme) events seem to be important for total erosion in semi-arid areas.

The concept of connectivity (Bracken and Croke, 2007) is important in the discussion about the effect of extreme events. During low magnitude, high frequency events hillslopes may only be connected to first-order streams or local footslopes, where sediment is then deposited. High magnitude events are large enough to connect hillslopes, through first order streams to main channels and floodplains. Thus, sediments deposited during earlier low magnitude events are being washed away and transported further downstream and eventually out of the system during high magnitude events. Without the sediments deposited during earlier storms, high magnitude events might not produce these high amounts of sediment. Thus, sediment production shows path dependency (dependency on initial conditions; e.g. Stallins, 2006, Wainwright and Millington, 2010) and factors such as erodibility of sediments, lithology and detachment- or transport limited systems influence erosion in response to event sequencing. However, during high magnitude events, mass wasting processes such as landsliding and undermining of gully banks might produce considerable amounts of sediments regardless of sediments deposited during earlier smaller events.

7.3.3. Non-linearity and its implications

Chapter 6 shows the difference between summing the simulated erosion of individual events and continuous simulation of events. In this chapter the effects of rainfall variability and events with increased erosivity are evaluated in a long-term (100 year) model simulation. Two processes can be highlighted: the non-linear response of erosion to rainfall variability and sequencing (Fig. 6.10 and 6.11; Murray *et al.*, 2009, Jerolmack and Paola, 2010, Van De Wiel and Coulthard, 2010) and the elimination of the effects of increased erosivity events over time due to topographic feedback (internal erosion and sedimentation dynamics). Although non-linearity is an important concept that should be kept in mind when simulating erosion and deposition at catchment scale, it is expected that the effects of extreme events will be visible in the erosional record and in the landscape, if their magnitude is significantly higher than that of average events (Jerolmack and Paola, 2010). For semi-arid areas with high natural variability this implies that for an event to leave an imprint in the landscape it has to be really extreme and of higher magnitude than compared with for instance temperate regions where rainfall variability is lower.

Related to non-linearity, net erosion dynamics show path dependency (Fig. 6.11b); the notion that future interactions and processes (e.g. erosion rates) are dependent or constrained by initial conditions (topography) (e.g. Stallins, 2006, Wainwright and

Millington, 2010). Net erosion response is different if preceding events are only of low magnitude than when they are of high magnitude.

Another implication of the non-linear and self-organizing behaviour of catchments is that predicting or extrapolating erosion rates for the future is impossible. Difference should be made between catchment response to rainfall variability and to trends in climate. Erosion may be predicted to increase if precipitation increases significantly over at least decadal time-scales, for instance wetter-colder decades or centuries such as the Little Ice Age. However, amounts of erosion for a specific event in the future will be impossible to predict due to non-linearity. An illustrative parallel is that of climate prediction itself: future climatic trends may be predicted within uncertainty limits but the weather of a specific date in (the far) future is impossible to predict.

7.4. Modelling landscape dynamics

In this thesis, two types of models have been used: the landscape evolution model LAPSUS and the event- and physically based OpenLISEM soil erosion model. Although some researchers and most engineers and policy makers may use erosion models to predict future erosion quantities and patterns, perhaps most scientists rather use models to understand landscape dynamics and the relevant processes, feedbacks and interactions among these processes (e.g. Hoffmann *et al.*, 2010, Cantón *et al.*, 2011). In this thesis, models are used for the latter purpose: to increase understanding of landscape dynamics and its drivers. In line with this purpose, the models (LAPSUS and OpenLISEM) have been developed (LAPSUS in chapter 3) and applied to conditions that they were not initially intended for (application of OpenLISEM to a relatively large catchment in chapter 5 and extending or shortening the time-scale of both models in chapter 6).

In this section, performance of each model is discussed, including limitations and possible improvements. The latter are discussed in relation to comparable existing models. Subsequently, the models are discussed in light of modelling approaches (reductionist versus synthesist).

7.4.1. Event-based OpenLISEM soil erosion model

In chapter 5, the OpenLISEM model was calibrated for four typical Mediterranean storm events of different magnitude (rainfall intensity and duration). Calibration was performed using the measured outlet hydrographs. The main conclusion was that, although possible to simulate the erosion dynamics of these different magnitude storms, each storm needed a different set of calibration parameters, most notably saturated hydraulic conductivity K_{sat}. In other words, it was not possible to simulate erosion of each storm with one parameter set. In chapter 6, this was obvious from the result that only

one event in the nine-year 1997-2006 record would produce over 90% of total erosion (Fig. 6.5), which did not match measured erosion from lower magnitude storms. The necessity of separate calibration for events of different magnitudes was also found by others (Hessel *et al.*, 2003, 2007) and may be explained by the fact that infiltration rates are dependent on rainfall intensity, as was demonstrated by rainfall simulation experiments and studies on natural rainfall variability (Yu *et al.*, 1997, Léonard *et al.*, 2006). In chapter 5, input characteristics such as antecedent moisture and vegetation characteristics were the same for each event. Differences in these characteristics between events may also partly explain the necessity to use different values for K_{sat} for each event. For example, Castillo *et al.* (2003) found that antecedent soil moisture strongly affects the runoff response during medium and low-intensity storms, but hardly affects peak discharge during high-intensity rainstorms. In addition, the effect of crusting on runoff production was not incorporated.

The OpenLISEM model was applied to the ~50 km^2 Prado catchment, while until then it had been applied to plots or small catchments up to a few square kilometres. However, discharge measurements were only available for the main outlet. Thus, no information was available for subcatchment response to rainfall and runoff. Ideally, more measurements of runoff and, importantly, sediment discharge, should be conducted at the outlets of individual subcatchments. In such a nested approach, the contributions of different areas in the larger catchment might be better incorporated in the simulation of the main hydrograph. Alternatively, incorporating Hydrological Similar Surfaces (HYSS; Kirkby *et al.*, 2002, Bull *et al.*, 2003) might improve spatial characterization of the area and hydrological response. Bull *et al.* (2003) describe a method to derive HYSS using land use, geology and slope classifications and test the method for the Nogalte catchment, which is located close to the Torrealvilla and Prado catchments, but constitutes a different lithology.

The OpenLISEM model was developed to simulate individual events, which can be done in detail due to its detailed output at the catchment outlet (hydrograph). However, the effects of multiple (sequences) of events cannot be evaluated with the current OpenLISEM version. As discussed in chapter 6, the OpenLISEM model could benefit from improvements to the spatial description of sediment deposition processes, so that a realistic output DEM can be simulated and the model can be used to simulate sequences of events. However, this would increase requirements of input parameters and calibration, which were already significant for single events, as discussed above.
Of the many soil erosion models that exist (for reviews see e.g. Jetten *et al.*, 1999, Merritt *et al.*, 2003, Aksoy and Kavvas, 2005), most physically-based models are event-based. Two examples of physically-based models that simulate on a continuous basis are WEPP and SHETRAN. The WEPP model (Water Erosion Prediction Project; Nearing *et al.*, 1989) is a daily continuous model simulating processes of infiltration, runoff, raindrop and flow

detachment, sediment transport, deposition, plant growth and residue decomposition (Flanagan *et al.*, 2007). The model represents sheet, rill and channel erosion. However, as with the OpenLISEM model, one of the main limitations of the model are its large computational and data requirements (Merritt *et al.*, 2003). Additionally, the watershed version of the WEPP model can be problematic for large scale catchments, as individual hillslope scale models are being summed up to the catchment scale, which increases overall data requirements even more, as well as model complexity (Merritt *et al.*, 2003). The SHETRAN model (Ewen *et al.*, 2000) is the sediment transport component of the SHE hydrological model (Abbott *et al.*, 1986a,b). In comparison to other physically-based models, the SHETRAN model can be applied to large catchments (< 2000 km^2) and includes processes of channel bank erosion, gullying and landsliding, besides standard processes of erosion due to raindrop and leaf drip impact and overland flow (Bathurst, 2002). It does not explicitly include rill erosion or crusting. Simulation time step is usually less than 2 h and is automatically reduced during and immediately after rainfall (Ewen *et al.*, 2000). An important limitation is, again, that extensive datasets are required for model parameterisation (see list in Ewen *et al.* (2000)). However, it would be interesting to compare results of OpenLISEM and SHETRAN. Detailed, physically-based soil erosion models that can simulate erosion and sediment dynamics for large catchments on a continuous basis have a common problem of high data requirements and associated uncertainty problems.

7.4.2. Landscape evolution model LAPSUS

To be able to simulate erosion and deposition dynamics in the research area, the LAPSUS model first had to be adapted to better simulate fluvial processes. Chapter 3 describes this implementation and tests the new model's behaviour on a simple artificial catchment. Sensitivity analysis, which should be a standard part of testing and presenting a new or adapted model, showed that the model was sensitive to changes in discharge and gradient exponents (Fig. 3.7) and to spatial resolution (Table 3.4 and Fig. 3.8). Next, in chapter 4 the adapted model was calibrated for the Torrealvilla catchment. The insights and dated sediments of chapter 2 were used to quantitatively simulate a sequence of erosion – sedimentation – erosion. On millennial time-scales these cycles are important, as opposed to net erosion over a certain time period. A landscape evolution model such as LAPSUS that includes complex response feedbacks is an appropriate tool to capture these alternating processes of erosion and sedimentation.

However, as most models, LAPSUS features some limitations that might be addressed in future studies. As shown and discussed in chapter 3, the model is sensitive for DEM resolution. This is to be expected for every spatial model and has been described in earlier studies (Schoorl *et al.*, 2000, Claessens *et al.*, 2005, Temme *et al.*, 2011b). Methods to

overcome resolution sensitivity exist (e.g. Stark and Stark, 2001), and future application of such methods to the LAPSUS model would be interesting to perform.

A second limitation lies in the lumped character of erodibility (*K*) and sedimentation potential (*P*) parameters. These include the effects of, for example, vegetation, lithology, cohesion and roughness and are used for calibration. Values of *K* and *P* can range various orders of magnitude (see chapters 4 and 6 and e.g. Temme *et al.*, 2009) and it is hard to compare calibrated values of *K* and *P* to measureable surface characteristics such as cohesion and thus to judge the values. On the other hand, data availability on detailed characteristics is often not available for long (past) time-scales. In chapter 6, values of *K* and *P* were spatially varied based on land use type, and measured values for cohesion, vegetation cover and roughness for these different land uses were used to restrict the relative values of *K* and *P* between the land uses.

A third limitation of LAPSUS, especially for a semi-arid area such as SE Spain and on shorter (decadal) time-scales, is the absence of a dynamic (re)infiltration procedure. Due to the lack of such re-infiltration processes, low-magnitude events as simulated by LAPSUS have spatial connectivity whereas connectivity is probably low during such low-magnitude events in semi-arid areas (e.g. Calvo-Cases *et al.*, 2003, Bracken and Croke, 2007, Buis and Veldkamp, 2008).

Finally, as concluded in chapter 4, not all processes that might be relevant in the landscape are yet included in the LAPSUS model. Processes that might in future be included in the model are, for instance, grain size distribution (Coulthard and Van De Wiel, 2007), lateral erosion or valley widening (Hooke, 2000a), the effects of base level change, an explicit feedback between vegetation and the water balance (e.g. increased infiltration with increased plant cover) and the interactions between water flow and vegetation patterning (Collins *et al.*, 2004, Saco *et al.*, 2007). However, the potential increased benefit of including these processes into the LAPSUS model is dependent on data availability for case studies. For lateral erosion, the landslide option of LAPSUS (Claessens *et al.*, 2005, 2007a,b) could be tested, which would avoid oversteepening of for example steep gully side walls.

An example of a landscape evolution model (LEM) with increased detail in time step is LEM CAESAR (Coulthard *et al.*, 2002, Coulthard and Van de Wiel, 2006, Van De Wiel *et al.*, 2007). The model can be used to simulate either catchments or river reaches. CAESAR uses a variable time step, related to the volume of erosion and/or deposition, which can vary between a fraction of a second during floods to a maximum of 30 min. (Coulthard *et al.*, 2002). Simulated processes include fluvial erosion and deposition, including different grain sizes and bed armouring, instantaneous mass movement, creep (monthly) and vegetation change (Coulthard *et al.*, 2002). As with continuous physically-based models (see previous section), the more detailed time steps of the CAESAR model means that input and computational requirements of CAESAR are higher than those of LAPSUS (e.g. hourly rainfall, grain size distribution data). However, more detailed outputs (hourly) and

sediment transport rates of individual events can be generated (Hancock *et al.*, 2010). It would be interesting to include the 'event-based' LEM CAESAR in the comparison of LEM LAPSUS and event-based soil erosion OpenLISEM such as done in chapter 6. A comparison of reduced-complexity CAESAR model to the more detailed OpenLISEM model could be used to test the importance of detailed surface and infiltration characteristics in simulating a hydrograph on the catchment scale.

7.4.3. Reductionist versus synthesist approach

As introduced in chapter 1, two contrasting approaches to modelling landscape dynamics exist: reductionism and synthesism (section 1.4). However, many models are not strictly reductionist or synthesist and the term reduced-complexity is often used, implying only an emphasis on simplicity (Nicholas and Quine, 2007). As can be seen from comparing Figs. 1.3 and 1.4, the physically and event-based OpenLISEM soil erosion model incorporates more processes and is therefore more inclined towards the reductionist type of models than the landscape evolution model LAPSUS, which can be called a reduced complexity model. The strong points and limitations of both models as identified in the previous sections (7.4.1 and 7.4.2) are in line with general advantages and disadvantages of synthesist and reductionist type of models (Brasington and Richards, 2007).

In the section 7.4.2, it was suggested to incorporate more, potentially relevant processes into the LAPSUS model. This suggests a shift from the more synthesist approach towards the reductionist approach (although the model would still be a reduced complexity model). However, a major drawback of incorporating more processes is increasing the amount of (unknown or difficult to measure) parameters and therewith model uncertainty (Temme *et al.*, 2011a, Van De Wiel *et al.*, 2011). Therefore, in reduced complexity modelling, this means that instead of highly accurate descriptions reflecting the state of the art in process understanding, it may be better to use less elaborate descriptions in landscape evolution models (Temme *et al.*, 2011a). In addition, inclusion of extra processes in a model should be justified by field observations (such as lateral erosion, see chapter 4), not only by increased model performance (Tucker, 2009). In line with Paola (2011), an interesting approach would be to include progressively fewer processes in a LEM and as such evaluate the relevance of and interactions between those processes. Such an approach would be feasible with LEM LAPSUS, as its structure allows for processes to be optionally (de)activated (e.g. Temme and Veldkamp, 2009, Temme *et al.*, 2011a).

7.5. Research implications

7.5.1. Implications for mitigation measures

Apart from the scientific understanding of landscape processes, insight in the relative importance of nature versus human activity on erosion rates is also relevant for erosion mitigation programs. If the natural system of erosion and deposition dynamics in relation to climate variability in a specific area is known, sustainable soil and water conservation measures may be designed. For instance, infiltration of rainfall could be promoted, e.g. by type specific re-vegetation after abandonment (Lesschen et al., 2008) to reduce erosion, instead of trying to retain sediments behind (small) checkdams, beyond which the clean water will have stronger erosional power (Hooke and Mant, 2000, Boix-Fayos et al., 2008). The concept of path dependency of erosional response (see section 7.3.3) could be used for the design of mitigation measures. For instance, mitigation measures could be designed to break (negative) path dependency or, sustain path dependency if it works desirable.

Also, even scientists who design soil and water conservation measures are not always aware that for instance gully erosion is a natural process and, moreover, that a gully may exist over long time-scales and that it is not necessarily the direct result of human (mis)management of natural resources (e.g. Kirkby and Bracken, 2009). Trying to elucidate this gully may not work, because of the natural system's dynamics. Thus, knowledge on natural erosion and deposition dynamics on broad spatial and temporal scales may prevent money and effort being wasted on fruitless soil conservation measures and the effectiveness of conservation measures should be evaluated at the catchment or regional scale (Cantón et al., 2011).

7.5.2. Methodological and scientific implications

The value of using models as tools in landscape dynamics research as found in this thesis include: (i) it allows to separate different processes and evaluate their relative importance, as shown in chapter 5 for the distinction between human and natural processes; (ii) the effects of scenarios of land use and climate change can be quantitatively evaluated (chapter 6); and (iii) it can lead to increased insight in processes of landscape response, such as non-linearity and self-organization (chapter 6). The latter processes make the prediction or extrapolation of future erosion rates difficult (see section 7.3.3). However, landscape evolution models enable to reproducibly explore complexity and landscape response.

Results from chapter 6 imply that large events can be important in semi-arid landscape evolution but that the quantitative evaluation and results depend on the method and/or model used, which in turn is dependent on data availability, quality and spatial and temporal resolution. At the catchment scale, factors influencing sediment delivery ratios include topographic configuration (e.g. sediment storage space) and landscape characteristics such as transport-limited or detachment-limited systems. The latter also influence the erosive effects of (extreme) event sequencing. For example, a detachment-limited system will generate less sediments if a second large event succeeds a first one than a transport-limited system in which sediments are readily available to be washed away.

There is an important difference between summing the simulated erosion of various individual events and simulating these events continuously over time. For example, the contribution to total erosion of a high magnitude event may be large (Puigdefabregas et al., 1999, Cammeraat, 2004), but its effects might not last in terms of topographical change. Moreover, by assessing the landscape response to different sequences of rainfall variability and extreme events (chapter 6), non-linearity and self-organization emerged as important processes of landscape evolution (Fig. 6.11). Both these processes would not have emerged if events were simulated individually instead of continuously over time. For these reasons, simulating erosion and deposition in a continuous way is preferred over single event simulation if the goal is to understand processes and interactions in catchment evolution. In addition, despite less detail in process description, reduced complexity (i.e. with emphasis on simplicity; Nicholas and Quine, 2007) modelling is advocated (Murray et al., 2009) for the simulation of landscape processes, interactions and feedbacks over long (past) time-scales. Main reasons are the explicit simulations of process interactions and the large data requirements of reductionist models; such data is hardly ever available for the long time past.

However, for shorter (e.g. decadal) time-scales and provided that input data can be reliably estimated, for instance using timeseries of satellite data, a more detailed model such as OpenLISEM could be developed, that is able to simulate sequences of events on a continuous basis.

7.5.3. Exploring the time-scale gap between triggers and landscape response

The central subject of this thesis was the gap in time-scales between rainfall events and landscape evolution, depicted in Fig. 1.1. This can be generalized to a time-scale gap between a trigger and subsequent landscape response in terms of soil redistribution. Fig. 7.1 schematically synthesises this time-scale gap for various processes of landscape dynamics and two spatial scales (catchment and hillslope). As can be seen, the difference between actual process activity and its effect in terms of time-scales of landscape

response can be large. An extreme example is an earthquake, which may take only seconds, but may cause millennial-scale landscape response (e.g. enhanced erosion and catchment adjustment due to base level lowering). Rill erosion is an example of a process which, after initial (short-term) rill formation, may be active until the next ploughing round, which is usually within a few months. As discussed in chapter 4, the time-scale of erosional effects is dependent on the spatial scale at which it is assessed. For example, the effects of tillage directly affect the tilled slopes (on-site effects). However, due to off-site changes in the water balance and transport capacity, the effects of tillage last longer on the catchment scale than on the hillslope scale.

Fig. 7.1 shows that, in general, the effect in terms of soil redistribution is shorter for individual hillslopes than for catchments. This is due to interactions and topographic feedbacks that are apparent on catchment scale, but are less profound at hillslope scales. This implies that simulation of hillslope processes could well be evaluated by more detailed models such as OpenLISEM, or models specialised in simulating a specific (hillslope) process (e.g. landsliding, gully initiation or tillage (Van Oost et al., 2000, 2005)). To simulate catchment scale landscape dynamics a model capable of simulating interactions and feedbacks between processes is needed.

Furthermore, Fig. 7.1 implies that contemporary landscape processes and dynamics may be (but not necessarily always are) the response to (long ago) past triggers. Therefore, assessing possible past triggers is essential for understanding present day landscape processes.
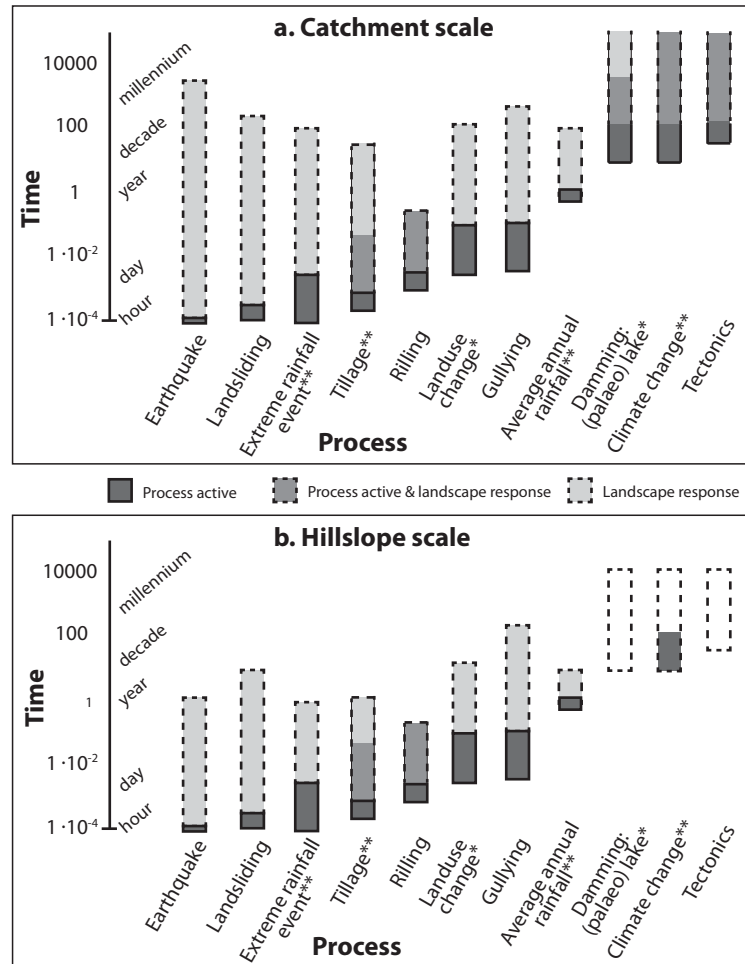
Fig. 7.1. Schematic visualization of time-scale of process activity and landscape response in terms of soil redistribution for various processes at the a). catchment spatial scale and b). hillslope scale. * = qualitatively / exploratively assessed in this thesis; ** = quantitatively assessed in this thesis.

7.6. General conclusions and research challenges

This thesis answered several research questions related to human versus natural erosion dynamics and the time-scale gap between individual events and long-term landscape evolution, using models as tools. The spatial scale assessed in this study is the catchment scale, so that landscape dynamics, interactions and feedback mechanisms are included in the analysis, as well as (changes in) connectivity and sediment storage. This leads to enhanced insights in landscape process functioning, revealing for example the

179

importance of non-linearity in landscape response to rainfall variability. (Sustainable) management of landscapes and ecosystems is usually assessed at the catchment or regional scale. Therefore, processes should also be assessed at that scale. Innovative aspects of this thesis research include the explicit simulation of anthropogenic processes over long-term (millennial) time-scales and the comparison of an event-based soil erosion model and a landscape evolution model with the aim to bridge the time-scale gap in erosion modelling. General conclusions of the thesis are:

- In a holistic approach combining fieldwork and modelling, triggers of landscape change can be identified and their temporal and spatial effects can be evaluated. Preferably, such an analysis of landscape processes and response is performed for a relatively large area and temporal scale, because upstream processes can influence those downstream and vice versa and because time-lags between triggers and landscape response can be large (Fig.7.1).

- Models can be promising tools for the evaluation of landscape dynamics. Such a model should be able to simulate:
  - Continuously over time, which is needed if the aim is to understand processes and interaction in catchment evolution over time;
  - Various processes individually or in combination so that their relative importance in landscape evolution can be quantitatively evaluated. In this way, human and natural processes can be evaluated separately and their individual contribution to erosion and deposition can be quantified.
  - Complex response feedbacks capable of capturing alternating sequences of erosion and deposition processes as well as temporally changing (dis)connectivity, local sediment storage and self-organizing and non-linear behaviour.

  A landscape evolution model such as LAPSUS meets these requirements, also for longer time-scales, but is less detailed than the physically based OpenLISEM model. For the latter model to meet the first requirement, a continuous OpenLISEM version could be developed.

- Simulated landscape response to climate variability and different sequencing of events demonstrates non-linearity and self-organization. Extreme events must have high magnitude and/or high frequency if they are to leave a net trace in the landscape. Furthermore, the effects of high magnitude events can be eliminated over time by topographic feedback and non-linearity. Thus, extreme events should be evaluated on longer time-scales and within the context of (potential) rainfall variation to be able to judge their effect on landscape dynamics.

Future research challenges

In this chapter, several suggestions for further research were given, mainly related to the limitations of the OpenLISEM and LAPSUS models. For the application of OpenLISEM to large catchments, methods to increase insight in spatial response of (sub)catchments are needed, such as a nested measurement approach or possibly applying Hydrological Similar Surfaces (HYSS). Furthermore, the possibility to simulate sequences of events could be added to the OpenLISEM model. For LAPSUS, the incorporation of a dynamic infiltration module, possibly related to vegetation changes is advocated, as well as the introduction of other processes such as lateral erosion and grain size distribution. In terms of model comparison, it was mentioned that it would be interesting to include the 'event-based LEM' CAESAR to the comparison of chapter 6. Other interesting research challenges include:

- To investigate the effects in terms of erosion and sedimentation dynamics of base level changes. These can for instance be caused by (palaeo- and historic) lake formation and disruption. Evidence of the existence of a palaeo-lake was found, but the trigger of the blocking event is unknown, as well as the nature, exact location and timing of the dam and its eventual failure. The effect of sediment transportation after dam failure by the Guadalentín river probably influenced erosion and sedimentation dynamics of the Torrealvilla catchment due to base level changes. The Puentes reservoir, which has been disrupted twice (in 1648 and 1802), may have caused similar changes.

- To include tectonic activity in the landscape reconstruction and modelling. This has not been included up to now, although the region in general is known to be tectonically active (Lorca earthquake, May 2009). For the Torrealvilla catchment in particular, tectonic activity could for instance have played a role in creating accommodation space for sedimentation in the lower part of the catchment. Quantifying how tectonics influenced sedimentation and erosion dynamics could be interesting.

- To combine vegetation patterning and erosion and sedimentation dynamics on the catchment scale. Self-organized vegetation patterns (e.g. tigerbush) are important in (dryland) ecology and related to sudden shifts in ecosystem functioning (e.g. Rietkerk *et al.*, 2004, Kefi *et al.*, 2007). Understanding the triggers that lead to such shifts is crucial to the sustainable management of ecosystems. Until now, models that describe vegetation patterns do not include the spatial interactions and feedbacks between vegetation dynamics (biotic) and soil redistribution (abiotic) processes in the landscape. These effects could be evaluated by incorporating a dynamic vegetation module in a LEM such as LAPSUS.

- To evaluate the effect of system characteristics (i.e. transport- or detachment limited, initial topographic conditions) on the results of event sequencing. The SE Spanish landscape of this thesis consists mainly of soft sediments in the valley and channel, constituting a transport-limited system. If a landscape is largely detachment limited, the effect of (extreme) event sequencing might be different. Perhaps most systems are not strictly detachment- or transport-limited, but may for example have soft sediments covering hard rock channels. Thresholds between system response may exist if going from transport- to detachment limited systems. In addition, initial topography (e.g. steep or shallow and long or short slopes; channel characteristics etc.) may influence erosion and sedimentation dynamics (path dependency; Stallins, 2006, Wainwright and Millington, 2010). These issues could be evaluated using a LEM and, for instance, different hypothetical DEMs.

- While this thesis focussed on the temporal scale of erosion dynamics, the spatial dynamics of events in landscape evolution is a continuing interesting topic. In section 7.3.2 the concept of connectivity was discussed. While some authors state that most sediments originate from the channels during (extreme) erosion events (e.g. Hooke and Mant, 2000), this might conceal the contribution of smaller events that were not connected to the channel network and that deposited sediment in or near the channel. As such, the channel might seem to produce the major part of the sediments eroded during a large event, however, the role of smaller events in providing sediments ready to be washed away might be underestimated. In general, the landscape can be seen as a conveyor belt for sediment transportation, which can be short (low magnitude events) or long (high-magnitude events). Thus, the role of a channel might only be that of a conveyor belt instead of producing sediments. Does each of these opposing roles of a channel leave a different topographic imprint, or, in other words, can the topography of a landscape reveal the functioning of the channel (for instance, a deeply incised channel with steep sidewalls in rolling hillslopes or a wide channel surrounded by steep slopes)?

- To test the further development of long-term (centennial – millennial) continuous models of landscape evolution in terms of process representation. Two general approaches can be distinguished: including more processes into a landscape evolution model such as LAPSUS or excluding processes from a physically based, detailed model such as (a continuous) OpenLISEM. Both approaches would gain insight in process relevance, dependent on (spatial) scales and they do not necessarily lead to the same result. Comparing both approaches would therefore give further insight in model functioning.
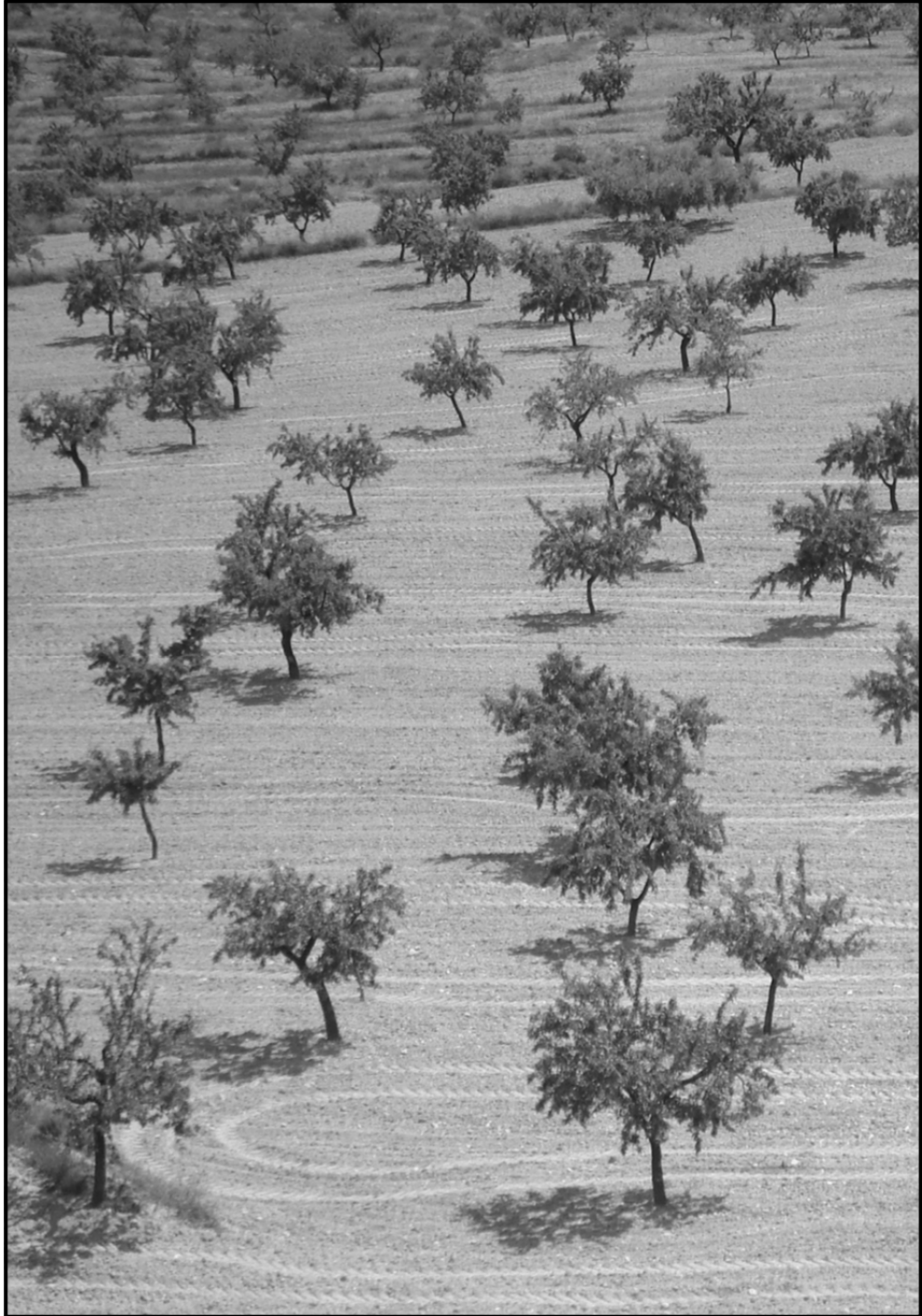
References

Abbott MB, Bathurst JC, Cunge JA, O'Connell PE, Rasmussen J. 1986a. An introduction to the European Hydrological System - Systeme Hydrologique Europeen, "SHE", 1: History and philosophy of a physically-based, distributed modelling system. *Journal of Hydrology* 87: 45-59.

Abbott MB, Bathurst JC, Cunge JA, O'Connell PE, Rasmussen J. 1986b. An introduction to the European Hydrological System - Systeme Hydrologique Europeen, "SHE", 2: Structure of a physically-based, distributed modelling system. *Journal of Hydrology* 87: 61-77.

Abu Ghazleh S, Kempe S. 2009. Geomorphology of Lake Lisan terraces along the eastern coast of the Dead Sea, Jordan. *Geomorphology* 108: 246-263.

Ahnert F. 1976. Brief description of a comprehensive process-response model of landform development. *Zeitschrift für Geomorphologie, Supplementband* 25: 25-49.

Aksoy H, Kavvas ML. 2005. A review of hillslope and watershed scale erosion and sediment transport models. *Catena* 64: 247-271.

Alexandrov Y, Laronne JB, Reid I. 2003. Suspended sediment concentration and its variation with water discharge in a dryland ephemeral channel, northern Negev, Israel. *Journal of Arid Environments* 53: 73-84.

Alonso-Sarría F, López-Bermúdez F, Conesa-García C. 2002. Synoptic Conditions Producing Extreme Rainfall Events along the Mediterranean Coast of the Iberian Peninsula. In *Dryland Rivers: Hydrology and Geomorphology of Semi-arid Channels*, Bull LJ, Kirkby MJ (eds). John Wiley & Sons, Chichester, UK.

Arnaud-Fassetta G, Bertrand F, Costa S, Davidson R. 2006. The western lagoon marshes of the Ria Formosa (Southern Portugal): Sediment-vegetation dynamics, long-term to short-term changes and perspective. *Continental Shelf Research* 26: 363-384.

Avni Y, Porat N, Plakht J, Avni G. 2006. Geomorphic changes leading to natural desertification versus anthropogenic land conservation in an arid environment, the Negev Highlands, Israel. *Geomorphology* 82: 177-200.

Bakker MM, Govers G, van Doorn A, Quetier F, Chouvardas D, Rounsevell M. 2008. The response of soil erosion and sediment export to land-use change in four areas of Europe: The importance of landscape pattern. *Geomorphology* 98: 213-226.

Ballarini M, Wallinga J, Wintle AG, Bos AJJ. 2007. A modified SAR protocol for optical dating of individual grains from young quartz samples. *Radiation Measurements* 42: 360-369.

Banwart S. 2011. Save our soils. *Nature* 474: 151-152.

Bartov Y, Enzel Y, Porat N, Stein M. 2007. Evolution of the Late Pleistocene Holocene Dead Sea Basin from Sequence Statigraphy of Fan Deltas and Lake-Level Reconstruction. *Journal of Sedimentary Research* 77: 680-692.

Bathurst JC. 2002. Physically-based erosion and sediment yield modelling: the SHETRAN concept. In *Modelling erosion, sediment transport and sediment yield*, Summer W, Walling DE (eds). IHP-VI Technical Documents in Hydrology, No. 60, Unesco, Paris, France. p. 47-67.

Bathurst JC, Kilsby C, White S. 1996. Modelling the Impacts of Climate and Land-Use Change on Basin Hydrology and Soil Erosion in Mediterranean Europe. In *Mediterranean Desertification and Land Use*, Brandt CJ, Thornes JB (eds). John Wiley & Sons, Chichester, UK.

Benito G, Thorndycraft VR. 2005. Palaeoflood hydrology and its role in applied hydrological sciences. *Journal of Hydrology* 313: 3-15.

Benito G, Thorndycraft VR, Rico M, Sánchez-Moya Y, Sopeña A. 2008. Palaeoflood and floodplain records from Spain: Evidence for long-term climate variability and environmental changes. *Geomorphology* 101: 68-77.

Benito G, Rico M, Sánchez-Moya Y, Sopeña A, Thorndycraft VR, Barriendos M. 2010. The impact of late Holocene climatic variability and land use change on the flood hydrology of the Guadalentín River, southeast Spain. *Global and Planetary Change* 70: 53-63.

Boardman J. 2006. Soil erosion science: Reflections on the limitations of current approaches. *Catena* 68: 73-86.

Boer M, Puigdefábregas J. 2005. Effects of spatially structured vegetation patterns on hillslope erosion in a semiarid Mediterranean environment: a simulation study. *Earth Surface Processes and Landforms* 30: 149-167.

Boix-Fayos C, Martínez-Mena M, Calvo-Cases A, Castillo VM, Albaladejo J. 2005. Concise review of interrill erosion studies in SE Spain (Alicante and Murcia): erosion rates and progress of knowledge from the 1980s. *Land Degradation & Development* 16: 517-528.

Boix-Fayos C, Martínez-Mena M, Calvo-Cases A, Arnau-Rosalén E, Albaladejo J, Castillo V. 2007. Causes and underlying processes of measurement variability in field erosion plots in Mediterranean conditions. *Earth Surface Processes and Landforms* 32: 85-101.

Boix-Fayos C, De Vente J, Martínez-Mena M, Barberá GG, Castillo V. 2008. The impact of land use change and check-dams on catchment sediment yield. *Hydrological Processes* 22: 4922-4935.

Bork HR, Li Y, Zhao Y, Zhang J, Shiquan Y. 2001. Land use changes and gully development in the Upper Yangtze River Basin, SW-China. *Journal of Mountain Science* 19: 97-103.

Bøtter-Jensen L, Andersen CE, Duller GAT, Murray AS. 2003. Developments in radiation, stimulation and observation facilities in luminescence measurements. *Radiation Measurements* 37: 535-541.

Bracken LJ, Kirkby MJ. 2005. Differences in hillslope runoff and sediment transport rates within two semi-arid catchments in southeast Spain. *Geomorphology* 68: 183-200.

Bracken LJ, Croke J. 2007. The concept of hydrological connectivity and its contribution to understanding runoff-dominated geomorphic systems. *Hydrological Processes* 21: 1749-1763.

Bracken LJ, Cox NJ, Shannon J. 2008. The relationship between rainfall inputs and flood generation in south-east Spain. *Hydrological Processes* 22: 683-696.

Brandt CJ, Thornes JB. 1996. *Mediterranean Desertification and Land Use.* John Wiley & Sons, Chichester, UK.

Brasington J, Richards K. 2007. Reduced-complexity, physically-based geomorphological modelling for catchment and river management. *Geomorphology* 90: 171-177.

Bridgland D, Westaway R. 2008. Climatically controlled river terrace staircases: A worldwide Quaternary phenomenon. *Geomorphology* 98: 285-315.

Brunsden D, Thornes JB. 1979. Landscape Sensitivity and Change. *Transactions of the Institute of British Geographers* 4: 463-484.

Buis E, Veldkamp A. 2008. Modelling dynamic water redistribution patterns in arid catchments in the Negev Desert of Israel. *Earth Surface Processes and Landforms* 33: 107-122.

Bull LJ, Kirkby MJ, Shannon J, Hooke JM. 1999. The impact of rainstorms on floods in ephemeral channels in southeast Spain. *Catena* 38: 191-209.

Bull LJ, Kirkby MJ, Shannon J, Dunsford HD. 2003. Predicting Hydrologically Similar Surfaces (HYSS) in Semi-Arid Environments. *Advances in Environmental Monitoring and Modelling* 1: 1-26.

Burt TP. 1998. Infiltration for soil erosion models: some temporal and spatial complications. In *Modelling Soil Erosion by Water*, Boardman J, Favis-Mortlock D (eds). Springer-Verlag, Berlin, Germany.

Cacho I. 2006. Western Mediterranean d18O and Uk37 Data and SST Reconstructions. IGBP Pages/World Data Center for Paleoclimatology.

Cacho I, Grimalt JO, Canals M, Sbaffi L, Shackleton NJ, Schönfeld J, Zahn R. 2001. Variability of the western Mediterranean Sea surface temperature during the last 25,000 years and its connection with the Northern Hemisphere climatic changes. *Paleoceanography* 16: 40-52.

Calmel-Avila M. 1998. Géomorphogenèse Holocène dans la Bas-Guadalentín, Bassin du Segura, Province de Murcie, Espagne. PhD Thesis, Université de Pau et des pays de l'Adour, France. 323p.

Calmel-Avila M. 2000. Procesos hídricos holocenos en el bajo Guadalentín (Murcia, SE España). *Rev. C. & G.* 14: 65-78.

Calvo-Cases A, Boix-Fayos C, Imeson AC. 2003. Runoff generation, sediment movement and soil water behaviour on calcareous (limestone) slopes of some Mediterranean environments in southeast Spain. *Geomorphology* 50: 269-291.

Cammeraat ELH. 2004. Scale dependent thresholds in hydrological and erosion response of a semi-arid catchment in southeast Spain. *Agriculture, Ecosystems & Environment* 104: 317-332.

Cammeraat LH, Imeson AC. 1998. Deriving indicators of soil degradation from soil aggregation studies in southeastern Spain and southern France. *Geomorphology* 23: 307-321.

Cammeraat E, van Beek R, Kooijman A. 2005. Vegetation Succession and its Consequences for Slope Stability in SE Spain. *Plant and Soil* 278: 135-147.

Candy I, Black S, Sellwood BW. 2004. Interpreting the response of a dryland river system to Late Quaternary climate change. *Quaternary Science Reviews* 23: 2513-2523.

Cantón Y, Solé-Benet A, de Vente J, Boix-Fayos C, Calvo-Cases A, Asensio C, Puigdefábregas J. 2011. A review of runoff generation and soil erosion across scales in semiarid south-eastern Spain. *Journal of Arid Environments* 75: 1254-1261.

Carrión JS, Fuentes N, González-Sampériz P, Sánchez Quirante L, Finlayson JC, Fernández S, Andrade A. 2007. Holocene environmental change in a montane region of southern Europe with a long history of human settlement. *Quaternary Science Reviews* 26: 1455-1475.

Carrión JS, Fernández S, Jiménez-Moreno G, Fauquette S, Gil-Romera G, González-Sampériz P, Finlayson C. 2010. The historical origins of aridity and vegetation degradation in southeastern Spain. *Journal of Arid Environments* 74: 731-736.

Castillo VM, Gomez-Plaza A, Martinez-Mena M. 2003. The role of antecedent soil water content in the runoff response of semiarid catchments: a simulation approach. *Journal of Hydrology* 284: 114-130.

Castro M, Martín-Vide J, Alonso S. 2005. The climate of Spain: Past, present and scenarios for the 21st century. In *A Preliminary Assessment of the Impacts in Spain due to the Effects of Climate Change (ECCE Project, Final Report)*, Moreno Rodríguez JM (eds). Ministerio de Medio Ambiente, Madrid, Spain.

Chow VT, Maidment DR, Mays LW. 1988. *Applied Hydrology*. McGraw-Hill: Maidenhead, UK. 572p.

Christensen JH, Hewitson B, Busuioc A, Chen A, Gao X, Held I, Jones R, Kolli RK, Kwon W-T, Laprise R, Magaña Rueda V, Mearns L, Menéndez CG, Räisänen J, Rinke A, Sarr A, Whetton P. 2007. Regional Climate Projections. In *CLimate Change 2007: The Physical Science Basis. Contribution of Working Group I to the Fourth Assessment Report of the Intergovernmental Panel on Climate Change*, Solomon S, Qin D, Manning M, Chen Z, Marquis M, Averyt KB, Tignor M, Miller HL (eds). Cambridge University Press, Cambridge, UK and New York, NY, USA.

Claessens L, Schoorl JM, Veldkamp A. 2007a. Modelling the location of shallow landslides and their effects on landscape dynamics in large watersheds: An application for Northern New Zealand. *Geomorphology* 87: 16-27.

Claessens L, Stoorvogel J, Antle J. 2010. Exploring the impacts of field interactions on an integrated assessment of terraced crop systems in the Peruvian Andes. *Journal of Land Use Science* 5: 259-275.

Claessens L, Heuvelink GBM, Schoorl JM, Veldkamp A. 2005. DEM resolution effects on shallow landslide hazard and soil redistribution modelling. *Earth Surface Processes and Landforms* 30: 461-477.

Claessens L, Verburg PH, Schoorl JM, Veldkamp A. 2006a. Contribution of topographically based landslide hazard modelling to the analysis of the spatial distribution and ecology of kauri (Agathis australis). *Landscape Ecology* 21: 63-76.

Claessens L, Lowe DJ, Hayward BW, Schaap BF, Schoorl JM, Veldkamp A. 2006b. Reconstructing high-magnitude/low-frequency landslide events based on soil redistribution modelling and a Late-Holocene sediment record from New Zealand. *Geomorphology* 74: 29-49.

Claessens L, Knapen A, Kitutu MG, Poesen J, Deckers JA. 2007b. Modelling landslide hazard, soil redistribution and sediment yield of landslides on the Ugandan footslopes of Mount Elgon. *Geomorphology* 90: 23-35.

Claessens L, Schoorl JM, Verburg PH, Geraedts L, Veldkamp A. 2009. Modelling interactions and feedback mechanisms between land use change and landscape processes. *Agriculture, Ecosystems & Environment* 129: 157-170.

Collins DBG, Bras RL, Tucker GE. 2004. Modeling the effects of vegetation-erosion coupling on landscape evolution. *J. Geophys. Res.* 109: F03004.

Combourieu Nebout N, Peyron O, Dormoy I, Desprat S, Beaudouin C, Kotthoff U, Marret F. 2009. Rapid climatic variability in the west Mediterranean during the last 25 000 years from high resolution pollen data. *Clim. Past* 5: 503-521.

Coulthard TJ. 2001. Landscape evolution models: a software review. *Hydrological Processes* 15: 165-173.

Coulthard TJ, Macklin MG. 2001. How sensitive are river systems to climate and land-use changes? A model-based evaluation. *Journal of Quaternary Science* 16: 347-351.

Coulthard TJ, Wiel MJVD. 2006. A cellular model of river meandering. *Earth Surface Processes and Landforms* 31: 123-132.

Coulthard TJ, Van De Wiel MJ. 2007. Quantifying fluvial non linearity and finding self organized criticality? Insights from simulations of river basin evolution. *Geomorphology* 91: 216-235.

Coulthard TJ, Kirkby MJ, Macklin MG. 1999. Non-linearity and spatial resolution in a cellular automaton model of a small upland basin. *Hydrol. Earth Syst. Sci.* 2: 257-264.

Coulthard TJ, Kirkby MJ, Macklin MG. 2000. Modelling geomorphic response to environmental change in an upland catchment. *Hydrological Processes* 14: 2031-2045.

Coulthard TJ, Macklin MG, Kirkby MJ. 2002. A cellular model of Holocene upland river basin and alluvial fan evolution. *Earth Surface Processes and Landforms* 27: 269-288.

Coulthard TJ, Lewin J, Macklin MG. 2005. Modelling differential catchment response to environmental change. *Geomorphology* 69: 222-241.

De Alba S, Lindstrom M, Schumacher TE, Malo DD. 2004. Soil landscape evolution due to soil redistribution by tillage: a new conceptual model of soil catena evolution in agricultural landscapes. *CATENA* 58: 77-100.

De Baets S, Poesen J, Knapen A, Barberá G, Navarro J. 2007. Root characteristics of representative Mediterranean plant species and their erosion-reducing potential during concentrated runoff. *Plant and Soil* 294: 169-183.

De Baets S, Torri D, Poesen J, Salvador MP, Meersmans J. 2008a. Modelling increased soil cohesion due to roots with EUROSEM. *Earth Surface Processes and Landforms* 33: 1948-1963.

De Baets S, Poesen J, Reubens B, Wemans K, De Baerdemaeker J, Muys B. 2008b. Root tensile strength and root distribution of typical Mediterranean plant species and their contribution to soil shear strength. *Plant and Soil* 305: 207-226.

De Jong SM, Jetten VG. 2007. Estimating spatial patterns of rainfall interception from remotely sensed vegetation indices and spectral mixture analysis. *International Journal of Geographical Information Science* 21: 529 - 545.

De Moor JJW, Kasse C, van Balen R, Vandenberghe J, Wallinga J. 2008. Human and climate impact on catchment development during the Holocene -- Geul River, the Netherlands. *Geomorphology* 98: 316-339.

De Roo APJ, Jetten VG. 1999. Calibrating and validating the LISEM model for two data sets from the Netherlands and South Africa. *Catena* 37: 477-493.

De Roo APJ, Wesseling CG, Ritsema CJ. 1996a. LISEM: A Single-Event Physically Based Hydrological and Soil Erosion Model for Drainage Basins. I: Theory, Input and Output. *Hydrological Processes* 10: 1107-1117.

De Roo APJ, Offermans RJE, Cremers NHDT. 1996b. LISEM: A Single-Event, Physically Based Hydrological and Soil Erosion Model for Drainage Basins II: Sensitivity Analysis, Validation and Application. *Hydrological Processes* 10: 1119-1126.

De Vente J. 2009. Soil Erosion and Sediment Yield in Mediterranean Geoecosystems - Scale issues, modelling and understanding. PhD Thesis, Katolieke Universiteit Leuven, Belgium. 264p.

De Wit A. 2001. Runoff controlling factors in various sized catchmnets in a semi-arid Mediterranean environment in Spain. PhD Thesis, Utrecht University, The Netherlands. 229p.

Dearing JA, Jones RT, Shen J, Yang X, Boyle JF, Foster GC, Crook DS, Elvin MJD. 2008. Using multiple archives to understand past and present climate-human- environment interactions: The lake Erhai catchment, Yunnan Province, China. *Journal of Paleolimnology* 40: 3-31.

Descroix L, Gautier E. 2002. Water erosion in the southern French alps: climatic and human mechanisms. *Catena* 50: 53-85.

Dotterweich M. 2008. The history of soil erosion and fluvial deposits in small catchments of central Europe: Deciphering the long-term interaction between humans and the environment -- A review. *Geomorphology* 101: 192-208.

Duller GAT. 2008. Single-grain optical dating of Quaternary sediments: why aliquot size matters in luminescence dating. *Boreas* 37: 589-612.

EEA. 2000. CORINE Land Cover 2000.

Eiroa Rodriguez JA. 2011. Tres útiles agrícolas andalusíes conservados en el Museo Santa Clara (Murcia). *Tudmir - Revista del museo Santa Clara Murcia* 2: 61-68.

European Commission. 2006. Soil protection - the long story behind the strategy. Technical report. Office for Official Publications of the European Communities, Luxembourg.

European Commission. 2011. Glossary of Soil Terms. Web page: http://eusoils.jrc.ec.europa.eu/ESDB_Archive/glossary/Soil_Terms.html. 30-12-2011.

Ewen J, Parkin G, O'Connell PE. 2000. SHETRAN: Distributed river basin flow and transport modeling system. *Journal of Hydrologic Engineering* 5: 250-258.

Faust D, Zielhofer C, Baena Escudero R, Diaz del Olmo F. 2004. High-resolution fluvial record of late Holocene geomorphic change in northern Tunisia: climatic or human impact? *Quaternary Science Reviews* 23: 1757-1775.

Flanagan DC, Gilley JE, Franti TG. 2007. Water Erosion Prediction Project (WEPP): Development history, model capabilities, and future enhancements. *Transactions of the ASABE* 50: 1603-1612.

Foster GR, Meyer LD. 1972. A closed-form soil erosion equation for upland areas. In *Sedimentation*, Shen HW (eds). Colorado State University, Fort Collins, CO, USA. 12:1 - 12:19.

Freeman TG. 1991. Calculating catchment area with divergent flow based on a regular grid. *Computers and Geosciences* 17: 413-422.

Fresco LO, Kroonenberg SB. 1992. Time and spatial scales in ecological sustainability. *Land Use Policy* 9: 155-168.

Fuchs M. 2007. An assessment of human versus climatic impacts on Holocene soil erosion in NE Peloponnese, Greece. *Quaternary Research* 67: 349-356.

Fuchs M, Buerkert A. 2008. A 20 ka sediment record from the Hajar Mountain range in N-Oman, and its implication for detecting arid–humid periods on the southeastern Arabian Peninsula. *Earth and Planetary Science Letters* 265: 546-558.

Fuchs M, Lang A. 2009. Luminescence dating of hillslope deposits-A review. *Geomorphology* 109: 17-26.

Fuchs M, Fischer M, Reverman R. 2010. Colluvial and alluvial sediment archives temporally resolved by OSL dating: Implications for reconstructing soil erosion. *Quaternary Geochronology* 5: 269-273.

García-Ruiz JM. 2010. The effects of land uses on soil erosion in Spain: A review. *Catena* 81: 1-11.

Geel T, Roep TB. 1998. Oligocene to middle Miocene basin development in the Eastern Betic Cordilleras, SE Spain (Vélez Rubio Corridor - Espuña): reflections of West Mediterranean plate-tectonic reorganizations. *Basin Research* 10: 325-343.

188

Gellis AC, Pavich MJ, Bierman PR, Clapp EM, Ellevein A, Aby S. 2004. Modern sediment yield compared to geologic rates of sediment production in a semi-arid basin, New Mexico: assessing the human impact. *Earth Surface Processes and Landforms* 29: 1359-1372.

Giorgi F, Lionello P. 2008. Climate change projections for the Mediterranean region. *Global and Planetary Change* 63: 90-104.

Gonzalez-Hidalgo JC, Pena-Monne JL, de Luis M. 2007. A review of daily soil erosion in Western Mediterranean areas. *Catena* 71: 193-199.

González-Hidalgo JC, de Luis M, Batalla RJ. 2009. Effects of the largest daily events on total soil erosion by rainwater. An analysis of the USLE database. *Earth Surface Processes and Landforms* 34: 2070-2077.

Gonzalez-Hidalgo JC, Batalla RJ, Cerdá A, de Luis M. 2010. Contribution of the largest events to suspended sediment transport across the USA. *Land Degradation and Development* 21: 83-91.

Gottdang A, Mous DJW, Van der Plicht J. 1995. The HVEE 14C system at Groningen. *Radiocarbon* 37: 649-656.

Govers G. 1990. Empirical relationships on the transporting capacity of overland flow. In *Erosion, transport and deposition processes*, Walling DE, Yair A, Berkowicz S (eds). IAHS: Wallingford, UK. p. 45-63.

Govers G, Van Oost K, Poesen J. 2006. Responses of a semi-arid landscape to human disturbance: A simulation study of the interaction between rock fragment cover, soil erosion and land use change. *Geoderma* 133: 19-31.

Govers G, Vandaele K, Desmet P, Poesen J, Bunte K. 1994. The role of tillage in soil redistribution on hillslopes. *European Journal of Soil Science* 45: 469-478.

Govers G, Quine TA, Desmet PJJ, Walling DE. 1996. The relative contribution of soil tillage and overland flow erosion to soil redistribution on agricultural land. *Earth Surface Processes and Landforms* 21: 929-946.

Haileslassie A, Priess J, Veldkamp E, Teketay D, Lesschen JP. 2005. Assessment of soil nutrient depletion and its spatial variability on smallholders' mixed farming systems in Ethiopia using partial versus full nutrient balances. *Agriculture, Ecosystems and Environment* 108: 1-16.

Haileslassie A, Priess JA, Veldkamp E, Lesschen JP. 2006. Smallholders' soil fertility management in the Central Highlands of Ethiopia: Implications for nutrient stocks, balances and sustainability of agroecosystems. *Nutrient Cycling in Agroecosystems* 75: 135-146.

Haileslassie A, Priess JA, Veldkamp E, Lesschen JP. 2007. Nutrient flows and balances at the field and farm scale: Exploring effects of land-use strategies and access to resources. *Agricultural Systems* 94: 459-470.

Hancock GR. 2009. A catchment scale assessment of increased rainfall and storm intensity on erosion and sediment transport for Northern Australia. *Geoderma* 152: 350-360.

Hancock GR, Coulthard TJ. 2011. Channel movement and erosion response to rainfall variability in southeast Australia. *Hydrological Processes* n/a-n/a.

Hancock GR, Willgoose GR, Evans KG. 2002. Testing of the SIBERIA landscape evolution model using the Tin Camp Creek, Northern Territory, Australia, field catchment. *Earth Surface Processes and Landforms* 27: 125-143.

Hancock GR, Lowry JBC, Moliere DR, Evans KG. 2008a. An evaluation of an enhanced soil erosion and landscape evolution model: a case study assessment of the former Nabarlek uranium mine, Northern Territory, Australia. *Earth Surface Processes and Landforms* 33: 2045-2063.

Hancock GR, Crawter D, Fityus SG, Chandler J, Wells T. 2008b. The measurement and modelling of rill erosion at angle of repose slopes in mine spoil. *Earth Surface Processes and Landforms* 33: 1006-1020.

Hancock GR, Lowry JBC, Coulthard TJ, Evans KG, Moliere DR. 2010. A catchment scale evaluation of the SIBERIA and CAESAR landscape evolution models. *Earth Surface Processes and Landforms* 35: 863-875.

Hancock GR, Evans KG, McDonnell J, Hopp L. 2011. Ecohydrological controls on soil erosion and landscape evolution. *Ecohydrology* (In Press).

Harrison S. 2001. On reductionism and emergence in geomorphology. *Transactions of the Institute of British Geographers* 26: 327-339.

Harvey AM, Wells SG. 1987. Response of Quaternary fluvial systems to differential epeirogenic uplift; Aguas and Feos river systems, Southeast Spain. *Geology* 15: 689-693.

Harvey AM, Silva PG, Mather AE, Goy JL, Stokes M, Zazo C. 1999. The impact of Quaternary sea-level and climatic change on coastal alluvial fans in the Cabo de Gata ranges, southeast Spain. *Geomorphology* 28: 1-22.

Hessel R, van den Bosch R, Vigiak O. 2006. Evaluation of the LISEM soil erosion model in two catchments in the East African Highlands. *Earth Surface Processes and Landforms* 31: 469-486.

Hessel R, Jetten V, Liu B, Zhang Y, Stolte J. 2003. Calibration of the LISEM model for a small Loess Plateau catchment. *Catena* 54: 235-254.

Hessel R, Gupta MK, Singh Datta P, Gelderman E. 2007. Application of the LISEM Soil Erosion Model to a Forested Catchment in the Indian Himalayas. *International Journal of Ecology and Environmental Sciences* 33: 129-142.

Heuvelink GBM, Schoorl JM, Veldkamp A, Pennock DJ. 2006. Space-time Kalman filtering of soil redistribution. *Geoderma* 133: 124-137.

Hoffmann T, Thorndycraft VR, Brown AG, Coulthard TJ, Damnati B, Kale VS, Middelkoop H, Notebaert B, Walling DE. 2010. Human impact on fluvial regimes and sediment flux during the Holocene: Review and future research agenda. *Global and Planetary Change* 72: 87-98.

Holmgren P. 1994. Multiple flow direction algorithms for runoff modelling in grid based elevation models: An empirical evaluation. *Hydrological Processes* 8: 327-334.

Hooke J. 2003. Coarse sediment connectivity in river channel systems: a conceptual framework and methodology. *Geomorphology* 56: 79-94.

Hooke JM. 2006. Human impacts on fluvial systems in the Mediterranean region. *Geomorphology* 79: 311-335.

Hooke JM. 2007. Monitoring morphological and vegetation changes and flow events in dryland river channels. *Environmental Monitoring and Assessment* 127: 445-457.

Hooke JM, Mant JM. 2000. Geomorphological impacts of a flood event on ephemeral channels in SE Spain. *Geomorphology* 34: 163-180.

Hooke JM, Brookes CJ, Duane W, Mant JM. 2005. A simulation model of morphological, vegetation and sediment changes in ephemeral streams. *Earth Surface Processes and Landforms* 30: 845-866.

Hooke RL. 2000a. On the history of humans as geomorphic agents. *Geology* 28: 843-846.

Hooke RL. 2000b. Toward a uniform theory of clastic sediment yield in fluvial systems. *Geological Society of America Bulletin* 112: 1778-1786.

Houben P, Wunderlich J, Schrott L. 2009. Climate and long-term human impact on sediment fluxes in watershed systems. *Geomorphology* 108: 1-7.

IGME. 1981. Mapa Geologico de Espana, 1:50.000, Sheet Lorca (953). Servicio de Publicaciones, Ministerio de Industria, Spain.

Jacobson RB, Miller AJ, Smith JA. 1989. The role of catastrophic geomorphic events in central Appalachian landscape evolution. *Geomorphology* 2: 257-284.

Jalut G, Esteban Amat A, Bonnet L, Gauquelin T, Fontugne M. 2000. Holocene climatic changes in the Western Mediterranean, from south-east France to south-east Spain. *Palaeogeography, Palaeoclimatology, Palaeoecology* 160: 255-290.

Jalut G, Dedoubat JJ, Fontugne M, Otto T. 2009. Holocene circum-Mediterranean vegetation changes: Climate forcing and human impact. *Quaternary International* 200: 4-18.

Jerolmack DJ, Paola C. 2010. Shredding of environmental signals by sediment transport. *Geophysical Research Letters* 37

Jester W, Klik A. 2005. Soil surface roughness measurement - Methods, applicability, and surface representation. *Catena* 64: 174-192.

Jetten V, De Roo APJ. 2001. Spatial analysis of erosion conservation measures with LISEM. In *Landscape Erosion and Evolution Modelling*, Harmon RS, Doe WW (eds). Kluwer Academic, New York, USA. p. 429-445.

Jetten V, Favis-Mortlock D. 2006. Modelling Soil Erosion in Europe. In *Soil Erosion in Europe*, Boardman J, Poesen J (eds). John Wiley & Sons, Chichester, UK.

Jetten V, Boiffin J, De Roo A. 1996. Defining monitoring strategies for runoff and erosion studies in agricultural catchments: a simulation approach. *European Journal of Soil Science* 47: 579-592.

Jetten V, de Roo A, Favis-Mortlock D. 1999. Evaluation of field-scale and catchment-scale soil erosion models. *Catena* 37: 521-541.

Jetten V, Govers G, Hessel R. 2003. Erosion models: quality of spatial predictions. *Hydrological Processes* 17: 887-900.

Kamphorst EC, Jetten V, Guerif J, Pitkanen J, Iversen BV, Douglas JT, Paz A. 2000. Predicting Depressional Storage from Soil Surface Roughness. *Soil Sci Soc Am J* 64: 1749-1758.

Kefi S, Rietkerk M, Alados CL, Pueyo Y, Papanastasis VP, ElAich A, de Ruiter PC. 2007. Spatial vegetation patterns and imminent desertification in Mediterranean arid ecosystems. *Nature* 449: 213-217.

Keijsers JGS, Schoorl JM, Chang KT, Chiang SH, Claessens L, Veldkamp A. 2011. Calibration and resolution effects on model performance for predicting shallow landslide locations in Taiwan. *Geomorphology* 133: 168-177.

Kirchner JW, Finkel RC, Riebe CS, Granger DE, Clayton JL, King JG, Megahan WF. 2001. Mountain erosion over 10 yr, 10 k.y., and 10 m.y. time scales. *Geology* 29: 591-594.

Kirkby MJ. 1971. Hillslope process-response models based on the continuity equation. In *Slopes, forms and processes*, Brunsden D (eds). Transactions of the IBG. Special Publication: 15-30.

Kirkby MJ. 1986. A two-dimensional simulation model for slope and stream evolution. In *Hillslope Processes*, Abrahams AD (eds). Allen & Unwin Inc., Winchester, UK.

Kirkby MJ. 1987. Modelling some influences of soil erosion, landslides and valley gradient on drainage density and hollow development. *Catena Supplement* 10: 1-14.

Kirkby MJ. 2010. Distance, time and scale in soil erosion processes. *Earth Surface Processes and Landforms* 35: 1621-1623.

Kirkby MJ, Bull LJ. 2000. Some factors controlling gully growth in fine-grained sediments: a model applied in southeast Spain. *Catena* 40: 127-146.

Kirkby MJ, Bracken LJ. 2009. Gully processes and gully dynamics. *Earth Surface Processes and Landforms* 34: 1841-1851.

Kirkby M, Bracken L, Reaney S. 2002. The influence of land use, soils and topography on the delivery of hillslope runoff to channels in SE Spain. *Earth Surface Processes and Landforms* 27: 1459-1473.

Kirkby MJ, Bracken LJ, Shannon J. 2005. The influence of rainfall distribution and morphological factors on runoff delivery from dryland catchments in SE Spain. *Catena* 62: 136-156.

Knox JC. 1972. Valley Alluviation in Southwestern Wisconsin. *Annals of the Association of American Geographers* 62: 401 - 410.

Knox JC. 2006. Floodplain sedimentation in the Upper Mississippi Valley: Natural versus human accelerated. *Geomorphology* 79: 286-310.

Kosmas C, Danalatos N, Cammeraat LH, Chabart M, Diamantopoulos J, Farand R, Gutierrez L, Jacob A, Marques H, Martinez-Fernandez J, Mizara A, Moustakas N, Nicolau JM, Oliveros C, Pinna G, Puddu R, Puigdefabregas J, Roxo M, Simao A, Stamou G, Tomasi N, Usai D, Vacca A. 1997. The effect of land use on runoff and soil erosion rates under Mediterranean conditions. *Catena* 29: 45-59.

Kroonenberg S. 2006. *De menselijke maat*. Atlas, Amsterdam, The Netherlands. 334p.

Kutílek M, Nielsen DR. 1994. *Soil Hydrology*. Catena Verlag, Reiskirchen, Germany.

Lang A. 2003. Phases of soil erosion-derived colluviation in the loess hills of South Germany. *Catena* 51: 209-221.

Leeder M. 2011. Complexity and the memory of landscape. *Nature* 469: 39.

Léonard J, Ancelin O, Ludwig B, Richard G. 2006. Analysis of the dynamics of soil infiltrability of agricultural soils from continuous rainfall-runoff measurements on small plots. *Journal of Hydrology* 326: 122-134.

Lesschen JP, Cammeraat LH, Nieman T. 2008. Erosion and terrace failure due to agricultural land abandonment in a semi-arid environment. *Earth Surface Processes and Landforms* 33: 1574-1584.

Lesschen JP, Schoorl JM, Cammeraat LH. 2009. Modelling runoff and erosion for a semi-arid catchment using a multi-scale approach based on hydrological connectivity. *Geomorphology* 109: 174-183.

Lesschen JP, Kok K, Verburg PH, Cammeraat LH. 2007. Identification of vulnerable areas for gully erosion under different scenarios of land abandonment in Southeast Spain. *Catena* 71: 110-121.

López-Bermúdez F. 1990. Soil erosion by water on the desertification of a semi-arid Mediterranean fluvial basin: the Segura basin, Spain. *Agriculture, Ecosystems & Environment* 33: 129-145.

López-Bermudez F, Romero-Diaz A, Martinez-Fernandez J, Martinez-Fernandez J. 1996. The El Ardal field site: soil and vegetation cover. In *Mediterranean Desertification and Land Use*, Brandt CJ, Thornes JB (eds). John Wiley & Sons, Chichester, UK. p. 169-188.

López-Bermúdez F, Conesa-García C, Alonso-Sarría F. 2002a. Floods: Magnitude and Frequency in Ephemeral Streams of the Spanish Mediterranean Region. In *Dryland Rivers: Hydrology and Geomorphology of Semi-arid Channels*, Bull LJ, Kirkby MJ (eds). Joh Wiley & Sons, Chichester, UK.

López-Bermúdez F, Barberá GG, Alonso-Sarría F, Belmonte Serrato F. 2002b. Natural Resources in the Guadalentín Basin (South-east Spain): Water as a Key Factor. In *Mediterranean Desertification: A Mosaic of Processes and Responses*, Geeson NA, Brandt CJ, Thornes JB (eds). John Wiley & Sons, Chichester, UK. p. 233-245.

LUCDEME. 1988. Hoja 953 - Lorca. Ministerio de Agricultura, Pesca y Alimentacion, Spain.

LUCDEME. 1993. Hoja 952 - Velez Blanco. Ministerio de Agricultura, Pesca y Alimentacion, Spain.

Machado MJ, Benito G, Barriendos M, Rodrigo FS. 2011. 500 Years of rainfall variability and extreme hydrological events in southeastern Spain drylands. *Journal of Arid Environments* 75: 1244-1253.

Magny M, Miramont C, Sivan O. 2002. Assessment of the impact of climate and anthropogenic factors on Holocene Mediterranean vegetation in Europe on the basis of palaeohydrological records. *Palaeogeography, Palaeoclimatology, Palaeoecology* 186: 47-59.

Martín-Puertas C, Valero-Garcés BL, Mata MP, González-Sampériz P, Bao R, Moreno A, Stefanova V. 2008. Arid and humid phases in southern Spain during the last 4000 years: the Zoñar Lake record, Córdoba. *The Holocene* 18: 907-921.

Martín-Puertas C, Jiménez-Espejo F, Martínez-Ruiz F, Nieto-Moreno V, Rodrigo M, Mata MP, Valero-Garcés BL. 2010. Late Holocene climate variability in the southwestern Mediterranean region: an integrated marine and terrestrial geochemical approach. *Clim. Past* 6: 807-816.

Martrat B, Grimalt JO, Lopez-Martinez C, Cacho I, Sierro FJ, Flores JA, Zahn R, Canals M, Curtis JH, Hodell DA. 2004. Abrupt Temperature Changes in the Western Mediterranean over the Past 250,000 Years. *Science* 306: 1762-1765.

Mather AE, Stokes M, Griffiths JS. 2002. Quaternary landscape evolution: a framework for understanding contemporary erosion, southeast Spain. *Land Degradation & Development* 13: 89-109.

Matmon A, Bierman PR, Larsen J, Southworth S, Pavich M, Caffee M. 2003. Temporally and spatially uniform rates of erosion in the southern Appalachian Great Smoky Mountains. *Geology* 31: 155-158.

191

Meehl GA, Stocker TF, Collins WD, Friedlingstein P, Gaye AT, Gregory JM, Kitoh A, Knutti R, Murphy JM, Noda A, Raper SCB, Watterson IG, J. WA, Zhao Z-C. 2007. Global Climate Projections. In *Climate Change 2007: The Physical Science Basis. Contribution of Working Group I to the Fourth Assessment Report of the Intergovernmental Panel on Climate Change*, Solomon S, Qin D, Manning M, Chen Z, Marquis M, Averyt KB, Tignor M, Miller HL (eds). Cambridge University Press, Cambridge, UK and New York, NY, USA.

Merritt WS, Letcher RA, Jakeman AJ. 2003. A review of erosion and sediment transport models. *Environmental Modelling & Software* 18: 761-799.

Meyer H, Hetzel R, Strauss H. 2010. Erosion rates on different timescales derived from cosmogenic 10Be and river loads: implications for landscape evolution in the Rhenish Massif, Germany. *International Journal of Earth Sciences* 99: 395-412.

Moret D, Arrúe JL, López MV, Gracia R. 2007. Winter barley performance under different cropping and tillage systems in semiarid Aragon (NE Spain). *European Journal of Agronomy* 26: 54-63.

Morgan RPC, Smith RE, Govers G, Poesen JWA, Auerswald K, Chisci G, Torri D, Styczen ME, Folly AJV. 1998. The European Soil Erosion Model (EUROSEM): documentation and user guide. version 3.6. Silsoe, Bedford, UK.

Mount JF, Cohen AS. 1984. Petrology and Geochemistry of Rhizoliths from Plio-Pleistocene Fluvial and Marginal Lacustrine Deposits, East Lake Turkana, Kenya. *Journal of Sedimentary Petrology* 54: 263-275.

Mulligan M, Wainwright J. 2004. Modelling and Model Building. In *Environmental Modelling: Finding Simplicity in Complexity*, Wainwright J, Mulligan M (eds). John Wiley & Sons, Chichester, UK. p. 7-73.

Muñoz-Carpena R, Regalado CM, Álvarez-Benedi J, Bartoli F. 2002. Field Evaluation of the New Philip-Dunne Permeameter for Measuring Saturated Hydraulic Conductivity. *Soil Science* 167: 9-24.

Murray A, Marten R, Johnston A, Martin P. 1987. Analysis for naturally occuring radionuclides at environmental concentrations by gamma spectrometry. *Journal of Radioanalytical and Nuclear Chemistry* 115: 263-288.

Murray AB, Paola C. 1994. A cellular model of braided rivers. *Nature* 371: 54-57.

Murray AB, Paola C. 1997. Properties of a cellular braided-stream model. *Earth Surface Processes and Landforms* 22: 1001-1025.

Murray AB, Paola C. 2003. Modelling the effect of vegetation on channel pattern in bedload rivers. *Earth Surface Processes and Landforms* 28: 131-143.

Murray AB, Lazarus E, Ashton A, Baas A, Coco G, Coulthard T, Fonstad M, Haff P, McNamara D, Paola C, Pelletier J, Reinhardt L. 2009. Geomorphology, complexity, and the emerging science of the Earth's surface. *Geomorphology* 103: 496-505.

Murray AS, Wintle AG. 2003. The single aliquot regenerative dose protocol: potential for improvements in reliability. *Radiation Measurements* 37: 377-381.

Nachtergaele J, Poesen J, Vandekerckhove L, Oostwoud Wijdenes D, Roxo M. 2001. Testing the Ephemeral Gully Erosion Model (EGEM) for two Mediterranean environments. *Earth Surface Processes and Landforms* 26: 17-30.

Nachtergaele J, Poesen J, Oostwoud Wijdenes D, Vandekerckhove L. 2002. Medium-term evolution of a gully developed in a loess-derived soil. *Geomorphology* 46: 223-239.

Nadal-Romero E, Martínez-Murillo JF, Vanmaercke M, Poesen J. 2011. Scale-dependency of sediment yield from badland areas in Mediterranean environments. *Progress in Physical Geography* 35: 297-332.

Nash JE, Sutcliffe JV. 1970. River flow forecasting through conceptual models part I -- A discussion of principles. *Journal of Hydrology* 10: 282-290.

Navarro Hervás F. 1991. *El Sistema Hidrográfico del Guadalentín*. Consejería de Política Territorial, Obras Públicas y Medio Ambiente, Murcia, Spain.

Nearing MA, Foster GR, Lane LJ, Finkner SC. 1989. A process-based soil erosion model for USDA-Water Erosion Prediction Project technology. *TRANS. ASAE* 32:

Nearing MA, Jetten V, Baffaut C, Cerdan O, Couturier A, Hernandez M, Le Bissonnais Y, Nichols MH, Nunes JP, Renschler CS, Souchere V, van Oost K. 2005. Modeling response of soil erosion and runoff to changes in precipitation and cover. *Catena* 61: 131-154.

Nicholas AP, Quine TA. 2007. Crossing the divide: Representation of channels and processes in reduced-complexity river models at reach and landscape scales. *Geomorphology* 90: 318-339.

Notebaert B, Verstraeten G, Rommens T, Vanmontfort B, Govers G, Poesen J. 2009. Establishing a Holocene sediment budget for the river Dijle. *Catena* 77: 150-163.

Onate JJ, Peco B. 2005. Policy impact on desertification: stakeholders' perceptions in southeast Spain. *Land Use Policy* 22: 103-114.

Orejas A, Sánchez-Palencia FJ. 2002. Mines, Territorial Organization, and Social Structure in Roman Iberia: Carthago Noua and the Peninsular Northwest. *American Journal of Archaeology* 106: 581-599.

Page MJ, Trustrum NA, Dymond JR. 1994. Sediment budget to assess the geomorphic effect of a cyclonic storm, New Zealand. *Geomorphology* 9: 169-188.

Panin AV, Fuzeina JN, Belyaev VR. 2009. Long-term development of Holocene and Pleistocene gullies in the Protva River basin, Central Russia. *Geomorphology* 108: 71-91.

Pantaleon-Cano J, Yll E-I, Perez-Obiol R, Roure JM. 2003. Palynological evidence for vegetational history in semi-arid areas of the western Mediterranean (Almeria, Spain). *The Holocene* 13: 109-119.

Paola C. 2011. In modelling, simplicity isn't simple. *Nature* 469: 38.

Parsons AJ, Wainwright J, Powell DM, Kaduk J, Brazier RE. 2004. A conceptual model for determining soil erosion by water. *Earth Surface Processes and Landforms* 29: 1293-1302.

Peeters I, Van Oost K, Govers G, Verstraeten G, Rommens T, Poesen J. 2008. The compatibility of erosion data at different temporal scales. *Earth and Planetary Science Letters* 265: 138-152.

Pelletier JD. 2004. Persistent drainage migration in a numerical landscape evolution model. *Geophys. Res. Lett.* 31: L20501.

Pérez Asensio M. 2007. Un edificio Romano de Tabernas en Lorca (Siglos I-V D.C.). *Alberca* 5: 67-79.

Pimentel D. 2006. Soil erosion: A food and environmental threat. *Environment, Development and Sustainability* 8: 119-137.

Pollen-Bankhead N, Simon A, Jaeger K, Wohl E. 2009. Destabilization of streambanks by removal of invasive species in Canyon de Chelly National Monument, Arizona. *Geomorphology* 103: 363-374.

Pons A, Reille M. 1988. The holocene- and upper pleistocene pollen record from Padul (Granada, Spain): A new study. *Palaeogeography, Palaeoclimatology, Palaeoecology* 66: 243-249, 255-263.

Preston N, Brierley G, Fryirs K. 2011. The Geographic Basis of Geomorphic Enquiry. *Geography Compass* 5: 21-34.

Puigdefabregas J, Alonso JM, Delgado L, Domingo F, Cueto M, Gutierrez L, Lázaro R, Nicolau JM, Sánchez G, Solé A, Vidal S. 1996. The Rambla Honda Field Site: Interactions of Soil and Vegetation Along a Catena in Semi-arid Southeast Spain. In *Mediterranean Desertification and Land Use*, Brandt CJ, Thornes JB (eds). John Wiley & Sons, Chichester, UK.

Puigdefabregas J, Sole A, Gutierrez L, del Barrio G, Boer M. 1999. Scales and processes of water and sediment redistribution in drylands: results from the Rambla Honda field site in Southeast Spain. *Earth-Science Reviews* 48: 39-70.

Pujante Martínez A. 2002. El Castillo de Puentes y las alquerías de du entorno: aproximación a la estructura del poblamiento. *Alberca* 1: 57-84.

Quine TA, Govers G, Poesen J, Walling D, van Wesemael B, Martinez-Fernandez J. 1999. Fine-earth translocation by tillage in stony soils in the Guadalentin, south-east Spain: an investigation using caesium-134. *Soil and Tillage Research* 51: 279-301.

Quine TA, Govers G, Walling DE, Zhang X, Desmet PJJ, Zhang Y, Vandaele K. 1997. Erosion processes and landform evolution on agricultural land - new perspectives from caesium-137 measurements and topographic-based erosion modelling. *Earth Surface Processes and Landforms* 22: 799-816.

Quinn P, Beven K, Chevallier P, Planchon O. 1991. The prediction of hillslope flow paths for distributed hydrological modelling using digital terrain models. *Hydrological Processes* 5: 59-79.

Regalado CM, Ritter A, Alvarez-Benedi J, Munoz-Carpena R. 2005. Simplified Method to Estimate the Green-Ampt Wetting Front Suction and Soil Sorptivity with the Philip-Dunne Falling-Head Permeameter. *Vadose Zone J* 4: 291-299.

Reimer PJ, Baillie MGL, Bard E, Bayliss A, Beck JW, Bertrand CJH, Blackwell PG, Buck CE, Burr GS, Cutler KB, Damon PE, Edwards RL, Fairbanks RG, Friedrich M, Guilderson TP, Hogg AG, Hughen KA, Kromer B, McCormac G, Manning S, Bronk Ramsey C, Reimer RW, Remmele S, Southon JR, Stuiver M, Talamo S, Taylor FW, Van der Plicht J, Weyhenmeyer CE. 2004. IntCal04 terrestrial radiocarbon age calibration, 0-26 cal kyr BP. *Radiocarbon* 46: 1029-1058.

Rietkerk M, Dekker SC, de Ruiter PC, van de Koppel J. 2004. Self-Organized Patchiness and Catastrophic Shifts in Ecosystems. *Science* 305: 1926-1929.

Rittenour TM. 2008. Luminescence dating of fluvial deposits: applications to geomorphic, palaeoseismic and archaeological research. *Boreas* 37: 613-635.

Roberts RG, Galbraith RF, Yoshida H, Laslett GM, Olley JM. 2000. Distinguishing dose populations in sediment mixtures: a test of single-grain optical dating procedures using mixtures of laboratory-dosed quartz. *Radiation Measurements* 32: 459-465.

Rodnight H, Duller GAT, Tooth S, Wintle AG. 2005. Optical dating of a scroll-bar sequence on the Klip River, South Africa, to derive the lateral migration rate of a meander bend. *The Holocene* 15: 802-811.

Saco PM, Willgoose GR, Hancock GR. 2007. Eco-geomorphology of banded vegetation patterns in arid and semi-arid regions. *Hydrol. Earth Syst. Sci.* 11: 1717-1730.

Schoorl JM, Veldkamp A. 2001. Linking land use and landscape process modelling: a case study for the Alora region (south Spain). *Agriculture, Ecosystems & Environment* 85: 281-292.

Schoorl JM, Veldkamp A. 2003. Late Cenozoic landscape development and its tectonic implications for the Guadalhorce valley near Álora (Southern Spain). *Geomorphology* 50: 43-57.

Schoorl JM, Sonneveld MPW, Veldkamp A. 2000. Three-dimensional landscape process modelling: the effect of DEM resolution. *Earth Surface Processes and Landforms* 25: 1025-1034.

Schoorl JM, Veldkamp A, Bouma J. 2002. Modeling Water and Soil Redistribution in a Dynamic Landscape Context. *Soil Sci Soc Am J* 66: 1610-1619.

Schoorl JM, Boix Fayos C, de Meijer RJ, van der Graaf ER, Veldkamp A. 2004. The 137Cs technique applied to steep Mediterranean slopes (Part II): landscape evolution and model calibration. *Catena* 57: 35-54.

Schulte L. 2002. Climatic and human influence on river systems and glacier fluctuations in southeast Spain since the Last Glacial Maximum. *Quaternary International* 93-94: 85-100.

Schulte L, Julià R, Burjachs F, Hilgers A. 2008. Middle Pleistocene to Holocene geochronology of the River Aguas terrace sequence (Iberian Peninsula): Fluvial response to Mediterranean environmental change. *Geomorphology* 98: 13-33.

Schumm SA. 1981. Geomorphic thresholds and complex resonse of drainage systems. In: *Fluvial geomorphology : a proceedings volume of the fourth annual geomorphology symposia series held at Binghamton, New York, September 27-28, 1973*, Morisawa M (eds). Allen & Unwin, London, UK. p. 299-310.

Schumm SA, Lichty RW. 1965. Time, space, and causality in geomorphology. *American Journal of Science* 263: 110-119.

Schütt B. 2006. Rekonstruktion, Abbildung und Modellierung der holozänen Reliefentwicklung der Cañada Hermosa, Einzugsgebiet des Rio Guadalentín (SE Iberische Halbinsel). *Nova Acta Leopoldina NF 94* 346:

Shannon J, Richardson R, Thornes JB. 2002. Modelling Event-based Fluxes in Ephemeral Streams. In *Dryland Rivers: Hydrology and Geomorphology of Semi-arid Channels*, Bull LJ, Kirkby MJ (eds). John Wiley & Sons, Chichester, UK p. 129 - 172.

Silva PG, Goy J, Zazo C, Lario J, Bardaji T. 1997. Paleoseismic indications along `aseismic' fault segments in the guadalentin depression (SE Spain). *Journal of Geodynamics* 24: 105-115.

Silva PG, Goy JL, Zazo C, Bardají T. 2003. Fault-generated mountain fronts in southeast Spain: geomorphologic assessment of tectonic and seismic activity. *Geomorphology* 50: 203-225.

Silva PG, Bardají T, Calmel-Avila M, Goy JL, Zazo C. 2008. Transition from alluvial to fluvial systems in the Guadalentín Depression (SE Spain) during the Holocene: Lorca Fan versus Guadalentín River. *Geomorphology* 100: 140-153.

Snyder NP. 2003. Importance of a stochastic distribution of floods and erosion thresholds in the bedrock river incision problem. *Journal of geophysical research* 108: 2117.

Sonneveld MPW, Schoorl JM, Veldkamp A. 2006. Mapping hydrological pathways of phosphorus transfer in apparently homogeneous landscapes using a high-resolution DEM. *Geoderma* 133: 32-42.

Stallins JA. 2006. Geomorphology and ecology: Unifying themes for complex systems in biogeomorphology. *Geomorphology* 77: 207-216.

Stark CP, Stark GJ. 2001. A channelization model of landscape evolution. *American Journal of Science* 301: 486-512.

Stolte J, Ritsema CJ, Veerman GJ, Hamminga W. 1996. Establishing temporally and spatially variable soil hydraulic data for use in a runoff simulation in a Loess region of The Netherlands. *Hydrological Processes* 10: 1027-1034.

Stolte J, van Venrooij B, Zhang G, Trouwborst KO, Liu G, Ritsema CJ, Hessel R. 2003. Land-use induced spatial heterogeneity of soil hydraulic properties on the Loess Plateau in China. *Catena* 54: 59-75.

Syvitski JPM, Vörösmarty CJ, Kettner AJ, Green P. 2005. Impact of humans on the flux of terrestrial sediment to the global coastal ocean. *Science* 308: 376-380.

Takken I, Beuselinck L, Nachtergaele J, Govers G, Poesen J, Degraer G. 1999. Spatial evaluation of a physically-based distributed erosion model (LISEM). *Catena* 37: 431-447.

Tebbens LA, Veldkamp A. 2000. Late Quaternary evolution of fluvial sediment composition: a modeling case study of the River Meuse. *Global and Planetary Change* 27: 187-206.

Tebbens LA, Veldkamp A, Van Dijke JJ, Schoorl JM. 2000. Modeling longitudinal-profile development in response to Late Quaternary tectonics, climate and sea-level changes: the River Meuse. *Global and Planetary Change* 27: 165-186.

Temme AJAM, Veldkamp A. 2009. Multi-process Late Quaternary landscape evolution modelling reveals lags in climate response over small spatial scales. *Earth Surface Processes and Landforms* 34: 573-589.

Temme AJAM, Schoorl JM, Veldkamp A. 2006. Algorithm for dealing with depressions in dynamic landscape evolution models. *Computers & Geosciences* 32: 452-461.

Temme AJAM, Baartman JEM, Schoorl JM. 2009. Can uncertain landscape evolution models discriminate between landscape responses to stable and changing future climate? A millennial-scale test. *Global and Planetary Change* 69: 48-58.

Temme AJAM, Baartman JEM, Botha GA, Veldkamp A, Jongmans AG, Wallinga J. 2008. Climate controls on late Pleistocene landscape evolution of the Okhombe valley, KwaZulu-Natal, South Africa. *Geomorphology* 99: 280-295.

Temme AJAM, Claessens L, Veldkamp A, Schoorl JM. 2011a. Evaluating choices in multi-process landscape evolution models. *Geomorphology* 125: 271-281.

Temme AJAM, Peeters I, Buis E, Veldkamp A, Govers G. 2011b. Comparing landscape evolution models with quantitative field data at the millennial time scale in the Belgian loess belt. *Earth Surface Processes and Landforms* 36: 1300-1312.

Temme AJAM, Schoorl JM, Claessens L, Veldkamp A. In Press. Quantitative modelling of landscape evolution. In *Quantitative Modelling in Geomorphology*, Baas A (eds). Elsevier, The Netherlands.

Thomas R, Nicholas AP, Quine TA. 2007. Cellular modelling as a tool for interpreting historic braided river evolution. *Geomorphology* 90: 302-317.

Thrana C, Talbot MR. 2006. High-frequency carbonate-siliciclastic cycles in the Miocene of the Lorca Basin (Western Mediterranean, SE Spain). *Geologica Acta* 4: 343-354.

Tomkins KM, Humphreys GS, Wilkinson MT, Fink D, Hesse PP, Doerr SH, Shakesby RA, Wallbrink PJ, Blake WH. 2007. Contemporary versus long-term denudation along a passive plate margin: the role of extreme events. *Earth Surface Processes and Landforms* 32: 1013-1031.

Trimble SW. 1981. Changes in Sediment Storage in the Coon Creek Basin, Driftless Area, Wisconsin, 1853 to 1975. *Science* 214: 181-183.

Trimble SW. 1983. A sediment budget for Coon Creek basin in the Driftless Area, Wisconsin, 1853-1977. *Am J Sci* 283: 454-474.

Tucker GE. 2009. Natural experiments in landscape evolution. *Earth Surface Processes and Landforms* 34: 1450-1460.

Tucker GE, Bras RL. 2000. A stochastic approach to modeling the role of rainfall variability in drainage basin evolution. *Water Resour. Res.* 36: 1953-1964.

Tucker GE, Hancock GR. 2010. Modelling landscape evolution. *Earth Surface Processes and Landforms* 35: 28-50.

Valentin C, Poesen J, Li Y. 2005. Gully erosion: Impacts, factors and control. *Catena* 63: 132-153.

Van De Wiel MJ, Coulthard TJ. 2010. Self-organized criticality in river basins: Challenging sedimentary records of environmental change. *Geology* 38: 87-90.

Van De Wiel MJ, Coulthard TJ, Macklin MG, Lewin J. 2007. Embedding reach-scale fluvial dynamics within the CAESAR cellular automaton landscape evolution model. *Geomorphology* 90: 283-301.

Van De Wiel MJ, Coulthard TJ, Macklin MG, Lewin J. 2011. Modelling the response of river systems to environmental change: Progress, problems and prospects for palaeo-environmental reconstructions. *Earth-Science Reviews* 104: 167-185.

Van Dijk AIJM. 2002. Water and sediment dynamics in bench-terraced agricultural steeplands in West Java, Indonesia. PhD Thesis, Vrije Universiteit, Amsterdam, The Netherlands.

Van Oost K, Govers G, Desmet P. 2000. Evaluating the effects of changes in landscape structure on soil erosion by water and tillage. *Landscape Ecology* 15: 577-589.

Van Oost K, Govers G, Van Muysen W. 2003. A process-based conversion model for caesium-137 derived erosion rates on agricultural land: an integrated spatial approach. *Earth Surface Processes and Landforms* 28: 187-207.

Van Oost K, Van Muysen W, Govers G, Deckers J, Quine TA. 2005. From water to tillage erosion dominated landform evolution. *Geomorphology* 72: 193-203.

Van Rompaey AJJ, Verstraeten G, Van Oost K, Govers G, Poesen J. 2001. Modelling mean annual sediment yield using a distributed approach. *Earth Surface Processes and Landforms* 26: 1221-1236.

van Wesemael B, Rambaud X, Poesen J, Muligan M, Cammeraat E, Stevens A. 2006. Spatial patterns of land degradation and their impacts on the water balance of rainfed treecrops: A case study in South East Spain. *Geoderma* 133: 43-56.

Vanacker V, Govers G, Poesen J, Deckers J, Dercon G, Loaiza G. 2003. The impact of environmental change on the intensity and spatial pattern of water erosion in a semi-arid mountainous Andean environment. *Catena* 51: 329-347.

Vanacker V, von Blanckenburg F, Govers G, Molina A, Poesen J, Deckers J, Kubik P. 2007. Restoring dense vegetation can slow mountain erosion to near natural benchmark levels. *Geology* 35: 303-306.

Vandekerckhove L, Poesen J, Oostwoud Wijdenes D, Nachtergaele J, Kosmas C, Roxo MJ, de Figueiredo T. 2000. Thresholds for gully initiation and sedimentation in Mediterranean Europe. *Earth Surface Processes and Landforms* 25: 1201-1220.

Vandenberghe J. 2008. The fluvial cycle at cold-warm-cold transitions in lowland regions: A refinement of theory. *Geomorphology* 98: 275-284.

Vanmaercke M, Poesen J, Verstraeten G, de Vente J, Ocakoglu F. 2011. Sediment yield in Europe: Spatial patterns and scale dependency. *Geomorphology* 130: 142-161.

Veihe A. 2002. The spatial variability of erodibility and its relation to soil types: a study from northern Ghana. *Geoderma* 106: 101-120.

Veldkamp A, van Dijke JJ. 2000. Simulating internal and external controls on fluvial terrace stratigraphy: a qualitative comparison with the Maas record. *Geomorphology* 33: 225-236.

Veldkamp A, Kok K, De Koning GHJ, Schoorl JM, Sonneveld MPW, Verburg PH. 2001. Multi-scale system approaches in agronomic research at the landscape level. *Soil and Tillage Research* 58: 129-140.

Verstraeten G, Prosser IP. 2008. Modelling the impact of land-use change and farm dam construction on hillslope sediment delivery to rivers at the regional scale. *Geomorphology* 98: 199-212.

Verstraeten G, Lang A, Houben P. 2009a. Human impact on sediment dynamics -- quantification and timing. *Catena* 77: 77-80.

Verstraeten G, Van Oost K, Van Rompaey A, Poesen J, Govers G. 2002. Evaluating an integrated approach to catchment management to reduce soil loss and sediment pollution through modelling. *Soil Use and Management* 18: 386-394.

Verstraeten G, Rommens T, Peeters I, Poesen J, Govers G, Lang A. 2009b. A temporarily changing Holocene sediment budget for a loess-covered catchment (central Belgium). *Geomorphology* 108: 24-34.

Vigiak O, van Loon E, Sterk G. 2006. Modelling spatial scales of water erosion in the West Usambara Mountains of Tanzania. *Geomorphology* 76: 26-42.

Vita-Finzi C. 1969. *The Mediterranean Valleys - Geological Changes in Historical Times.* Cambridge University Press, London, UK.

Wagner LE, Yu Y. 1991. Digitization of profile meter photographs. *Transactions of the American Society of Agricultural Engineers* 34: 412-416.

Wainwright J. 2006. Degrees of separation: Hillslope-channel coupling and the limits of palaeohydrological reconstruction. *Catena* 66: 93-106.

Wainwright J, Millington JDA. 2010. Mind, the gap in landscape-evolution modelling. *Earth Surface Processes and Landforms* 35: 842-855.

Waldmann N, Stein M, Ariztegui D, Starinsky A. 2009. Stratigraphy, depositional environments and level reconstruction of the last interglacial Lake Samra in the Dead Sea basin. *Quaternary Research* 72: 1-15.

Walling DE, Quine TA. 1991. Use of 137Cs measurements to investigate soil erosion on arable fields in the UK: potential applications and limitations. *Journal of Soil Science* 42: 147-165.

Wallinga J. 2002. Optically stimulated luminescence dating of fluvial deposits: a review. *Boreas* 31: 303 - 322.

Wallinga J, Hobo N, Cunningham AC, Versendaal AJ, Makaske B, Middelkoop H. 2010. Sedimentation rates on embanked floodplains determined through quartz optical dating. *Quaternary Geochronology* 5: 170-175.

Ward PJ, van Balen RT, Verstraeten G, Renssen H, Vandenberghe J. 2009. The impact of land use and climate change on late Holocene and future suspended sediment yield of the Meuse catchment. *Geomorphology* 103: 389-400.

Webster R, Oliver MA. 2007. *Geostatistics for Environmental Scientists.* John Wiley & Sons, Chichester, UK.

White KD. 1967. *Agricultural implements of the Roman world.* Cambridge, UK.

Wilkinson BH. 2005. Humans as geologic agents: A deep-time perspective. *Geology* 33: 161-164.

Willgoose G. 2005. Mathematical Modeling of Whole Landsdcape Evolution. *Annual Review of Earth and Planetary Sciences* 33: 443-459.

Willgoose G, Bras RL, Rodriguez-Iturbe I. 1991a. A coupled channel network growth and hillslope evolution model: 1. Theory. *Water Resour. Res.* 27: 1671-1684.

Willgoose G, Bras RL, Rodriguez-Iturbe I. 1991b. A coupled channel network growth and hillslope evolution model: 2. Nondimensionalization and applications. *Water Resour. Res.* 27: 1685-1696.

Wintle AG, Murray AS. 2006. A review of quartz optically stimulated luminescence characteristics and their relevance in single-aliquot regeneration dating protocols. *Radiation Measurements* 41: 369-391.

Woolhiser DA, Smith RE, Giraldez JV. 1996. Effects of Spatial Variability of Saturated Hydraulic Conductivity on Hortonian Overland Flow. *Water Resour. Res.* 32: 671-678.

Yu B, Rose CW, Coughlan KJ, Fentie B. 1997. Plot-Scale Rainfall-runoff Characteristics and Modeling at Six Sites in Australia and Southeast Asia. *Transactions of the ASABE* 40: 1295-1303.

Zazo C, Dabrio CJ, Goy JL, Lario J, Cabero A, Silva PG, Bardají T, Mercier N, Borja F, Roquero E. 2008. The coastal archives of the last 15 ka in the Atlantic-Mediterranean Spanish linkage area: Sea level and climate changes. *Quaternary International* 181: 72-87.

Zielhofer C, Faust D, Linstädter J. 2008. Late Pleistocene and Holocene alluvial archives in the Southwestern Mediterranean: Changes in fluvial dynamics and past human response. *Quaternary International* 181: 39-54.
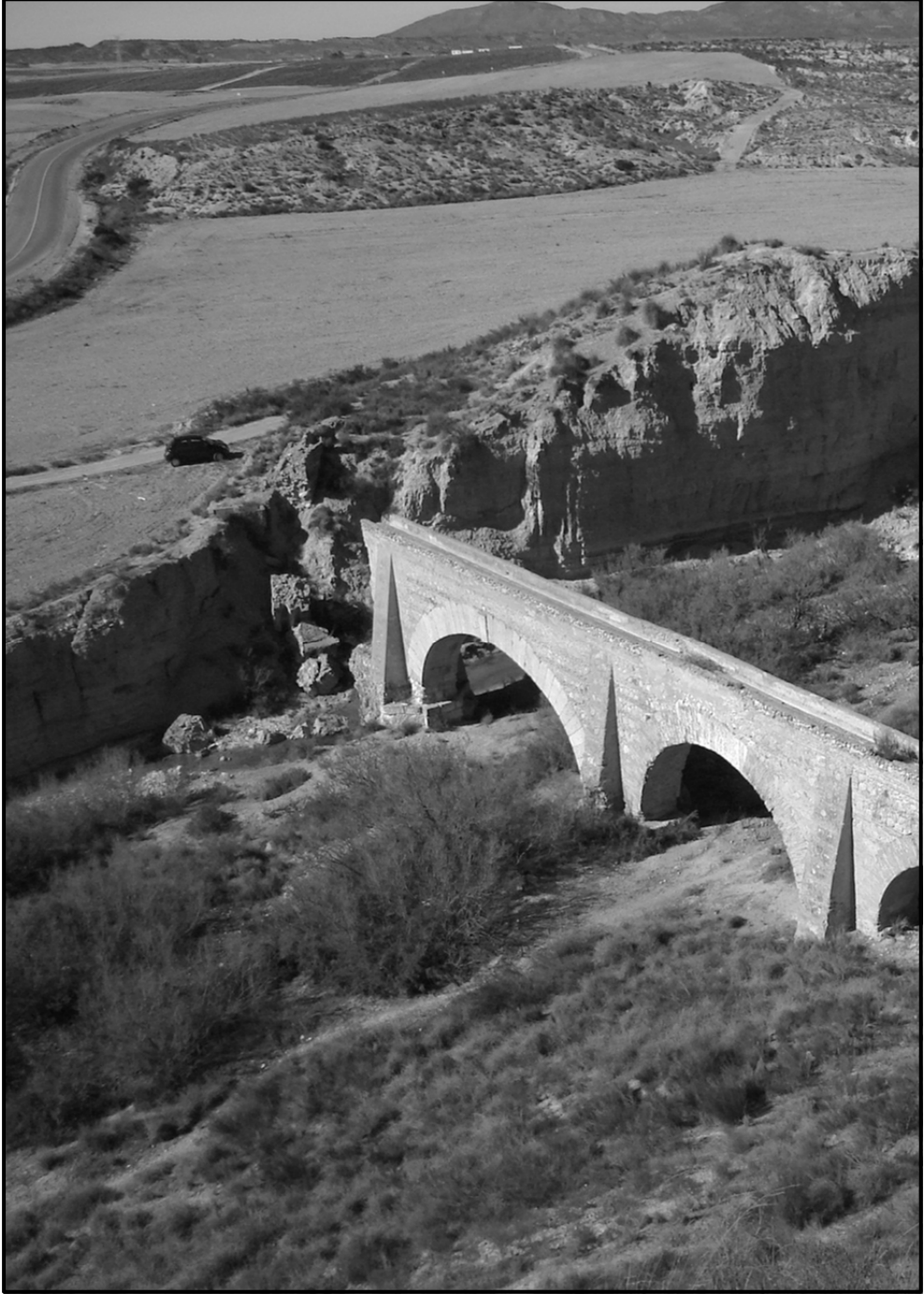
Summary

In erosion research spatial and temporal scales as well as research methods differ. In many studies erosion is assessed on plot-slope-small catchment scale and on short, contemporary ('human') time-scales. Event based changes are addressed and field experiments are conducted. On the other hand, in geosciences, research is conducted on the landscape regional scale and on time-scales of landscape evolution. Decadal changes are addressed and landscape evolution models (LEMs) are used as tools. This thesis aimed to bridge the gap between these two contrasting approaches with focus on the time-scale gap between rainfall events and landscape evolution and the relative contribution of human activity to natural erosion.

The first chapter introduces three themes central to this thesis: natural versus human-induced erosion, the time-scale gap in landscape dynamics and approaches to modelling landscape dynamics. In chapter 2 the geomorphological functioning of the study area (Upper Guadalentín Basin, SE Spain) was investigated with the aim to get insight into Late Pleistocene and Holocene landscape development. A schematic model of erosion and sedimentation dynamics was developed for three parts of the Upper Guadalentín river. From this analysis, it was deduced that the studied rivers are not in equilibrium, evidenced by their out-of-phase sedimentation pattern. This was hypothesized to be due to the influence of a palaeo-lake. A tentative correlation of the younger deposits to human impact after the Roman and Moorish occupation was made, but local processes and internal river dynamics were concluded to have played a more important role in landscape dynamics than external drivers.

In chapter 3 the landscape evolution model LAPSUS (LandscApe ProcesS modelling at mUlti dimensions and Scales) was adapted to better simulate fluvial processes without changing the existing model equations and structure. Depending on simulated climatic conditions, the model should be able to reproduce alternating aggradation and incision behaviour in a river floodplain area. In this model development phase an artificial DEM and experimental set-up were used to test the model's functionality. Results showed that the adapted model reproduced alternating aggradation - due to divergent flow in the floodplain and sediment supply under cold conditions - and incision due to reduced sediment supply and resulting clean water erosion during simulated warm conditions. These results can be explained by interactions between hillslopes and floodplains, as the former provide the sediments that are deposited in the latter. Sensitivity and resolution analysis showed that the model is sensitive to changes in the discharge and gradient

exponents and convergence factor for water routing and that model behaviour is influenced by DEM resolution.

Subsequently, in chapter 4, the adapted model was calibrated for the study area. The insights from the conceptual model and the dated sediments of chapter 2 were used to quantitatively simulate a sequence of erosion – sedimentation – erosion processes. In addition, the potential contribution of tillage erosion (i.e. human impact) was analysed over a millennial time-scale and large catchment scale, which has not before been attempted. Generally, model results showed that tillage erosion added to deposition in the lower floodplain area, but neither water erosion alone nor water plus tillage erosion together could exactly reproduce the observed amounts of erosion and sedimentation for the case study area. This implies that other processes, not included in the model, and / or input and model assumptions and uncertainties, play a role. In addition, scale effects were apparent: on hillslopes, tillage importantly contributes to erosion and fills local depressions. On the catchment scale, sediments from tillage erosion eventually reach the floodplain area, where they contribute to aggradation, but to a lesser extent than on hillslopes, also depending on the connectivity within the catchment.

In chapter 5, the event-based soil erosion model OpenLISEM was calibrated for four typical Mediterranean storms of different magnitudes of rainfall intensity and duration. In addition, the relative contribution of these different magnitude storms to total erosion was explored. The main conclusion was that to simulate the erosion dynamics of these different magnitude storms, each storm needed a different set of calibration parameters. An event-index (EVI) was developed which combines the most important characteristics of (Mediterranean) rainfall events: total precipitation, maximum rainfall intensity and event duration. Hitherto, the OpenLISEM model had been applied to small catchments up to a few square kilometres. In chapter 5, the model was calibrated for the ~50 km^2 Prado catchment. Some drawbacks for the calibration of the model to such a large catchment were found, mainly due to spatial variability in values of saturated hydraulic conductivity. This confirmed the need for (enhanced) spatially distributed calibration and validation of model results. Scenario calculations show that, although ~50% of soil erosion occurs as a result of high frequency, low intensity rainfall events, large magnitude, low frequency events potentially contribute significantly to total soil erosion.

Chapter 6 brings together the two models and for the first time compares a landscape evolution model (LAPSUS) and an event-based soil erosion model (OpenLISEM). To try and bridge the time-scale gap between these two models, the time-scales for which each model was originally developed were deliberately extended (OpenLISEM) or shortened (LAPSUS). Calibration of OpenLISEM using average erosion rates derived from long-term simulations with LAPSUS (chapter 4) and, vice versa, calibration of LAPSUS on event-scale (from chapter 5) did not give satisfactory results, suggesting that the gap between the different time-scales of both models is too large to be bridged directly. Calibration of

LAPSUS on annual basis using the summed OpenLISEM erosion and deposition values for each year resulted in a good reproduction of these values by LAPSUS. Thus, when keeping to the time-scale that the model was originally intended for, but calibrating the model using simulation results from the event-based model, short-term variability could successfully be introduced in longer-term modelling of landscape development. In addition, the erosive effects of different sequencing of rainfall variation, climate and land use change were explored on a centennial time-scale. Results showed non-linear behaviour between rainfall input and simulated net erosion. Simulated net erosion for increased rainfall erosivity (with equal total rainfall) was compared to the erosive effect of varying rainfall sequencing, showing that mean annual net erosion of up to 15% increased erosivity is not significantly different from annual mean net erosion of the original simulations. Semi-arid areas may be relatively less sensitive to changes in erosivity, because of high natural rainfall variability. Similarly, single events must be very high and/or frequent if they are to leave a signal in the landscape that is beyond the scope of natural rainfall variability. Scenarios of human impact, although they should be seen as model explorations, show that land use changes can have a large effect on erosion dynamics, larger than climate variability and change, especially for reforestation. Comparing the two models, landscape evolution models such as LAPSUS have the advantage over event-based models that they are capable of simulating landscape dynamics on a continuous basis over long time-scales, which allows evaluation of topographic feedback mechanisms, temporally changing (dis)connectivity and local sediment storage and non-linear, self-organizing behaviour. Chapter 6 showed that these feedback mechanisms are important in landscape erosion and deposition dynamics and catchment evolution.

Finally, chapter 7 combines results of chapters 2-6 and discusses them in light of the three main themes of this thesis that were introduced in the first chapter. Implications of the research are discussed: for mitigation measures as well as methodological and scientific implications. The time-scale gap between triggers and landscape response in terms of soil redistribution is explored for the hillslope and catchment spatial scales. For the first, detailed models are suited to simulate various processes. For the latter, reduced complexity models may be more applicable due to the need to be capable to simulate spatial interactions and feedbacks that emerge at the catchment scale. General conclusions include (i) the need for a holistic (fieldwork and modelling) approach to be able to identify triggers of landscape change and their temporal and spatial effects; (ii) landscape evolution models (LEMs) are promising tools to evaluate landscape dynamics because of continuous (temporal) simulation of various processes, including complex response feedbacks and non-linear behaviour; and (iii) the effects of extreme events on landscape dynamics should be evaluated on longer time-scales and within the context of (potential) rainfall variability. Finally suggestions for further research are given.

Samenvatting

In erosie-onderzoek worden verschillende ruimtelijke schalen, tijdschalen en onderzoeksmethoden gebruikt. Veel studies kijken naar erosie op veld-, helling- of klein stroomgebiedsschaal en op korte, hedendaagse ('menselijke') tijdschalen. Erosie en depositie na een regenbui worden geanalyseerd m.b.v. veldexperimenten. Aan de andere kant wordt geowetenschappelijk onderzoek gedaan op de regionale en landschapsschaal en op tijdschalen van landschapsevolutie. Erosie en depositie worden geanalyseerd over decennia m.b.v. landschapsevolutie modellen (LEMs). Het doel van dit proefschrift is het overbruggen van deze twee verschillende methodes. De focus ligt daarbij op het verschil in tijdschaal tussen regenbuien en landschapsevolutie en op de relatieve bijdrage van menselijke activiteiten aan natuurlijke erosie.

In het eerste hoofdstuk worden de drie centrale thema's van dit proefschrift geïntroduceerd: (1) natuurlijke tegenover door mensen veroorzaakte erosie, (2) het verschil in tijdschaal, en (3) verschillende modelleermethoden in landschapsdynamiek. In hoofdstuk 2 wordt de geomorfologie van het onderzoeksgebied (Guadalentín Basin, zuidoost Spanje) onderzocht met als doel inzicht te krijgen in landschapsprocessen tijdens het Laat Pleistoceen en Holoceen. Een conceptueel model van erosie en sedimentatie dynamiek wordt ontwikkeld. Hieruit blijkt dat het sedimentatiepatroon van de drie rivieren uit fase is; ze zijn niet in evenwicht. De oorzaak hiervan is de invloed van een, inmiddels verdwenen, paleomeer. De jongere sedimenten kunnen worden gecorreleerd aan menselijke invloed; nl. erosie na het verdwijnen van de Romeinse en Moorse bezetting. Echter, de belangrijkste conclusie is dat lokale processen en interne rivierdynamiek een belangrijkere rol hebben gespeeld in de landschapsdynamiek in het onderzoeksgebied dan externe factoren zoals klimaatverandering.

Landschapsevolutiemodel LAPSUS (LandscApe ProcesS modelling at mUlti dimensions and Scales) wordt in hoofdstuk 3 zodanig aangepast dat fluviatiele processen beter gesimuleerd kunnen worden, maar zonder dat daarbij de bestaande modelvergelijkingen en –structuur veranderen. Het model moet, afhankelijk van het klimaat, afwisselend aggradatie en incisie simuleren in een riviervlakte. Resultaten laten zien dat het aangepaste model afwisselend aggradatie – door divergerende waterstroming en toevoer van sediment tijdens koude omstandigheden – en incisie simuleert, de laatste door verminderde toevoer van sediment tijdens warme omstandigheden en daarmee samenhangende erosie.

Dit laat een interactie zien tussen hellingen en rivieren; de eerste produceren het sediment dat wordt afgezet in de riviervlakte door de rivier. Voor dit aangepaste model zijn in hoofdstuk 3 bovendien een gevoeligheids- en resolutieanalyse gedaan.

Vervolgens wordt dit aangepaste model in hoofdstuk 4 gecalibreerd voor het onderzoeksgebied. De inzichten uit het conceptuele model en de gedateerde sedimenten uit hoofdstuk 2 worden gebruikt om een reeks van erosie – sedimentatie – erosie te simuleren. Bovendien wordt de potentiele bijdrage van ploegerosie (menselijke invloed) geanalyseerd op een tijdschaal van duizenden jaren en op grote stroomgebiedsschaal, iets wat niet eerder is gedaan. Over het algemeen heeft ploegerosie bijgedragen aan sedimentatie in de riviervlakte, maar de simulaties konden niet exact de geobserveerde hoeveelheden erosie en sedimentatie reproduceren. Dit geeft aan dat andere processen die niet in het huidige model zitten, en/of input en model aannames en onzekerheden een rol spelen. Bovendien waren schaaleffecten duidelijk: op de hellingen draagt ploegen sterk bij aan erosie en sedimentatie en worden lokale depressies gevuld. Op de stroomgebiedsschaal bereiken de sedimenten, geërodeerd door ploegen, uiteindelijk de riviervlakte waar ze bijdragen aan depositie. Echter, dit is een indirect effect en is afhankelijk van factoren zoals connectiviteit binnen het stroomgebied.

In hoofdstuk 5 wordt het regenbui-gebaseerde erosiemodel OpenLISEM gecalibreerd voor vier typische mediterrane buien van verschillende lengte en regenval intensiteit. Ook wordt de relatieve bijdrage van deze verschillende buien aan totale erosie berekend. De belangrijkste conclusie is dat een andere parameter set nodig is om de erosie als gevolg van de verschillende buien goed te kunnen simuleren. Een 'event-index (EVI)' die de belangrijkste eigenschappen van typische mediterrane regenbuien combineert (nl. totale hoeveelheid neerslag, maximale intensiteit en lengte van de bui), is ontwikkeld. Tot nog toe werd het OpenLISEM model toegepast op kleine stroomgebieden van enkele vierkante kilometers. In hoofdstuk 5 wordt het model toegepast op het ~50 km² stroomgebied van de Prado. Nadelen hiervan zijn voornamelijk gerelateerd aan ruimtelijke variatie in waterdoorlatendheid. Dit bevestigt de noodzaak voor (verbeterde) ruimtelijke calibratie en validatie van de modelresultaten. Scenarios laten zien dat, hoewel ~50% van de totale erosie het gevolg is van vaak voorkomende buien met lage intensiteit, heftige regenbuien die niet vaak voorkomen in hoge mate bijdragen aan totale erosie.

Hoofdstuk 6 brengt de twee modellen samen en vergelijkt voor het eerst een landschapsevolutiemodel (LAPSUS) en een regenbui-gebaseerd erosiemodel (OpenLISEM). Om te proberen het verschil in tijdschaal tussen de twee modellen te overbruggen is de tijdschaal waarvoor elk model oorspronkelijk was ontwikkeld met opzet verlengd (OpenLISEM) of verkort (LAPSUS). Calibratie van OpenLISEM met gemiddelde erosiesnelheden, verkregen van de lange termijn simulatie met LAPSUS (hoofdstuk 4) en, vice versa, calibratie van LAPSUS op tijdschaal van één bui (uit hoofdstuk 5), leidden niet

tot bevredigende resultaten. Dit suggereert dat het verschil in tijdschaal tussen beide modellen te groot is om direct te kunnen overbruggen. Calibratie van LAPSUS op jaarlijkse tijdschaal met de gesommeerde erosie en depositie waarden van OpenLISEM voor elk jaar geeft goede resultaten. Ook zijn de effecten van verschillende volgorde van regenbuien, van klimaatverandering en landgebruiksverandering verkent op een tijdschaal van honderden jaren. Resultaten laten een niet-lineaire relatie zien tussen regenval input en gesimuleerde netto erosie. Gesimuleerde gemiddelde jaarlijkse netto erosie als gevolg van tot 15% hogere regenval erosiviteit (maar gelijke totale regenval) is niet significant verschillend van gesimuleerde gemiddelde jaarlijkse netto erosie als gevolg van verschillende volgorde van regenbuien. Semiaride gebieden zijn mogelijk minder gevoelig voor veranderingen in erosiviteit omdat ze gekarakteriseerd worden door een van nature hoge variatie in regenval (intensiteit). Evenzo moeten individuele regenbuien erg heftig zijn en/of vaak voorkomen om een herkenbaar spoor achter te laten in het landschap dat groter is dan dat door natuurlijke variatie in regenval. Scenarios van menselijke invloed, hoewel enkel bedoeld als model verkenningen, laten zien dat landgebruiksverandering, met name herbebossing, grote invloed kan hebben op erosiedynamiek, groter dan dat van klimaatverandering. Landschapsevolutiemodellen zoals LAPSUS hebben het voordeel ten opzicht van bui-gebaseerde erosiemodellen dat ze landschapsdynamiek kunnen simuleren op continue basis over lange tijdschalen. Dit maakt het mogelijk om topografische terugkoppelingsmechanismen te evalueren, alsook door de tijd veranderende (dis)connectiviteit, lokale accumulatie van sediment en niet-lineair, zelf-organiserend gedrag. Hoofdstuk 6 laat zien dat zulke terugkoppelings-mechanismen belangrijk zijn in landschapsevolutie processen.

Hoofdstuk 7 combineert de resultaten van hoofdstukken 2-6 in het licht van de drie hoofdthema's van dit proefschrift. Implicaties van het onderzoek worden besproken: voor erosiemaatregelen als ook methodologische en wetenschappelijke implicaties. Het verschil in tijdschaal tussen trigger en landschapsreactie in termen van herverdeling van sediment wordt verkent voor de helling- en de stroomgebiedsschaal. Voor de hellingschaal zijn gedetailleerde modellen geschikt om verschillende processen te simuleren. Voor de stroomgebiedsschaal zijn 'reduced complexity' modellen meer geschikt door de noodzaak om ruimtelijke interacties en terugkoppeling te kunnen simuleren die optreden op deze schaal. Algemene conclusies zijn (i) de noodzaak van een holistische aanpak (veld- en modelleerwerk) om triggers van landschapsverandering en hun ruimtelijke en temporele effecten te kunnen identificeren; (ii) landschapsevolutie-modellen (LEMs) zijn veelbelovende modellen om landschapsdynamiek mee te evalueren doordat ze op continue basis verschillende processen kunnen simuleren, inclusief complex response terugkoppelingsmechanismen en niet-lineair gedrag; en (iii) de effecten van extreme regenbuien op landschapsdynamiek moeten worden geëvalueerd op langere tijdschalen en in de context van (mogelijke) variabiliteit in regenval. Als laatste worden suggesties gedaan voor verder onderzoek.

205

Resumen

En investigación sobre la erosión de suelo los métodos utilizados se adaptan a las diferentes escalas espaciales y temporales de estudio. En muchos trabajos se evalúa la erosión a escala espacial de campo, de parcela, de ladera o de cuenca pequeña y a escalas temporales cortas y contemporáneas ('humana'). Se evalúa erosión y sedimentación tras los eventos lluviosos y con experimentos de campo. Por otro lado, en las Geo-ciencias, los trabajos de investigación se desarrollan a escala regional y de paisaje y a escalas temporales que abarcan la evolución del mismo. Se evalúan cambios decenales y se utilizan modelos de evolución del paisaje (LEMs). El objetivo de esta tesis es conectar estas dos diferentes aproximaciones metodológicas y líneas de investigación contrastadas, poniendo el énfásis en la escala temporal entre un evento y la evolución del paisaje, analizando la contribución relativa de la actividad humana a la erosión natural.

El primer capítulo introduce tres temas centrales de esta tesis: la erosión natural versus la erosión inducida por el hombre, la diferencia de escala temporal en la dinámica de erosión y los métodos de modelización de la erosión. En el capítulo 2 el funcionamiento geomorfológico del área de investigación (Cuenca Alta del Guadalentín, SE de España) se ha explorado con el objetivo de entender la evolución del paisaje del Pleistoceno tardío y Holoceno. Se desarrolló un modelo conceptual sobre la dinámica de erosión y sedimentación sobre tres partes de la cuenca del Alto Guadalentín. A través de este análisis, se dedujo que los ríos estudiados no se encuentran en equilibrio, puesto ello en evidencia por su patrón de sedimentación fuera de fase. Se hipotetiza que ello puede ser debido a la influencia de un paleo-lago. Se realizó una correlación tentativa entre los depósitos más jóvenes y el impacto humano tras la ocupación romana y árabe, pero se llegó a la conclusión que los procesos locales y la dinámica interna de los ríos parecen haber tenido un papel más importante que los factores externos.

En el capítulo 3 el modelo de evolución del paisaje LAPSUS (LandscApe ProcesS modelling at mUlti dimensions and Scales) fue adaptado para simular mejor los procesos fluviales. En esta fase de desarrollo del modelo, y con un propósito experimental, se utilizó un DEM artificial para probar la funcionalidad del modelo. Los resultados mostraron que el modelo adaptado pudo simular fases de agradación - debido a un flujo divergente en la llanura de inundación y el suministro de sedimentos durante condiciones climáticas frías - e incisión, por un suministro reducido de sedimento y la erosión resultante durante condiciones climáticas cálidas. Estos resultados se deben a las interacciones entre las laderas y llanuras de inundación, las primeras suministran los sedimentos que se depositan en las segundas.

Después, en el capítulo 4, el modelo fue calibrado para el área de investigación. El modelo conceptual y los sedimentos datados del capítulo 2 se han utilizado para simular cuantitativamente una secuencia de erosión - sedimentación - erosión. Además por primera vez la contribución potencial de la erosión por laboreo (el impacto humano), se analizó durante milenios y a escala espacial de cuenca. En general, los resultados del modelo muestran que la erosión por laboreo contribuye a la deposición en la llanura de inundación, pero ni la erosión hídrica por sí sola o conjuntamente con la erosión por laboreo podrían llegar a los valores observados de erosión y sedimentación en el área de estudio. Todo ello implica que otros procesos, no incluidos en el modelo, y/o entradas de datos, asunciones e incertidumbres juegan un papel fundamental en la simulación de los procesos geomórficos. Además, los efectos de escala fueron evidentes: en laderas, la labranza contribuye de manera importante a la erosión. En cuencas, los sedimentos de la erosión de labranza llegan al final a la zona inundable, donde contribuyen a la agradación, pero dependiendo de la (des)conectividad dentro de la cuenca.

En el capítulo 5, el modelo de la erosión del suelo OpenLISEM que simula erosión causada por eventos lluviosos fue calibrado para cuatro eventos típicos del Mediterráneo de diferente duración, magnitud e intensidad de lluvia. Además, se estudió la contribución relativa de estos eventos de diferente magnitud a la erosión total. La principal conclusión fue que, para simular la dinámica de erosión de estos eventos de diferente magnitud, cada evento necesita un conjunto diferente de parámetros de calibración. Se desarrolló un índice de evento (Event Index, EVI) que combina las características más importantes de los eventos mediterráneos: precipitación total, intensidad máxima de la precipitación y duración del evento. Hasta ahora, el modelo OpenLISEM se había aplicado a pequeñas cuencas de unos pocos kilómetros cuadrados. En el capítulo 5, el modelo fue calibrado para la cuenca del Prado (~50 km2). La calibración del modelo para una cuenca de este tamaño más grande fue complicada debido principalmente a la variabilidad espacial de la conductividad hidráulica. Se precisado una mejor calibración y validación espacial de los resultados del modelo. Las estimaciones realizadas para diferentes escenarios muestran que, aunque ~50% de la erosión del suelo es causada por eventos de alta frecuencia y baja intensidad, los eventos de gran magnitud y baja frecuencia pueden contribuir significativamente a la erosión total del suelo.

El capítulo 6 reúne los dos modelos de este estudio y por primera vez se combina un modelo de evolución del paisaje (LAPSUS) y un modelo de erosión de suelo basado en eventos (OpenLISEM). Para intentar cerrar la laguna entre las dos escalas temporales a las que trabaja cada uno de ellos, ambas fueron deliberadamente manipuladas, prolongada (OpenLISEM), o reducida (LAPSUS). La calibración de OpenLISEM utilizando el valor medio de erosión derivado de simulaciones a largo plazo con LAPSUS (capítulo 4) y, viceversa, la calibración de LAPSUS a escala de evento (derivado del capítulo 5) no produjeron resultados satisfactorios, lo que sugiere que la laguna entre las diferentes

208

escalas temporales de los dos modelos es demasiado grande para ser ligada directamente. La calibración de LAPSUS para una escala anual utilizando las valores de erosión simulados por OpenLISEM sumados anualmente, resultó en una buena reproducción de estos valores por LAPSUS. Además, los efectos erosivos de las diferentes secuencias de la variación de la lluvia, cambio climático y el uso del suelo se analizaron en una escala temporal centenaria. Los resultados mostraron un comportamiento no-lineal entre la precipitación y la erosión neta simulada. La erosión media anual neta aumentando la erosividad de la lluvia (manteniendo el total de precipitación) hasta un 15% no es significativamente diferente del efecto erosivo producido al variar la secuencia de las precipitaciones. Las zonas semiáridas pueden ser relativamente menos sensibles a los cambios en la erosividad de la lluvia, debido a la alta variabilidad de las precipitaciones naturales. Del mismo modo, los eventos individuales deben ser de muy elevada intensidad y/o frecuecia para dejar una señal en el paisaje diferente al de la variabilidad de la precipitación natural. Los escenarios de impacto humano explorados con el modelo muestran que los cambios de uso del suelo pueden tener un gran efecto sobre la dinámica de la erosión, especialmente las reforestaciones, mayor que el efecto de la variabilidad climática y el Cambio Climático. Al comparar los dos modelos, los modelos de evolución del paisaje, como LAPSUS, tienen la ventaja sobre los modelos basados en eventos que son capaces de simular la dinámica del paisaje de forma continua en períodos largos, lo que permite la evaluación de los mecanismos de retroacción topográfica, cambios temporales de (des)conectividad, acumulación de sedimentos localmente y un comportamiento no-lineal de auto-organización.

Finalmente, el capítulo 7 combina los resultados de los capítulos 2-6 y se analizan los mismos bajo el enfoque de tres temas principales de esta tesis. Se discuten las implicaciones de esta investigación tanto a nivel de medidas de mitigación como las implicaciones metodológicas y científicas. Las diferencias de escala temporal entre los motores de cambio del paisaje y su respuesta en términos de redistribución del suelo se explora para laderas y cuencas. La escala de ladera es adecuada para simular procesos diversos con modelos de detalle. Para la escala de cuenca los modelos de complejidad reducida pueden ser más aplicables por su versatilidad para simular interacciones y retroacciones espaciales que surgen a esta escala. Las conclusiones generales incluyen: (i) la necesidad de un método holístico (trabajo de campo y modelización) para poder identificar los motores de cambio del paisaje y sus efectos temporales y espaciales; (ii) los modelos de evolución del paisaje (LEMs) son modelos prometedores para evaluar la dinámica del mismo, por su capacidad de simular varios procesos continuamente, incluyendo los efectos indirectos de respuestas complejas y el comportamiento no-lineal, y (iii) los efectos de eventos extremos en la dinámica del paisaje deben ser evaluados a escalas temporales más largas y en el contexto de variabilidad (potencial) de las precipitaciones. Finalmente se dan algunas sugerencias para investigaciones futuras.
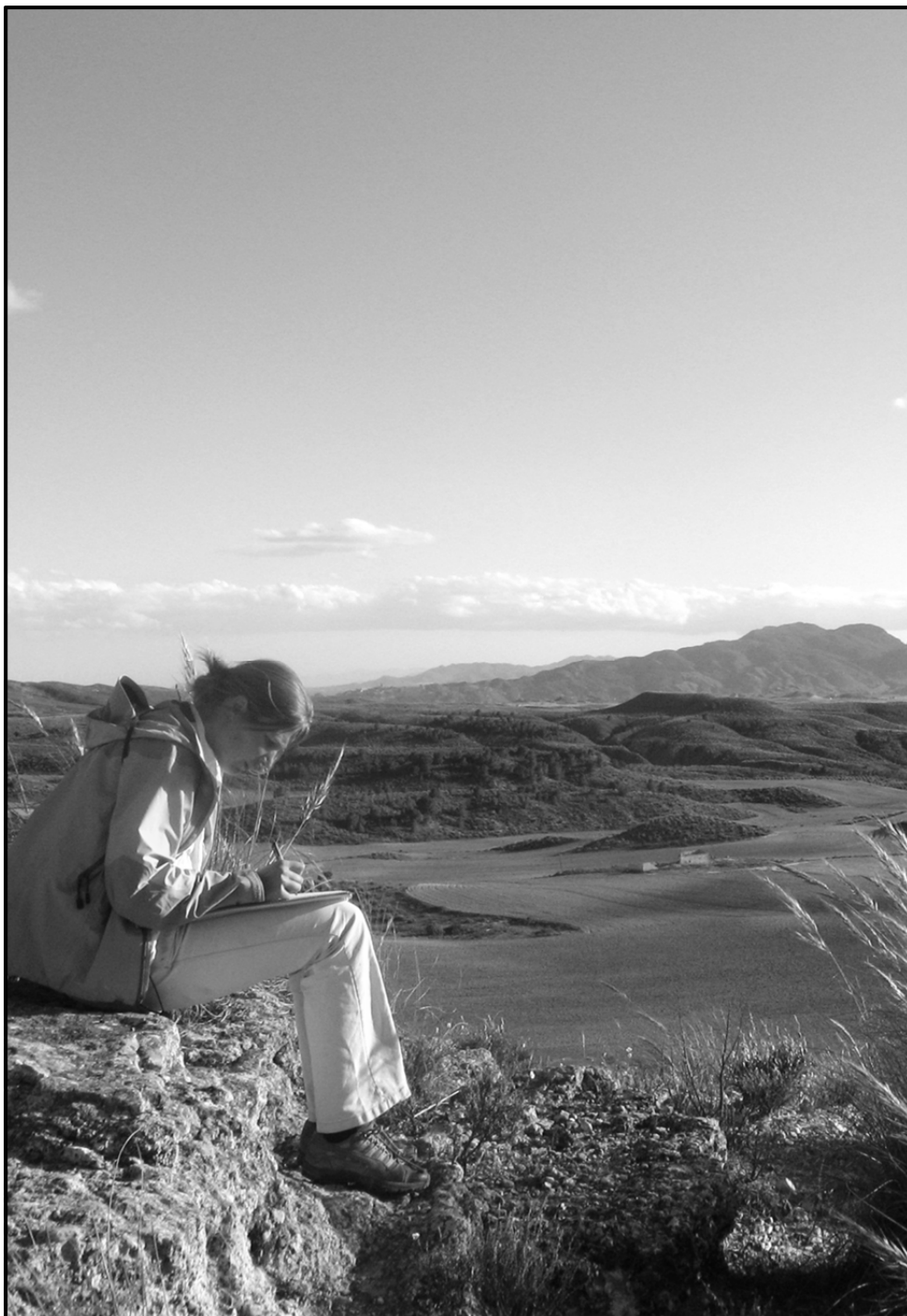
About the author

Curriculum Vitae

Jantiene Elise Marianne Baartman was born on 12th April 1981 in Culemborg, the Netherlands. She attended secondary school at Kon. Wilhelmina College in Culemborg, where she obtained her VWO diploma in 1999. Before continuing her studies at university, Jantiene wanted to broaden her view of the world. She spend eight months travelling and working on a voluntary programme as a primary school teacher and programme coordinator of a child-welfare organisation in a small village in Bolivia. In 2000 she started studying Soil, Water and Atmosphere at Wageningen University. As an extension to the BSc. programme, she participated in the 6-month 'From Mountain to Fjord: geology and ecology of Western Norway' programme at the Sogn og Fjordane University College, Sogndal, Norway. In her third year, she specialised in Soil Science and Geology, obtaining her BSc. degree in 2004. She continued with an MSc. in soil science, with specialisation in soil inventorisation and land evaluation, graduating in 2006. For her first MSc. thesis, Jantiene did fieldwork in the mangrove forests of Vietnam, including laboratory analyses, studying the relation between soil characteristics and mangrove distribution in the Dong Nai River Delta. For her second and major MSc. thesis, she travelled to South-Africa, where she did fieldwork and wrote a thesis on reconstructing the palaeo-environmental changes and landscape evolution using palaeosol sequences in colluvial sediments. Finally and knowing that she wanted to continue in science, Jantiene did her internship at research institute Alterra, applying the soil erosion model LISEM to a case study in Samoa. Her second thesis inspired Jantiene to continue in research and during her internship at Alterra she met Prof. Coen Ritsema who had just acquired funding for a large research project on land degradation and desertification (the DESIRE project). Coincidentally, a call for PhD research proposals was issued by the PE&RC research school. The PhD research proposal that Jantiene wrote together with her supervisors was selected for funding. Thus, in 2007, Jantiene started her PhD research as a collaboration between the Land Dynamics (LAD) and Land Degradation and Development (LDD) groups of Wageningen University.

In her holidays, Jantiene likes to be active: mountaineering (both sports- and alpine climbing), hiking and mountainbiking. During winter, she enjoys fresh powdersnow during tour skiing adventures. In the Netherlands, Jantiene enjoys mountainbiking, hiking and dancing, as well as drinking a beer with friends!

Publication list

Baartman, J.E.M., Veldkamp, A., Jetten, V.G., Temme, A.J.A.M., Schoorl, J.M. Exploring the role of rainfall variability and exterme events in long-term landscape evolution. *Catena (in review).*

Baartman, J.E.M., Temme, A.J.A.M., Schoorl, J.M., Braakhekke, M.H.A., Veldkamp, A. Did tillage erosion play a role in millennial scale landscape development? *Earth Surface Processes and Landforms (Accepted).*

Baartman, J.E.M., Van Gorp, W., Temme, A.J.A.M., Schoorl, J.M., 2012. Simulating sediment dynamics due to hillslope – river interactions at the catchment scale and on annual timescales using a landscape evolution model. *Earth Surface Processes and Landforms (In press).*

Baartman, J.E.M., Jetten, V.G., Ritsema, C.J., De Vente, J. 2012. Exploring effects of rainfall intensity and duration on soil erosion at the catchment scale using openLISEM – Prado catchment, SE Spain. *Hydrological Processes* 26: 1034 – 1049.

Baartman, J.E.M., Veldkamp, A., Schoorl, J.M., Wallinga, J., Cammeraat, L.H., 2011. Unravelling Late Pleistocene and Holocene landscape dynamics: The Upper Guadalentín Basin, SE Spain. *Geomorphology* 125: 172 – 185.

Temme, A.J.A.M., **Baartman, J.E.M.**, Schoorl, J.M., 2009. Can uncertain landscape evolution models discriminate between landscape responses to stable and changing future climate? A millennial-scale test. *Global and Planetary Change* 69: 48 – 58.

Temme, A.J.A.M., **Baartman, J.E.M.**, Botha, G.A., Veldkamp, A., Jongmans, A.G., Wallinga, J., 2008. Climate controls on late Pleistocene landscape evolution of the Okhombe valley, KwaZulu-Natal, South Africa. *Geomorphology* 99: 280 – 295.

Baartman, J.E.M., Van Lynden, G.W.J., Reed, M.S., Ritsema, C.J., Hessel, R., 2007. Desertification and land degradation: origins, processes and solution – A literature review. DESIRE Scientific Report no. 4, ISRIC, The Netherlands

PE&RC PhD Education Certificate

With the educational activities listed below the PhD candidate has complied with the educational requirements set by the C.T. de Wit Graduate School for Production Ecology and Resource Conservation (PE&RC) which comprises of a minimum total of 32 ECTS (= 22 weeks of activities)
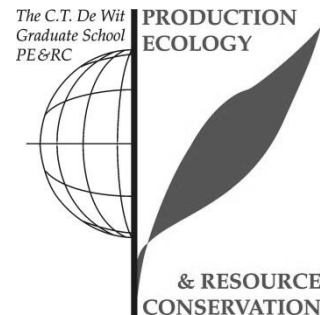
Writing of project proposal (4.5 ECTS)
- Natural and human-induced erosion: combining short-term event-based research and landscape evolution modelling (2007)

Post-graduate courses (13 ECTS)
- Land science: bringing concepts and theory into practice; PE&RC, LAD (2007)
- The art of modelling; PE&RC (2008)
- Land dynamics: getting to the bottom of Mount Kenya: analysis of land dynamics and sustainable development in an interdisciplinary perspective; PE&RC, LAD (2009)
- Summer School on geomorphology: complex response of earth surface processes to environmental change; Junge Geomorphologen, Heimbuchental, Germany (2010)

Laboratory training and working visits (4 ECTS)
- Working visit to Prof. MJ Kirkby; University of Leeds, UK (2007)
- OSL-dating preparation techniques; NCL-TU, Delft (2008)
- LISEM Modelling workshop; ITC, Enschede (2010)

Invited review of (unpublished) journal manuscript (1 ECTS)
- Catena: human versus natural factors in land instability; case studies in N Spain (2011)

Deficiency, refresh, brush-up courses (0.3 ECTS)
- Erosion processes and modelling (2007)

Competence strengthening / skills courses (3.1 ECTS)
- PhD Competence assessment; WGS (2007)
- Techniques for writing and presenting a scientific paper; WGS (2008)
- Mobilising your scientific network; WGS (2009)
- Afstudeervak organiseren en begeleiden; DO (2010)

PE&RC Annual meetings, seminars and the PE&RC weekend (1.2 ECTS)
- PE&RC Annual meeting "Collapse" (2007)
- Symposium "The role of long-term landscape reconstruction for understanding current-day rates of landscape change" (2008)
- PE&RC Annual meeting "Intelligent communication" (2009)
- Contribution to PE&RC weekend (2011)

Discussion groups / local seminars / other scientific meetings (7.2 ECTS)

- Spatial Methods PhD discussion group (2007-2011)
- NBV Themadagen (2007-2011)
- KNAG-dag (2008)
- Nederlands Aardwetenschappelijk Congres (NAC9) (2008)
- DESIRE PhD Meeting (2010)
- Scaling and Governance Conference (2010)

International symposia, workshops and conferences (15.7 ECTS)

- Cost 634 conference "Soil and Hillslope Management using scenario analysis and runoff-erosion models: a critical evaluation of current techniques; Florence, Italy (2007)
- Invited speaker at colloquium series on landscape modelling; Trier University, Germanay (2009)
- International Conference on Desertification; Murcia, Spain (2009)
- Fluvial Archives Group (FLAG) Biennial meeting "Long term river evolution and fluvial dynamics"; Portugal (2010)
- European Geosciences Union; Vienna, Austria (2010, 2011)
- DESIRE Final meeting; Almeria, Spain (2011)

Lecturing / supervision of practical's / tutorials (5.2 ECTS)

- Bodem-water I; 6 days (2007-2009)
- Field training land science; 10 days; Spain (2008)
- Geologie, bodem en landschap van de Rijn-Maas delta; 0.5 day (2009)
- Integratievak bodem, water atmosfeer; 1 day (2009)
- Erosion processes and modelling; 8 days (2009-2010)
- Research approaches to land and water management; 2 days (2009-2010)
- Bodem-water II; 3 days (2009-2010)

Supervision of 5 MSc students; 40 days

- Landscape dynamics in the context of natural and human-induced erosion: an overview of erosion rates in SE Spain
- Literature research of erosion and sedimentation processes in the Guadalentin Basin and the implementation of LISEM for the Prado catchment in SE Spain
- Reconstructing Late Quaternary landscape development for a dryland catchment; SE Spain
- Setting up a sampling design for the LISEM model for the Torrealvilla catchment in South-East Spain
- Statistical analysis of field-based measurements for a sediment yield model (LISEM) in the Torrealvilla catchment; SE Spain